Corrosion-Induced Durability Issues and Maintenance Strategies for Post-Tensioned Concrete Bridges

PUBLICATION NO. FHWA-HRT-22-090

SEPTEMBER 2022

U.S. Department of Transportation
Federal Highway Administration

Research, Development, and Technology
Turner-Fairbank Highway Research Center
6300 Georgetown Pike
McLean, VA 22101-2296

FOREWORD

This final report presents the research findings of a three-year synthesis study on four topics concerning corrosion-induced durability issues in grouted post-tensioned (PT) tendons and maintenance strategies to address these issues. The topics covered are major cases of corrosion in the field, key findings of national and international laboratory studies, the current understanding of corrosion mechanisms, and maintenance strategies aimed at controlling PT tendon corrosion.

This final report is expected to be of interest to bridge engineers from Federal, State, and local transportation departments as well as to parties engaged in bridge-related research.

Cheryl Allen Richter, P.E., Ph.D.
Director, Office of Infrastructure
Research and Development

Recommended citation: Federal Highway Administration, *Corrosion-Induced Durability Issues and Maintenance Strategies for Post-Tensioned Concrete Bridges* (Washington, DC: 2022) https://doi.org/10.21949/1521873.

TECHNICAL REPORT DOCUMENTATION PAGE

1. Report No. FHWA-HRT-22-090	2. Government Accession No. N/A	3. Recipient's Catalog No. N/A
4. Title and Subtitle Corrosion-Induced Durability Issues and Maintenance Strategies for Post-Tensioned Concrete Bridges		5. Report Date September 2022
		6. Performing Organization Code: HRDI-30
7. Author(s) Seung-Kyoung Lee (ORCID ID 0000-0001-7367-5197)		8. Performing Organization Report No. N/A
9. Performing Organization Name and Address SK Lee & Associates, Inc., 10813 Fieldwood Drive Fairfax, VA 22030		10. Work Unit No. HRDI-30
		11. Contract or Grant No. DTFH6117D00017
12. Sponsoring Agency Name and Address Office of Infrastructure Research and Development Federal Highway Administration 6300 Georgetown Pike McLean, VA 22101-2296		13. Type of Report and Period Covered Final Report February 2018–September 2022
		14. Sponsoring Agency Code HRDI-30

15. Supplementary Notes
The technical contact was Frank Jalinoos (HRDI-30), and the contracting officer's representative was Cara Fitzgerald (HRDI-1).

16. Abstract
Prestressed concrete structures utilize prestressing force, which can be applied using a pre-tensioning or post-tensioning method. The Walnut Lane Bridge in Philadelphia, PA was the first precast post-tensioned (PT) bridge in the United States. It opened to traffic in the late 1950s and had to be replaced in 1990 after nearly 40 years of service due to improper tendon grouting and other deficiencies. Generally, for most of the second half of the 20th century, the durability of PT bridges in the United States was rated as good to excellent, even as PT bridges in Europe experienced tendon corrosion problems. Then, in 1999, the first failed tendon caused by corrosion in the United States was found in the Niles Channel Bridge in Florida. Since then, six other states—Virginia, Texas, Minnesota, Kansas, Indiana, and South Carolina—also experienced tendon corrosion problems in eight major PT bridges. Materials, specifications, construction methods, and inspection techniques for PT bridges have progressed greatly over the last two decades. Prepackaged non-bleed/thixotropic grout, flexible fillers, and corrosion-resistant strands exemplify improved materials. Additionally, tightened grout specifications and improved grout-injecting procedures can now minimize grout deficiencies. Another encouraging trend is the increasing use of advanced inspection tools such as high-powered borescopes, ground-penetrating radars, impact echoes, and magnetic-based nondestructive evaluation (NDE) systems. However, performing NDEs of prestressing steel in many critical structural locations prone to corrosion, such as the anchorage area, is still challenging. Additionally, once it is discovered, damaged prestressing steel often cannot be replaced. As PT bridges age, especially those constructed before 2001 with neat cement grout, more durability problems are likely to surface, with PT tendon corrosion likely to be a primary cause. This final report presents important findings from a 3-yr synthesis study on four aspects of corrosion-induced durability issues in grouted PT tendons, as follows: major cases of corrosion in the field, key findings of national and international laboratory studies, mechanisms of corrosion, and maintenance strategies for corrosion control.

17. Key Words	18. Distribution Statement
Corrosion, segregated grout, chloride ions, sulfate ions, post-tensioned tendon, carbonation, prestressed steel, pitting corrosion, crevice corrosion	No restrictions. This document is available to the public through the National Technical Information Service, Springfield, VA 22161. http://www.ntis.gov

19. Security Classif. (of this report)	20. Security Classif. (of this page)	21. No. of Pages	22. Price
Unclassified	Unclassified	205	N/A

Form DOT F 1700.7 (8-72) Reproduction of completed page authorized

SI* (MODERN METRIC) CONVERSION FACTORS

APPROXIMATE CONVERSIONS TO SI UNITS

Symbol	When You Know	Multiply By	To Find	Symbol
		LENGTH		
in	inches	25.4	millimeters	mm
ft	feet	0.305	meters	m
yd	yards	0.914	meters	m
mi	miles	1.61	kilometers	km
		AREA		
in^2	square inches	645.2	square millimeters	mm^2
ft^2	square feet	0.093	square meters	m^2
yd^2	square yard	0.836	square meters	m^2
ac	acres	0.405	hectares	ha
mi^2	square miles	2.59	square kilometers	km^2
		VOLUME		
fl oz	fluid ounces	29.57	milliliters	mL
gal	gallons	3.785	liters	L
ft^3	cubic feet	0.028	cubic meters	m^3
yd^3	cubic yards	0.765	cubic meters	m^3
	NOTE: volumes greater than 1,000 L shall be shown in m^3			
		MASS		
oz	ounces	28.35	grams	g
lb	pounds	0.454	kilograms	kg
T	short tons (2,000 lb)	0.907	megagrams (or "metric ton")	Mg (or "t")
		TEMPERATURE (exact degrees)		
°F	Fahrenheit	5 (F-32)/9 or (F-32)/1.8	Celsius	°C
		ILLUMINATION		
fc	foot-candles	10.76	lux	lx
fl	foot-Lamberts	3.426	$candela/m^2$	cd/m^2
		FORCE and PRESSURE or STRESS		
lbf	poundforce	4.45	newtons	N
lbf/in^2	poundforce per square inch	6.89	kilopascals	kPa

APPROXIMATE CONVERSIONS FROM SI UNITS

Symbol	When You Know	Multiply By	To Find	Symbol
		LENGTH		
mm	millimeters	0.039	inches	in
m	meters	3.28	feet	ft
m	meters	1.09	yards	yd
km	kilometers	0.621	miles	mi
		AREA		
mm^2	square millimeters	0.0016	square inches	in^2
m^2	square meters	10.764	square feet	ft^2
m^2	square meters	1.195	square yards	yd^2
ha	hectares	2.47	acres	ac
km^2	square kilometers	0.386	square miles	mi^2
		VOLUME		
mL	milliliters	0.034	fluid ounces	fl oz
L	liters	0.264	gallons	gal
m^3	cubic meters	35.314	cubic feet	ft^3
m^3	cubic meters	1.307	cubic yards	yd^3
		MASS		
g	grams	0.035	ounces	oz
kg	kilograms	2.202	pounds	lb
Mg (or "t")	megagrams (or "metric ton")	1.103	short tons (2,000 lb)	T
		TEMPERATURE (exact degrees)		
°C	Celsius	1.8C+32	Fahrenheit	°F
		ILLUMINATION		
lx	lux	0.0929	foot-candles	fc
cd/m^2	candela/m2	0.2919	foot-Lamberts	fl
		FORCE and PRESSURE or STRESS		
N	newtons	2.225	poundforce	lbf
kPa	kilopascals	0.145	poundforce per square inch	lbf/in^2

*SI is the symbol for International System of Units. Appropriate rounding should be made to comply with Section 4 of ASTM E380. (Revised March 2003)

TABLE OF CONTENTS

LIST OF FIGURES

LIST OF TABLES

LIST OF ABBREVIATIONS

AASHTO	American Association of State Highway and Transportation Officials
AC	alternating current
AE	acoustic emission
ASBI	American Segmental Bridge Institute
ASTM	American Society for Testing and Materials International
BV	bleed water voids
CEBTP	Centre Expérimental de Recherches et d'Études du Bâtiment et des Travaux Publics (Center for Experimental Research and Studies of Building and Construction)
CPP	cyclic potentiodynamic polarization
CR	corrosion rate
EDS	energy dispersive X-ray spectroscopy
EIC	environmentally induced cracking
EIT	electrically isolated tendon
EIS	electrochemical impedance spectroscopy
EN	European Standard
FDOT	Florida Department of Transportation
FHWA	Federal Highway Administration
fib	Fédération Internationale du béton (International Federation for Structural Concrete)
GPR	ground penetrating radar
GUTS	guaranteed ultimate tensile strength
HDPE	high density polyethylene
HE	hydrogen embrittlement
HRWR	high-range water reducer
HSSS	high-strength stainless steel
IE	impact echo
ISO	International Organization for Standardization
LPR	linear polarization resistance
MFL	magnetic flux leakage
MIC	microbiologically influenced corrosion
MITT	modified inclined tube test
MnDOT	Minnesota Department of Transportation
NBI	National Bridge Inventory
NDE	nondestructive evaluation
NDT	nondestructive testing
OCP	open circuit potential
PCA	Portland Cement Association
PE	polyethylene
PG	pressure grouting
PT	post-tensioned
PTI	Post-Tensioning Institute
PVG	pressure-vacuum grouting
R&D	research and development

RH	relative humidity
SCC	stress corrosion cracking
SEM	scanning electron microscopy
SETRA	Service d'Etudes Techniques des Routes et Autoroutes (French Technical Department for Transport, Roads, and Bridges)
SSRT	slow strain rate testing
TxDOT	Texas Department of Transportation
VDOT	Virginia Department of Transportation
VG	vacuum grouting
VPI	vapor phase inhibitor
VTRC	Virginia Transportation Research Council
XRD	X-ray diffraction

MEASUREMENTS, CHEMICAL COMPOUNDS, AND VARIABLES

C	capacitance
Cs	specific capacitance
D	loss factor
E	potential
E_{corr}	corrosion potential
$(E_{corr})_{\text{macro-anode}}$	corrosion potential at macro-anode
$(E_{corr})_{\text{macro-cathode}}$	corrosion potential at macro-cathode
E-log i	potential log current density
E_{pit}	pitting potential
E_{prot}	protection potential
i	current density
I_{corr}	corrosion current
$(i_{corr})_{\text{macro-anode}}$	corrosion current density at macro-anode
$(i_{corr})_{\text{macro-cathode}}$	corrosion current density at macro-cathode
$i_{critical}$	critical current density
$i_{passive}$	passive current density
ksi	kips per square inch
mil	0.001 of an inch
mpy	mil per yr
mA	milliampere
mV	millivolt
mV_{CSE}	mV versus copper-copper sulfate reference electrode
mV_{SCE}	mV versus saturated calomel reference electrode
L	inductance
ppm	parts per million
psi	pound per square inch
R	resistance
ρ	specific resistance
Ag/AgCl	silver/silver chloride
Ca	calcium
Ca^{2+}	calcium ion
$Ca_6Al_2(SO_4)_3(OH)_{12}\cdot 26H_2O$	ettringite
$CaCO_3$	calcite
$Ca(OH)_2$	calcium hydroxide
Cl^-	chloride ion
CO_2	carbon dioxide
e^-	electron
Fe	iron
Fe^+	ferrous ion
$FeCl_2$	ferrous chloride
$Fe(OH)_2$	ferrous hydroxide
$Fe(OH)_3$	ferric hydroxide
FeOOH	goethite
Fe_3O_4	magnetite

$FeSO_4$	ferrous sulfate
H^+	hydrogen ion
HCl	hydrochloric acid
H_2O	water molecule
H_2SO_4	sulfuric acid
K^+	potassium ions
K_2O	potassium oxide
KOH	potassium hydroxide
Mo	molybdenum
Na^+	sodium ion
NaCl	sodium chloride
Na_2O	sodium oxide
NO_3^-	nitrate ion
NaOH	sodium hydroxide
O	oxygen
O_2	oxygen molecule
OH^-	hydroxyl ion
P	phosphorus
SO_3	total sulfur (sulfur trioxide)
SO_4^{2-}	sulfate ion
Zn	zinc
$ZnPO_4$	zinc phosphate

CHAPTER 1. INTRODUCTION

Prestressed concrete structures use prestressing force, which compresses concrete members by a pretensioning or post-tensioning method. The externally applied compressive force compensates for the weakness of concrete in tension. To make pretensioned concrete members, multiple 7-wire strands are tensioned in a prestressing bed, based on a predetermined design load, before concrete is poured. In this way, the pretensioned strands are in direct contact with the concrete. After the concrete hardens and reaches a target compressive strength, the strands are cut free from the bed, and a compressive force is introduced in the concrete at locations that would otherwise be in tension. For post-tensioned (PT) concrete members, two types of tendons are used—bonded or unbonded, depending on the timing of installing the duct, tensioning the strands, and filling the duct with grout.

For bonded tendons, the ducts need to be installed in the form before the concrete is cast. First, the concrete is poured until it gains a targeted compressive strength to withstand the prestressing force. Next, a bundle of the prestressing steel, which can be composed of wires, 7-wire strands, or bars, is inserted into the duct and stressed against an anchor point to a predetermined level of stress. Once the steel is stressed and properly anchored, the annular space between the interior of the duct and the prestressed steel is filled with cementitious grout. A strong bond between the prestressing steel and the duct transfers the prestressing force to the surrounding concrete through the grout. Typically, internal tendons embedded within the concrete structure and filled with grout are bonded.

A tendon that is not embedded in concrete and cannot transfer prestressing force to concrete is called an unbonded tendon. For unbonded tendons, the ducts and prestressing steel are installed after the concrete is hardened. The steel is then stressed against the anchorages and, subsequently, the ducts are filled with cementitious grout (or flexible fillers in some recent cases). Since such tendons are not embedded in the concrete, they are not considered part of the structural components. External tendons are classified as unbonded, regardless of their filler materials (grout, wax, or grease).

Injected filler materials can provide additional benefits for corrosion protection as physical barriers to water and air, i.e., oxygen (O_2) and carbon dioxide (CO_2). Cementitious grout can also be beneficial, providing a high-pH environment to form a protective, passive film (an invisible oxide film) on the steel surface. However, if the passive film is compromised by aggressive anions such as chloride ions (Cl^-) and sulfate ions (SO_4^{2-}), and carbonation of the surrounding grout occurs (i.e., the pH falls below 9), prestressed steel can begin to corrode.[1]

The observed PT tendon corrosion problems were all linked to water or moist environments and grout voids, although other issues also sometimes factored in. Water can enter from external sources or can form internally through the grout bleeding phenomenon. Grout voids can be formed due to poor-quality grouting operations and from bleed water that is eventually evaporated or reabsorbed into the hardened grout. Once corrosion initiates, it propagates at a rate controlled by many factors, including oxygen availability; moisture content; the grout's electrical resistance; the degree of carbonation; ion concentrations; and grout segregation leading to bleeding, variable water-cement ratios, and other issues.

In reinforced concrete structures, corrosion causes a reduced cross-sectional area in ordinary reinforcing steel. However, this reduction is generally not a primary concern because it is preceded by concrete cracking and spalling. These visual indications of deterioration serve as warning signs, and appropriate action can be taken before it is too late. Conversely, section loss of prestressing steel in prestressed concrete structures can be a serious problem for two reasons, as follows:

First, prestressing steel is susceptible to localized corrosion, i.e., pitting corrosion and crevice corrosion, in addition to uniform corrosion. Noncorroding steel is subjected to the constant stress of about 55 to 65 percent of its ultimate tensile strength; corroding steel's section loss increases the tensile stress locally at the corroding area. Once growing corrosion damage reduces the cross-sectional area to a critical level, the tensile stress exceeds the tolerable limit. Consequently, the corrosion-damaged area yields and then fails by ductile fracture.

Second, the strength of prestressing steel is usually four to five times greater than that of ordinary reinforcing steel. Therefore, the former has a smaller cross-sectional area than the latter for an identical loading condition. If both types of steel experience the same corrosion rate (CR), the prestressing steel will likely lose its cross-sectional area faster than the ordinary reinforcing steel.[(2)] Even though PT bridges are designed to have sufficient structural redundancy globally, the corrosion of prestressing steel can impose an inherent risk of sudden, localized failure of affected bridge components with little warning.

Also, the prestressing steel's high strength characteristics can make the steel vulnerable to environmentally induced cracking (EIC), such as hydrogen embrittlement (HE) and stress corrosion cracking (SCC), which result in brittle fracture. Even though HE- and SCC-related problems have rarely been reported, the possibility of their occurrence exists under certain exposure conditions.

Constructing a durable PT bridge and maintaining it throughout its service life can be achieved—if every step is done correctly during construction and maintenance. The satisfactory performance of PT bridges depends on the quality of individual bridge components; the workmanship of the construction; and the attention paid to detail during design, construction, and maintenance. A collective protection system provided by concrete cover, ducts, and grout is the primary defense against any service environment. If stringent requirements to ensure satisfactory performance are not met in any of these areas, corrosion problems can occur in the localized areas containing deficiencies and compromise the entire bridge's durability. At a macroscopic level, poor design, construction choices, and workmanship appear to be the underlying problem when PT bridges fail—not inherent problems with PT construction technology.[(3)]

A compounding factor is that the prestressing steel is always buried in a grout/duct system (for grouted external tendons) or in a grout/duct/concrete system (for grouted internal tendons) such that ongoing corrosion damage cannot be easily detected before it is too late. To make the matter worse, there are no reliable and economic nondestructive evaluation (NDE) and nondestructive testing (NDT) technologies readily available to assess tendon condition during routine PT bridge inspections. The most challenging PT bridge components to inspect are anchorage zones, diaphragms, and deviation blocks, where a heavily reinforcing steel network is enclosed in massive concrete. These field conditions obstruct the effective use of many nondestructive

technologies. As early as 1998, Poston and Wouters recommended developing better NDT techniques and field trials to ensure the satisfactory performance of grouted PT bridges in a National Cooperative Highway Research Program (NCHRP) report.[3] Yet even now, it is common to employ the semi-invasive method of drilling small holes for borescope inspection, on special occasions and only at selected locations, due to the destructiveness of the process and its high costs.

European countries started experiencing PT tendon problems earlier than the United States. In the United Kingdom, the Bickton Meadows Footbridge, a precast segmental bridge, collapsed in 1967 due to the corrosion of prestressing steel. The entire prestressing steel in Braidley Road Bridge, which was constructed in 1968, was replaced in the late 1970s. In 1985, a single-span segmental bridge, the Ynys-y-Gwas Bridge, also suddenly collapsed due to the corrosion of internal tendons.[3-8]

After the collapse of the Ynys-y-Gwas Bridge, nine segmental bridges were subsequently inspected. Grout voids were found in seven of these, and severely corroded tendons were found at two locations in one of the bridges. Despite widespread grout deficiencies, it was concluded that the inspected tendons were generally in good condition. The Taf Fawr Bridge, constructed in 1964, experienced significant corrosion that led to its rebuilding in 1995. Hammersmith Flyover suffered from the severe corrosion of internal and external tendons and went through extensive repair and rehabilitation work from 2011 to 2015.[3-8]

These corrosion problems seemed largely due to poor design choices and low-quality construction rather than the PT systems' intrinsic susceptibility to corrosion. The U.K. Department of Transport banned external tendons in bridges in 1977 and the construction of new grouted internal PT bridges in 1992 until design and construction standards could be reviewed. In 1996, the United Kingdom moratorium on cast-in-place grouted PT bridge construction was removed. The moratorium on precast, segmental grouted PT bridge construction remains in place because of concerns with the corrosion protection of internal tendons at the joints between the precast segments.[3-8]

A survey done in 1998 of 107 Swiss bridges found that 13 percent had grouting deficiencies. A French study done of 163 bridges in 1999 found that 12 percent were not grouted. In Belgium, the Melle Bridge collapsed in 1992 due to hidden corrosion damage on the prestressing steel.[3-8] (More corrosion-related problems observed in Europe will be presented in chapters 3 and 4.)

In the United States, the Walnut Lane Bridge, located in Philadelphia, PA, was the first precast PT bridge. It was constructed between 1949 and 1950 and opened to traffic in late 1950. It had three spans, and each span consisted of 13 79-inch-tall PT I-girders. In each girder, 256 0.276-inch-diameter, high strength, stress-relieved wires were placed in four rectangular ducts, 64 wires in each duct. To protect the prestressed wires from corrosion, a conventional grout was injected into the ducts.

After the bridge's opening, prestressing applications in bridges and building construction spread rapidly because of their many benefits, including increased load-bearing capacity, improved crack control, and the slenderness of structural elements. In particular, closing concrete cracks and preventing future crack development under tension imposed by service loading can improve

the durability of the concrete members by minimizing entry of harmful external elements such as water, oxygen, and deicing salts. However, the Walnut Lane Bridge was replaced in 1990 after nearly 40 yr of service due to improper tendon grouting and other deficiencies.[2,3,9,10]

From the mid-1960s through the early 2000s, while PT bridges in Europe experienced tendon corrosion problems, the durability of PT bridges in the United States continued to be rated as excellent, despite the severe deterioration of Walnut Lane Bridge. According to National Bridge Inventory (NBI) data surveys by the American Segmental Bridge Institute (ASBI) published in 2007, the durability of segmental concrete bridges in the United States was considered better than that of non-U.S. bridges built with other materials. This superior durability was attributed to the relatively small number of tendon problems reported in the United States and their significantly smaller repair costs. These costs were only a fraction of the costs that were routinely accepted to repair or replace bridges constructed of other materials. For example, 2006 NBI inspection data showed an average superstructure condition rating on the NBI scale of 7.1 for all 273 segmental concrete bridges in the United States, indicating good condition with no structural deficiencies. NBI inspection data for 2011 still showed an average superstructure condition rating of 6.9 for all 363 concrete segmental and concrete cable-stayed bridges (approximately 460 segmental bridges), with only seven bridges noted as structurally deficient.[10-13]

The first notable tendon deficiency reported in the United States was at the Interstate 75/Interstate 595 Sawgrass Interchange in Florida in 1996. The Florida Department of Transportation (FDOT) discovered efflorescence at some of the anchor blocks, water leakage at some joints, and grout void problems in six bridges. Three yr later, a failed external tendon was found in the Niles Channel Bridge in Florida. This tendon failure was the first corrosion-induced incident in the United States. This tendon failure was the first corrosion-induced incident in the United States.

Following the unexpected tendon problem in Niles Channel Bridge, statewide inspections were conducted in 2000. They found that the Mid-Bay Bridge in Okaloosa County had two failed tendons and nearly two dozen tendons with corrosion problems. Additionally, the Sunshine Skyway Bridge in St. Petersburg had many corrosion problems, including one failed tendon, and the Seabreeze Bridge on State Road 430 in Daytona also had tendon corrosion problems. These bridges were constructed before 2001 and used neat cement grout.

In the following yr, FDOT revised grouting specifications and allowed only approved prepackaged, non-bleed/thixotropic grout materials. Later, FDOT started implementing five strategies related to enhanced PT systems: fully grouted tendons, multilayered anchor protection, watertight bridges, enhanced PT systems, and multiple tendon paths to raise performance in design, construction, and maintenance.[12,14-18] After tendon corrosion problems and other deficiencies—such as cracked polyethylene (PE) ducts and grout voids— were observed in Florida, the durability of PT bridges in the United States became a concern to bridge owners and maintenance engineers. The problems experienced by FDOT were the first wave of PT corrosion problems in the United States.[19]

In a national response to PT tendon corrosion problems, the Post-Tensioning Institute (PTI) introduced a new specification in 2012 and updated it in 2019. This document, titled

Specifications for Grouting of Post-Tensioned Structures (PTI M55.1-19), intended to minimize bleed water and improve grouting practices. ASBI also formed a grouting committee in 2000, which issued the document *Interim Statement on Grouting Practices* in December 2000 and initiated the Grouting Certification Training Program, with the first training session held in August 2001. A joint document of PTI and ASBI, *Specification for Multistrand and Grouted Post-Tensioning* (PTI/ASBI M50.3-19), was published in 2019. With these changes, improved practices for grout material selection and construction practices were implemented successfully. In Europe, the International Federation for Structural Concrete (*fib*) issued *Fib Bulletin No. 33: Durability of Post-Tensioning Tendons*, a compilation of reports on the topic. Additionally, an International Organization for Standardization (ISO) specification and three European standards (ENs) were also published.[20-26]

A second wave of PT tendon issues began in Florida in 2011 when FDOT discovered a new type of corrosion problem in the tendons that contained a newly introduced, prepackaged, non-bleed/thixotropic grout material. The affected bridges included the John Ringling Causeway Bridge in Sarasota, commonly known as the Ringling Bridge; the Charles E. Bennett Memorial Bridge, commonly referred to as the Wonderwood Bridge, in Jacksonville; the Interstate 4/Selmon Expressway Connector, also known as the Crosstown Connector, in Tampa; and the Interstate 95/Interstate 295 interchange in Jacksonville.[14,15,18,19,27] In the case of the Ringling Bridge, two external tendons failed prematurely due to corrosion after less than eight yr of service, and 15 more external tendons suffered from excessive section loss. The observed corrosion problems were mainly associated with grout segregation, resulting in high moisture content, high pH, pasty and chalky texture, and locally elevated sulfate ions.

Between 2007 and 2019, six other states—Virginia, Texas, Minnesota, Kansas, Indiana, and South Carolina—also experienced tendon corrosion problems in eight major PT bridges. Then, in June 2020, the latest corrosion problem was discovered in the internal tendons on the southbound Roosevelt Bridge in Stuart, FL. The discovery of serious tendon problems often led to temporary closures of the bridges during emergency repairs and tendon replacements. The majority of the tendon corrosion problems observed in the United States have been attributed to aggressive environments, a low volume of PT construction, contractors with a lack of experience or expertise in PT construction, inadequate construction supervision, lack of design details, and failures to correct construction problems.[12]

Many advancements related to PT bridges have been made over nearly two decades in the areas of materials, specifications, construction methods, and inspection techniques. Prepackaged non-bleed/thixotropic grout products, flexible fillers, and corrosion-resistant strands are good examples of improved materials. Tightened grout specifications and improved grout injecting procedures can minimize grout deficiencies. The increasing use of advanced inspection tools—such as high-power borescopes, ground penetrating radars (GPRs), impact echoes (IEs), and magnetic-based NDE systems—is also an encouraging trend. However, it is still difficult to inspect prestressing steel nondestructively in many critical locations that are known to develop corrosion problems. In addition, damaged steel cannot be replaced in most cases. These issues are challenges for bridge owners and maintenance engineers.

As PT bridges age, especially those constructed with neat cement grout before 2001, more durability problems will surface, and PT tendon corrosion will likely continue to be a primary

cause. This final report presents the important research findings of a 3-yr synthesis study related to four topics concerning corrosion-induced durability issues in grouted PT tendons and maintenance strategies to address these issues. The topics covered are major cases of corrosion in the field, key findings of national and international laboratory studies, the current understanding of corrosion mechanisms, and maintenance strategies aimed at controlling PT tendon corrosion.

CHAPTER 2. OBJECTIVES AND SCOPE OF WORK

This report presents important findings of a three-yr synthesis study involving a historical overview spanning over three decades of grouted PT system durability problems associated with tendon corrosion and corrosion control methods.

The scope of work for this synthesis study was divided into four topics, as follows:

- Reported major field corrosion cases.
- National and international laboratory studies.
- Corrosion mechanisms.
- Corrosion control methods.

Reported field corrosion cases are reviewed in chapter 3, based on corrosion investigation reports and presentation materials prepared by bridge owners and their consultants, technical articles, and news media. Starting from a tendon failure on the Niles Channel Bridge in 1999, notable tendon corrosion cases in the United States are discussed chronologically. Miscellaneous corrosion problems experienced in four states are also presented. Additionally, corrosion problems encountered in foreign countries are summarized at the end of the chapter.

Laboratory studies carried out by domestic and international government agencies, consultants, and universities from 1992 to 2019 are reviewed in chapter 4. Covered topics include grout development; bleeding phenomena; the characterization of deficient grout; alternative fillers; corrosion mechanisms; and the corrosion resistance of grout, ducts, and strands.

Corrosion mechanisms responsible for PT tendon corrosion are discussed in chapter 5 based on fundamental electrochemistry and findings from field investigations and laboratory studies. Corrosion characteristics in normally hardened grout and segregated grout are presented separately. Finally, a hypothetical case of a sequential corrosion process in segregated grout is presented.

Lastly, various corrosion control methods currently available or tried in the field are examined in chapter 6. These included electrically isolated tendons (EITs), cathodic protection, regrouting, corrosion-resistant strands, flexible filler, the impregnation method, air drying with inert gas, and other considerations. Protection of anchorage zones and temporary corrosion protection are also briefly reviewed.

CHAPTER 3. MAJOR CORROSION PROBLEMS ENCOUNTERED IN THE FIELD

This chapter compiles corrosion problems observed in eight major PT bridges in the United States chronologically. Reviewing these cases highlights the serious nature of corrosion-induced durability problems experienced by the PT bridges and identifies potentially problematic conditions. The last section presents additional corrosion problems observed in other PT bridges in the United States and other countries.

1. NILES CHANNEL BRIDGE: FLORIDA[12,17]

The Niles Channel Bridge is a 4,557-ft-long precast box girder bridge with a deck width of 38.5 ft that connects Summerland Key and Ramrod Key. It was built in 1983 using a low-level, span-by-span method (the 4th bridge constructed with this method in Florida). The bridge has six grouted external PT tendons in each span, and each tendon contains 19 0.6-inch 7-wire strands filled with neat cement grout.

In 1999, bridge inspectors discovered that one of 234 external tendons on the Niles Channel Bridge had failed after 16 yr in service due to intensive corrosion in a grout void formed by bleed water. The void was located behind an anchor head at an expansion joint diaphragm. Recharging water contaminated with airborne chloride in the void was responsible for the corrosion. Inspectors speculated that the water leaked through the expansion joints and ran down the inner faces of the segment diaphragms onto the anchorage in question. Figure 1-A shows some of the damaged strands still attached to the anchor head, and figure 1-B shows the corroded interior condition of the anchorage trumpet associated with the failed tendon.

This incident was regarded as the first PT tendon failure by corrosion in the United States and triggered statewide investigations of PT bridges in Florida.

A. Failed strands. [17]

Source: FHWA.

B. Interior of anchorage trumpet.

Figure 1. Photos. Failed tendon in the Niles Channel Bridge.

2. MID-BAY BRIDGE: FLORIDA[17,28-32]

The Mid-Bay Bridge is a 19,265-ft-long, precast segmental concrete box girder bridge spanning the Choctawhatchee Bay between Destin and Niceville, FL. Like the Niles Channel Bridge, it was built using a span-by-span construction method and used a neat cement grout. It opened to traffic in 1993. Each of its spans has six tendons, and each tendon has 19 0.6-inch, 7-wire strands in four-inch PE ducts.

In August 2000, during a routine inspection, a failed tendon was pulled from an expansion joint diaphragm due to severe corrosion in the anchorage zone, as shown in figure 2. This incident was regarded as the second PT tendon failure by corrosion in the United States.

Figure 2. Photo. Failed tendon in the Mid-Bay Bridge.[17]

The strong bond between the grouted steel pipe and the failed tendon section pulled the steel pipe from the expansion joint diaphragm during the tendon rupture. The failure pattern resembled the failed tendon observed in the Niles Channel Bridge.

A second deteriorated tendon, which was not ruptured but severely damaged, was discovered in another span. The PE duct was cracked, and 11 strands were fractured in the free length of the tendon. It was apparent that the penetration of moisture and air through the cracked ducts caused corrosion to start. The tendon's condition is shown in figure 3.

Figure 3. Photo. Severely damaged tendon.[17]

These corrosion problems prompted FDOT to launch emergency inspections: visual crack inspections; vibration testing; the sounding of all ducts; and borescope inspections of all 1,728 anchorages. Each PT tendon was also subjected to magnetic flux leakage (MFL) testing to locate significant section losses nondestructively. The MFL testing was able to locate potential corrosion problems and wire fractures in two tendons. At the end of the inspections, 11 severely corroded tendons out of 846 tendons were replaced, and anchor voids were regrouted using the vacuum grouting (VG) method. The measured chloride concentrations in the grout samples were below the threshold for corrosion.

Hartt and Venugopalan carried out a field investigation on the Mid-Bay Bridge's failed tendon and other tendons. Although the duct cracking problem was the primary focus of their investigation, some of their findings were related to segregated grout, which contributed to severe corrosion of the PT tendons. A parallel petrographic analysis was also conducted using grout samples collected at the site. Following are the findings of their research.[29]

- Many external tendon anchorages located at high points were partially empty, and some of the exposed strands throughout the cracked ducts were broken. The grout was made with Type I cement and an expansive admixture (0.53 percent by weight of cement). The estimated upper limit of the water-cement ratio was 0.45.

- Uneven cover around the strands was noted.

- Rust stains were observed on strands with no grout cover.

- The spatial location of the exposed strands was primarily between 4 and 8 o'clock.

- Nonuniformly distributed microscopic (4 mil or smaller) and macroscopic voids were observed in many areas. It appeared that the expansive admixture generated the microscopic voids.

- Glassy aluminum powder particles, a component of the expansive admixture, were observed on the grout's surface.

- Periodic circumferential hairline shrinkage cracks were present in the grout along the entire tendon length.

- The grout was dry, and no moisture traces were found wherever the duct was removed.

- A white powdery deposit, a sign of grout segregation, was observed along a void channel on a tendon. It was believed that the channel was formed by air and bleed water during the grout segregation process. Figure 4 shows a photograph of this condition.

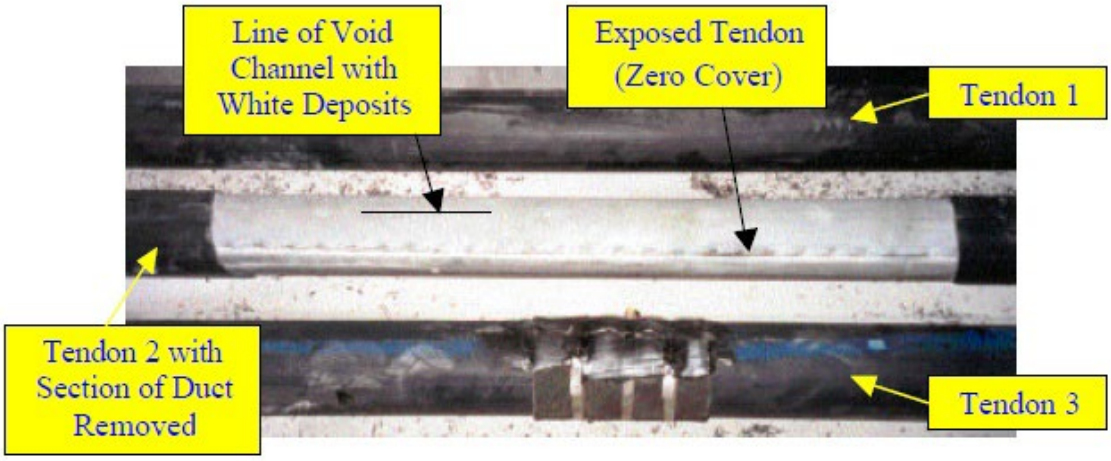

Figure 4. Photo. Void channel and exposed strand.[29]

The quantity of white powdery deposit was directly proportional to the cross-sectional area of the void channel. These channels and a white powdery deposit were mostly observed in the top half of the tendon—but in some cases, they also extended along the underside of individual strands or several closely grouped strands. White chalky grout was also found in an eight-ft-long section of a tendon. However, the grout in the lower half of the tendon was typically dark gray, well consolidated, and showed no signs of segregation.

The investigators concluded that grout segregation occurred along the tendon in the presence of excess bleed water. Eventually, evaporation or reabsorption of bleed water into the grout resulted in a void at the exit anchorage area. It appears that this investigation reported the first domestic case of grout segregation-related problems, which were limited to isolated areas with no significant physical deficiencies.

The grout in two tendons revealed high pH values except within a thin top layer (16 mil). The white powdery deposit at the top of a tendon had a pH in the range of 8 ± 1 before cleaning with

a wire brush. The lowest pH was 6. After cleaning, the pH increased to 12 ± 1. At the bottom, the 0.25-inch-thick grout was carbonated with pH 8 ± 1. The broken wires were found in this layer. The deeper grout, which exhibited a dark gray color, had pH 12 ± 1 again. Figure 5 shows a photograph of the grout after pH measurements were completed.

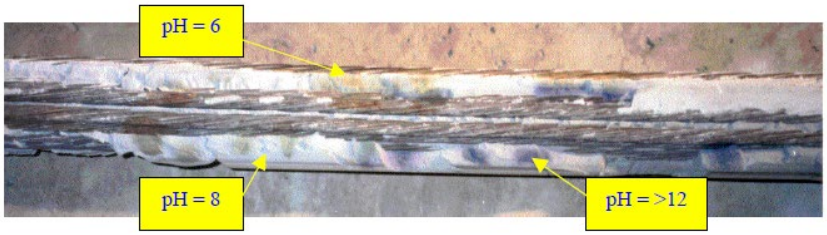

Figure 5. Photo. Variation of the grout pH.[29]

The investigators noted that the bleed water could be corrosive when it was carbonated and when an expansive admixture reduced its pH. Moreover, the carbonated grout (i.e., pH 8 ± 1) severely corroded four wires in the presence of oxygen and moisture. They speculated strand corrosion within grout voids and carbonated grout would reinitiate during periods of high humidity. They hypothesized strand corrosion would also reinitiate in condensed water that had been previously absorbed into the grout during occasional temperature drops below the dew point. The measured chloride concentrations were too low (90 and 120 parts per million [ppm] by weight of cement) to play a role in the corrosion process.

Corrosion potential data collected on two tendons indicated no active corrosion. This corrosion-free condition was attributed to the dried grout and low relative humidity (RH). However, a visual inspection of several exposed anchorages revealed wet and acidic liquid corrosion products, indicating ongoing active corrosion. Dried corrosion products of the same type were also observed as spherical rust particles along the base of the bottom strands. The investigation concluded the following:

Grout segregation occurred along the tendon in the presence of excessive bleed water. The bleed channels and a white powdery deposit were mostly observed in the top half of the tendon. Evaporation or reabsorption of bleed water into the grout resulted in a void at the anchorage zone. Moisture and air penetrated the cracked ducts, resulting in depassivation and corrosion of the strands.

Eventually, grout carbonation, segregated grout, and excessive bleed water were collectively responsible for rapid tendon corrosion in the presence of oxygen, carbon dioxide, and moisture, irrespective of chloride concentration.

An indepth petrographic analysis of grout samples acquired from four locations offered valuable information about the characteristics of segregated grout at the macroscopic and microscopic levels: unit weight, degree of cement hydration, water-cement ratio, grout pH, the extent of carbonation, void density, void distribution, void interconnectivity, and the difference between white and gray grout. The following summarizes the analysis results.

There was evidence that the grout mix remained fluid for an abnormally long time. When the grout was still fluid, many phenomena took place, including segregation/sedimentation of solid matters, stratified layers, significant variations in water-cement ratio, nonuniform void distribution, and migration and coalescence of the air voids. Also, hydration reactions occurred at different rates in different portions of the grout. Each affected the grout quality negatively.

Color differences in the grout samples were caused by variations in water-cement ratios and degrees of hydration. Stratification of cement paste was observed due to grout bleeding. Bleeding may have been promoted by high water-cement ratio, prolonged initial set, a long pumping range caused by single end injection, or a combination of two or more of these factors. In some areas, sedimentation of solid particles and movement of air bubbles had occurred during the grout's flowable state.

The highest water-cement ratio of 1 or greater was estimated within a 0.12-inch layer at the outer grout surface. This layer was highly porous, very soft, and weak. The second highest water-cement ratio of 0.6–0.7 was estimated within 0.12 to 0.39 inches from the duct surface. The hardened grout's water-cement ratio away from the duct surface was in the normal range of 0.42–0.50. Figure 6 illustrates the distribution of the estimated water-cement ratios in the segregated and normal grout areas.

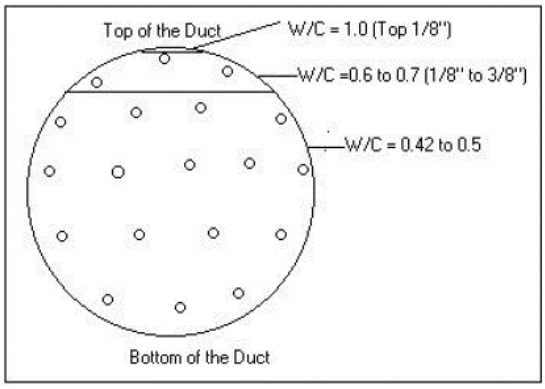

Figure 6. Illustration. Schematic representation of estimated water-cement ratios in segregated and normal grout areas.[29]

The hydration of portland cement progressed as a function of the water-cement ratio of the cement paste. It was determined that when the water-cement ratio exceeded 0.6, there were relatively few unhydrated portland cement clinker particles in the interior of the samples in a matrix of calcium silicate hydrate and calcium hydroxide. There was a correlation between the cement paste color and the amount of unhydrated portland cement particles: an increase in the unhydrated cement particles resulted in a darker paste. Overall, the degree of hydration in the samples was estimated to be more than 90 percent.

In the cement paste with a high water-cement ratio and a porous layer, the pH was between 9 and 10. The grout was not carbonated at depths below 0.24 inches from the duct surface, where the pH values were between 12 and 13. The surfaces of the air voids also showed light carbonation

(pH between 9 and 10), suggesting that these voids might have been exposed to air containing CO_2. Figure 7 schematically illustrates the distribution of grout pH in the tendon's cross-section.

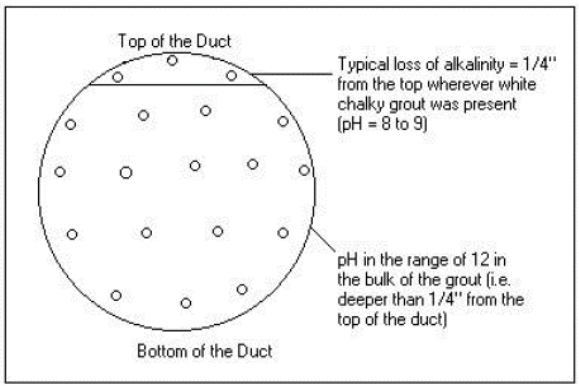

Figure 7. Illustration. Schematic of grout pH distribution.[29]

According to energy dispersive X-ray spectroscopy (EDS) analysis results, there were higher concentrations of oxide phases based on aluminum, iron, potassium, and sulfur in the white paste. There was also widespread evidence of the accumulation of secondary deposits (calcium hydroxide platelets) and fibrous ettringite crystals (a calcium sulfoaluminate hydrate) on grout void surfaces and within the larger pores of the higher water-cement ratio cement paste.

The average air void content in the grout was about 10 percent. There were small regions without voids. In other areas, voids were interconnected and clustered to form a frothy condition with an estimated 20 to 40 percent total void content. These clustered regions could lead to a physical discontinuity in the grout between adjacent air voids. The void tears might be related to different rates of stiffening and hardening in the stratified grout layers, as influenced by the local water-cement ratio. In regions where the grout remained open, air voids had migrated to a point where hardening had already begun and collected there. The permeable void volume ranged from 41.3 to 45.4 percent.

In 2018, reoccurring corrosion problems were discovered on seven tendons in the Mid-Bay Bridge during a biennial bridge inspection. A follow-up investigation in 2019 revealed that two corroded tendons were close to each other in the same span, which forced FDOT to close the bridge for eight d for emergency repair work. A total of eight tendons were replaced at the end. It was unclear whether the previous investigations in 2000 failed to detect ongoing corrosion problems or if new corrosion started somewhere else later. Going forward, FDOT planned to conduct condition assessments of all tendons with a hammer-sounding method every six months.

3. SUNSHINE SKYWAY BRIDGE: FLORIDA[14,17,19,28,33,34,35]

The Sunshine Skyway Bridge is a 29,040-ft-long, precast segmental box girder bridge across Tampa Bay in Florida. The bridge was constructed with the span-by-span method and opened to traffic in 1987. The high-level approaches are supported by nearly elliptical hollow precast segment columns with a mix of internal and external tendons. The vertical tendons holding the column segments together are bonded internally within the thicker wall region and run externally

along the upper part's inner walls. The tendons are composed of 12, 17, and 18 0.5-inch-diameter strands housed in a three-inch primary duct. This bridge uses a neat cement grout. The upper ends of these tendons are anchored in the cap and form a u-loop configuration in the footing. In the thick wall region, the three-inch-diameter primary duct is inside a five-inch-diameter corrugated PE secondary duct cast inside a precast segment wall. Figure 8 illustrates how the precast segmental column was constructed.

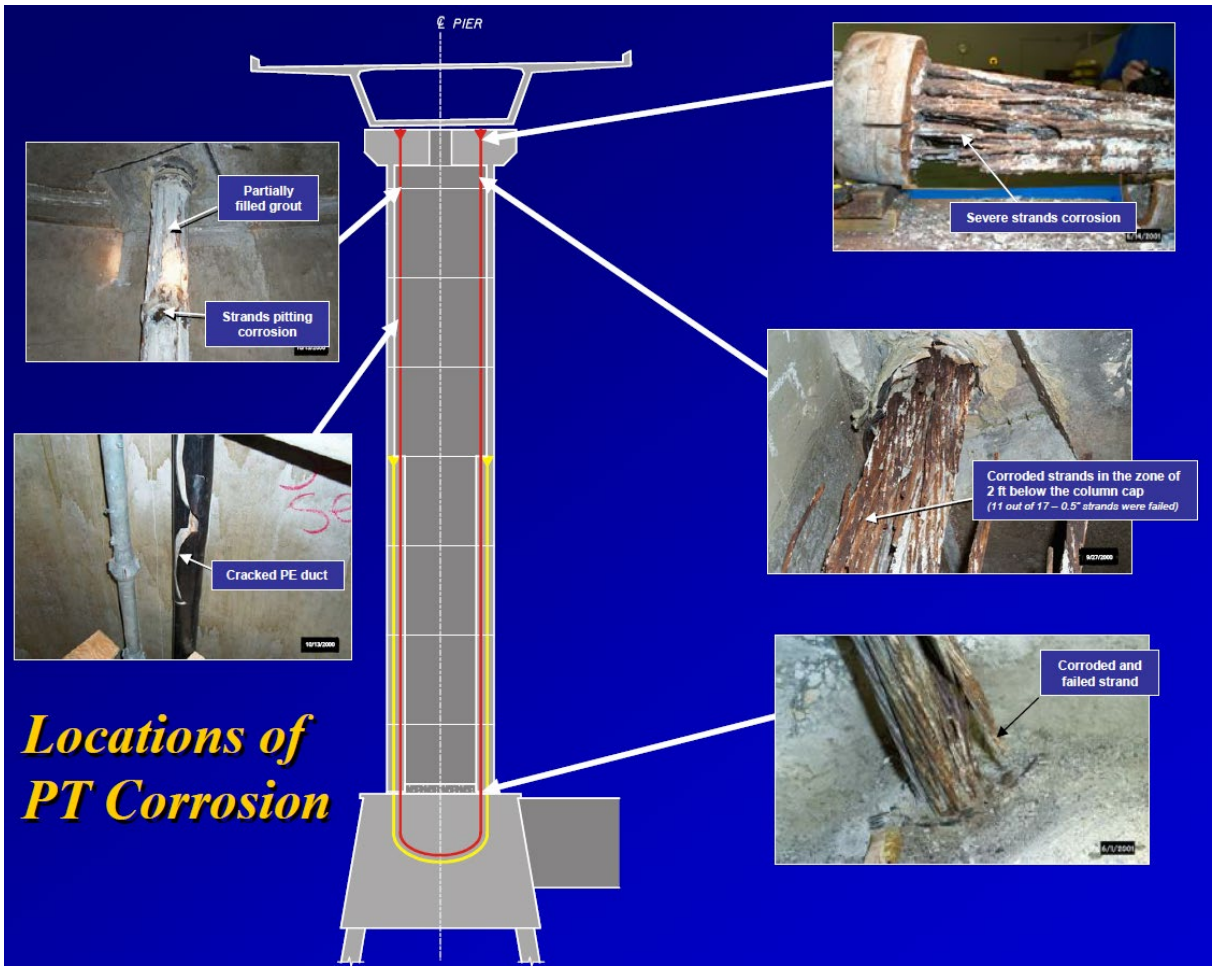

Figure 8. Schematic and photos. Column structure and locations of tendon corrosion.[14]

During a special inspection of the bridge in September 2000, severe corrosion was discovered in a tendon housed in a northbound column: 11 out of 17 0.5-inch strands were fractured at 2 ft below a column cap. As a result, further inspections were performed on all the other high-level approach columns (including comprehensive destructive testing on about 10 percent of the columns), the superstructure, and the cable anchorage of the main span. Figure 8 also shows the locations and actual conditions of the discovered tendon corrosion.

In the column cap region, issues were identified in the anchor pour-back areas on the top of the cap. These problematic areas included deteriorated surface areas and surface irregularities, cracked pour-back, and surrounding concrete materials. Rainwater and condensation bearing

airborne chloride could reach the strands in the void formed in the anchor trumpet and cracked ducts. Grout voids and soft chalky grout were also found in the trumpet due to bleed water.

In addition, severe strand corrosion accompanied by partial or complete failures was discovered within the cap region at various locations. Three out of four tendons cored in the inspected column's cap showed severe corrosion (right middle and top left photos in figure 8) and failure in the trumpet areas (top right photo in figure 8).

In the external region, more deficiencies were found, as follows:

- Severe duct splitting was found on 37 tendon legs in 21 columns (bottom left photo in figure 8). Portions of the ducts on 148 tendon legs in 57 columns were unsound and exhibited a hollow sound (indicating a grout void area) when tapped with a hammer. The neoprene boot duct coupler in the external tendon region contained grout voids with severe pitting and strand corrosion.

- No strand corrosion was observed at locations where the ducts were uncracked, regardless of voids, which appeared to be sealed from water and oxygen. Strand failure in the free length was identified only in the southeast tendon in a northbound column. Vibration tests showed that none of the external tendons had lost tension force in their free length except for the one shown in figure 8 and at a few locations where the test results were inconclusive, with no other critical deficiencies observed.

In the thick wall region, three deficiencies were found, as follows:

- The primary ducts at the base of the columns were not centered within the secondary corrugated duct, leading to no grout protection.

- Twenty percent of the three-inch primary ducts had sustained damage such as dents and cracks.

- Severe corrosion, including strand failure, was found only within a recessed area at the base of two columns (bottom right photo in figure 8). This area was exposed in a wet-dry zone, and the primary grout had very high levels of chloride and sulfate ions at the bottoms of 28 columns.

In the superstructures, no tendon failed in the box girders, but many tendon deficiencies were found, as follows:

1. Cracked PE ducts.

2. Cracked pour-back material.

3. Grout voids, indicated by hollow sounding.

4. Evidence of grout leaks from duct couplers.

5. Water leaks from deck joints and water ponding in local areas.

6. Pitting corrosion.

One of the inspected external tendons contained soft/wet grout, which proved that the segregated grout could occur in old neat cement grout. The tendon in question is shown in figure 9.

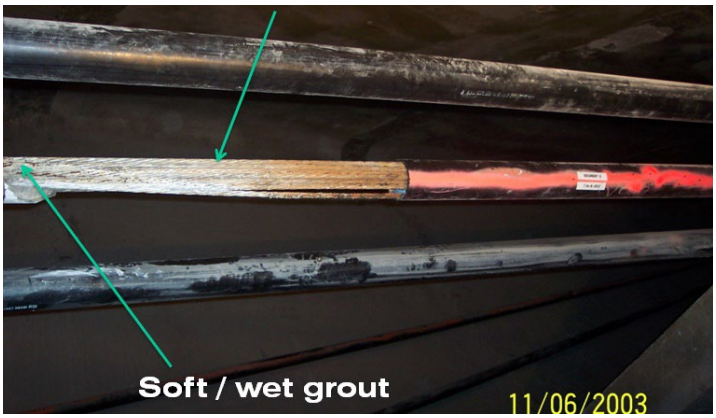

Figure 9. Photo. Sunshine Skyway Bridge tendon containing soft/wet grout.[35]

From the aforementioned findings, several important lessons were learned to improve the durability of similar structures, as follows:

1. Epoxy joints can leak, and hollow PT precast column segments with epoxy joints are not recommended, especially in wet-dry zones (15 ft above or below the mean high-water elevation).

2. Pour-back located in areas with aggressive contaminant intrusion opportunities should be avoided where possible. If necessary, special PT protection and anchorage details should be developed. Epoxy-based materials are recommended as pour-back instead of cementitious materials.

3. The grouting operation for a tall vertical tendon should be planned carefully and monitored. Only prepackaged thixotropic grout should be used. After grouting is completed, the anchorage areas should be inspected after 48 h to ensure that the grout adequately fills the trumpets.

4. An electro-fusion coupler or a similar type of coupler must be used for connecting the PE ducts, not a neoprene duct coupler with a stainless-steel strap. The latter cannot provide a waterproof connection.

Following the inspection, many deficiencies in the 76 high-level approach columns were repaired. The deteriorated north column was rehabilitated by adding mild reinforcing dowel bars into the support footings and filling the core of the hollow pier with concrete poured from the deck.

4. VARINA-ENON BRIDGE: VIRGINA[36-44]

The Varina-Enon Bridge, the only cable-stayed bridge in Virginia, opened to traffic in 1990 and carries Interstate 295 over the James River between the counties of Chesterfield and Henrico. The bridge is 4,680 ft in length and consists of two parallel approach structures (southbound and northbound bridges) and a single structure on the cable-stayed main span. It has a total of 480 grouted external tendons and 360 PT bars. Each box has eight external tendons, and each tendon has 19 0.6-inch strands encased in a four-inch, high density polyethylene (HDPE) duct.

In 2001, grout voids were found in many tendons, but the strands did not appear corroded. At that time, it was estimated that grout bleeding was approximately 4 percent in properly batched grout (water-cement ratio < 0.42). This estimation meant that two three-ft-long voids at the high points adjacent to the anchor plates could be formed in a typical 150-ft-long draped tendon. Field inspections also found three issues: First, tendons were not appropriately sealed at metal straps used to connect HDPE duct to steel pipe at diaphragms and bulkheads. Second, some vent tubes were sealed incorrectly. Third, holes were often drilled in the HDPE ducts to check for voids. However, inadequate corrosion protection was considered the local issue. Following the discovery of the voids, the Virginia Department of Transportation (VDOT) carried out vacuum regrouting in 2003–2004 to fill the grout voids in 55 percent of the tendons.

In May 2007, a routine inspection discovered one failed tendon in the southbound bridge. Even though the tendon was regrouted in 2004, it still failed by corrosion at a bridge age of 17 yr. Figure 10 shows the failed tendon.

Source: FHWA.

A. Section attached to the diaphragm.

Source: FHWA.

B. Opposite section on a deviation block.

Figure 10. Photos. Failed tendon in the Varina-Enon Bridge.

Corrosion also damaged another tendon due to ponding water near a clogged drain hole in the bottom slab of a box girder. Both tendons were replaced in 2007. In late 2007, MFL testing was conducted on approximately 17 mi of external tendons (approximately 3,200 sections) and identified a severely corroded tendon. A closeup of its corroded wires is shown in figure 11.

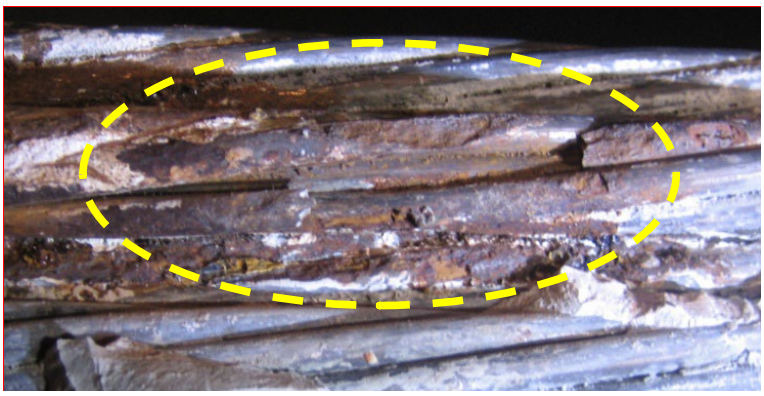

Source: FHWA.

Figure 11. Photo. Closeup of corroded wires.

Additional inspections were conducted after removing two-ft-long duct sections from the selected 20 tendons. Incomplete regrouting and broken wires were discovered in two tendons in the northbound bridge. Subsequently, clear plastic tubes with one or two plastic valves were installed over 11 opened sections, exhibiting different levels of corrosion. The transparent tubes allowed the inspectors to monitor the strand conditions. Figure 12 shows one of the tendon sections being monitored.

Source: FHWA.

Figure 12. Photo. Condition monitoring section covered with a clear plastic tube.

In 2015, four tendons were injected with an impregnated type of corrosion inhibitor. (More about this trial will be discussed in chapter 6.)

Large longitudinal grout voids were often discovered between 3 and 9 o'clock when the selected tendon sections were opened. Some strands were partially exposed without any recognizable corrosion. However, their bottom portions were filled with well-hydrated grout. The top section of the exposed grout appeared porous, weak, and covered with white powdery grout. The defective grout condition indicated that grout segregation had occurred during grouting. Figure 13 shows a representative condition of the segregated grout, including white powdery grout, sporadically exposed strands, and the grout void.

Source: FHWA.

Figure 13. Photo. Typical condition of the segregated grout.

In 2007, the Virginia Transportation Research Council (VTRC) and an independent laboratory investigated some of the retrieved tendon sections from the Varina-Enon Bridge. Figure 14 shows the interior condition of the failed tendon section shown in figure 10-B after it was opened with a circular saw.

Source: FHWA.

Figure 14. Photo. Interior condition of a failed tendon section.

A thin regrouting layer distinguished by a whitish color and rust stains can be seen near the fracture point. The original grout in this area was chalky and fragmented.

Laboratory analysis revealed that all grout samples taken from the failed tendon had less than 0.003 percent acid-soluble (total) chloride by weight of cement, which was well below the corrosion threshold. On the other hand, the repair grout contained an elevated level of sulfate ions. From these findings, it was speculated that excessive sulfate in the repair grout might be responsible for such a rapid corrosion failure. The indepth petrographic analysis of grout samples extracted from the failed tendon was carried out at an independent laboratory to determine the grout's corrosivity and physical characteristics. The following is a summary of the petrographic analysis.

The original gray grout was an unsanded neat paste of ordinary portland cement and water. The estimated water-cement ratio was 0.45 to 0.55 or higher (possibly greater than 0.65). The lower water-cement ratio was found where the grout was medium to dark gray, and the higher water-cement ratio was found in the pale gray and soft grout. Some settled dark cement lumps along the bottom end of the HDPE duct suggested that the grout had a high water content and experienced bleeding before setting. Deposits of ettringite—a hydrous reaction product of calcium aluminate with calcium sulfate in portland cement—were abundant in grout cracks and air voids near the cracks throughout the gray grout, but the overall amount of ettringite in the grout was small.

Overall, the gray grout had high water content, as evidenced by the abundance and large crystal size of portlandite (calcium hydroxide). High water content resulted in segregation, at least locally, forming a soft layer (about 0.125-inch thick) with an exceptionally high water-cement ratio at the surface of this location. Based on the abundance of cement lumps, the gray grout was thought to be a consequence of either lumpy, prehydrated cement or an incomplete mix. Voids and microcracks in the gray grout near another grout layer contained ettringite deposits.

The repair grout material was found in the portion of the tendon next to the zone of strand failure (trailed off within a four-ft section of the failed area). It appeared to have been placed in the tendon after the original gray grout. The tendon in question had a 20-mil thick layer of sanded

gypsum grout at the top surface. The repair grout contained minor amounts of a soft and whitish paste consisting of abundant cement paste, moderate amounts of clear siliceous sand, and minor amounts of small nonentrained air voids. The pH values of the samples were somewhat lower than that of normally hardened grout. The total sulfur (SO_3) content of the white grout samples ranged from about 29 to 32 percent, which was substantially higher than expected for the portland cement-only grout. Additional free calcium sulfate, likely in the form of gypsum, was also present as the major binder component.

In 2012, another round of field investigation and petrographic analysis examined 13 external tendons and 18 vertical PT bars based on previous inspection records. Twelve of 13 locations were at high points near pier diaphragms. The other location was at a low point between two deviation blocks where water had been temporarily collected at the bottom of the box. Inspection locations for the PT bars were randomly selected among those in empty grout vent tubes. The key findings of this investigation are summarized as follows:

- Four of the inspected tendons appeared to contain new repair grout placed after the original construction.

- Two of the most severely corroded tendons exhibited approximately 2.9 and 4.4 percent section losses, respectively.

- The areas exposed to air or covered with a very thin grout layer corroded the most, whereas every strand completely encased in grout exhibited little to no corrosion.

- Twelve of 13 tendons exhibited small voids with exposed steel in the top half of the duct, except where voids had been filled by new grout.

- The grout at the top of the duct in voided areas was typically white and exhibited a soft, chalky consistency, indicative of grout separation or the presence of excess bleed water at the time of construction.

- The grout in the bottom half of the duct was typically light gray with a hard consistency. Eight tendons (62 percent) exhibited circumferential cracking in the grout.

- Corrosion potential varied from -164 to +249 millivolts (mV) versus copper-copper sulfate reference electrode (mV_{CSE}). These potential readings indicated a 90 percent probability of no active corrosion.

- CR ranged from 0.001 to 0.546 mil per yr (mpy), which were considered low to moderate.

- The pH at the grout/strand interface ranged from 11 to 13. Therefore, corrosion was not expected to occur there. However, five tendons exhibited low pH (<11) at the top of the duct. The maximum depth of the carbonation was 0.2 inches. No strands were embedded in the low pH grout layer.

- The new repair grout exhibited the highest moisture content at 33 percent. All the original grout samples had a moisture content of less than 28 percent.

- Total chloride contents ranged from 0.001 to 0.014 percent by grout weight. It is unlikely that chloride-induced corrosion would be an issue.

- All dark grout samples contained sulfate content ranging from 1.02 to 2.21 percent like the original grout samples tested. However, a light-colored repair grout sample from a southbound tendon contained a significantly higher sulfate content of 16.2 percent. This tendon was adjacent to the tendon that failed in 2007.

- All 18 vertical PT bars (5 percent of the total number of bars) were only partially buried in the grout, and most bars were at least partially coated with grout even within the voided area. The void lengths, measured from the entrance of the grout vent tubes to the top of the grout surface, ranged from 10 to 140 inches.

- A borescope inspection revealed that all inspected PT bars exhibited at least minor surface rust, but no significant section loss was observed. The exposed strands also sustained only minor surface corrosion.

- Large voids found in two northbound tendons extended from the test location through the pier diaphragm to the anchor plate. These tendons' trumpet interior was approximately half empty, and 10 to 12 strands were exposed or only partially covered with grout. The strands and anchor plates exhibited heavy surface rust.

Petrographic analysis of 10 original grout samples determined the following:

- All samples were composed of neat portland cement grouts.

- No aggregate or supplementary cementitious materials were observed.

- The grout samples generally contained a moderate water-cement ratio of approximately 0.40 to 0.45.

- The grouts ranged widely in air-void volumes from 0.3 to 8.4 percent and did not appear purposefully air-entrained.

- The outer surface conditions of all grout samples were smooth.

- The depth of carbonation ranged from negligible to 0.47 inches from the formed outer surfaces.

- Small amounts of corrosion products were observed in the strand impressions in all but two samples.

- Secondary portlandite (calcium hydroxide) commonly lined or filled air voids, while ettringite was not commonly observed. These compunds indicated no significant moisture movement through the bulk of the grout.

- Some moisture cycling might have occurred at the grout's outer surfaces due to condensation.

- Sulfate contents ranged from 1.7 to 2.6 percent, but the true range is likely wider due to variations in water-cement ratio and cement content.

- The most common crystalline component of the grout samples was portlandite.

- In all grout samples, ettringite was present in small amounts, but thaumasite, which can develop in the presence of sulfates and carbonate ions, was absent entirely.

- Gypsum was not evident in any of the samples.

- Higher percentages of carbonate (primarily calcite) appeared in three grout samples that exhibited excessive carbonation.

- Microcracking by drying shrinkage was common, with some distinct crazing on the outer formed surfaces.

In 2017, a transverse tendon failed because of corrosion near the parapet in the main span. A follow-up investigation assessed the condition of transverse tendons in two cable-stayed spans (98 tendons per span) using IE and inspection holes. Visual inspections of over 20 tendons confirmed that many locations were fully grouted but contained weak grout. Vertical tendon inspections of the superstructure and substructure found 43 voids out of 72 locations inspected, and 24 tendons (16 at the top of the pier anchors and 8 in the box anchors) exhibited significant corrosion.

An acoustic emission (AE) monitoring system was recently installed on the bridge as the most economical technology for detecting real-time wire breaks and making decisions concerning tendon replacement. The system monitors some longitudinal external tendons, the transverse internal tendons, the cable stays, the piers, and the towers. The system has been in operation since October 2020, and no wire breaks had been reported as of April 2021.

5. CLINE AVENUE BRIDGE: INDIANA[45-48]

The Cline Avenue Bridge is a 6,600-ft-long, cast-in-place concrete box girder bridge over the Indiana Harbor and Ship Canal in Indiana. It opened to traffic in 1983. A routine inspection identified significant longitudinal and transverse cracking in the bridge deck and more cracking in the webs and diaphragms. Indiana DOT was concerned enough about the condition of the PT tendons to conduct a field investigation in 2003.

Out of 1,063 total tendons in the bridge, 277 tendons (26 percent) were inspected using drilling and borescope inspection. A total of 33 voids were found at high points. Eight of them exposed the strands, but none was corroded. After the borescope inspection, the voids were filled using

the VG method. The investigators concluded that most of the PT system functioned with little corrosion (no section loss). The exception was at a few couplers, where significant duct voids resulted in some cross-section losses.

However, a later-yr routine inspection revealed significant corrosion of PT tendons and reinforcing steel bars caused by water seeping through cracks in the bridge deck. Indiana DOT determined that the level of corrosion compromised structural integrity beyond viable repairs. Consequently, the bridge was permanently closed in November 2009 after 26 yr of service.

6. RINGLING CAUSEWAY BRIDGE: FLORIDA[35,49-56]

The Ringling Causeway Bridge is a 3,094-ft-long, 106-ft-wide precast segmental box girder bridge spanning Sarasota Bay and the Intracoastal Waterway of the Gulf of Mexico in Florida. It was completed in 2003. The bridge consists of 11 spans supported by four fixed and five expansion piers plus two abutments. The box girders have a three-cell configuration with a variable depth from 8.85 to 16.4 ft held by internal and external tendons. Half of a span between piers consists of 12 12-ft-long precast segments. This bridge is the first to use segmental duct couplers and prepackaged non-bleed/thixotropic grout in Florida. Each of the external tendons contains 22 0.6-inch 7-wire strands in a four-inch-diameter HDPE duct.

Corrosion failure of an external tendon was discovered in January 2011, and another external tendon failed in July 2011 after less than eight yr of service. These tendon failures were the first incident involving a prepackaged grout product, which had been believed to be a solution to grout-related problems. Therefore, FDOT's investigative work is covered extensively in the following subsections.

6.1 Description of Failed Tendons

The first tendon failure occurred in the upper horizon portion of a sloped tendon section adjacent to an upper deviator. Figure 15 shows, on the left, the as-discovered condition when the failed tendon fell to the girder floor, and on the right, the complete separation of entire strands due to severe corrosion.

© 2011 FDOT.

Figure 15. Photos. Ringling Causeway Bridge's first failed tendon: Ruptured tendon and ruptured section.[35]

Figure 16 shows the other end of the failed tendon (see figure 16-A) and the upper deviator containing the steel pipe and the interior condition of the galvanized steel pipe that contained the failed tendon (see figure 16-B).

© 2011 FDOT.

A. Closeup of the other end of the ruptured tendon.

© 2011 FDOT.

B. Overview of the deviator and interior condition of the steel pipe.

Figure 16. Photos. More photographs associated with the first failed tendon.[52]

This tendon exhibited severe corrosion mostly concentrated on the strands in the upper portion. Except for the heavily corroded strands there, the failure mode of the remaining strands appeared ductile, as evidenced by necking signs at the ruptured ends of the wires. The corroded-in-two wire tips suggested that the failed tendon must have been exposed to a very corrosive environment for some time. Corrosion was also observed in the upper portion of the galvanized steel pipe in the upper deviator (see figure 16-B). Although there is no initial photograph of the pipe's condition, two distinctive rust lines on the interior wall indicated that there was likely water or watery grout up to the rusty watermarks for an unknown duration after grouting.

The strands in the upper horizontal region of the tendon were not fully embedded in grout, and the cross-section in some locations appeared more than half empty. The grout filled into the bottom was well consolidated and hardened with a thin white chalky layer at the grout/void interface. Cementitious residues on the upper part of the strands suggested that the tendon might have been initially filled up to that level.

The grout in other sections filled the duct, but strands were partially exposed in the voids. Tight confinement of the strands against the HDPE duct wall appeared to create some voids. Most voids in the sloped tendon sections were still associated with a continuous longitudinal groove (bleed channel) at the 12 o'clock orientation. An upward movement of liquid and gases and subsequent severe grout segregation in a plastic state might have contributed to forming the large voids, segregated grout, and imprints of bubbles. As a result, the grout was moist and soft throughout. Unlike brittle and easily breakable grout found in the upper horizontal region, the segregated grout in this region remained claylike. It changed the color from dark gray to white upon drying in laboratory air.

Figure 17 shows the condition of the second failed tendon at the time of discovery. Severe corrosion damage took place at the west face of the upper deviator.

Figure 17. Photo. Second failed tendon.[35]

Figure 18 shows the affected deviator (see figure 18-A) and interior of the galvanized steel pipe (see figure 18-B). Horizontal bands of corrosion products can be seen on the pipe's interior wall between 8 and 10 o'clock.

A. Deviator of the failed tendon.

B. Interior condition of the steel pipe.

Figure 18. Photos. More photographs associated with the second failed tendon.[52]

Figure 19 shows a close-up photograph of the failure location.

Courtesy of FDOT.

Figure 19. Photo. Closeup of the second failed tendon.

The condition of the failed section was inspected through the gap between the slipped HDPE duct and the galvanized pipe assembled with the neoprene coupler. Severe corrosion damage was not as localized as in the first failed tendon. Instead, corrosion and strand fracture were observed at several locations within a 20-ft section. The remaining strands showed a ductile fracture with necking. Severe corrosion of the strands within the galvanized steel pipe in the upper deviator was also observed.

Segregated soft/wet grout was observed throughout the region of corrosion failure. A large amount of segregated grout was also observed at a low point anchorage zone, where severe corrosion of the anchor head and strands occurred. Figure 20 shows the soft/wet grout inside the anchorage zone.

Courtesy of FDOT.

Figure 20. Photo. Interior of low-point anchorage of the second failed tendon.

While the hardened grout adhered to the anchor head's upper and lower areas, severe corrosion was observed in the middle area between them. A lack of adhered grout there suggested that the area was initially occupied by a mixture of air and bleed water before corrosion took place in the absence of protective grout.

Unlike the first failed tendon, large voids were not present in the second failed tendon. Instead, highly segregated, poor-quality grout material filled significant portions of the tendon. Some

tendon segments had minor void spaces caused by a closely packed strand bundle against adequate grout flow in the HDPE duct. Also, stratification of the black layer and signs of gas venting were observed at the grout's top surface. There were significant amounts of soft/wet grout adjacent to both sides of the upper deviator, where the duct separation was initially observed. The segregated grout had a strong odor resembling ammonia. Stratification of silica fume particles and intermixing of the white chalky grout were also observed. The sedimentation did not directly cause grout segregation and stratification because different forms of segregated grout were interspersed within the cross-section. Severe corrosion typically occurred in the wet plastic grout area.

To determine the corrosion tendency of individual strands exposed to various forms of segregated grout in the failed tendon sections, the investigators measured their open circuit potentials (OCPs) or corrosion potentials. Figure 21 shows the cumulative fractions of the OCP data.

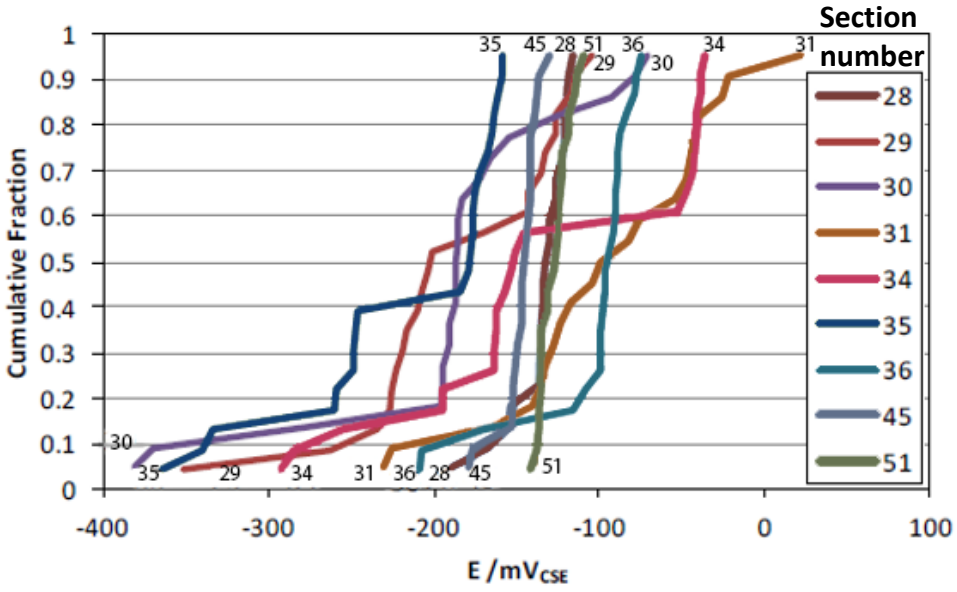

Figure 21. Graph. Strand OCPs in a failed tendon by section number.[51]

A wide range of the measured OCPs highlighted differences in grout corrosivity, even within a short distance apart. Some segments, such as 29, 30, and 35, exhibited active OCPs (below -350 mV_{CSE}). These differences were attributed to the moisture content, chloride and sulfate concentrations, and oxygen availability.

6.2 Other Findings

After the second tendon failure, field investigations were performed for all 132 external draped tendons. The scope of the investigations included understanding why and how such rapid tendon failures occurred; characterizing the grout's consistency; locating segregated grout, voided areas, and corroded strands; and repairing or replacing the affected tendons.

6.2.1 Description of Segregated Grout

The segregated grout was characterized as having a soft/wet—claylike—consistency (moisture content 50—80 percent), sedimented black layer with silica fume, and white chalky (moisture content 20—50 percent) appearance. Figure 22 shows three distinctively different areas of segregated grout.

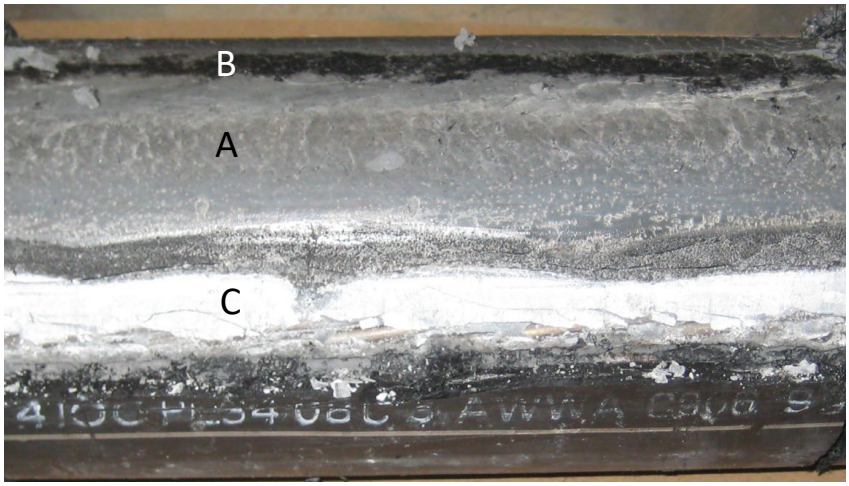

A = soft/wet grout; B = sedimented silica fume; C = white chalky grout.

Figure 22. Photo. Stratified segregated grout.[50]

During inspections of other tendons, soft/wet grout was present at numerous locations and could be present in large regions. The segregated grout had other characteristics such as high CR, high pH, high sulfate concentration, other soluble ionic contents, and no significant chloride concentration. In addition to different material properties, the segregated grout and normally hardened grout exhibited different colors. For instance, the segregated grout tended to have a white or light gray color contrasted with the normally hardened grout's dark gray color.

Figure 23 and figure 24 show a soft/wet field grout sample that never hardened and chalky grout inside the corroded strands, respectively.

Source: FHWA.

Figure 23. Photo. Claylike texture of a soft/wet grout sample.

Courtesy of FDOT.

Figure 24. Photo. Interior condition of strands filled with chalky grout.

It was not clearly understood how the segregation process of the identical prepackaged grout product could produce such distinctively different grout textures and material properties.

Figure 25 shows an excavated area with four features commonly exhibited by many tendons filled with segregated grout, starting from top to bottom as follows: incomplete grout filling, i.e., a grout void; severely corroded bare strands surfaced above normally hardened grout; remnants of thin grout coating over some of the exposed strands; a layer of sedimented silica fume particles; and normally hardened grout.

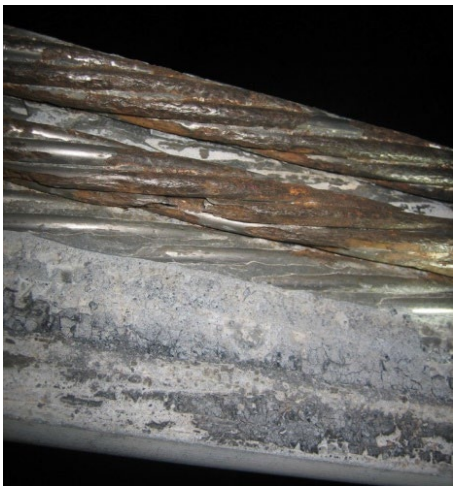

Courtesy of FDOT.

Figure 25. Photo. Closeup of segregated grout in a half-filled tendon.

The silica fume particles could surface on bleed water during grout pumping, moving through the duct, and during the initial plastic stage. When the bleed water evaporated or was reabsorbed into the segregated grout, lightweight particles such as silica fume clustered over the grout surface. A black deposit layer of silica fume particles was also present in the bleed channels. The normally hardened grout beneath the segregated grout preserved protective properties to maintain corrosion-free strands.

The observed corrosion problems were mainly associated with segregated grout, which was much more likely to develop strand corrosion than normally hardened grout. For example, figure 26 shows severely corroded strands embedded in the deficient grout, which was cracked, soft, and very thin. The inset at the right bottom corner shows the grout's initial condition exhibiting a network of grout cracking before it was removed.

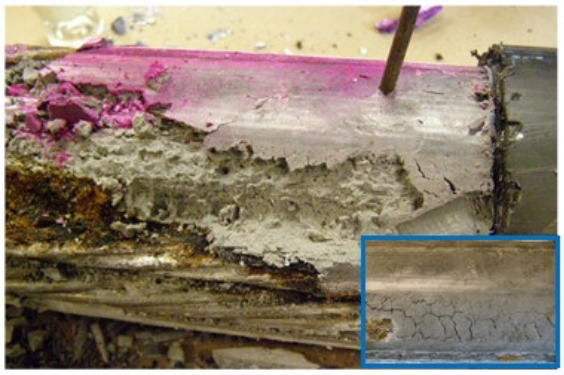

Figure 26. Photos. Severe corrosion associated with soft grout.[50]

Two interesting features observed from the photograph are the grout's softness (tested with a screwdriver) and the presence of the black-colored magnetite, which can form in the oxygen-starving environment.

Figure 27 shows two significantly corroded strands covered with a thin grout coating; figure 28 shows a photograph taken from an undisturbed, inclined section upon opening, respectively.

Figure 27. Photo. Closeup of severely corroded strands in a rejected tendon.[49]

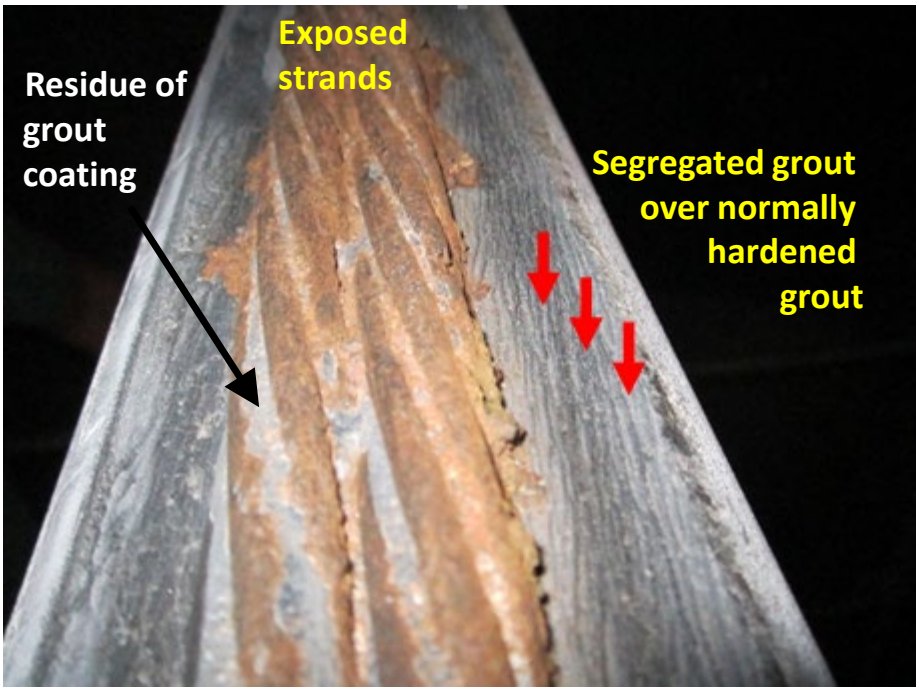

Courtesy of FDOT.

Figure 28. Photo. Undisturbed condition of an opened tendon.

The grout condition shown in the two figures revealed important features regarding the initial grout condition of the sloped tendon sections, as follows:

- Corrosion was observed on the strands exposed to the void space only.
- Remnants of thin grout coating were observed over the exposed strands, suggesting the segregated grout initially rose above the strand level and then receded.
- The exposed, uncoated strand surface started corroding at a later time.
- The grout coating's thinness indicated a strong possibility that the initial grout might have been quite watery, with a small amount of cement paste in the bleed water.
- The initially placed grout material might have mostly receded rather quickly, because the top surface of the hardened grout appeared to be normal (see figure 28).
- The normal hardening process would not be possible during prolonged exposure to excessive bleed water or with the presence of a severely segregated grout layer.
- The hardened grout's top surface exhibited small longitudinal ridges, as indicated by the three arrows in figure 28.
- This wrinkled surface texture must have been created by liquid (i.e., bleed water) flowing back down along the sloped section while the grout was still soft enough to be carved by the moving water.

- Some anchorage zone grout caps were drilled and opened, and then the exposed anchor heads' conditions were inspected.

Figure 29 shows an anchorage zone's interior condition after its grout cap was removed.

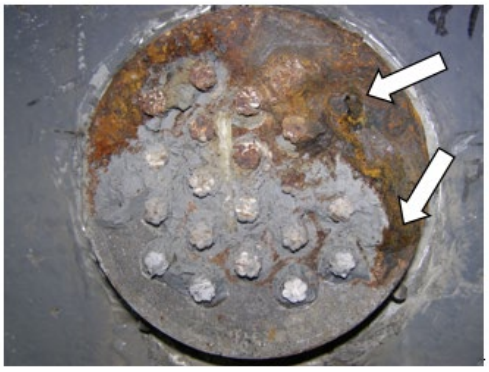

Courtesy of FDOT.

Figure 29. Photo. Exposed anchorage zone after a grout cap was removed.

The space created between the grout cap and anchor head was filled with fragments of the segregated grout, and the steel surface showed corrosion. Permanent corrosion damage under the corrosion products did not look significant. The corrosion products concentrated in the upper part of the anchor plate suggested that bleed water was responsible for the active corrosion. The partially cleaned anchor head exhibited trails of liquid corrosion products oozing out of two strands' cut ends, as indicated by two arrows. The flowable corrosion by-products must have formed behind the anchor head and traveled through the strands' interstitial space.

6.2.2 Data Analysis

A total of 655 couplers out of 1,416 inspected couplers (46 percent) contained grout voids, and 1,236 duct couplers of the 1,416 inspected couplers (87 percent) were replaced. As discussed previously, 15 tendons, in addition to two already failed tendons, were replaced. The tendons to be replaced were selected through structural analysis. A technical advisory group formed by FDOT recommended permitting a cross-sectional loss of up to one strand among 22 0.6-inch strands per tendon.

Almost one-third of the voids measured less than 1/16 inches in size. More than half of the voids exposed strands, but only 5 percent of the voids larger than 1/16 inches showed corrosion. This percentage seems somewhat low compared to the initial assessment of the extent of the grout problems. Figure 30 shows a bar graph for three types of grout conditions in the grout voids bigger than 1/16 inches based on the unpublished FDOT inspection data.[1]

[1]Theryo, T.S., Lepore, R., Green, D., and Lee, M. 2012. Ringling Causeway Bridge External Tendon Investigation Summary, Parsons Brinckerhoff Summary Report. Internal Document. Tampa, FL: FDOT.

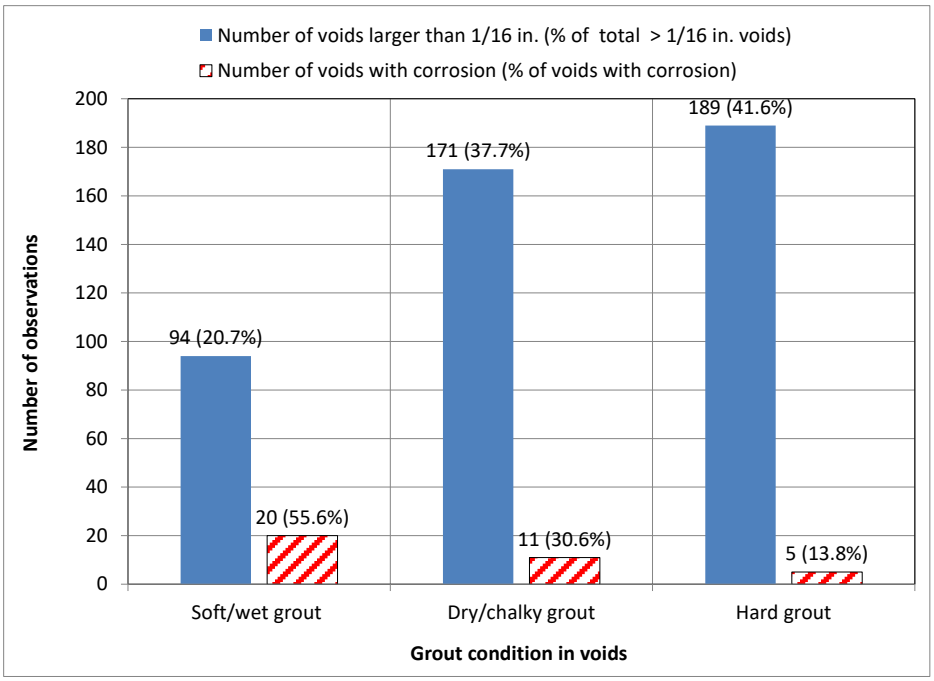

Source: FHWA.

Figure 30. Graph. Grout condition in relation to number of voids and amount of corrosion.

Overall, normally hardened grout was the most frequent grout type in the voids with 42 percent of the observations, followed by dry chalky grout with 38 percent and soft/wet grout with 21 percent. However, 56 percent of the corrosion was observed in the soft/wet grout, followed by 31 percent in the dry chalky grout and 14 percent in the hardened grout. These data confirmed that the deficient grout was much more likely to develop strand corrosion than the normally hardened grout (i.e., 86 versus 14 percent).

7. PLYMOUTH AVENUE BRIDGE: MINNESOTA[28,57-60]

The Plymouth Avenue Bridge is the first cast-in-place segmental box girder PT bridge constructed in Minnesota and opened in 1983. It consists of two parallel twin concrete box girders with varying depths of 10 to 13 ft and carries Plymouth Avenue over the Mississippi River on the north side of Minneapolis, Mn. This bridge has a total length of 943 ft with a deck width of 75.5 ft for four lanes of traffic and two pedestrian sidewalks. Among five spans, span numbers 1, 2, 4, and 5 were cast-in-place on falsework, and the 260-ft main span (span 3) was constructed using form travelers in unidirectional, cast-in-place cantilever construction. Each internal tendon contains 19 0.5-inch-diameter 7-wire strands in a 3.5-inch metal duct.

During an annual inspection in 2010, slab cracking and rust stains were observed in the box girders. A follow-up inspection revealed significant cracking, rust stains, and the corrosion of internal continuity tendons buried in the bottom slab under the delaminated concrete. The bridge was closed for nearly 1 yr to carry out detailed inspections and subsequent repairs, and it was strengthened with the installation of five additional external tendons in each box girder. Each new tendon contains 12 0.6-inch strands. The new tendons were installed through new concrete

deviation blocks attached to the bottom slab and anchored in the concrete blisters newly formed at the girder ends.

The investigation determined that chloride-bearing water from the deck was leaked through the misaligned drainage pipe sections inside the box girders and deicing salts accumulated in the bottom slab triggered corrosion of the internal tendons and adjacent reinforcing steel. A schematic of the drainage system is shown in figure 31.

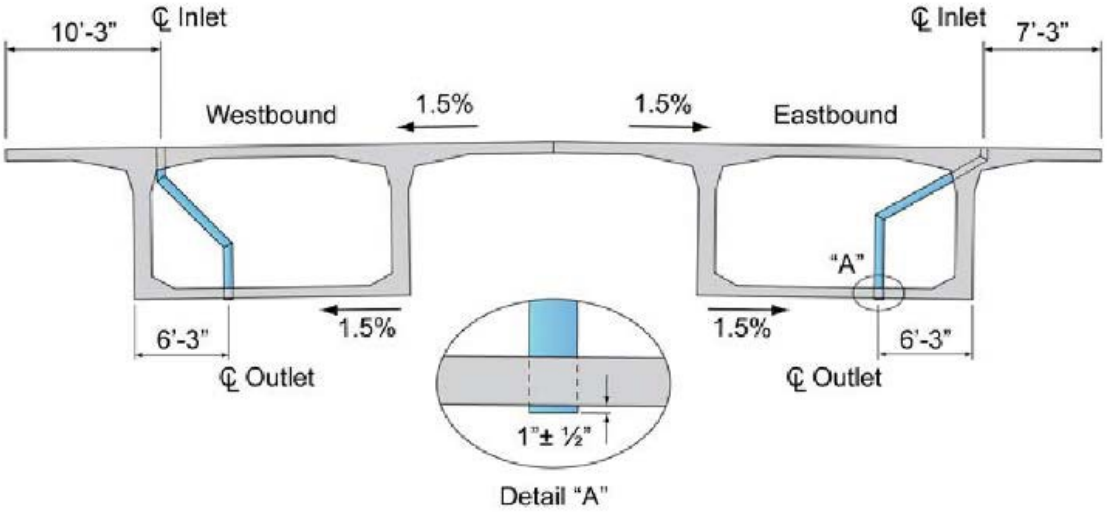

Figure 31. Illustration. Schematic of drainage system.[28]

The exterior bottom slab surface of the eastbound and westbound box girders also exhibited longitudinal cracks, efflorescence, rust stains, and concrete spalling. A very short drainage outlet pipe beyond the bottom slab (see detail "A" in figure 31) caused the corrosive water to wet the nearby bottom slab and initiated corrosion. Figure 32 shows an interior view of concrete damage and severely corroded tendons in the bottom slab (see figure 32-A) and an exterior view of another location experiencing similar damage (see figure 32-B).

A. Interior condition.

B. Exterior condition.

Figure 32. Photos. Plymouth Avenue Bridge's severely damaged bottom slab.[28]

The bottom slab had large patched areas over the base concrete. These patches were delaminated and allowed direct ingress of moisture, chloride, and oxygen to the tendons and structural reinforcing bars.

Figure 33 shows the as-excavated condition of three internal tendons beneath the delaminated concrete (see figure 33-A) and a closeup of a corroded tendon (see figure 33-B).

A. Corroded tendons exposed.

B. Closeup of a corroded tendon.

Figure 33. Photos. Corroded internal tendons beneath delaminated concrete.[28]

It was observed that the metal duct was corroded away, and grout and corrosion products mingled with severely corroded strands such that individual wires could not be distinguished. Nearby concrete contained a high level of acid-soluble chloride concentration (nearly 0.8 percent by weight of grout) at 0.8 inches deep.

On the contrary, an internal tendon in excellent condition was uncovered in an area where a large crack was directly over the tendon. A representative condition is shown in figure 34.

Figure 34. Photo. Exposed internal strands exhibiting excellent condition.[28]

A good quality grout without moisture was observed there. The grout contained 0.075 percent acid-soluble chloride concentration by weight of grout, which explained its corrosion-free condition.

Spot checks were done at high points on the box girder webs and other areas of interest, like areas with moisture present on the web surface. It was concluded that the web tendons were in good condition and appeared fully grouted with a normal (nonsegregated) grout. Although the grout used in this bridge would likely be neat cement grout (i.e., a nonthixotropic), the overall quality of the grout was considered very good.

8. WANDO RIVER BRIDGE: SOUTH CAROLINA[61-69]

The Interstate 526 Wando River Bridge (formerly the James B. Edwards Bridge), completed in 1989, connects Mount Pleasant and Daniel Island over the Wando River in Charleston, SC. It is the only segmental box girder bridge in the state and was constructed using a span-by-span method for the two approach units and a balanced cantilever method for the main span. The bridge has two 7,900-ft-long parallel structures carrying eastbound and westbound traffic. Each structure consists of 51 precast, segmental PT box girder spans and contains 696 longitudinal internal and external tendons, including 240 external tendons in the approach span units and 60 external tendons in the main span units. Each tendon has 19 0.6-inch, 7-wire strands. The bridge also has 84 additional tendons composed of segments of concrete foundation.

The first failed external tendon was discovered in September 2016 when the “M 1-South” tendon was loosened in the main span of the westbound structure. However, the bridge had issues since its completion in 1989—and since 2010, it had gone through several indepth inspections. A routine biannual inspection in May 2010 and a subsequent walk-through in August 2010 noted many deficiencies related to inadequate corrosion protection of the PT tendons, including the following:

- White deposit material (a sign of water infiltration) coming out of the ducts and couplers and pour-back at anchorage.

- Leaky segment joints.

- Rust stains oozing out of tendon penetration on a diaphragm.
- Unprotected grout holes in PE ducts.
- Unsealed grout vent tubes.
- Improper duct couplers and extensive use of duct tape for duct connection.
- Connection problems with ducts, diaphragms, and deviators.
- An improper external tendon entry point at the top deck.
- Incorrect drain locations.
- Inadequate corrosion protection of PT bar anchors.

Following the cursory walkthrough inspection in 2010, a comprehensive field investigation was carried out in 2011. The key findings of the investigation are summarized below.

Various locations on 31 tendons were accessed and inspected, and, where appropriate, samples were taken and analyzed. The primary investigation of the external tendons was performed by the visual inspection method with the help of a borescope. Even though there were grout voids, no strands were visible inside the voids. Also, there was a significant amount of corrosion products, presumably from a metal duct.

Water droplets observed in the anchorage area indicated that water was responsible for the active corrosion there. Most of the locations selected for investigation exhibited white-colored deposit material at pour-backs, unsealed holes in PE ducts, and duct connections adjacent to deviator blocks and diaphragms. In some cases, active water leakage was observed. The main composition of the white-colored material was calcium carbonate, which accumulated after water that had infiltrated the PT system evaporated. One confirmed water source was an open grout vent tube in a diaphragm that extended directly up to the deck. There might be more locations where the grout vent tubes were partially filled or filled with poor-quality grout.

Other factors conducive to corrosion included incomplete grouting; extensive grout carbonation; and defective grout exhibiting excessive porosity, cracks, and absorption. Galvanic coupling of the tendons and dissimilar metals in the anchorage zone may also have increased corrosion.

After the first tendon failure was discovered in November 2016, an extensive investigation was performed from January 2017 to March 2018. Major investigation findings are summarized as follows:

- Water was present inside box girders due to excessive leakage from the deck joints and the exiting of tendons from the deck slab, within the diaphragms, and at low points of the tendon.
- Efflorescence was formed at and near areas with water leakage.

- Exposed grout appeared very wet, soft, and pasty and sometimes had voids along the top of the tendon and on the corroding strands.

- Anchorage caps contained water, efflorescence dripped from anchors, anchor heads were severely corroded, and grout filling did not appear to have been completed initially.

- Multiple one-inch-diameter holes in the PE ducts revealed, upon excavation, corrosion and grout deterioration.

- One strand was loose at three locations.

- Water poured from an opened tendon.

- HDPE ducts showed numerous bulges.

- Borescope inspections revealed moisture inside the anchorage zones.

These problems were also noted during the 2011 investigation, but the magnitude of the problems seemed to increase further over the following seven years.

A laboratory investigation was performed with six strand sections retrieved from the failed tendon and ten 5-ft tendon sections from a span far away from the failure location. A visual evaluation of the grout revealed that, for the full lengths of all the tendon sections, the exposed grout was typically gray to dark gray with a good, hard consistency, except for segments of horizontal bands containing porous, loose grout or white, chalky grout. These bands were indications that grout segregation occurred during construction.

A 0.8-inch-thick grout sample collected from the tendon failure location suggested that the duct was 80 percent empty. No strand impressions were found in the thin grout sample except for two short lines of rust. Since the strands were not encased in good quality grout, any moisture intrusion into the duct would have led to significant strand corrosion. This sample exhibited acceptable quality in terms of moisture content (5.9 percent), chloride concentration (0.044 percent by weight of the grout sample), and sulfate concentration (2.13 percent by weight of the grout sample). However, the pH around the exterior surface was 5, whereas the grout interior still exhibited high pH.

Corrosion potential and CR measured at each of ten away-from-the failure tendon sections indicated that they were all in the passive state. The probability of no corrosion was 90 percent (corrosion potential more positive than −200 mV_{CSE}) and the rate of corrosion was very low (less than 0.24 mpy). The pH at the grout/strand interface was high, ranging from 12 to 13. The moisture contents in the grout samples varied within the normal range (between 15.2 to 21.4 percent). The acid-soluble chloride concentrations ranged from 0.011 to 0.015 percent by weight of cement at the corroded section, but sulfate concentrations varied from 2.98 to 3.98 percent by the weight of the grout sample. Since some sulfate concentrations were higher than 3 percent and grout carbonation was confirmed, sulfate-induced corrosion could not be excluded.

A parallel petrographic analysis of the grout samples recovered away from the failed tendon indicated the following:

- The grout pieces and wire imprint surfaces were not carbonated.
- The strands were embedded in good quality, well-hydrated, noncarbonated grout.
- The strands were not observed to be corroded at the sampling locations.
- The grout's water-cement ratio was estimated to be 0.43 when it was placed.
- The grout contained entrapped air voids in between 5 and 9 percent of the grout paste, which was considered high.
- Entrapped air voids were clustered on the surfaces, in contact with the duct and some wire imprint surfaces, in small regions of some grout pieces.
- The observed air voids and bands of grout segregation were attributed to grout bleeding before the initial set.
- Grout samples fractured at some time before the grout sampling.
- The sampled tendon sections' laboratory analysis indicated corrosion would not be likely to occur on them in the future.

Based on the investigation findings, it was concluded that the failure occurred in the area of a grout void and exposure to recharged water (or moist air). These unfavorable conditions led to severe strand corrosion and, eventually, tendon ruptured. Nearby strands encased in poor-quality grout also experienced corrosion damages, even without chloride. When the strands were completely encased in the good quality grout, corrosion was not observed.

Another failed tendon (M-5) was discovered in the westbound structure near the first failed one during a weekly routine walkthrough inspection in May 2018. This tendon failure led to an emergency closure of the westbound structure for nearly three weeks. Examining the fractured strands revealed that 107 wires (80.5 percent) were ruptured by corrosion and the remaining 26 wires (19.5 percent) by overstressing in the presence of reduced cross-sectional areas. During the replacement of the damaged tendon, two extra external tendons were added for increased structural redundancy.

9. POST-TENSIONED BRIDGES IN TEXAS[70,71,72]

During the construction of the Carbon Plant Road Bridge (Corpus Christy, TX) in 2010, two problems were noted on PT straddle caps. Each cap had five internal tendons, and each tendon contained 13 to 19 strands. They were grouted with a commercially available, prepackaged, non-bleed/thixotropic grout product. When the grout caps were removed, grout voids, exposed strands, and segregated grout were found. Also, water was pouring out beneath the grout cap. Figure 35 shows defective grout conditions.

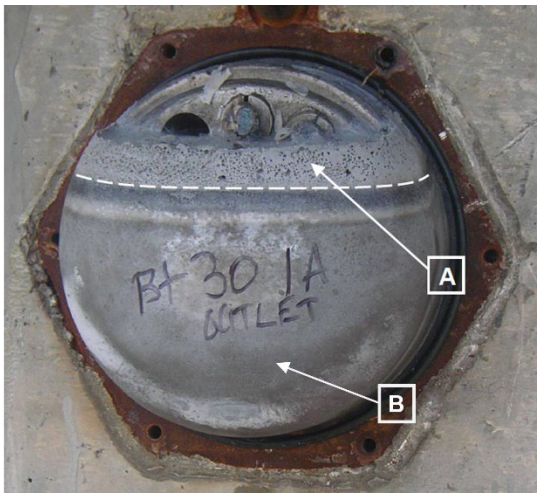

Source: FHWA.

Figure 35. Photo. Grout voids and segregated grout layers in Carbon Plant Road Bridge.[72]

Labels A and B indicate the segregated grout and normally hardened grout, respectively. The segregated grout was described as being soft like clay and containing numerous tiny air bubbles. It also contained a high level of chloride—up to 5.27 percent by weight of cement.

The petrographic analysis revealed that the grout segregation made both the cementitious material and water migrate to the surface of the inlets. Also, a comparison of both grout materials showed considerable variation in fineness and significant variation in chemistry. For example, the silica fume present in the "A" material was not uniformly distributed, indicating poor mixing efficiency. Much of the mixing water also migrated upward and likely carried the water-soluble ions to the surface, which resulted in high ionic concentrations in the segregated grout. Additionally, according to Texas Department of Transportation (TxDOT) construction records, some grouting operation-related incidents and concerns were observed. The following highlights some of the issues:

- The specification required a grouting plan for the work, but each of three contractors used slightly different procedures.
- TxDOT personnel expressed concerns about the quality of the grout mixing.
- Fifteen tendons encountered issues with blowouts or other procedural failures (out of 19 tendons grouted), leading to excessive grout loss from the anchorages during grouting.
- One grout cap remained secured by only three of the required six bolts and blew off under grouting pressure.
- Bolts secured a grout cap with no washers. When the pressure rose, the grout cap was forced over the bolt heads, causing a rupture and significant grout loss.
- Someone pumped grout under high pressure while the outlet valve was closed. A significant loss of grout occurred when the valve was finally opened.

- Communication cited as lacking between the contractor in charge of grouting and the general contractor's grouting personnel.

- Contract personnel reported that tendons were "burped" to relieve any air or bleed water; any incorrect burping could have caused grout voids to form in the tendon anchorages.

- Injected grout failed to fill the anchorage zones, evidenced by the incomplete filling in the spaces between the wedges, the exposed strand tails (cut ends), and the clean wedge plate.

These issues suggest that many causes, independently or jointly, may yield deficient grout in actual job site situations. A grouting operation is a complicated process that requires well-written construction specifications, tight grout specification and strict enforcement, the right materials, the maintenance of proper mixing and injection conditions, skilled operators, adequate grout transportation and storage, and grout consumption before the expiration date. Deficient or poor-quality grout can be produced due to a lack of understanding of proper grouting practices by the contractor's personnel, insufficient supervision by the contractor's personnel, poor communication between the contractor's personnel and the general contractor, and problems with contractor-supplied equipment.

Shahawy and Cox performed condition evaluations of three PT bridges in Texas: a 5-yr-old US Route 183 segmental bridge in Austin, an 8-yr-old Y-segmental bridge in San Antonio, and a 12-yr-old cable-stayed segmental bridge in Port Arthur. The investigators noted the following deficiencies:

- Many locations contained grout voids, and the voids were generally close to the end anchorages.

- The anchorage zones revealed air cavities, trails of bleed water, and soft and chalky grout.

- Pairs of solid grout sections contained voids between them in many cases, indicating air was entrapped there. This entrapment was likely due to pump cavitation where the grout level was insufficient and the pump running dry for an extended period.

- A high pumping rate could have caused turbulent flow, leading to more entrapped air and bleed water.

- Expansive gases and bleed water formed some grout voids. Before the grout's initial setting, the captured air or gas from expansive agents could rise to a high point.

- Grout injected from a high point may have experienced turbulence and captured air in the grout column.

- Free water moving to the tendon's high points allowed the remaining grout to settle back away from the anchor. This settling back was potentially aggravated by excessive water in the grout. Gravity-induced separation of cement took place in the grout mix.

- Several PT tendons contained only traces of grout or were virtually empty.
- Excessive bleed water entrapped in the tendons and moisture intruding into the voids caused strand corrosion at various locations within the voids.

Investigators concluded that the observed tendon conditions were severe, considering the age of the ’ridges,' and raised questions about the durability of the primary PT tendons.

10. ADDITIONAL POST-TENSIONED BRIDGES IN MINNESOTA[28,58,73]

In 2010, the University of Minnesota Duluth reviewed the condition of PT tendons in approximately 40 PT bridges constructed before 2003 in Minnesota. After the preliminary evaluation of 10 bridges representing various bridge types, accessible areas of three PT bridges (Plymouth Avenue Bridge, Duluth Bridge, and Coon Rapids Bridge) were visually evaluated with limited invasive inspections. The Plymouth Avenue Bridge case was already presented. The inspection findings of the other bridges are summarized below.

Duluth Bridge (MnDOT Bridge Identification [ID]: 69818 N/S), constructed in 1985, is a pair of approximately 2,730-ft-long, northbound and southbound bridges on Interstate 35. Each superstructure consists of multicell box girders and I-beam sections. The box girder portion contains internal PT tendons. Each parabolic-shaped metal duct installed in the web contains up to 37 strands to consitute an internal tendon. The selected inspection spots did not reveal any grout problems or tendon corrosion.

Coon Rapids Bridge (MnDOT Bridge ID: 02037 E/W) was built in 1997. It consists of twin structures carrying eastbound and westbound traffic on US Route 10. The eastbound structure spans 479 ft and consists of three spans with five girder lines (a total of 15 tendons). The westbound structure spans 597 ft and consists of four spans with five girder lines (a total of 15 tendons). The structures have precast segmental box girder sections containing three tendons per girder/web (as many as 27 strands per tendon). The box girders’ 9-ft height results in a significant vertical rise of the tendon profile between the low points at mid-span and the high points at piers.

Figure 36 shows a representative condition of internal tendons at low points.

A. Exposed tendons.

B. Closeup of the middle tendon.

Figure 36. Photos. Exposed ducts at a low point of tendon profile on Coon Rapids Bridge.[28]

They were filled with good-quality grout, and only some bleed channels could be seen on top of the grout. Acid-soluble chloride concentrations in two grout samples were 0.046 and 0.062 percent. The grout samples taken from other locations also contained acceptable levels of chloride.

However, grout voids were discovered at 29 out of 90 high points (32 percent) inspected within three spans. A typical grout void occupied the roughly upper half of the duct's cross-section and was at least 10 ft long. The grout surface usually exhibited a white chalky texture. The poor condition suggested the grout segregation had occurred during grouting. Interior surfaces of the metal ducts showed light to moderate corrosion. Figure 37 shows two locations exhibiting moderate corrosion on the duct surface and chalky grout (see figure 37-A) and a smooth grout surface and little corrosion on the duct surface (see figure 37-B).

A. Corroded duct interior.

© 2012 MnDOT.

B. Corrosion-free duct interior.

Figure 37. Photos. Voided internal tendons at high points.[28]

The strands were exposed in approximately half of the grout voids, but significant corrosion or light surface corrosion was not observed at any of these locations. Figure 38 shows two locations at high points of the tendon profile, where the strands exposed above the grout surface were partially covered with grout coating (see figure 38-A) or fully covered (see figure 38-B).

© 2012 MnDOT.

A. Exposed strands.

© 2012 MnDOT.

B. Another group of exposed strands.

Figure 38. Photos. Exposed strands in the grout voids at high points.[28]

Numerous repair patches in the box girders could provide access paths for water and air. The corrosion on the duct's interior surface confirmed the presence of moisture and oxygen in the grout voids. Approximately one-third of the grout voids were filled with a repair grout using vacuum-assisted or pressure grouting (PG) repair techniques to mitigate future corrosion problems.

11. ADDITIONAL POST-TENSIONED BRIDGES IN FLORIDA[17,35,50,51,53]

As briefly mentioned in chapter 1, some of the balanced cantilever PT bridges at the Interstate 75/Interstate 595 Sawgrass Interchange built between 1986 and 1989 experienced water-leaking problems through the segment joints. Efflorescence also came from the top slab continuity tendons. Figure 39 shows the interior condition of the water-leaking box girders.

Figure 39. Photo. Interior view of water-leaking box girders at the Sawgrass Interchange.[17]

FDOT discovered one top continuity tendon that was nearly empty for more than 300 ft. Later, the grout void was repaired by regrouting after drilling multiple holes into the duct from the deck in 1996.

After the Ringling Bridge tendon problem was discovered, FDOT inspected other bridges using the prepackaged, non-bleed/thixotropic grout products. They found that at least five bridges contained some types of deficient grout. The affected bridges included Interstate 4/Crosstown Connector in Tampa, Wonderwood Bridge in Jacksonville, and Interstate 95/Interstate 295 Interchange in Jacksonville. The extent of the grout deficiencies varied significantly among the bridges.

The Interstate 4 Connector project involved the construction of 29 concrete segmental bridges in the Tampa Bay area. The Interstate 4 Connector consists of 2,765 segments accommodating 2,868 longitudinal tendons and 252 short transverse tendons. In an earlier phase of the project, 10 out of 63 longitudinal tendons were found to contain segregated grout, characterized as puttylike soft grout. None of the short transverse tendons contained segregated grout. The deficient grout was found mainly in the tendons filled with one particular grout product. No segregation had been observed after switching to another grout product.

The Wonderwood Bridge was built in 2003 and carries State Road 116 over the intracoastal waterway in Jacksonville. To increase structural capacity, more strands were jammed into the ducts and restricted the flow of grout. The bridge experienced significant grouting problems, including soft/wet grout during construction using a prepackaged grout product. Two inspections were carried out in 2012. The inspectors found 16 corroded metal ducts, 15 tendons with minor strand corrosion, and 14 tendons with soft/wet grout. Figure 40 shows four opened internal tendons where soft/wet grout was found.

A. Exposed tendon condition 1.

B. Exposed tendon condition 2.

© 2014 FDOT.

C. Exposed tendon condition 3.

© 2014 FDOT.

D. Exposed tendon condition 4.

Figure 40. Photos. Soft/wet grout found in the Wonderwood Bridge.[35]

While the metal ducts were corroded in the vicinity of deficient grout, as shown in the top photographs (see figure 40-A and figure 40-B), all the exposed strands shown in figure 40 did not exhibit corrosion despite the presence of the soft/wet grout.

Ettringite was present in the grout samples extracted from the bridge. The moisture content in the soft/wet grout samples ranged from 30 to 66 percent by weight of the sample, whereas those in the hardened grout samples were between 12 and 18 percent. Up to 12,000 ppm of sulfate ions and elevated levels of potassium and sodium ions were contained in the deficient grout. The chloride concentration determined in the leachate was generally low, regardless of grout quality.

12. ADDITIONAL POST-TENSIONED BRIDGES IN VIRGINA[42,43]

The PT bridges in Virginia constructed since 2001 have used prepackaged grout products. Smart Road Bridge was the first bridge to use this type of commercial grout in its 226 longitudinal tendons. The IE technique was used on 16 tendons (with a total length 5,300 ft), and OCPs and CRs were measured on seven tendons. Also, grout samples were collected from nine tendons, and 4 oz of water were collected from one of the anchorage zones.

It was concluded that the overall conditions of the grout and strands were very good throughout the bridge except for several grout voids in four tendons. Less than 0.3-inch-thick shallow voids

were found in three tendons. Also, a 33-ft-long section with no grout was found in one top cantilever tendon. The exposed strands showed moderate corrosion. Regrouting using the VG method was recommended for the voided section.

Two other PT bridges constructed in 2006, the Lord Delaware and Eltham Bridges, experienced tendon corrosion problems due to improper grouting work. Between the two bridges, all 84 tendons in 28 continuous, 880-ft-long spliced girders likely contained segregated (soft) grout, water, and voids. IE inspection identified the problem areas and inspection holes revealed soft grout and water. Elevated levels of iron and sulfate ions were found in the sampled water. Water, efflorescence, and rust stains could be seen on the exterior surface as well. Figure 41-A shows a stream of water coming out of an internal tendon through an inspection hole, and figure 41-B shows a sign of ongoing tendon corrosion.

A. Water coming out.

B. Concrete cracks showing efflorescence.

Figure 41. Photos. Deteriorated internal tendons in Lord Delaware and Eltham Bridges.[42]

13. EUROPE

European countries started experiencing PT tendon problems earlier than the United States. The following presents some field cases observed in Europe.

13.1 France

Godart, Lacombe, and Aubagnac reported five cases of external PT tendon failures that occurred in France between 1994 and 2005. The affected PT bridges were 8, 10, 18, 19, and 21 yr old, with a mean age of 15 yr.[74] Their paper, *Failures of External Tendons in Prestressed Concrete Bridges: Causes, Investigations, Remediation and Prevention*, appeared to be the first technical report discussing the segregated grout phenomenon observed in multiple PT bridges in France. The following section summarizes three of the tendon failure cases discussed.

First, a prestressed concrete bridge built in 1986 over the Durance River experienced a tendon failure near an anchorage in 1994. The duct had no grout and was partially filled with water. Of 109 wires analyzed, 21 were disconnected by corrosion damage, and the others were failed by overstressing. The water collected from the anchor caps had a high pH. The grout samples removed from the trumpets showed a whitish, pasty consistency, sometimes accompanied by moisture and corroded wires. The failed tendon was replaced in 1996, and all tendons in the downstream box girders were replaced in 2000.

Second, the Saint-Cloud Viaduct over the Seine River opened to traffic in 1974. It is a 3,280-ft-long, 67-ft-wide, multicell box girder bridge. All internal tendons are embedded in four webs. After construction, the bridge had to be strengthened with additional external tendons in 1979. One of them, a 1,000-ft-long external tendon, failed at the lowest point between two deviators in 1998. The location of the failure was close to a regrouting injection hole. A grout pocket exhibited a consistency like “wet sandy paste” without any coherence, and the pH of the deficient grout ranged from 12 to 14. Examination of the broken wires indicated that most of the wires exhibited SCC.

Third, the Riviere d’Abord Bridge was opened to traffic in 1991. It is a 500 ft-long, three-span segmental box girder bridge constructed by a balanced cantilever method. One of the external tendons failed at an anchor zone in the upper part of a pier segment in 2001. The autopsy discovered a substantial amount of whitish paste on the surface of the strands and in the affected anchorage. A conglomeration of good grout and whitish paste was observed in some sections of the failed tendon. Corrosion and some broken wires were also found there. Water was not observed, but the whitish grout was sometimes wet.

The authors also reported other cases related to segregated grout. External tendons of a box girder bridge under construction in 1994 showed anomalies at the upper points of the tendons, which had been grouted with cement containing an admixture. Some tendons showed incomplete fillings or soft/wet grout consistency that subsequently hardened upon exposure to air. In 1995, inspections carried out on other bridges that were under construction revealed the same type of grout problem existed in these bridges, leading to the belief that the defective grout was a rather widespread issue. They measured “hyper basic” water collected in the anchoring caps where a

tendon failure occurred and explored the possibility of corrosion in such a high pH environment (no published reports for the follow-up study were found).

13.2 United Kingdom

In the United Kingdom, the Bickton Meadows Footbridge collapsed in 1967 due to the corrosion of prestressing steel. Additionally, the Ynys-y-Gwas Bridge, a single-span segmental bridge, collapsed due to the corrosion of internal PT tendons in 1985 without warning. Also, the Taf Fawr Bridge, built in 1964, experienced major corrosion and was rebuilt in 1995. All the prestressing steels in Braidley Road Bridge, built in 1968, were also replaced in the late 1970s. These incidents led U.K. authorities to ban external PT tendons in bridge structures in 1977. In 1992, they banned all new construction of PT bridges containing grouted internal tendons until design and construction standards could be reviewed.

In 1996, the U.K. ban on cast-in-place, grouted PT bridge construction was lifted. However, the ban on precast, segmental grouted PT bridge construction remained in place due to concerns regarding the corrosion of internal tendons in the precast segment joints.[4,5,6] Recently, Hammersmith Flyover in West London suffered from the severe corrosion of internal and external PT tendons and went through extensive repair and rehabilitation work from 2011 until 2015.[41]

In 2001, Woodward published an overview of the durability of PT bridges in the United Kingdom titled "Durability of Post-Tensioned Tendons on Road Bridges in the UK," which was published in *fib Bulletin No. 15: Durability of Post-Tensioned Tendons*.[7] According to the overview, the first problem involving a major PT bridge structure in the United Kingdom was noticed in the early 1970s and was associated with grout voids and water. The water permeated through the concrete cracks into the tendons and expanded upon freezing. However, only slight corrosion of the ducts was observed. Additionally, an adjacent bridge showing no external signs of distress yet was observed to have continuous voids along the entire lengths of 62 percent of the ducts, and two additional ducts were completely empty. Some ducts also contained water and moist grout. Although prestressing wires in the grouted ducts showed surface corrosion, they were generally in good enough condition to conclude that the presence of some grout in a duct provided a protective environment. Wire fractures were observed at an air/water interface in a partially grouted duct; meanwhile, intact wires were found 24 inches away from the wire fracture location. In other cases, the wires in the empty ducts exhibited a wide range of conditions, from near-perfect to having extensive surface corrosion.

Subsequent investigations of 12 bridges built between 1958 and 1977 found grout voids in over 50 percent of the ducts examined. In general, the ducts were dry. The void sizes varied significantly, and their distributions were uneven. The voids were concentrated at high points over the piers. Some of the voids were large enough to expose the strands, and a thin film of cement paste was usually present over the strands. There was no evidence of severe corrosion except slight pitting on a strand in a virtually empty duct.

After the sudden collapse of the Ynys-y-Gwas Bridge, nine segmental PT bridges were inspected. Grout voids were found in seven of them, and severely corroded tendons were

observed at two locations in one bridge. Despite widespread grout deficiencies, the tendons were generally in good condition.

Following the moratorium in 1992, special inspections of 447 bridges started in 1993 in three phases.[7] These bridges were registered on a database, and full entries for 281 bridges were made. Most of the bridges had good durability records. The collected field data were classified in terms of severity and incidence. Severity was subdivided into void size and extent of corrosion. According to an analysis of compiled data, grout voids of various sizes were found in over 50 percent of the bridges, as shown in figure 42.

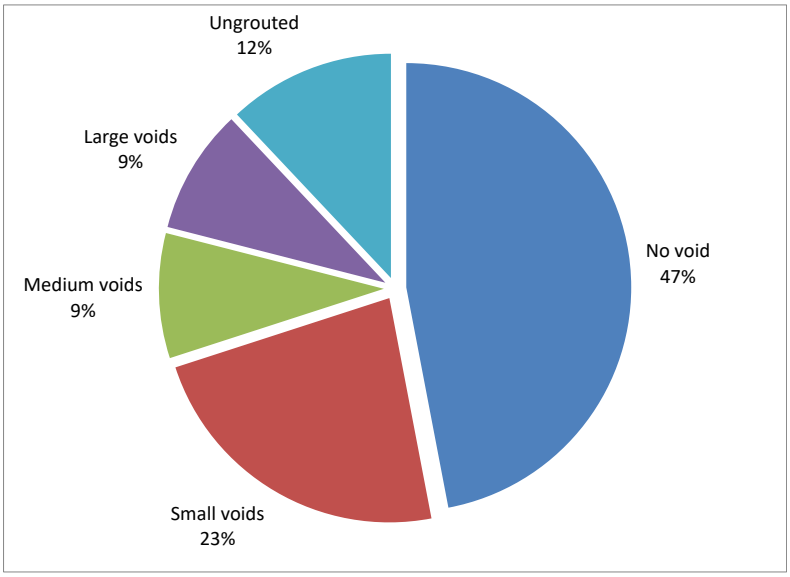

Source: FHWA.

Figure 42. Graph. Distribution of void sizes for 447 UK bridges.

About 36 percent of the inspected locations contained voids large enough to allow the strands to be at least partially exposed. Also, the older bridges showed a noticeable trend of having larger voids.

Figure 43 presents another pie chart related to the distribution of corrosion severity constructed with the data included in the paper entitled "Durability of Post-Tensioned Tendons on Road Bridges in the UK."[7]

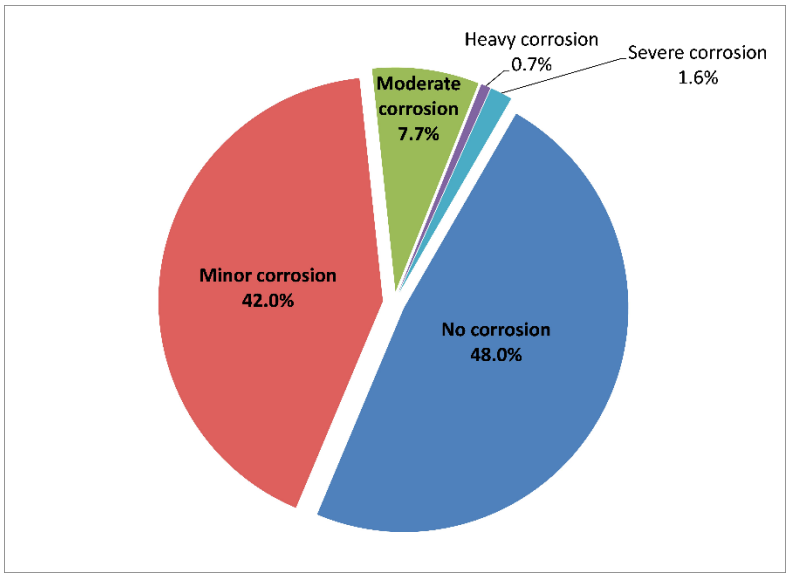

Source: FHWA.

Figure 43. Graph. Distribution of corrosion severity for 447 UK bridges.

Exactly 90 percent of the bridges were in good condition, exhibiting either no or minor corrosion. Also, most observed corrosion fell into an "isolated in occurrence" category. Woodward used the term "substantial corrosion" to describe the degree of corrosion. According to his subjective classification, corrosion was more prevalent in older bridges. The bridges constructed in the 1950s were the worst, accounting for approximately 25 percent of the samples exhibiting substantial corrosion. Those built since the late 1970s were the best, with very little substantial corrosion.

Woodward also reported that water was found in 13 percent of a smaller sample group of 281 bridges, sometimes with chloride in the grout. Most of the water-containing tendons had voids in the ducts that could be potential sites for future deterioration. Even though voids were common, and many ducts contained exposed strands, very few strands showed signs of severe corrosion after several decades of service.

Woodward stated in his conclusions: "The isolated voids in themselves are not a major problem if the ducts are well sealed from the atmosphere and the presence of even a thin layer of grout over the surface of the wires provided effective corrosion protection." At the same time, he also questioned the longevity of the protective grout layer and pointed out the difficulty of detecting insidious deterioration in PT bridges.

In 2004, Pearson-Kirk et al. reported on the results of field investigations of various PT bridges in the United Kingdom and France, as well as on Boston's Central Artery/Tunnel Project (also known as the Big Dig Project) in the United States. Some of the results from Pearson-Kirk et al. are summarized in figure 44. [(75,76)]

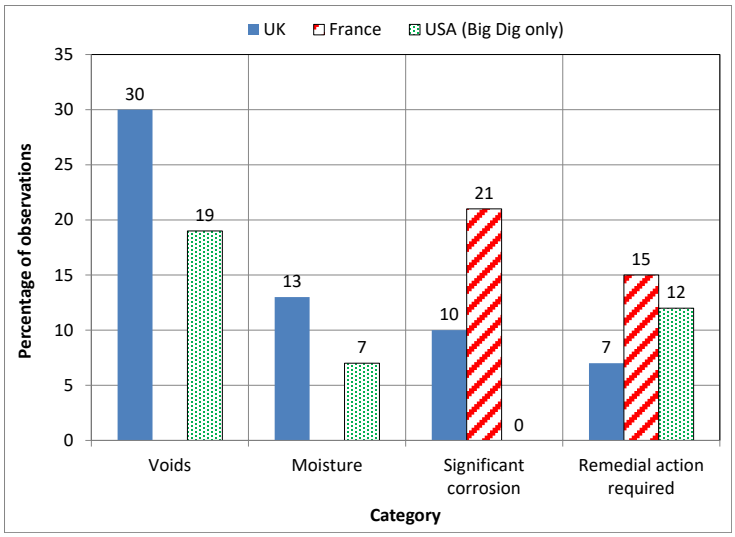

Source: FHWA.

Figure 44. Graph. UK and France PT bridges and Boston Big Dig investigation results.

It is unusual to see that 21 percent of the observations revealed significant corrosion in the French data. Because there were no pertinent data available for France related to grout void and moisture, it was not possible to explain such a high percentage of significant corrosion. Despite many voids, no reportable corrosion was found in the Big Dig Project, which was still new at the time.

13.3 Austria

In 2002, a special report published by VSL International Ltd. referred to field investigations of 10 bridges located in Vienna, Austria, citing a report by Eichinger et al. that is not easily available today.[77] During the field investigations, more than 10,000 spots on the 10 bridges were reportedly opened to record grout conditions and severity levels of tendon corrosion. The complete data subsets related to the discovered grout voids and severity levels of corrosion are reconstructed in the pie charts shown in figure 45 and figure 46.

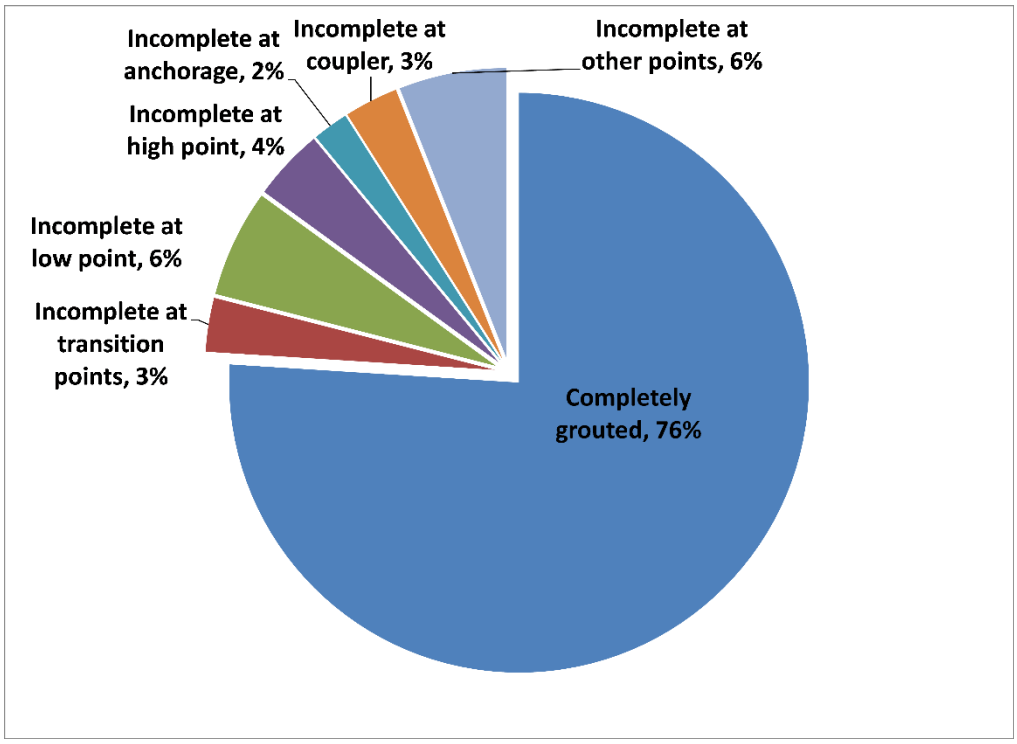

Source: FHWA.

Figure 45. Graph. Distribution of grout voids for 10 bridges in Vienna, Austria.

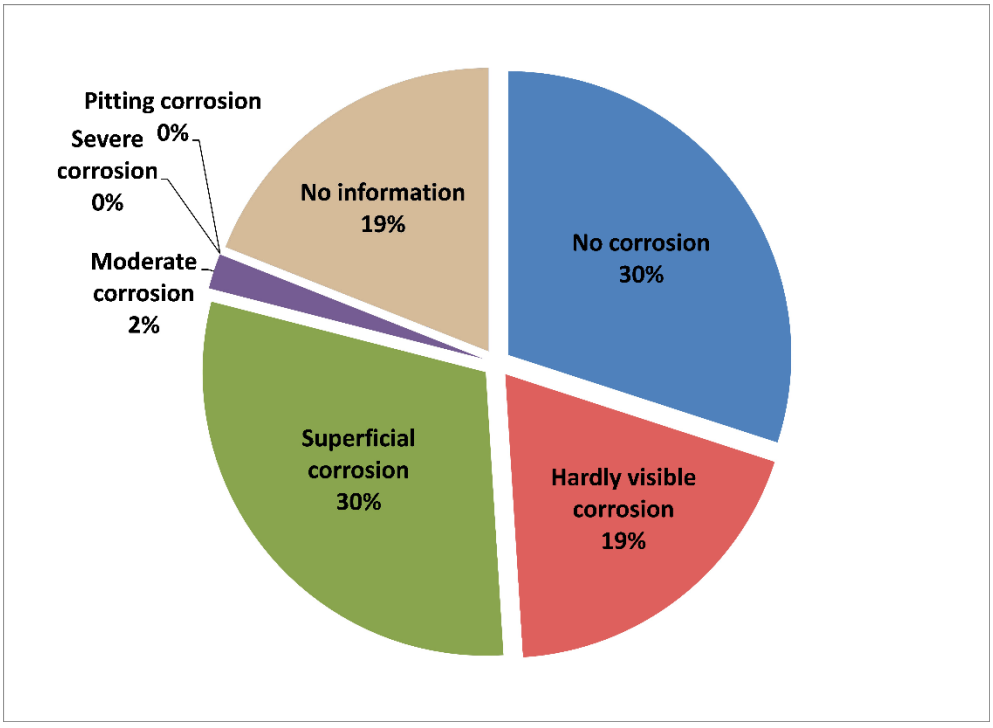

Source: FHWA.

Figure 46. Graph. Distribution of corrosion type for 10 bridges in Vienna, Austria.

Investigation results indicated that the actual performance and durability of the PT tendons were excellent: 76 percent of the opened locations were filled with grout, and the remaining 24 percent were not. Among the incomplete grout filling cases organized in figure 45 and figure 46, the majority showed no corrosion (30 percent), hardly visible minor corrosion (19 percent), and superficial corrosion (30 percent). Only 2 percent showed moderate corrosion, and no severe or pitting corrosion was observed. Minor and superficial corrosion could be removed with a soft cloth.

The same VSL report also mentioned that significant corrosion problems were found in the United Kingdom, France, Denmark, Germany, Italy, and Japan. Anchorage inspections were carried out for approximately 63 percent of the bridges investigated in the United Kingdom Among the anchorages inspected, 75 percent contained no or minor corrosion, 19 percent contained moderate corrosion, and 6 percent contained heavy corrosion with significant section loss (the presence of wire fractures or severe corrosion where at least half of the tendon wires were fractured).

13.4 Germany

In 2006, Weiher and Zilch conducted a survey on PT bridge conditions in Germany.[78] A total of 125 PT bridges that exceeded a total length of 300 ft were selected. The bridges represented about 60 percent of the bridge deck area of German PT bridges at that time. The overall condition of the selected bridges was assessed by surveying the bridge owners with a questionnaire. The gathered results were classified into three damage categories: serious, medium, and slight. Serious damage referred to fractures of the tendon affecting the loading capacity. Medium damage was defined as a situation in which serious damage, due to tendon corrosion and incompletely filled ducts, would be possible in a very short time. Slight damage included concrete spalling at PT elements and corrosion developed in the anchorage zones and ducts. Figure 47 features a stacked column chart showing the reported survey data from the perspective of the relationship between yr of construction and level of damage.

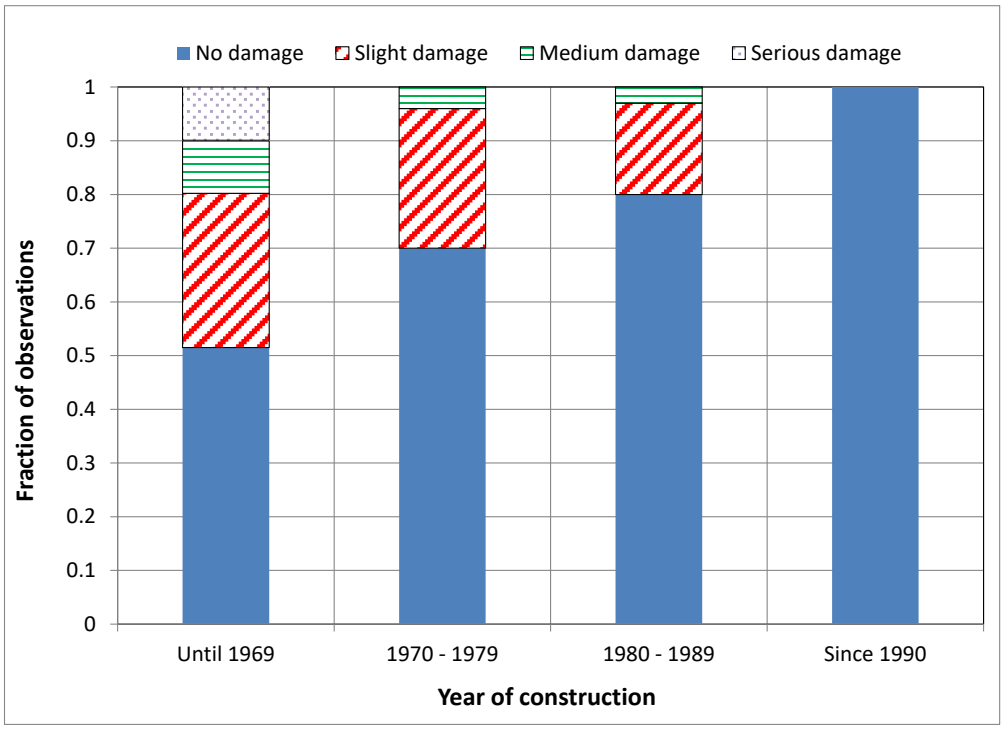

Source: FHWA.

Figure 47. Graph. Relationship between construction year and corrosion damage in German bridges.

As expected, younger bridges experienced less corrosion damage: Almost 50 percent of the bridges built before 1970 exhibited corrosion damage, and 10 percent had serious damage. In contrast, none of the bridges built after 1970 exhibited serious corrosion damage, and only 4 percent had medium damage. The bridges built since 1990 did not show any damage. Figure 48 shows the data for all the bridges in terms of the corrosion damage type.

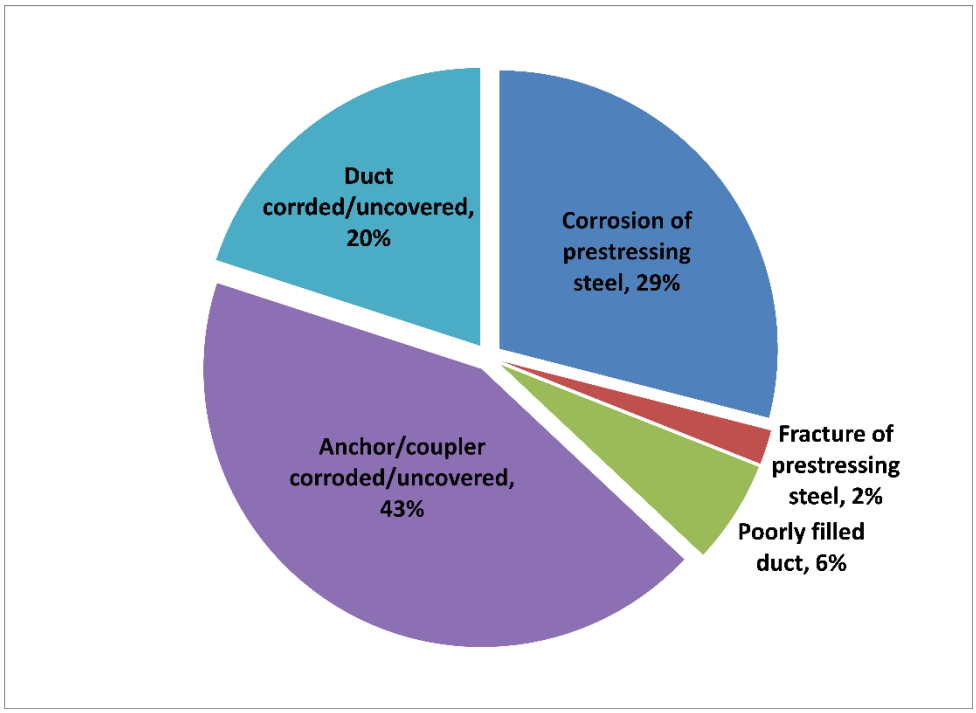

Source: FHWA.

Figure 48. Graph. Distribution of corrosion damage type for 125 German PT bridges.

For all of the 125 bridges in the German study, most of the corrosion damage fell into the slight damage category, and only 2 percent fell into the serious damage category, i.e., fracture of the prestressed strands.

13.5. Italy

According to a survey of available literature, four PT bridges in Italy were reported to experience serious corrosion problems or structural failure. The following summarizes each case.

13.5.1 Unidentified Bridge[24,79,80]

An unidentified segmental box girder PT bridge experienced failure of an external tendon less than two yr after it was completed. Follow-up investigations then led to the replacement of additional tendons. The bridge spans supported by the external tendons ranged from about 164 to 410 ft. Each tendon contained 27 7-wire steel strands inside HDPE ducts that were filled with grout mixed at the construction site. The grout had a water-cement ratio of 0.32 with the addition of a commercial admixture. The fresh grout was able to pass the inclined tube and wick-bleed tests and thus was expected to fill the ducts without any segregation problems.

The inclined sections between the last deviation points and the anchorages of the failed tendon showed deep localized corrosion damage on the wires in contact with the segregated grout. It was apparent that corrosion was associated with the whitish unhardened paste. Laboratory investigations, which will be discussed in more detail in chapter 4, were carried out to determine causes for the grout segregation and unprecedented rapid tendon failure.

13.5.2 Petrulla Viaduct[81]

Petrulla Viaduct is situated along State Road 626 in the Salso Valley in Sicily. It was built in the mid-80s. The viaduct consists of 12 simply supported precast PT I-beams, each 131 ft long. Its 37-ft-wide deck was supported by four beams equally spaced at 9.4 ft. In July 2014, one span of the viaduct collapsed, injuring four people. The collapsed span is shown in figure 49.

Figure 49. Photo. Petrulla Viaduct after its collapse.[81]

While the exterior concrete appeared visually to be in good condition, investigations revealed construction flaws, including a lack of grout in the internal tendons (see figure 50-A) and improperly sealed grout vent tubes (see figure 50-B). Severe corrosion of the metal ducts was also observed (see figure 51).

A. Empty duct indicating lack of grout in the internal tendon.

B. Improperly sealed grout vent tubes.

Figure 50. Photos. Flaws found in the internal tendons.[81]

Figure 51. Photo. Metal ducts perforated by corrosion.[81]

These deficiencies indicated that the PT tendon work was not carried out correctly. Lack of adequate concrete cover, leaking joints, and inadequate concrete workability also contributed to the deterioration of the PT tendon system.

13.5.3 La Reale Viaduct[81]

La Reale Viaduct, part of the Fossano bypass road, consists of simply supported PT box girders, each 101 ft long and 29 ft wide, and a cast-in-place concrete deck slab. Each of the eight parabolic tendons contains 19 0.8-inch strands. One ramp of La Reale Viaduct collapsed in 2017, as shown in figure 52.

Figure 52. Photo. Collapsed La Reale Viaduct ramp.[81]

Visual inspections confirmed that the collapse was triggered by a shear failure in one of the joints due to the absence of the equilibrating action of the prestressing force. Even though the overall external condition appeared to be good, the strands did not have sufficient grout protection at the collapsed joint, which led to a corrosion-induced tendon failure. Lack of redundancy in the prestressing members, inadequate grout injection inside the tendons, and inaccessibility for structural inspections were noted. Figure 53 shows the severely corroded PT tendons of the collapsed ramp after they were extracted from the concrete.

Figure 53. Photos. Severely damaged tendons extracted from collapsed La Reale Viaduct ramp.[81]

European field data indicated that the probability of severe corrosion in the PT tendons was relatively low even though grout voids and exposed strands were reasonably common in

hardened grout, especially in older bridges. However, severe corrosion or even the fracturing of strands can occur after a relatively short period of exposure to segregated grout.

14. CANADA

In "Internal Post-Tensioning Tendons: Many Problems and Sometimes Solutions," Gilles reported on a 2005 incident involving a fracture of sheathed strands.[82] Several liters of trapped water were observed in an anchorage in the downward tendons. The injected wax was floating over the water in the anchorage in question. This aggressive environment allowed the development of SCC just behind the anchor head. The author stated that high-strength steel (278 ksi) stressed at 80 percent of the ultimate tensile strength was a contributing factor for the observed SCC development. He added that SCC might begin to appear if wire stress exceeded 174 ksi.

15. JAPAN

In 2001, Mutsuyoshi discussed PT bridges in Japan in the paper "Present Situation of Durability of Post-Tensioned PC [prestressed concrete] Bridges in Japan," which was published in *Fib Bulletin No. 15: Durability of Post-Tensioned Tendons,* after inspecting 120 prestressed concrete bridges.[83] Chloride was found to be the most frequent cause of corrosion (14 out of 24 PT bridges), and poor-quality grout was responsible for most tendon breakage (12 out of 22 PT bridges). This high failure rate for tendons proved that grout quality was essential, and the stressed strands had a low tolerance for deficient grouts.

The author randomly selected 84 PT bridges constructed between 1962 and 1985 to examine grout quality using X-ray and an "impact-elastic wave method." A total of 640 tendons in 340 main girders were investigated, and the results were published. Figure 54 shows the distribution of five grout conditions in the main tendons and lateral tendons.

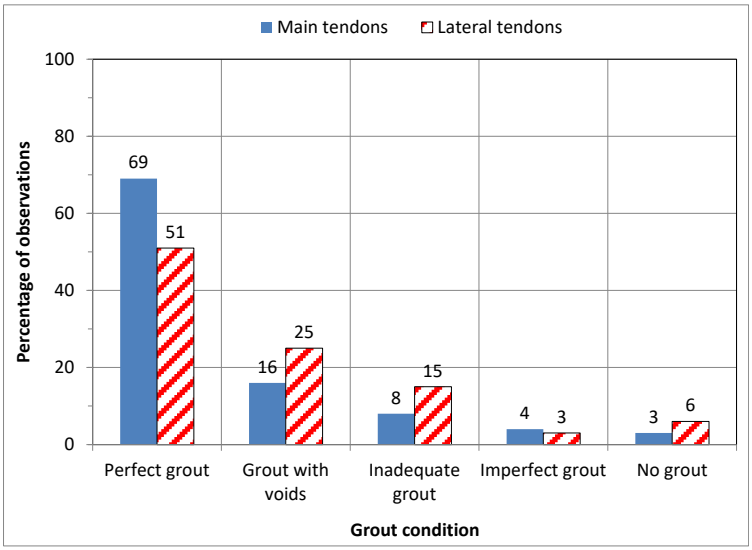

Source: FHWA.

Figure 54. Graph. Grout condition per tendon type in Japanese PT bridges.

Approximately 69 percent of the main tendons and 50 percent of the lateral tendons contained sound grout. The remaining tendons (30 percent of the main tendons and 50 percent of the lateral tendons) contained some grout defects ranging from minor voids to no grout, as shown in figure 54. The author did not provide a detailed description of each grout condition.

The author also investigated the effect of tendon length on grout conditions. The tendons shorter than 15 ft contained negligible deficient grout. The tendons between 15 and 62 ft long had a slightly higher percentage of having perfect grout condition than the longer tendons (80 percent versus less than 70 percent). It was clear that longer tendons tended to develop problematic grouts more, especially grout voids, than shorter ones. The author also offered additional field data related to grout condition versus tendon type (wire, strand); anchor position (end, top); yr of construction; and free space in the duct after strands were installed. However, none of the data showed statistically significant relationships.

16. SOUTH KOREA[84]

In 2016, bridge inspectors of Seoul Metropolitan Facility Management Corporation discovered failed external tendons due to corrosion in two precast segmental box girder PT bridges, the Cheong-Rung Creek Bridge and the Seo-Ho Bridge, during routine walkthrough inspections. Major corrosion problems found in the two bridges are described in section 16.1 and 16.2.

16.1 Cheong-Rung Creek Bridge

This bridge is part of a beltway highway system around the city of Seoul and opened to traffic in 1999. The bridge's overall length is 6,037 ft, and the bridge section containing the failed tendon is 1,378 ft long with a total width of 89 ft and a box width of 34 ft. The single-cell box girder contains 12 external tendons and eight internal tendons (10 tendons on each side of the box). Each external tendon contains 15 0.6-inch 7-wire strands in a four-inch-diameter PE duct, and each internal tendon contains 19 0.6-inch 7-wire strands in a 3.5-inch metal duct.

All the tendons were filled with neat cement grout mixed at the construction site. Even though construction records indicated an expansive admixture was used in the grout mix, its presence could not be confirmed in petrographic analysis of several grout samples. One external tendon failed due to corrosion in February 2016. Figure 55 shows the failed tendon when discovered.

Figure 55. Photo. Cheong-Rung Creek Bridge's failed tendon as discovered.[84]

An immediate field investigation discovered that five other tendons adjacent to the failed one at the same pier were also severely corroded. Figure 56 shows an external tendon that was found to contain two strands that were severed by corrosion when the PE duct was removed (see figure 56-A) and water droplets (circled with yellow dashed lines) on a downward-sloped section of the failed tendon (see figure 56-B).

A. Severely corroded strands.

B. Water droplets on two corroded strands.

Figure 56. Photos. Exposed strands in the failed tendon.[84]

Acid-soluble chloride analysis results of 41 grout samples indicated that the areas close to the failed tendon were contaminated with a very high level of chloride ions (up to 11,755 ppm by weight of the sample). In contrast, other areas farther away from the failure location contained a low level of chloride (less than 300 ppm).

Since empty grout vent tubes could provide a water path from the deck surface to the high points of the external tendons inside the diaphragms, extensive efforts were made to locate empty grout vent tubes from the deck surface. As a result, it was determined that 44 out of 73 (60 percent) of the grout vent tubes identified from the deck were empty, and the water droplets shown in figure 56-B were remnants from water leaking before the tendon failure.

Other locations of the bridge also experienced corrosion problems. Figure 57 shows a corroded anchorage zone consisting of an assembly of corroded strands and an anchor head extracted from a diaphragm close to the failed tendon.

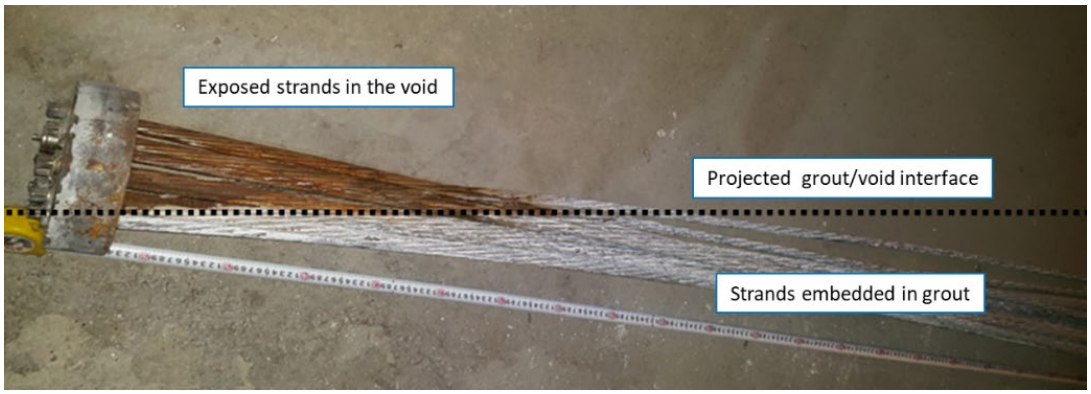

Figure 57. Photo. Corroded anchorage zone.[84]

The anchorage zone's corrosion pattern was distinctively different than that of the failed tendon because of a large grout void formed behind the anchor head. The projected plane of the interface where the remaining grout and void meet is indicated by a horizontal, dashed line in figure 57. The dashed line separates the corrosion-free strand section embedded in the grout from the corroding section exposed to the void space. Like the tendons that failed in the Niles Channel Bridge, Sunshine Skyway Bridge, and Mid-Bay Bridge, this tendon would also have eventually failed at the interface where the remaining grout and the void met if recharged water had filled in the voided anchorage zone for a prolonged period.

More than 11,500 pit depths were measured on 286 wire samples extracted from 49 strand segments. The wire samples were selected to represent various corrosion damage conditions and acid cleaned to remove stubborn products of corrosion before being measured. The outer wires removed from the fractured strands exhibited the most severe corrosion damage (maximum section loss of 97 percent), whereas the other outer wires exhibited moderate corrosion damage (maximum section loss of less than 35 percent). Based on the pit depth data, the failed tendon's estimated corrosion rate was roughly 39 mpy. Much less corrosion damage was found on the center wires, regardless of sampling location, than was found on the outer wires. These data suggested that the outer wires protected the center wires.

A field investigation revealed different forms of segregated grout because of poor grouting operations. High cement-water cement ratios in the grout were suspected. Some forms of the segregated grout were similar to forms observed in the United States; others were unique to this bridge. None of the grout samples contained sufficient levels of background chloride and sulfate ions to trigger corrosion. Some representative conditions of the deficient grout are presented in the following paragraphs and figures.

Figure 58 shows the segregated grout exhibiting a porous and frosty texture (see figure 58-A) over the normally hardened solid grout at the bottom half (see figure 58-B).

A. Porous and frosty grout.

B. Normal grout formed in the bottom of a tendon (view from below).

Figure 58. Photos. Various grout conditions.[(84)]

The defective grout contained numerous tiny bubbles and had no strength, which allowed a knife to penetrate easily, as shown in figure 58-A. Large grout voids were also observed frequently in most of the opened tendons. They appeared to be formed by a violent grout segregation process assisted by entrapped air. Figure 59 shows the remnants of air (or gas) bubbles adhered to the interior surface of the duct with a matching condition on the segregated grout (see figure 59-A) and a closeup of segregated grout containing large air bubbles (see figure 59-B). Both conditions must have formed during watery grout's initial segregation process.

A. Air bubbles in segregated grout.

B. Close-up of the segregated grout.

Figure 59. Photos. Segregated grout containing air bubbles.[(84)]

Soft/wet grout was found in many opened tendon sections as well. Some grout samples contained more than 50 percent moisture content (mean moisture content = 38 percent). The cause or origin of the wet grout could not be determined. However, the wet grout did not result in corrosion of the strands. Figure 60 shows a thumbprint next to a spot cut out with a knife on a claylike soft/wet grout (see figure 60-A) and a freshly exposed strand showing no corrosion soon after the wet grout was removed with fingers (see figure 60-B). The latter condition reconfirmed that soft/wet grout itself does not always trigger corrosion.

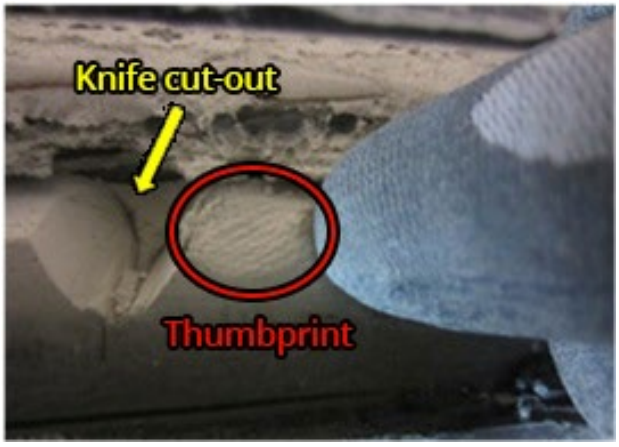

A. Thumbprint and knife cut-out on soft/wet grout.

B. Exposed strand without corrosion.

Figure 60. Photos. Exposed soft/wet grout.[84]

As shown in figure 61, many sections of the examined strands were covered with a thin grout coating (see figure 61-A) or partially buried in porous, frosty segregated grout (see figure 61-B).

A. Thin grout coating.

B. Exposed strands in segregated grout.

Figure 61. Photos. Strand conditions in deficient grout.[84]

Neither condition—having a thin grout coating or being buried in porous, frosty segregated grout—induced corrosion damage aside from atmospheric surface corrosion. It was apparent that the segregated grout did not cause any corrosion—despite excessive moisture contents—probably due to low levels of chloride and sulfate ions. However, it was uncertain whether the bridge would remain corrosion-free throughout its lifespan.

It was concluded that the corrosion-induced tendon failure was caused by excessive chloride ions carried by leaking water from the deck via empty grout vent tubes. This conclusion was based on the gathered evidence, i.e., heavily chloride-contaminated grout near the failure location, water droplets near the failure location, and empty grout vent tubes connected to the bridge deck. Incomplete grout filling and bleed water may also have been lesser factors in the corrosion problem. After the investigation, seven external tendons were replaced with new mono-strands (galvanized strands plus wax impregnation inside HDPE sheathing) and wax-filled anchorages.

16.2 Seo-Ho Bridge

The Seo-Ho Bridge is also part of Seoul's beltway highway system and opened to traffic in 1997. The bridge's overall length is 15,912 ft, and it has a double-cell box girder width of 58 ft. Each box girder contains 16 longitudinal external tendons (five on each side of the web and three on either side of the center web). Each external tendon contains 27 0.5-inch 7-wire strands in a 4.3-inch-diameter PE duct. All its tendons were filled with neat cement grout mixed at the construction site. Like Cheong-Rung Creek Bridge, this bridge experienced corrosion problems after 17 years of service. Two major corrosion problems observed in this bridge are described in this section.

The first corrosion problem involved an external tendon that suffered from severe corrosion damage where a 43-ft-long grout void formed across four deviation blocks in its bottom, horizontal section, running parallel to the girder floor. Such an abnormally large and extended grout void could likely be caused by excessive bleed water and entrapped air in the horizontal region during the grout injection. The corroded-in-two wires and other wires exhibiting significant section loss were mostly concentrated between two deviation blocks in the middle of the span. No water was found in the empty duct at the time of the investigation. Instead, many small pieces of the segregated grout were piled up in the form of chalky grout at the bottom of the duct. Figure 62 shows small fragments of chalky grout (see figure 62-A) and a closeup of the severely corroded strands in contact with the chalky grout (see figure 62-B).

A. Chalky grout fragments.

B. Severely corroded strands.

Figure 62. Photos. Severely corroded strands exposed to chalky grout on Seo-Ho Bridge.[84]

The presence of the chalky grout next to the corroded strands indicated that the segregated grout must have played a major role in the corrosion process.

A neighboring tendon section also showed severe corrosion beneath thick corrosion products that were mingled with grout residue. Figure 63 shows the corroded strands upon duct opening (see figure 63-A) and the cleaned strands after the corrosion products were removed from the affected area (see figure 63-B).

A. Before removal of corrosion products.

B. After cleaning the strands.

Figure 63. Photos. Corroded strands before and after cleaning.[84]

These photographs were believed to be snapshots of serious, ongoing corrosion, but they were not representative of the worst condition seen with this corrosion problem, which is shown in figure 62-B.

The second corrosion problem was discovered near a thick pier diaphragm in another span. When a suspicious-looking external tendon was opened, some loosened strands were observed, initially at one location. Later, entire strands completely severed by corrosion were discovered at a nearby location. This failure also occurred in a horizontal bottom section between a pier diaphragm and the third deviation block. An approximately 44-ft-long, virtually empty duct started from the anchorage zone inside the diaphragm. Figure 64 shows some loosened strands coming out of the diaphragm (see figure 64-A) and strands completely severed by corrosion near an anchor head inside the diaphragm (see figure 64-B).

A. Loosened strands.

B. Completely separated strands.

Figure 64. Photos. Failed strands in the second damaged tendon.[(84)]

Same as with the corrosion-damaged tendon shown in figure 63, no water was found in the empty duct section. While the physical conditions were very similar, this tendon must have failed in the voided area without intimate contact with the segregated grout. This speculation was based on the observation that no grout was found there.

Another tendon in the same span had a similar condition, with an approximately 23-ft-long grout void. The majority of the strands extracted from the empty duct section inside a diaphragm did not have noticeable amounts of grout residue on the surface. Instead, they were covered with corrosion products that resembled those formed under atmospheric conditions. Figure 65 shows two close-up photographs of moderately corroded strands.

A. Corroded strands.

B. Other corroded strands.

Figure 65. Photos. Closeups of corroded strands near anchor head.[84]

Some strands had small droplets of solidified corrosion products, instead of grout, indicated by yellow dashed lines. A similar condition was observed in the Mid-Bay Bridge.[29]

The failed tendon also had several forms of segregated grout along the tendon length. Figure 66 shows a small soft/wet grout band along the tendon length (see figure 66-A) and chalky grout (see figure 66-B).

A. Localized soft/wet grout.

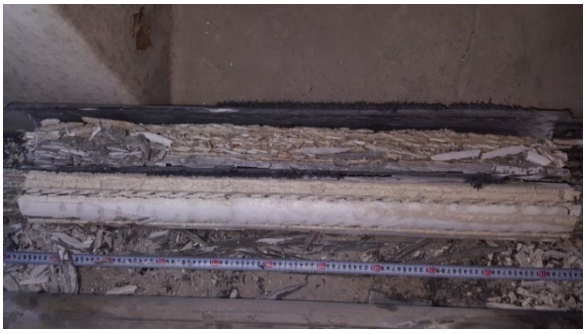

B. A large collection of chalky grout.

Figure 66. Photos. Segregated grout in an opened external tendon.[84]

Large bleed channels formed at 12 o'clock were also frequently observed in this tendon. The width of the bleed channels varied from less than 0.5 inches to wider than 2.5 inches. These grout conditions suggested that a significant bleeding problem took place during grouting.

Surface corrosion was observed occasionally on the strands partially buried in the segregated grout. Figure 67 shows the undisturbed condition of two exposed stands when a duct was removed (see figure 67-A) and the cleaned condition of the same strands after the segregated grout and surface rust were removed (see figure 67-B).

A. As-exposed condition.

B. Cleaned condition.

Figure 67. Photos. Exposed strands before and after removal of segregated grout and rusts.[(84)]

Minor surface corrosion can be seen on the cleaned strands inside the opened external tendon. The grout around the cleaned strands exhibited a brush mark, indicating that it was soft, like clay. Laboratory investigations, including petrographic analysis of grout samples and corrosion products, revealed the following:

- High water-cement ratios rendered overall grout quality poor: Three grout samples were over 0.55, and the others were between 0.45 and 0.55.
- Cement hydration appeared highly advanced or substantially complete, and many grout samples might not have had sufficient alkalinity to inhibit corrosion.
- Evidence indicated segregation of grout was extensive.
- Moisture content varied in 71 grout samples between 21.6 percent and 44.3 percent.
- The edges of the grout fragments and wet grout surfaces showed severe carbonation.
- Acid-soluble chloride analysis of 45 grout samples showed that 42 samples (93 percent) contained less than 0.04 percent by the sample weight. The remaining three contained less than 0.07 percent.
- The corrosion observed in this bridge most likely not related to chloride.
- The total sulfur in terms of SO_3 and water-soluble sulfate concentrations measured 2.19–5.54 percent and 0.02–0.80 percent of the sample weight, respectively. Four of the eight water-soluble sulfate concentrations exceeded 0.1 percent, which could be a concern for corrosion.
- The two highest water-soluble sulfate concentrations measured 0.80 and 0.37 percent, both in powder form of the segregated grout. The release of water-soluble sulfate ions was closely related to the grout segregation phenomenon.

- Based on over 6,100 pit depth measurements, mean section losses were estimated to be 8.7 mil in the areas dominantly exhibiting uniform corrosion and 37.8 mil in the areas dominantly exhibiting pitting and crevice corrosion.

It was concluded that the root cause of the segregated grout problem stemmed from poor grouting operations. In turn, the grout segregation resulted in an excessive amount of bleed water and large grout voids, likely augmented by entrapped air in the horizontal tendon sections. Different forms of segregated grout randomly filled the tendons without a consistent pattern, and some were carbonated. These conditions could not protect the exposed strands properly. Subsequently, severe corrosion damage occurred in the voided areas and in some carbonated grout. Excessive amounts of water-soluble sulfate ions released from the segregated grout in local areas also contributed to initiating and accelerating corrosion.

At the end of the investigation, seven tendons were replaced, and an additional 132 extra tendons (each containing 16 0.6-inch 7-wire strands) were installed through reserved tendon holes to provide adequate structural redundancy.

17. HONG KONG[85]

The Shenzhen Bay Bridge, opened to traffic in 2007, is a six-lane bridge that goes across the bay between Lau Fau Shan, Hong Kong and Shekou in Shenzhen, China. It is 18,045 ft long and consists of two sections: the Hong Kong Section (11,483 ft) and the Shenzhen Section (6,562 ft). The bridge consists of a multispan, concrete viaduct plus two cable-stayed steel bridges over two navigation channels. The Hong Kong section's concrete viaduct is a twin deck structure with a single-cell, trapezoidal box girder (49.2 ft wide and 12.5 ft deep) constructed by the precast segment method. The precast segments were assembled by multiple internal and external PT tendons.

During a routine inspection in February 2019, Hong Kong Highway Department staff discovered a ruptured external tendon (designated T3) in the concrete viaduct of the Hong Kong section. Prior multiple inspections conducted in 2018 and 2019 did not find any sign of its imminent failure.

The ruptured T3 was installed in 2005 and consisted of 37 0.6-inch 7-wire strands in a 6.3-inch-diameter HDPE duct filled with cementitious grout material. The length of T3 was about 919 ft, spanning from pier 1 (P1) to pier 5 (P5). Eight pairs of external tendons (T1 through T8) pass through high points at five pier diaphragms and multiple deviation blocks installed at the bottom slab.

Figure 68 shows an overview of the failed P5 anchor head (see figure 68-A) and an end view of the anchor head (see figure 68-B).

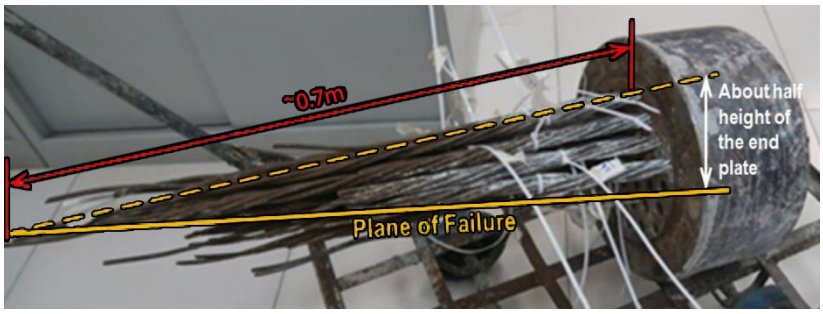

A. Overview of failed P5 anchor head shows strands attached. Modified by FHWA.

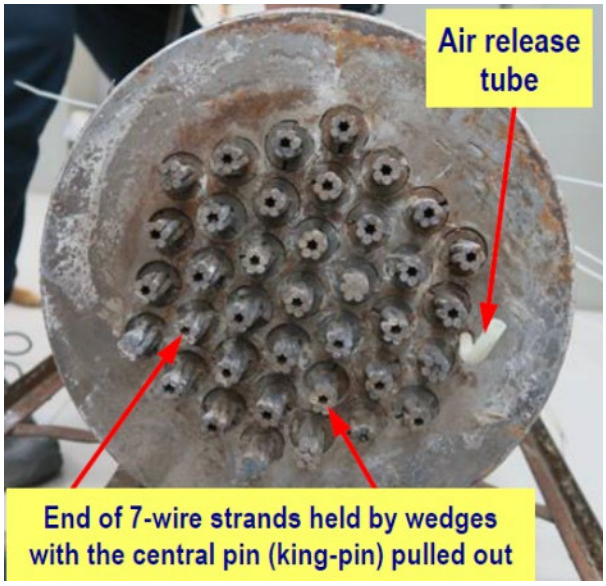

B. End view.

Figure 68. Photos. Corroded P5 anchor head on Shenzhen Bay Bridge (Hong Kong).[85]

About half of the upper portion of the strands attached to the P5 anchor head were failed and showed signs of serious corrosion—significant section loss and sharp wire tips—on most of the wires along a horizontal plane. The lower half of the strands on the same anchor head were embedded in the grout and mainly failed by overstressing. Most of the ruptured wires in this area exhibited a cup-and-cone fracture morphology, which indicated ductile failure by the necking process. No evidence of wire embrittlement and shear-type failure was observed.

White powdery paste, probably caused by grout bleeding, was observed on the strands near the P5 anchor head. The strands that were recovered from the mid-height section—between the upper and lower halves—of the P5 anchor head showed transitional corrosion morphologies from superficial corrosion to moderate corrosion without significant section loss. The strands at the opposite side (P1) anchor head were uniformly covered with whitish cementitious material, and all the exposed strands exhibited no sign of corrosion.

The grout contained a commercially available admixture for shrinkage compensation and

thixotropic properties that allowed a low water-cement ratio of about 0.25. Chemical analyses of grout samples collected at the failed tendon, including two anchor heads, did not indicate any corrosive conditions: The chloride content was less than 0.1 percent, and the pH level was between 12 and 13.5. Also, EDS analysis at the corroded surface and at the base metal interface revealed no signs of any aggressive elements.

However, the grout vent tube at the P5 anchor head was not filled with grout, and traces of grout residue were observed inside the tube. Similar morphology was found at the interfacial region between the air pocket and the segregated grout layer. Figure 69 illustrates corrosive conditions near the failed P5 anchor head schematically.

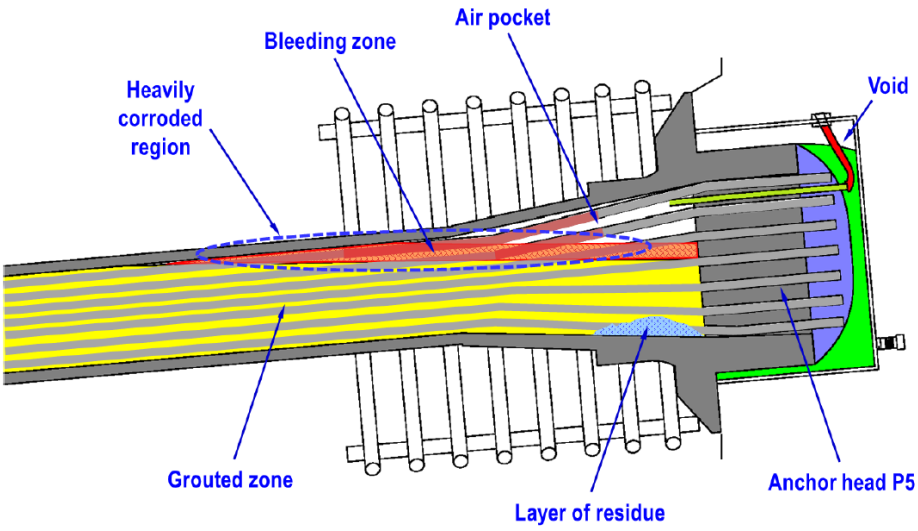

Figure 69. Illustration. Schematic of corrosive conditions near P5 anchor head.[85]

It was speculated, based on a pressure test conducted in the duct prior to stressing the tendon, that a high water-cement ratio, originating from the bleed water and possibly the residual water as well, had created deficient grout. The residual water collected at the duct's low point would have been pushed through in front of the fresh grout mix toward the anchorage zones at piers 1 and 5. The mixture of fresh grout and excessive water at the grout front may have promoted grout segregation. The grout vent tube at the P1 anchor head did not appear to experience any blockage problem. From these observations, investigators suspected unbalanced grout pressures had formed at the P1 and P5 anchor heads due to uneven distances from the grout injection point: 361 ft (P1) versus 558 ft (P5). Figure 70 illustrates a situation of unbalanced pumping pressure along the failed T3 tendon.

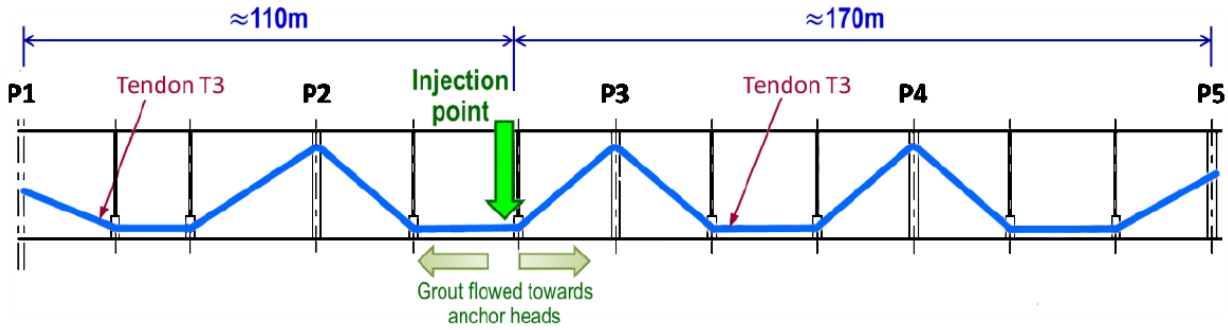

From the injection point to P1 = 361 ft (~110 m); from the injection point to P5 = 558 ft (~170 m).

Figure 70. Diagram. Uneven distances between injection point and P1 and P5 anchor heads.[85]

As the fresh grout was pumped toward the P5 anchorage zone, the pumping pressure may have been reduced as the duct length increased. In the presence of partial blockage in the grout vent tube, the reduced pressure may have prevented the entrapped air from being freely released at the P5 anchor head. On the other hand, the grout pressure at the P1 anchor head should have been sufficient to prevent an air pocket there.

Investigators concluded that three factors that occurred during the grouting operation had contributed to the failure of the T3 tendon: The segregation of grout due to excessive water in the duct, a lower pumping pressure toward the P5 anchor head than toward the P1 anchor head, and the partial blockage of the grout vent tube at the P5 anchor head. As a result, the anchorage zone contained an air pocket behind the P5 anchor head, where the bleed water was able to evaporate and then condense again. In addition, the interfacial zone between the top layer of the segregated grout and the air pocket contained a permeable and weakened cementitious material in the form of a white powdery paste. These conditions created a corrosive environment where intensive corrosion took place on the steel strands exposed to the interfacial zone. Ultimately, significant corrosion-induced section loss reduced the strands' load-carrying capacity and then led to the rupture of the T3 tendon near the P5 anchor head.

CHAPTER 4. LABORATORY STUDIES

Since 1990, more than 20 laboratory studies related to PT systems have been performed globally to develop and evaluate tendon fillers (mainly cementitious grout) and research characteristics of deficient grout, corrosion mechanisms and corrosion control methods, and other related topics. This chapter presents the major findings of selected laboratory studies conducted in the United States and Europe. Whenever possible, the studies are presented in chronological order. The topics of the selected studies include grout segregation and bleeding, grout voids, corrosion mechanisms, corrosion control methods, alternative corrosion-resistant materials, flexible fillers, and the corrosivity of chloride and sulfate ions in the grout. This chapter also covers the findings of several indepth petrographic analyses conducted as part of forensic investigations.

1. CORTEST COLUMBUS TECHNOLOGIES [86]

From 1988 to 1991, the Federal Highway Administration (FHWA) sponsored a laboratory study to develop new grouts and create accelerated corrosion testing methods. Additionally, the study sought to analyze how these new grouts performed in relation to corrosion compared to conventional grouts. The study's researchers discovered that the use of silica fume in a water-cement ratio of 0.365 grout mix significantly reduced pressure-induced bleeding seen in neat portland cement grout. By adding 10 percent of silica fume by weight of cement and a superplasticizer (0.19 fluid ounces per pound [fl oz/lb]), only 16 percent of the water was lost at 80 pounds per square inch (psi). At 20 percent silica fume and a higher dosage of superplasticizer (0.47 fl oz/lb), initial water loss did not occur until 30 psi, and only 6 percent of the water was lost at 80 psi. An anti-bleed admixture (1.5 percent by weight of cement) with a low water-cement ratio and silica fume effectively reduced pressure-induced grout bleeding.

The researchers also studied how additives could delay the onset of corrosion. A grout mix with a water-cement ratio of 0.32 containing 33 percent fly ash by weight of cement and a superplasticizer tripled the time to initiate corrosion relative to standard grout (Type II cement with a water-cement ratio of 0.44). A calcium nitrite corrosion inhibitor and superplasticizer improved corrosion performance at a water-cement ratio of 0.365. The best corrosion protection was offered by a grout mix containing 10 percent silica fume replacement by weight of cement and a superplasticizer. This grout took a longer time to initiate corrosion and displayed a slower increase in CR than other examined grout mixtures.

On another note, the researchers warned that the use of expansive additives such as aluminum powder should be reconsidered because these types of agents could not provide uniform and controlled expansion at the right time during the hydration process. They reasoned that the expansive admixtures contributed to an expansion by gas only when the grout was in a fluid or plastic state. Once the grout had hardened, these additives could not expand further, leading to drying shrinkage and overall volume reduction.

2. THE UNIVERSITY OF WISCONSIN AT MILWAUKEE [87]

From 1989 to 1992, Ghorbanpoor and Madathanapalli performed another FHWA-sponsored laboratory study to identify the most appropriate grout mix for PT bridges. The following section summarizes their major findings, which emphasized the relationship between grout properties and the corrosion of 7-wire strands.

The researchers evaluated 15 different grout mixes by manipulating quantities of various grout ingredients, including Type I portland cement, silica fume, an expanding/fluidifying/water-reducing admixture, a superplasticizer, and other miscellaneous admixtures. These admixtures included a superplasticizer/thickener/expansion agent, a dispersant/thixotropic agent, and a gas-generating agent. The researchers conducted the following evaluations:

- Testing for expansion and shrinkage.
- Testing with the Gelman pressure test.
- Testing for compressive strength.
- Testing for flow.
- Testing for permeability.
- Testing for the pH of bleed water collected from the Gelman pressure test.
- Testing for grout setting times with the Vicat apparatus.
- Examining for visual corrosion.

Most tests were carried out in transparent tubes measuring 2 inches in diameter and 52 inches tall. Tubes were filled up to the 39.4-inch mark with test grout mixes. Some of the specimens contained a 52-inch-long 7-wire strand.

As the percentage of silica fume replacement increased, shrinkage in the grout mixes decreased. This occurrence was attributed to microfine particles of silica fume that provided additional surface area and occupied fine pores in the mix. As a result, the grout mixes containing silica fume retained more water and reduced shrinkage.

Except for grout mixes containing the expanding/fluidifying/water-reducing admixture, increasing the percentage of silica fume also increased the mix's compressive strength and decreased the amount of bleed water. Researchers thought that the grout mixes with 20 to 25 percent silica fume replacement and a superplasticizer were most suitable for grouting tendons of PT bridges. In particular, a mix of 25 percent silica fume by weight of cement, 50 oz. superplasticizer per 100 lb of cement, and a water-cement ratio of 0.4 outperformed all other mixes. This mix exhibited low permeability, high compressive strength, minimal bleeding, good corrosion protection, and good flowability. All admixtures used in this study experienced less bleeding than was experienced by the control grouts.

As the water content increased for higher water-cement ratio mixes, the initial setting time also increased. More bleed water was observed when higher water-cement ratio mixes were used and the strands were in the tubes. For these samples, it took more than 20 h for the grout to reabsorb the bleed water. Grouts without strands in the tubes showed 2 to 12 percent more expansion than those with strands in the tubes. As expected, the compressive strength of the mixes decreased as the water-cement ratio increased.

The pH values of the bleed water samples from all the grout mixes measured in the vicinity of 13. After six months of testing, the strands were removed, cleaned with a wire brush, and examined. The control grouts contained no admixtures. No corrosion was observed on the strands buried in the control grouts with water-cement ratios of 0.35 and 0.40. However, a strand in the control grout with a water-cement ratio of 0.45 showed a 0.5-mil thick layer of corrosion that was caused by the bleed water before it was completely reabsorbed after 9 h.

The grout mixes containing the expanding/fluidifying/water-reducing admixture caused additional bleed water in the presence of strands compared to other mixes without it. The bleed water in the test tubes was responsible for the corrosion of the strands. The mixes containing 1 percent expanding/fluidifying/water-reducing admixture showed pitting corrosion in the bleed water. However, no corrosion was observed in the fully buried sections.

Corrosion pits larger than 115-mil wide and 13-mil deep were found in two mixes: a water-cement ratio of 0.35 plus 1 percent expanding/fluidifying/water-reducing admixture and a water-cement ratio of 0.45 plus 1 percent expanding/fluidifying/water-reducing admixture. The addition of a 0.5 percent expanding/fluidifying/water-reducing admixture in a grout mix (water-cement ratio of 0.4 with 20 percent silica fume and 47 oz. of superplasticizer per 100 lb of cement) improved the grout performance by providing some expansion. However, bleed water was also increased and caused corrosion of the strands. All specimens containing the expanding/fluidifying/water-reducing admixture exhibited very low compressive strength, higher porosity, and higher permeability than those made without the admixture.

The researchers concluded that if there was no void in the tendon, using the expanding/fluidifying/water-reducing admixture as an admixture would not significantly affect corrosion. However, void-free grout was difficult to achieve, and thus the admixture had a potentially detrimental effect on compressive strength, bleed water, and corrosion.

3. THE UNIVERSITY OF TEXAS AT AUSTIN

The Ferguson Structural Engineering Laboratory at University at Texas at Austin carried out a long-term research program related to corrosion performance and durability of PT tendons from 1993 to 2013. This 20-yr program consisted of two research projects, 0-1405 and 0-4562, sponsored by TxDOT and the FHWA.

3.1 Project 0-1405[88,89]

The first laboratory study, TxDOT Project 0-1405, was carried out from 1993 to 2003. Its objectives were to examine the use of the PT system in bridge substructures, identify existing technology to improve durability and address durability concerns, develop and carry out an experimental testing program, and develop durability design guidelines and recommendations for PT bridge substructures.

To meet these objectives, four experimental programs were developed, as follows:

- Grout studies to develop improved and high-performance grout with desirable fresh properties for providing good corrosion protection to prestressing strands.

- A series of long-term macrocell corrosion tests to investigate protecting internal tendons installed in precast segments from corrosion.

- Long-term corrosion tests to study the effects of post-tensioning on corrosion protection using 27 large-scale specimens.

- Additional long-term corrosion tests to examine corrosion protection in vertical columns.

3.1.1 Improved High-Performance Grout

Shokker et al. performed a laboratory study to develop a high-performance grout for PT tendons.[89] For this study, three grout mixes were tested in the draped parabolic mockup ducts. The first one was a grout with a water-cement ratio of 0.33 and 2 percent anti-bleed admixture. This grout had the best performance in the fresh property tests and a good performance in the accelerated corrosion tests. It was a very workable grout if kept agitated, and bleed water was not noticed in the duct at any time. Autopsy slices revealed no grout voids along the entire length of the duct. This mix was recommended for situations requiring high resistance to bleed (vertical rises of up to 114 ft based on results from the Gelman pressure test) and good corrosion protection. The researchers noted the anti-bleed admixture dosage might need to be adjusted slightly depending on conditions and product, but the dosage should be kept to a minimum to ensure maximum corrosion protection without sacrificing necessary workability.

The second grout mix contained a 30 percent fly ash with a water-cement ratio of 0.35 and 0.06 fl oz/lb superplasticizer. It had the best performance in the accelerated corrosion tests. This grout was very workable, and no voids were observed during pumping. Approximately 10 min after pumping, a long and very thin void was observed near the intermediate crest. Within 24 h, the water in the void was reabsorbed, and the void was no longer noticeable. Upon autopsy, no voids were found in any of the duct slices. This mix was recommended for situations requiring high resistance to corrosion without extreme bleed conditions (vertical rise of lower than 3.3 ft). This grout might be adequate for larger vertical rises (3.3–16.5 ft), but field testing should be performed, if necessary. The researchers noted the superplasticizer dosage might need to be adjusted according to the conditions (and brand used), but the dosage should be kept to a minimum to ensure maximum corrosion protection without sacrificing necessary workability.

The third grout mix was the standard TxDOT grout, which had a water-cement ratio of 0.44 and a 0.9 percent expanding/fluidifying/water-reducing admixture. The original mix of this grout was untestable because the grout never fully set and crumbled when touched. A follow-up retest with a new admixture was successful, so the original failed test was most likeley caused by the accidental use of old admixture that had expired. The retested grout was very workable and easy to pump. Immediately after pumping, bleed water was visible in the duct. Bubbles traveled to the intermediate crest, where a large void pocket formed. After 24 h, the bleed water was reabsorbed, and a large void remained at the intermediate crest.

The last two mixes had the same performance in the standard bleed test, but field testing showed significantly better bleed characteristics of the fly ash-containing grout than the TxDOT standard mix. The researchers noticed the TxDOT standard grout behaved with a more “loose” flow

pattern than the others. They hypothesized that this type of flow would form frequent air pockets because the grout initially filled only the lower half of the duct as it moved along the duct.

3.1.2 Ducts for Internal Tendons

Severe duct destruction and pitting were found in most specimens made with galvanized steel ducts. After 8 yr of testing, the primary chloride penetration into the tendon was through corroded ducts. The effect of the splices decreased as the duct began to corrode away, allowing more chloride ions to penetrate the grout and then the strand. On the other hand, the plastic ducts performed very well in the corrosive environment. Thus, plastic ducts should be used in chloride exposure conditions.

The industry-standard splice and the heat-shrink splice for the galvanized steel duct did not appear to effectively prevent moisture and chloride from reaching the grout. These harmful species seeped through the sides of the splice and got trapped between the ducts. No correlations were observed between splice type and amount of chloride ingress. Filled epoxy joints, in conjunction with unspliced plastic ducts, showed very good protection compared with the galvanized duct counterpart. The researchers concluded that better splicing systems were needed to avoid moisture and chloride penetration and subsequent corrosion at construction joints.

3.1.3 Segment Joints

Dry joints and incompletely filled epoxy joints of the macrocell specimens showed poor performance, as dry joints acted like preset cracks. On the other hand, thin epoxy joints offered substantially improved corrosion protection when compared to dry joints. Therefore, a correctly applied epoxy joint-filling method should be used to maintain water tightness at the joints.

The gaskets used in epoxy-jointed specimens did not allow for complete epoxy application at the joints but did allow moisture and chloride to enter the ducts. This problem might become worse under field conditions. The gaskets used at the duct ends also trapped moisture and induced crevice corrosion on the galvanized steel ducts.

3.1.4 Levels of Post-Tensioning

As levels of post-tensioning or concrete precompression increased, corrosion protection increased due to lowering permeability and better resistance to wicking effects, particularly for dry joint specimens.

3.1.5 Post-Tensioned Bars or Strands

Epoxy coating or galvanized coating showed enhanced general corrosion protection with respect to plain PT bars or strands. However, under very severe localized attacks in a crack or joint location, corrosion activity could still be severe, leading to unexpected failure. The epoxy-coated strand used in this test program only had a coating covering the exposed portion of the outer wires, and the interstices of the strand were not protected by epoxy filling. Since the flow-filled, epoxy-coated strand offered better performance than the nonflow-filled, epoxy-coated strand, the latter should not be used in aggressive environments. Also, a more resilient epoxy coating should

be used. Galvanized strand could delay the onset of corrosion, but it should be treated as a last line of defense against corrosion.

3.1.6 Anchorage Protection

The use of encapsulated anchorage protection systems appeared very promising. Because water can travel through strand interstices in the tendon, all anchorages should be fitted with permanent grout caps to reduce the risk of water entering through the anchor heads. Also, similar metals should be used in anchorage components to prevent galvanic (dissimilar metal) corrosion.

3.2 Project 0-4562[90-94]

After completing TxDOT Project 0-1405, a second laboratory study was carried out from 2003 to 2013. A new set of specimens—smaller-scale specimens than those made for Project 0-1405—was fabricated to evaluate the corrosion performance of new products intended for highly aggressive exposure conditions. Specimen dimensions were six ft long, 17 inches wide, and 13 inches deep. A three-ft-long and 13-inch-wide ponding well was installed in the middle of the top surface. PT force was applied through two internal tendons in the specimen and maintained self-equilibrium with PT bars at the bottom of the specimen. Many PT-related products were evaluated in this study: conventional 7-wire strand, hot-dip galvanized strand, copper-clad strand, stainless steel-clad strand, stainless-steel strand, flow-filled epoxy-coated strand, EIT, and various duct couplers. The following sections summarize researchers' conclusions after specimen autopsies were performed.

3.2.1 Ducts

3.2.1.1 Galvanized Ducts

The galvanized ducts performed very poorly even though they were continuous without physical connections. Every duct autopsied showed section loss and pitting. These corrosion damages were normally located at grout voids and transverse cracks in the concrete. The autopsied conditions of the galvanized ducts after six yr and four yr of exposure were similar. Most of the ducts from both testing periods exhibited pitting corrosion on their bottom inner surface. Therefore, it was recommended that galvanized ducts never be used in any aggressive environment due to their susceptibility to corrosion.

3.2.1.2 Plastic Ducts and Couplers

Plastic ducts sustained some scratching and gouging during threading and tensioning but were structurally intact**.** The greatly improved durability of the plastic ducts prevented most ducts from getting damaged during casting and post-tensioning or even during the highly aggressive chloride exposure testing. Therefore, it was recommended that they should be used in aggressive environments all the time.

The plastic ducts with couplers had grout chloride concentrations well above the corrosion threshold because the duct couplers or attachments could not be perfectly sealed. The two heat-shrink coupler types examined were very brittle at the time of autopsy and showed signs of breaches. Several of the mechanical snap-on couplers also showed signs of breaches. These cases

indicated that the sealing capability of the mechanical snap-on couplers and the bond of the heat shrink for the slip-on couplers were not adequate to prevent chloride ions from entering the ducts. Chloride concentrations were also very elevated in the continuous plastic ducts where grout vents were not an integral part of the coupler. For maximum water tightness, grout hoses should have a positive attachment to the grout vent tube.

3.2.2 Grout

Because grout was injected with a hand pump, the grout in the autopsied specimens was not always well consolidated and showed poor quality. In addition, the anti-bleed grout was heavily segregated, and, as a result, the anti-bleed admixture was not effective.

All tendons had chloride concentrations along the tendon length above the corrosion limit of 0.033 percent by grout weight. After the six-yr exposure testing, average chloride concentrations were approximately 19 percent higher than they were after the four-yr exposure testing.

3.2.3 Anchorage

Corrosion was found on the anchor heads and strand cut ends during the autopsy. In the case of the anchorages covered with caps, the strand ends were in much better condition. There was no appreciable difference between the galvanized and nongalvanized bearing wedge plates. Anchorage pour-back quality appeared to play a greater role in anchorage protection than the galvanized anchorage heads.

3.2.4 Strands

All the strand types showed low levels of corrosion. Among the four-yr exposure specimens, corrosion was more severe within the anchor heads than in the ponding areas. However, after 6 yr of exposure testing, both areas showed similar levels of corrosion. The following sections briefly discuss the corrosion performance of individual strand materials.

3.2.4.1 Conventional Strand

Even though the conventional strand met all industry requirements for mechanical properties, it showed the worst corrosion resistance. The outer wires of the conventional strands had light corrosion and exhibited discoloration. The corrosion observed on the inner wires was more severe than the corrosion observed on the outer wires.

3.2.4.2 Hot-Dip Galvanized Strand

The hot-dip galvanized strand performed worse than any other alternative strand material. Its corrosion damage was similar to that of a conventional strand. This particular galvanized strand product was galvanized after individual wires were wound. Thus, it was possible to make much of its interstitial space bare steel as it was not covered with molten zinc during the galvanizing process. In many cases, the exterior wires exhibited corrosion on the zinc coating as well as on the underlying steel, and heavy corrosion also occurred on the bare inner wires. This poor performance demonstrated the strand could transport moisture down its entire length.

The hot-dip galvanized strand's condition in the anchorage regions was similar to its condition in the ponding area. It had a very strong bond with surrounding grout and was difficult to remove. Small bubbles found in the interstices of some of the galvanized strand suggested the zinc might have reacted with the grout chemically. The six-yr testing specimens showed more extensive corrosion than the four-yr specimens. The presence of the galvanized coating only delayed the onset of corrosion. Therefore, hot-dip galvanized strand should not be regarded as a primary line of defense against corrosion.

3.2.4.3 Copper-Clad Strand

In general, copper and its alloys have good corrosion resistance. The copper-clad strand was composed of individual steel wires encased in copper cladding. The copper layer was metallurgically bonded to the steel so that the bond between the copper and the steel was very strong, but copper is softer and weaker than the steel.

The autopsied copper-clad strands in the saltwater ponding area exhibited a glossy black patina on all wires. The patina was darker and glossier on the inner wires than on the outer wires. The condition of the strands in the anchorage region was similar to the condition of the strands from the ponding region. Also, occasional tiny red spots were observed on the copper surface. It turned out that the wedges penetrated the copper cladding and caused the underlying steel to corrode there. The copper-clad strand performed better than the galvanized strand but worse than the stainless-clad and stainless-steel strands.

3.2.4.4 Nonflow-Filled, Standard Epoxy-Coated Strand

The nonflow-filled, standard epoxy-coated strand offered no advantage over the conventional strand from a durability standpoint. Because the epoxy coating did not also fill strand interstices, moisture could spread throughout the length of the strands.

3.2.4.5 Flow-Filled, Epoxy-Coated Strand

The flow-filled, epoxy-coated strand was autopsied after six yr of exposure testing. The inner and outer wires had corrosion ranging from mild pitting to light corrosion over the majority of their lengths and did not perform as well as expected. It was speculated that the corrosion probably existed before the strand was coated. The condition of the epoxy coating was good, with tiny holes, slight scratches, and slight gouges. The underlying steel was the same as that used in the conventional strand, so the mechanical properties were equivalent to the conventional strand and met all mechanical specifications.

The flow-filled, epoxy-coated strand outperformed the conventional epoxy-coated strand and all other strand types in corrosion resistance. This is because the epoxy gets in the interstitial areas and prevents moisture from initiating corrosion in these areas. As a result, when submerged in a chloride solution, encased in grout, or fully exposed, this type of epoxy-coated strand exhibited the least corrosion damage.

3.2.4.6 Stainless-Steel Strand

The stainless-steel strand performed very well on all corrosion tests. Its performance was only slightly behind the flow-filled, epoxy-coated strand. The stainless-steel strand in the saltwater ponding region showed very little corrosion after 4 yr and 6 yr. It appeared to be brand new in most areas. Some light corrosion occurred in the anchorage region. Additionally, this strand type had a very weak bond with the surrounding grout, resulting in debonding during the autopsy.

3.2.4.7 Stainless-Clad Strand

Stainless-clad strand benefited both from the strength of conventional steel and the corrosion protection of stainless steel. Its cladding process was similar to that of the copper-clad strand. The bond between the underlying steel and the stainless-steel cladding was very strong.

The stainless-clad strand was autopsied after six yr of exposure testing. Its condition was similar to that of the stainless-steel strand, with some discolorations and light corrosion spots. The stainless-clad strands bonded better to the grout than the stainless strands.

3.2.4.8 Strand Comparison

In conclusion, the flow-filled, epoxy-coated strands performed the best and conventional strands the worst. The second-best performing materials were the stainless-clad and stainless-steel strands. The third best performing materials were copper-clad and hot-dip galvanized. Since all the tests indicated that the flow-filled epoxy-coated strand performed the best, it was regarded as the best choice for satisfactory long-term performance in very aggressive environments.

3.2.5 Electrically Isolated Tendons

The EIT specimens were constructed so that the tendons were electrically isolated from the remainder of the specimens. Encapsulation was achieved using special anchorages, an isolating insert between the bearing plate and anchor head, and robust and watertight connections between the plastic duct and plastic trumpet. A permanent grout cap was installed over the anchor head to isolate the tendon further. In theory, the alternating current (AC) impedance measurements of an EIT could indicate whether the EIT lost its integrity or not. Moisture was observed when an EIT showing reduced AC impedance was cut open from the anchorage plate during autopsy, but it was also noted that the EIT was barely monitorable by AC impedance measurement.

The collected data indicated that strand corrosion in the fully encapsulated tendon was comparable to the nonencapsulated tendons in other specimens over both 4 and 6 yr of exposure testing. The actual corrosion conditions of the conventional strands encased in the EITs and the conventional PT system were similar. Except for the apex of the duct, where chloride concentrations were very near the corrosion threshold, chloride concentrations were well above the corrosion threshold. These chloride concentration data suggested that the poor bond of the heat shrink and the poor seal of the coupler had allowed chloride ions to enter the duct.

4. UNIVERSITY OF SOUTH FLORIDA[33,95,96]

Almost all the earlier corrosion problems observed in the Florida PT bridges were associated with grout voids and bleed water in the vicinity of the anchorage zone. Therefore, as part of the effort to understand corrosion in the anchorage zone, Powers, Sagues, and Virmani performed a laboratory investigation to examine the galvanic corrosion of dissimilar metals in the presence of water that could have been bleed water or recharged water that entered later. The dissimilar metals studied were the steel strands, ductile cast-iron anchor head, and forged-steel wedge plate.[33] The following section summarizes the study's findings after 166 days of testing.

The grout mix was made with Type I portland cement with a water-cement ratio of 0.45. It contained a 1 percent aluminum-based expansive admixture. A control mix was also made with the same proportions without the admixture. During standard grout testing, some specimens were vibrated for 4 h soon after the grout was placed to simulate a modest vibration under typical job site conditions. The control mix developed 1.8 and 6.2 percent bleed water by volume under the stationary condition and the vibrated condition, respectively. Comparatively, the mix containing the expansive admixture developed 1.9 and 10.2 percent bleed water by volume under the same conditions. Thus, this mix tended to induce more bleed water than the grout mix without it.

The bleed water-prone mix containing the expansive admixture showed wide variations in grout color corresponding to height. The lower portion of the specimen was dark and dense in appearance, but the specimen exhibited an increasingly lighter color higher up. At the uppermost portion of the specimen (about 0.04 inches high), the grout was almost white and chalky. The control mix showed relatively uniform consolidation and grout color throughout.

In an actual experiment with the anchorage mockup specimens, the expansive admixture containing specimens developed about 7.6 percent bleed water by volume under the four-h vibration. The pH of the bleed water was higher than 12.2. After 24 h of curing, only a trace amount of free water remained on the top of the specimen due to evaporation and reabsorption into the grout.

The grout immediately adjacent to the strands from the top of the grout and approximately 1.2 inches deep from the top exhibited a white, wet, pasty, chalklike texture, which suggested grout segregation. The segregated grout had a pH value of 8.7 ± 0.5 and a chloride content of 440 ppm. The pH values of the grout near the bottom of the specimen were higher than 12. The chloride concentration was 69 ppm, which was consistent with the expected background chloride concentration. It was assumed that unbound chloride ions rose to the top during the exaggerated bleeding process of the four-h vibration. The researchers did not report the sulfate concentration data.

An autopsy indicated that the strands buried in the grout were free of corrosion, but extensive pitting corrosion was observed on the strand surface in the segregated grout-void transition zone, coinciding with a band of 0.4 ± 0.2 inches from the top surface of the segregated grout. The corrosion-affected section had red to dark brown corrosion products. The examination of some wires that were separated from three strands revealed the heaviest pitting damage mostly coincided with the top of the grout. The observed penetration depth was as much as 7 percent of the wire diameter. Such a corrosion attack was considered very severe despite a short testing

duration of 166 days. Unfavorable conditions—low pH and segregated, poor-quality grout—must have promoted depassivation and subsequent corrosion damage in the transition zone. The researchers explained that the observed pH of 8.7 ± 0.5 could be due to the rapid carbonation of the segregated (porous and chalky) cement paste in the transition zone by CO_2 from the external atmosphere.

Furthermore, the chloride content in the transition zone was approximately six times greater than in the bulk of the grout, indicating a possible chloride-induced corrosion mechanism. They theorized that the lowered pH (less hydroxyl ion concentration [OH^-]) and higher chloride concentration increased the ratio of [Cl^-]/[OH^-], leading to intensive corrosion. Corrosion at the transition zone was further accelerated by macrocell corrosion established between the small active area in the segregated grout-void transition zone and the large passive steel strands embedded in the normal grout.

A follow-up laboratory study was conducted to investigate the cause of the steel depassivation, location, extent of macrocell corrosion, and timing of corrosion in PT anchorage assembly. A total of seven specimens were fabricated in two groups using commercial ductile iron PT anchorage assemblies containing unstressed, high strength 7-wire strands; two types of grout; and simulated grout voids. Three 'P' group specimens were made of conventional cement grout with a commercial aluminum-based expansive admixture. Four 'S' group specimens were made of a low-bleed, prepackaged grout product. The S specimens and P specimens were subject to several water-recharging events, with a freshwater solution and a 0.01 normality sodium chloride (NaCl) aqueous solution, respectively.

The researchers reconfirmed the PT system's vulnerability to corrosion at the grout/void interface due to the depassivation process between CO_2 in the air space and the high-pH grout. They did not expect a thin layer of hydrated grout on the steel surface would be highly protective, because the depassivation of thin grout-coated steel exposed to the mockup's simulated grout void (air space) would occur relatively quickly upon the intrusion of external air containing CO_2. The RH would determine the extent of subsequent corrosion in the void.

For the strands covered with thicker grout coating, depassivation and subsequent corrosion would be determined by water in the void. The corrosion proceeded at a substantial rate (see below) even though total external chloride contamination was modest. Also, increased chloride concentration could exist in the void due to chloride-bearing water from the grout surface or accumulated chloride ions initially present in the bleed water that leached from the segregated grout.

As a result, severe corrosion damage induced by the corrosion process was observed on the interior surface of the anchor block and the strands, primarily in the P group specimens. Rust distribution on the strands varied greatly among the three specimens, depending on the amount of grout residue on the strand bundles left by bleed water. The incidence of air-space corrosion in the P group specimens appeared to be a direct consequence of high internal RH (approximately 90 percent), which often resulted in condensation visible on the specimens' transparent covers.

The observation of corrosion under these conditions was consistent with the earlier experimental data showing a sharp increase in CR when the RH exceeded approximately 75–80 percent. The

macrocell corrosion current and the potential data indicated that corrosion at the grout/void interface might be sustained for months after a water-recharging event. The electrically connected anchor head and the wedge plate developed a mixed potential to act together as an efficient net cathode. Depending on the type of grout and the extent of the air exchange with the outside environment, air-space corrosion could proceed much longer after a water-recharging event.

The researchers estimated that the corrosion of strands in the void could be considerable, especially in grouts that supported a high internal RH. Their preliminary calculations predicted that air-space corrosion in the mockups in 100 percent RH could result in severe corrosion with a maximum pit depth of 7.9 mils after 1 yr. Suppose penetration depth progressed linearly and fracture occurred at a roughly 30 percent reduction in a cross-sectional area. In that case, individual strand breaks could occur in as little as ~3.5 yr of exposure conditions like those simulated in the laboratory.

5. PORTLAND CEMENT ASSOCIATION[97]

During research and development (R&D) for the Portland Cement Association (PCA), Bricker and Schokker investigated the corrosiveness of bleed water by employing three types of laboratory specimens: bare strands immersed in aqueous bleed solutions without chloride ions, small-scale grouted specimens, and large-scale grouted specimens in inclined tubes. They manufactured eight grout mixes using Types I and II portland cement; five chemical admixtures (an anti-bleed admixture, a superplasticizer, an organic corrosion inhibitor, an inorganic calcium nitrite corrosion inhibitor, and an expansive admixture); and combinations of the admixtures. They also included three prepackaged commercial grouts in their tests. With the grout mixes employed, they tried to determine the effects of grout ingredients on the corrosiveness of the bleed water. The Schupack pressure bleed test method was used to extract the necessary bleed test solutions from the fresh grout mixes. Table 1 lists the major ionic concentrations in the bleed test solutions.

Table 1. Chemical analysis of bleed test solutions.

	Concentration (ppm)				
Mix Type	**SO_4^-**	**Cl^-**	**Ca^{2+}**	**K^+**	**Na^+**
PL	15,700	66	660	15,400	2,540
SP	16,600	80	610	16,200	2,930
OC	14,800	57	560	14,200	2,310
IC	9,500	68	580	14,500	2,310
EX	18,400	69	910	14,100	3,600
IX	17,000	75	710	13,900	3,500

PL = 0.45 water-cement ratio (w/c) plain grout; SP = 0.35 w/c grout with superplasticizer; OC = 0.45 w/c grout with organic corrosion inhibitor; IC = 0.45 w/c grout with inorganic calcium nitrite corrosion inhibitor; EX = 0.42 w/c grout with expansive admixture; IX = 0.44 w/c grout with inorganic corrosion inhibitor and expansive admixture.

In all the sampled solutions, the concentration of chloride ions was very low, but the concentration of sulfate ions was substantially high. However, their report did not elaborate on

what role the elevated level of sulfate ions played in the corrosion process. In addition, potassium ions (K^+) and sodium ions (Na^+) were also present in the bleed water samples.

The 0.5-inch-diameter, 7-wire strands were immersed in extracted 1.69 oz bleed test solutions that were isolated from the atmosphere in sealed cylinders for 6 mo. Initial pH values of the test solutions ranged from 13 to 13.7. The final pH values taken after the strands were removed ranged from 9.4 to 11.2. Carbonation was thought to be responsible for the pH drop in the sealed test cells. The researchers observed corrosion products forming on the strands typically within 1 to 2 weeks after the strands were immersed in the test solutions. Upon cleaning the strands, intensive pitting corrosion damage was usually observed near the bleed water/air interface and on the exposed or submerged portions of some strands. The researchers assumed that the passivity of the steel would be lost at the low pH conditions. Figure 71 features a bar graph illustrating the relationship between grout mix and pit depth data obtained from the strand specimens.

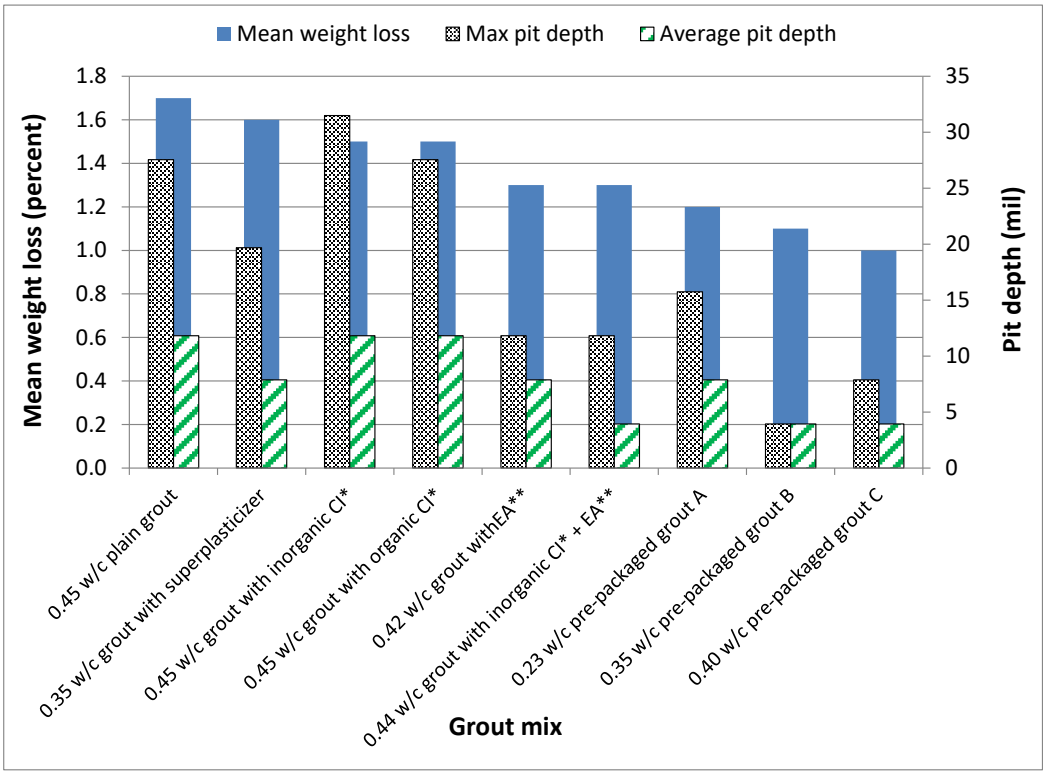

Source: FHWA.
*CI = corrosion inhibitor; **EA = expansive admixture; w/c = water-cement ratio.

Figure 71. Graph. Corrosion damage data based on grout mix type from PCA R&D.

Although no clear trends could be observed about cement type, admixture, or combinations of admixtures, it was apparent that the strands were susceptible to corrosion by aqueous bleed solutions alone. Also, despite some discrepancies among the experimental data, the plain grout mixes did not perform as well as the prepackaged commercial grout products. For example, the bleed solutions extracted from the plain grout without any admixture and the two prepackaged grouts yielded the highest and lowest weight losses and pit depths, respectively.

The initial pH values of the bleed water in the small-scale grouted specimens were in the range of 13.4–13.8. After the extracted bleed water was added to the grouted specimens, the pH increased to 13.9–14.3. During the remaining exposure period, the pH of the bleed water remained nearly constant with time. This observation was contradictory to the reduced pH observed in the earlier aqueous bleed solutions used in the strand specimens. The researchers speculated that the ability to maintain the high pH for the duration of the experiment came from calcium hydroxide leaching from the grout's cement paste. However, corrosion products still appeared on the strands near the bleed water/air interface within a week after the specimens were cast. It was confirmed later that the concentrated corrosion attack occurred only at the bleed water/air interface.

The researchers eliminated the possibility of chloride-induced corrosion because of the negligible chloride concentration in the test solutions. Instead, they suspected the carbonation-induced corrosion mechanism for the small-scale grouted specimens: high pH bleed water became carbonated (pH 8–9) at the interface when calcium hydroxide in the solutions reacted with O_2 and CO_2 in the sealed containers. As a result, corrosion could proceed without chloride ions at the bleed water/air interface, where the passivity of the strand there would be lost due to the low pH by carbonation.

The large-scale inclined grouted specimens made with transparent tubes showed the bleeding process well. The bleed water could be seen separating from the fresh grout in the tubes and flowing along the top of the tubes (12 o'clock) toward the high point of the specimens. The expansive admixture, added to the water-cement ratio grout with expansive admixture per the manufacturer's recommended dosage, provided a 5 percent expansion of the plastic grout. This grout also exhibited significant bleed water and resulted in a hardened grout exhibiting a visibly porous structure. The researchers stated that the quality of the hardened grout was more important than expanding the plastic grout. Therefore, the use of expansive admixtures for PT applications should be avoided. The grout mixes in 3 out of 4 specimens completely reabsorbed the bleed water that had formed initially in the fresh grout. The portion of the prestressing strands left exposed to the receding bleed water in the sealed tube developed a uniform layer of light surface corrosion in each specimen.

6. THE PENNSYLVANIA STATE UNIVERSITY GROUTING LABORATORY[98]

Schokker and Musselman performed a small-scale laboratory corrosion test at The Pennsylvania State University (Penn State) Grouting Laboratory to understand the corrosion mechanism of the gypsum-based repair grout suspected to have been used in the Varina-Enon Bridge in Virginia. This laboratory study was part of a full-scale tendon failure investigation of the bridge. They employed single 7-wire strand specimens embedded in a prepackaged grout and a commercial gypsum grout (used for a fast-setting underlayment) for the study.

No corrosion was observed on the specimens placed in the prepackaged grout, but significant pitting corrosion was observed at the inclined gypsum grout/void interface, after 2 mo of testing, in the sealed polyvinyl chloride tubes. The largest pits were approximately 1/16 of an inch deep. The strand section in the voided space above the gypsum grout interface was also corroded without direct contact with the grout. Figure 72 shows a corroded strand in gypsum grout (see figure 72-A) and the same strand after it was cleaned (see figure 72-B).

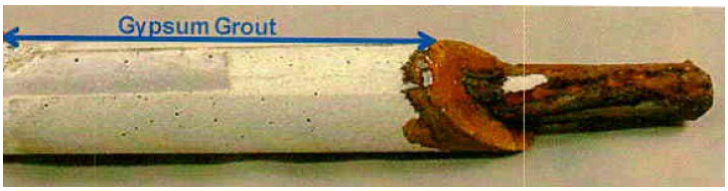

A. Corroded strand before removing gypsum grout.

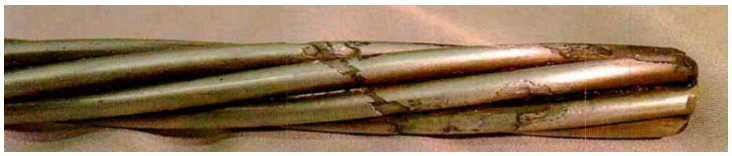

B. Cleaned strand after grout removal.

Figure 72. Photos. Corrosion-damaged strand in gypsum grout.[98]

7. TEXAS A&M UNIVERSITY[5,99,100,101]

Trejo et al. carried out three laboratory studies under a comprehensive five-yr research program titled "Effect of Voids in Grout, Post-Tensioned Concrete Bridge Construction" supported by TxDOT.[100] The following sections summarize key findings in the three laboratory studies.

7.1 Effects of Voids on Strand Corrosion and Capacity Reduction

A 12-month study was conducted to investigate the effects of voids on strand corrosion and capacity in the grouted PT tendons. A total of 298 grouted specimens containing 0.6-inch-diameter, 41-inch-long 7-wire strands were cast with the following variables:

- Grout types (2): Class A (portland cement and water, water-cement ratio = 0.44) and Class C (a prepackaged commercial grout, water-cement ratio = 0.27).
- Moisture contents (2): high (two weeks ponding with chloride solutions and two weeks of drying) and low (continuous exposure to a 0.0001 percent chloride concentration at the ambient condition).
- Chloride concentrations (5): 0.0001, 0.006, 0.018, 0.18, 1.8 percent by weight of aqueous solutions.
- Void types (5): no void, parallel voids, orthogonal voids, inclined voids, and bleed water voids.
- Stress levels (2): no stress and 150 ksi (56 percent of the guaranteed ultimate tensile strength [GUTS]).

The most significant localized corrosion was observed at or near the grout/void interface for all the voided specimens. The specimens exposed to test solutions containing 0.018–1.8 percent chloride concentrations during the wetting cycles experienced pitting corrosion. Those exposed

to 0.006 percent chloride concentration exhibited no pitting corrosion except for severe localized corrosion at the grout/void interface. From this finding, the researchers suggested that the chloride threshold value for the PT strands is likely between 0.006 and 0.018 percent by the weight of aqueous solutions.

This study determined that condensation could lead to higher CRs, but high humidity alone did not result in the same deterioration level. When the strands were directly exposed to moisture with and without chloride, a reduction of significant strand capacity occurred (assumed to be caused by pitting corrosion), and grout voids played a significant role. If the strands were embedded completely in the grout, both unstressed and stressed strands experienced similar capacity reductions. However, when voids were present in the parallel void and orthogonal void specimens, the stressed strands experienced much higher capacity losses (more corrosion damage) than the unstressed counterparts. The largest mean capacity reduction was observed when the stressed strands intersected the voids perpendicularly in the grout exposed to 0.006 and 1.8 percent chloride concentrations. The moisture with no or negligible chloride concentration in the voids also resulted in localized corrosion and reduced strand capacity by up to 11.4 percent over the 12-mo exposure period.

The study concluded that stress level was a statistically significant parameter affecting strand corrosion and remaining tension capacity in void conditions. Also, the void type and the grout/void interface had a statistically significant influence on corrosion and a subsequent reduction in the tension capacity of strands. Therefore, it was concluded that is important to protect the ducts and strands from water and chloride and eliminate grout voids to prevent or minimize the strand capacity reduction. Depending on the reliability model, a PT bridge could fail as early as 21 yr after construction if the strands were subjected to high-chloride environments.

In addition, three repair grouting methods, i.e., PG, pressure-vacuum grouting (PVG), and VG, were evaluated in terms of filling capabilities, filling performance, and economic feasibility. Although the different repair methods did not show significant differences at a 95 percent confidence level, the PG method exhibited a lower filling capability than the others, possibly due to backpressure. This backpressure might have been developed because the single grout port in each specimen was located on the anchor plate, and there were no grout outlets or vents elsewhere on the test setup. This method is known to require less preparation for work and be more cost-effective than the other methods. Relief valves or air outlets typically must be installed to avoid duct bursting and improve grouting (the rest of the duct should be airtight).The VG method utilizes a vacuum pump to reduce pressure in the duct by 80 percent. Once the pressure stabilizes, the vacuum pump is closed off from the system, and fresh grout is allowed to fill the voids. FDOT recommended the VG method to fill the voids in PT bridges because this method can fill voids effectively. However, if the duct system is not completely airtight, the air from outside may leak into the duct system. In that case, it is difficult to form an airtight tendon and maintain constant vacuum pressure inside the tendon. It may take weeks or even months to make the tendons airtight. Thus, the VG method is practically unfeasible and economically less viable.

The PVG method utilizes advantages of the PG and the VG methods. Therefore, this study recommended the PVG method for filling voids in the field, as the PG and PVG methods are more economical methods for repairing voids than the VG method. It was also recommended

that repairing with grouts be performed after potential issues with accelerated corrosion at the existing/repair grout interface were investigated.

7.2 Void Detection and Assessment by Sounding Technique

External tendon mockups were designed, fabricated, and tested to evaluate the sounding inspection method. Each mockup consisted of a lower anchorage, a deviator block, an upper anchorage, and 19 strands inside a transparent four-inch-diameter acrylic duct. Transparent acrylic ducts were used to facilitate visibility during the initial and repair grouting procedures. To straighten the strands and mimic field conditions, the strands were tensioned to 0.8 kips per square inch (ksi), which is equal to 0.3 percent of their ultimate strength. After stressing the strands, the interstitial spaces between the stands and duct were filled with Class A grout through the grout hole near the lower anchorage using a hand grout pump. Artificial voids were then formed in the top anchorage zone and at five locations along the duct to simulate improper grouting procedures. The voids in the mockups were visually inspected and drawn on a specially developed void-mapping sheet.

The sounding inspection method used a steel tapping hammer to identify voids in the ducts by detecting a high pitch and irregular sound while tapping. Sounding results were recorded at every inch in surveyed intervals of 1 ft on the mockups. Although the assessment of sounding was subjective and depended on the inspector’s judgment, it was classified as high- and low-pitched sounds. Void profiles found by both sounding and visual inspection methods were provided in the void maps for every specimen.

The study determined that the sounding technique underestimated the void size, especially extremely small voids. But correlation analysis revealed a highly positive linear correlation (correlation coefficient = 0.906) between the actual void locations in the test specimens and the sounding test results. Therefore, it was concluded that sounding inspection by experienced personnel could be an effective inspection tool in the field for locating voids because of its ease of application and relative accuracy. However, considering the uncertainty associated with the sounding technique, a detailed inspection using a borescope was recommended to confirm void locations.

7.3 Laboratory Evaluation of Prepackaged Grout Materials

For this study, three prepackaged PTI Class C grout products and a grout conforming to TxDOT grout specifications were employed to characterize fresh and hardened grout properties, develop a simple test procedure for evaluating fallibility of the grouts, and develop new specifications or modify existing specifications for durable grouts. In addition, three 2-by-4-inch cylindrical grout samples were cast for each mix to measure the grout pore solutions' pH values by expressing the pore solutions after 28 d of curing. Table 2 summarizes the characteristics of four grout mixes.

Table 2. Summary of grout characteristics.

Grout Type	Water-Powder Ratio*	Mean Wet Density (oz/in^3)	Mean Pore Water pH	Mean Chloride Diffusion Coefficient (x10^{-8}, in^2/s)	Wick-induced Bleed (%)	Fluidity (s)	Initial Setting Time (h)	Comp. Strength (ksi)	Volume Change (%)
Portland cement Type I grout	0.44	1.08	12.92	1.01	2.05	4.95	4.81	6.84	0
Grout 1**	0.30	1.21	12.91	0.20	0	10.32	5.12	11.24	0
Grout 2**	0.26	1.21	12.87	0.34	0	13.03	9.34	11.57	0
Grout 3**	0.27	1.13	12.95	0.17	0	9.99	9.47	9.17	0

*Recommended by manufacturers.
**Prepackaged.
Comp. strength = compressive strength.

The pH values of the expressed pore water listed in table 2 were lower than those reported in other studies discussed in this report. Chloride diffusion coefficient data indicated that the prepackaged grouts offered more than five times better corrosion protection than the plain cement grout. The superior properties of the prepackaged commercial grouts could also be seen by the bleeding and compressive strength data.

Every Class C grout met the TxDOT grout specifications (DMS-4670), whereas Class A grout (portland cement Type I and water only) did not meet them.[102] The grouts containing gas-generating components were disqualified because they might result in creating entrapped voids. Grouts with expansive admixtures were also disqualified because the grout expansion could result in the cracking of HDPE ducts, leading to durability issues. Finally, the grouts containing aluminum powder were disqualified because the aluminum powder contributed to the expansion by liberating hydrogen gas, forming voids within the grout, and resulting in durability issues.

8. TEXAS DEPARTMENT OF TRANSPORTATION[70,102,103]

As mentioned in chapter 3, TxDOT discovered two problems on the PT straddle caps for Carbon Plant Road Bridge over Interstate 37. When the grout caps were removed, free water came out of the anchorage zone, and voids with exposed strands were noted. The segregated grout marked "A" in figure 35 never hardened and had the consistency of clay with many air bubbles. It was saturated with unbound water. The grout marked "B" did harden properly without any deficiencies. Both the "A" and "B" materials were sampled for testing in the laboratory to investigate why the grout was stratified and if there were any potential durability problems with the "A" grout.

Table 3 lists chloride analysis results of segregated grout sample "A" and normally hardened grout sample "B."

Table 3. Chloride concentrations in grout samples.

Tendon ID	Sampling Location	Grout Condition	Chloride Concentration (ppm)		Instrument Used
			Acid-soluble	Water-soluble	
1-A	Inlet	Deficient "A" sample	52,700	—	XRF
1-A	Inlet	Deficient "A" sample	—	21,330	IC
2-B	Inlet	Deficient "A" sample	5,700	—	SEM/EDS
1-B	Inlet	Normal "B" sample	4,100	—	SEM/EDS
2-B	Inlet	Normal "B" sample	2,200	—	SEM/EDS
1-A	Outlet	Normal "B" sample	5,400	—	SEM/EDS

ID = identifier; XRF = X-ray fluorescence; IC = ion chromatography; SEM = scanning electron microscopy.
—Not available.

High levels of chloride, potassium, and sodium ions were found in the segregated grout samples. Typically, water-soluble chloride concentration accounts for 70 to 90 percent of the total chloride concentration. In this case, water-soluble chloride concentration was still very high but was less than 50 percent of the total chloride concentration (21,330 versus 52,700 ppm). The grout segregation might be responsible for the mobility of free ionic species.

The grout used in the referenced project was a commercially available, prepackaged grout product. Since it was a zero-bleed/thixotropic, high-performance grout, it was not supposed to have bleeding, grout segregation, and any large voids in the tendons or anchorages. Most of the acquired grout bags were used before the end of their shelf life, and the last lot of grout exceeded the shelf-life by about two weeks. The investigator suspected that exceeding the grout's shelf life could affect the physical properties such as anti-bleed performance and fluidity.

The elevated chloride concentration in this grout product and its segregation problem triggered several national research studies to determine chloride threshold values for grout materials and the grout segregation phenomenon.

9. GEORGIA INSTITUTE OF TECHNOLOGY[104]

An extensive laboratory study was conducted to evaluate the corrosion resistance of conventional 7-wire and various high-strength stainless steel (HSSS) alloy strands as part of corrosion mitigation techniques for coastal prestressed concrete bridge substructures. This study consisted primarily of electrochemical corrosion testing, mechanical testing, and microstructural characterization. Small single-wire and 7-wire strand specimens were fabricated with their as-received surface condition for electrochemical corrosion testing. The prepared specimens were

exposed to a simulated concrete pore solution with additions of NaCl, and their corrosion characteristics were evaluated using the cyclic potentiodynamic polarization (CPP) technique. Even though this study produced a lot of useful data, only limited results related to surface characterization, corrosion morphologies, and corrosion characteristics are presented in the following sections.

9.1 Characterization of the Prestressing Steel Surface

The chemical composition of the conventional prestressing steel used in this study was typical for cold-drawn, 0.6-inch, 7-wire strands. Figure 73 shows an electron micrograph of prestressing steel obtained by wet etching in a 2 percent nital solution.

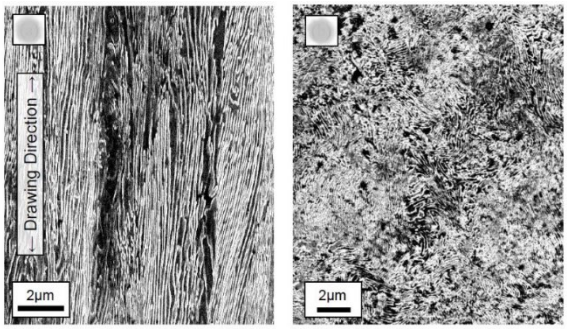

2 µm = 0.00007874 inches.

Figure 73. Photomicrographs. Pearlitic microstructure of prestressing steel: longitudinal orientation and transverse orientation.[104]

It consisted of a highly anisotropic pearlitic microstructure with alternating lamellae of ferrite (white) and cementite (black) oriented longitudinally in the cold drawing direction.

A photomicrograph shown in figure 74 shows the disturbed surface condition of the as-received zinc phosphate ($ZnPO_4$) surface coating on the prestressing steel, which contained flaws generated during cold drawing and subsequent thermomechanical processing during strand production.

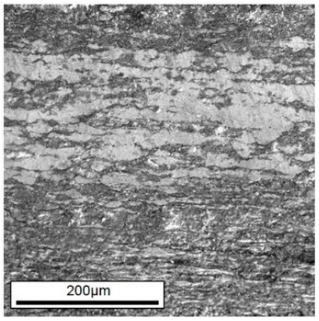

200 µm = 0.007874 inches.

Figure 74. Photomicrograph. As-received $ZnPO_4$ surface coating on prestressing steel.[104]

Scanning electron microscopy (SEM) and EDS analyses were performed on prestressing steel samples to characterize imperfections on as-received $ZnPO_4$ surface coatings. Figure 75 shows a photomicrograph highlighting the heterogeneity present in a 0.0016 in^2 area of the coating at an impingement site between two wires in a 7-wire strand sample. EDS results performed at three spots are also shown in figure 75.

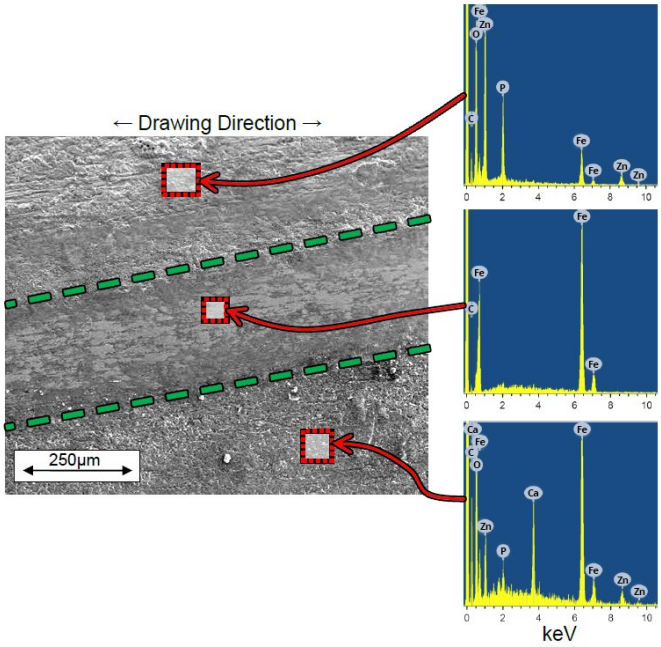

© 2011 R. Moser. Modified by FHWA.
250 µm = 0.009843 inches.

Figure 75. Photomicrograph. Typical imperfect $ZnPO_4$ surface coating and energy dispersive X-ray spectroscopy results.[104]

In the center of the backscattered image shown in figure 75, a bright diagonal imperfection band (marked by two dashed lines) shows a helical twist at the impingement site between the prestressing strand's outer wire and center wire. EDS analysis of this band indicated that most of the $ZnPO_4$ coating had been abraded off, as evidenced by the middle EDS spectrum showing only iron (Fe). Adjacent to this band of imperfection, the surface coating remained intact: Both zinc (Zn) and phosphorus (P) were present in the top and bottom EDS spectra. In many cases, trace amounts of calcium (Ca) were also detected in the surface coating. These Ca deposits were likely residual coatings from stearate-type drawing lubricants, which were not completely removed during postprocessing stress relief and cleaning treatments.[105]

9.2 Corrosion Characteristics of Conventional 7-Wire Steel Strand

CPP tests were employed to determine the conventional 7-wire steel strand's resistance to corrosion initiation at various chloride concentrations in a highly alkaline solution of simulated pore water (pH 13.6). The single-wire specimens extracted from the 7-wire strands were also tested for comparison purposes. All experiments were performed at 75 °F. A preconditioning time of 120 min was used for each specimen to ensure the formation of a stable passive film on the steel surface. Appropriate amounts of chloride ions were controlled by adding NaCl to the

chloride-free pore water solution in amounts of up to 35,500 parts per million (ppm) in increments of 3,550 ppm s.

Potentiodynamic scans began at -25 mV versus the OCP of the specimen and polarized the specimen in the positive potential direction until a current density of 1.62 milliampere (mA)/in^2 was reached. At that point, the scan direction was reversed in the negative potential direction until the specimen's potential was brought back down to -25 mV versus the original OCP. A scan rate of 0.1 mV/s was used for all CPP tests.

9.2.1 Single Wire Specimens

Figure 76 shows five examples of CPP curves obtained from single wires exposed to chloride-free and four chloride concentrations (24,850; 28,400; 31,950; and 35,500 ppm).

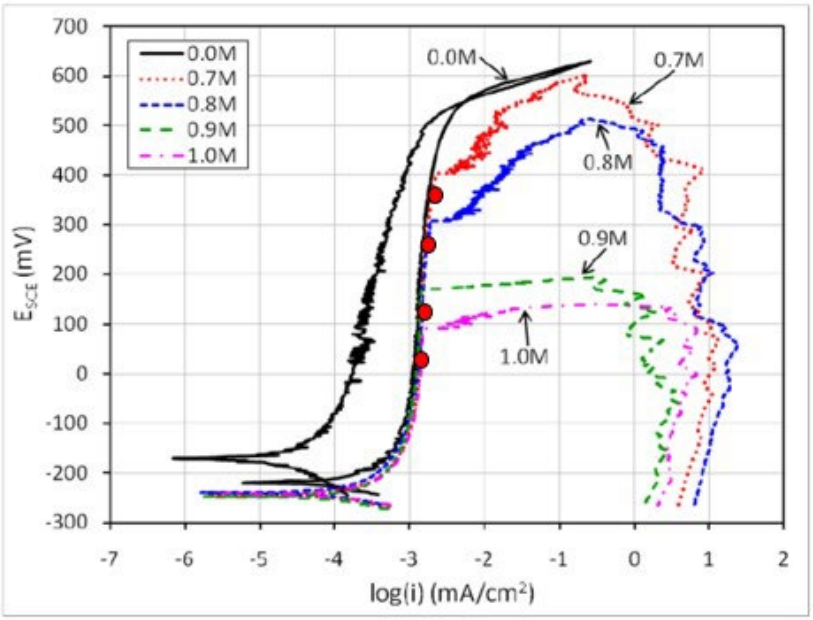

0.1 molarity (M) = 3,550 ppm; 1 mA/cm^2 = 6.5 mA/in^2.
E_{SCE} = potential versus saturated calomel reference electrode.

Figure 76. Graph. CPP data from single-wire specimens.[104]

After a 120-min sample conditioning period, relatively positive OCPs roughly between -150 and -240 mV versus saturated calomel reference electrode (mV$_{SCE}$) were measured for all wire specimens. The forward anodic polarization scan in the chloride-free solution started from the most positive OCP of about -150 mV$_{SCE,}$ reached the potential in the oxygen evolution region above approximately +500 mV$_{SCE}$, and then backed down close to the initial OCP in the reversed scan. Since the reversed anodic polarization curve was similar to the forward one, the hysteresis loop bound by the forward and reversed polarization curves was small, indicating that there was not much pitting damage on the specimen. As chloride concentration increased, resistance to corrosion initiation decreased accordingly, as evidenced by a continuous decrease in the passivity breakdown potential indicated by four small circles in the figure and the enlarged

hysteresis loops. This trend indicated easy pitting corrosion started at higher chloride concentrations.

9.2.2 Seven-Wire Strand Specimens

Figure 77 shows five examples of CPP curves obtained from 7-wire strand specimens exposed to a chloride-free concentration and four chloride concentrations (7,100; 10,650; 14,200; and 35,500 ppm).

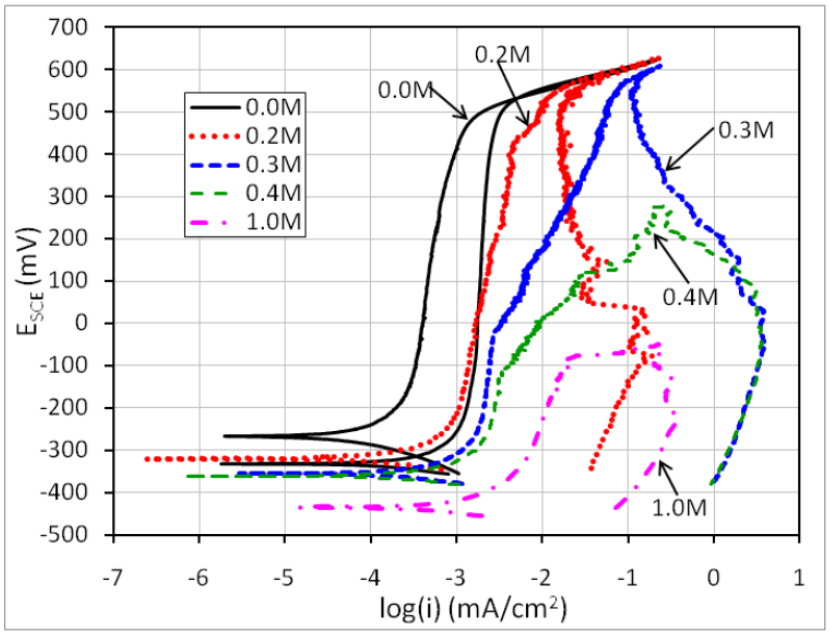

0.1 molarity (M) = 3,550 ppm; 1 mA/cm^2 = 6.5 mA/in^2.

Figure 77. Graph. CPP data from 7-wire strand specimens.[104]

Different OCPs were obtained between -250 mV_{SCE} in chloride-free and -450 mV_{SCE} in 35,500 ppm solutions after preconditioning. In the chloride-free solution, no corrosion initiation was observed, like the wire case in figure 76. The lowest chloride concentration to initiate corrosion was 7,100 ppm, and higher chloride concentrations made pitting corrosion start easily, as with the wire specimens.

9.2.3 Corrosion Tendency: Single Wire Specimens Versus 7-Wire Strand Specimens

Figure 78 shows a graph comparing the mean passivity breakdown potentials determined for all the wire and strand specimens at each chloride concentration.

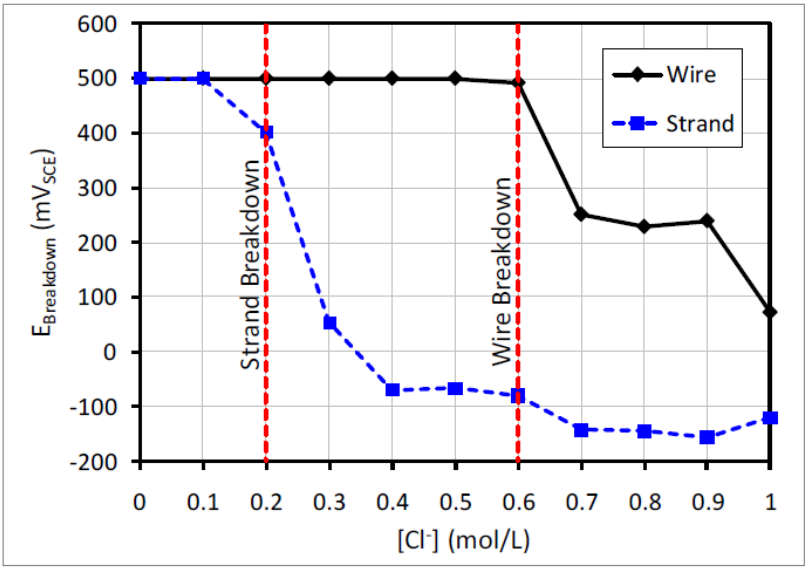

0.1 mol/L = 0.1 molarity (M) = 3,550 ppm.
$E_{Breakdown}$ = passivity breakdown potential.

Figure 78. Graph. Passivity breakdown potentials of wire and strand specimens.[104]

The passivity breakdown potential of +500 mV_{SCE} applicable to the wire and strand specimens represented the potential above which oxygen gas evolved. The mean breakdown potential data in figure 78 clearly showed that strand geometry had a negative impact on chloride-induced corrosion. For example, the mean passivity breakdown potential of the single-wire specimens started at 21,300 ppm, whereas the 7-wire strand specimens began at a far lower concentration of 7,100 ppm. The crevices formed on the 7-wire strand must be responsible for 67 percent less chloride concentration to initiate corrosion than the single wires.

9.2.4 Corrosion Morphologies

The researcher divided imperfections in the $ZnPO_4$ surface coating into two types, as follows:

- Type 1—Mechanical scratches and blemishes in the coating; present as either carbon-rich lines from wearing on the drawing die or bare metal "streaks" aligned in the drawing direction of the wire before stranding operations.

- Type 2—Abrasion of the coating due to relative displacement between the wires (impingement sites); present as bare metal "streaks" running helically with the strand's twist.

Figure 79 shows two specimens tested at passivity breakdown potential to determine preferential surface sites for corrosion initiation.

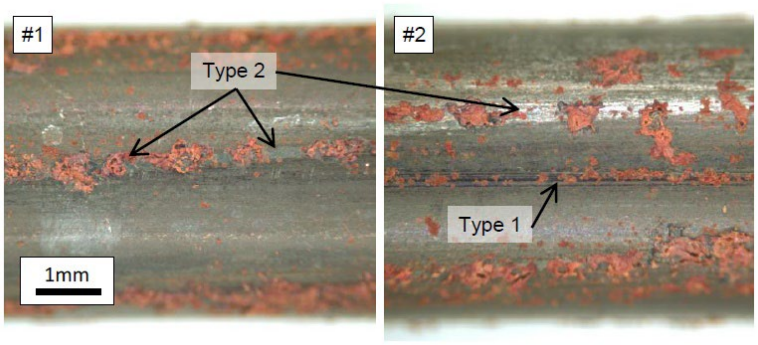

Figure 79. Photos. Corrosion initiation at surface imperfect sites: Type 1 and 2 defects.[104]

Corrosion started at type 1 and type 2 imperfections before general corrosion of the $ZnPO_4$ coated surface. Corrosion was initiated on both specimens at type 2 defect sites where corrosion products were aligned with the helical twist of outer wires around the center wire. Corrosion is also shown at the type 1 defect on a carbon-rich black streak aligned in the drawing direction. These observations suggested that the surface coating's imperfections played an integral role in providing sites for corrosion initiation. Such effects would not be detected by experiments conducted on polished samples. Particularly, type 2 defects occurred at the crevices in the 7-wire prestressing strands and could aggravate the crevice corrosion process.

X-ray diffraction (XRD) analysis using post CPP specimens identified that whisker-type corrosion products in the pits were primarily goethite (FeOOH). Extensive pitting was observed at the base of the whisker formations. Figure 80 shows an SEM photomicrograph of a typical pit observed at the base of a whisker formation.

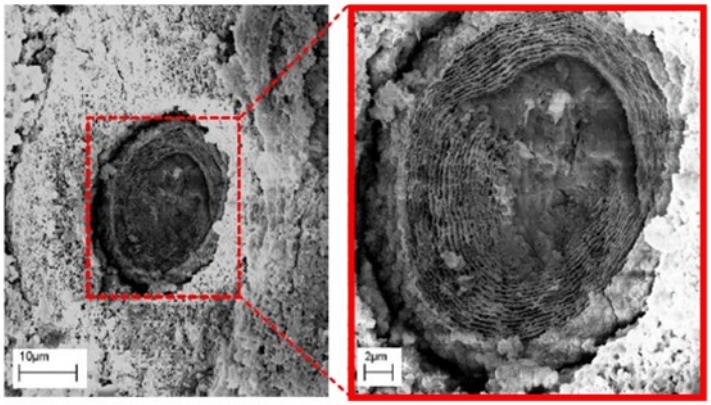

1 µm = 0.00003937 inches.

Figure 80. Photos. Typical pitting corrosion morphology: Pit mouth and closeup of inside of pit.[104]

The diameters of the pits ranged from 0.2 to 0.8 mils and typically exhibited concentric circular deposits of corrosion products on the pit walls.

When corrosion products were removed in the uniform corrosion areas, corrosion damage was found to be preferentially aligned in the drawing direction of the prestressing steel, as shown in figure 81.

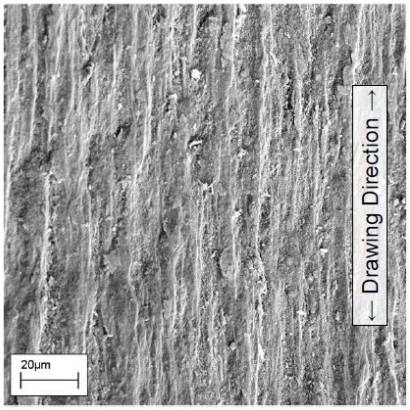

20 µm = 0.0007874 inches.

Figure 81. Photomicrograph. Uniform corrosion damage preferentially aligned in the cold drawing direction.(104)

It was concluded from the CPP experiment that type 2 impingement sites inside the crevice formed by the wires influenced the initiation of localized corrosion on the 7-wire strands. In comparison, type 1 imperfections in $ZnPO_4$ surface coatings provided sites for initiating localized corrosion on the wires and the 7-wire strands. Once localized corrosion initiated at individual imperfect spots, corrosion propagated similarly in both wires and strands, spreading out into a more uniform attack on the surface coating with time.

9.3 Corrosion Characteristics of High-Strength Stainless Steel Alloys

Another laboratory investigation was performed using CPP tests among six candidate stainless steel alloys based on their mechanical properties, corrosion resistance, cost, and availability. The selected alloys were two austenitic grades (304 and 316), three duplex grades (2,101; 2,205; and 2,304), and a precipitation-hardened martensitic grade (17-7). The following section summarizes key findings.

In alkaline solutions, all candidate alloys exhibited acceptable corrosion resistance at chloride concentrations up to 8,875 ppm. As chloride concentrations increased to 17,750 ppm, only grades 2,205 and 2,304 exhibited good corrosion resistance. Grade 2,205 was still resistant to corrosion at 35,500 ppm. In carbonated solutions, grades 2,205 and 2,304 exhibited high and moderate corrosion resistance at 17,750 ppm, respectively. The superior corrosion resistance of grade 2,205 was thought to be from its 3.2 percent molybdenum (Mo) content, which could enhance corrosion resistance in the acidic conditions developed inside the crevice region of the strand during corrosion propagation.

On the other hand, the other alloys showed reduced corrosion resistance. The corrosion resistance of grade 316 cold-drawn wire was found to be less than its austenitic counterpart grade

304. The poor corrosion resistance of grade 316 was attributed to the presence of sulfur-bearing precipitates and strain-induced martensite (α′-martensite). Corrosion morphology in grades 304, 316, and 17-7 was similar, with large pits distributed across the wire surface. A lacy-patterned pitting mechanism was identified around the pit's rim, which might have been caused by the aggressive nature of the CPP technique.

Based on all the CPP data, grades 2,205 and 2,304 showed the most promise for corrosion-resistant prestressing reinforcement. They were also identified as optimal HSSSs for further investigation to determine the influence of stranding on corrosion resistance and susceptibility to brittle fracture by SCC and HE.

Slow strain rate testing (SSRT) of grades 2,205 and 2,304 showed no damage by SCC at a chloride concentration of 17,750 ppm in alkaline and carbonated solutions. However, damage by HE was observed in both materials after SSRTs. HE cracking was isolated to the necked region of SSRT specimens. Brittle fracture by HE had only occurred on the surface of the specimen, and the rest of the fracture was ductile.

10. UNIVERSITY OF KANSAS[106]

O'Reilly et al. evaluated corrosion performance of the prestressing strands exposed to dissimilar grouts using portland cement grout, gypsum grout, and four commercially available prepackaged grouts. The researchers conducted pore water solution analysis and rapid macrocell corrosion tests. (The report excluded test results for a prepackaged grout mix.) As the pore water volume decreased with curing time in some cases, some data were also not available, especially on the 7th d.

The pH of the grout products varied from 13 to 13.63, depending on the water-to-solids ratio. According to the limited pH data (three sets to compare), a higher water-to-solids ratio resulted in the same or a lower pH than the lower water-to-solids ratios. The sodium and potassium concentrations were much higher than the chloride and sulfate concentrations. However, there were no consistent trends for sulfate concentrations except that one prepackaged grout contained the highest sulfate concentration (over 1,300 ppm) in the recommended water-to-solids ratio mix on the 1st d and the highest water-to-solids ratio mix on the 7th d. It exceeded the gypsum grout with a sulfate concentration of 870 ppm on the 1st d; no data was available on the 7th d. This was an unexpected result because gypsum grout was supposed to have a very high sulfate concentration among commercially available grout products.

The corrosion of strands exposed to the prepackaged grouts increased as the sulfate concentration in the grout pore solution increased. The researchers predicted that gypsum grout would cause accelerated strand corrosion when combined with portland cement grout, or any commercially prepackaged grout, due to its significantly lower pH and higher sulfate concentration.

The researchers believed that sulfate could compromise passive film on steel like chloride. The strands in contact with gypsum grout and the simulated gypsum grout pore solution experienced a high level of corrosion damage by a combination of three factors: much lower pH (13.0), more negative corrosion potential caused by differences in grout pH, and elevated sulfate

concentration in the gypsum pore solution. They suggested that pH had a greater effect on corrosion than sulfate concentration, at least for grouts evaluated in their study.

11. UNIVERSITY OF NORTH FLORIDA[107]

Corrosion could occur in regions with severely segregated grout and be further aggravated by macrocell corrosion formation associated with new repair grout. The segregated old grout acted as a macro-anode, and the new repair grout acted as a macro-cathode. Rafols conducted a laboratory study at the University of North Florida to determine the extent of macrocell corrosion in two different simulated grout materials and reported the findings in a master's thesis titled "Corrosion of Post-Tensioned Tendons Repaired With Dissimilar Grout." Unstressed mockups were made with sections retrieved from failed tendons and samples immersed in simulated pore solution containing various pH levels and constituent concentrations. Corrosion activity of the mockups was monitored through macrocell current, linear polarization resistance (LPR), OCP, potentiodynamic scans, and electrochemical impedance spectroscopy (EIS). All samples were repaired or constructed with commercially available, prepackaged grouts.

Ongoing corrosion activity at the existing grout/void interface, where moisture might accumulate before the casting of repair grout, could be significantly reduced after regrouting the void. Commercially available repair grouts showed differences in solution resistance in the cement paste. Measured resistance values were up to 10 times greater than and corrosion currents were significantly lower than those measured in neat cement grout with a water-cement ratio of 0.45. Cathodic reduction reaction capacity also appeared lower for repair grouts than for the control grout. No evidence of corrosion development was found when both existing and repair grouts were free of material deficiencies.

However, significant corrosion activity was noted in the presence of nonhomogeneous and segregated grout. This activity was attributed to the high sulfate concentration that could be liberated from the segregated grout and to the grout having high moisture content. Early exposure to sulfate concentration as low as 0.13 percent by weight of the sample may have prevented steel passivation from forming and resulted in early high CRs. Macrocell coupling between deficient grout and nondeficient repair grout (or normally hardened grout) increased corrosion in the segregated grout.

12. FLORIDA INTERNATIONAL UNIVERSITY[50,51,108,109]

In 2012 and 2013, two extensive corrosion studies were published investigating segregated grout problems discovered in Ringling Bridge in 2011.[108,109] Additionally—and apart from the field investigation presented in the previous chapter—several laboratory experiments, grout analyses, and miscellaneous data analyses were performed by researchers at FDOT's State Materials Office and later continued at Florida International University. Lau reported on this work in a report titled *Corrosion of Post-Tensioned Tendons With Deficient Grout.*[51] The following section summarizes some of this work, which focused on increasing the understanding of underlying issues involving segregated grout. Small-scale corrosion test cells were made with three- to four-inch-long tendon sections cut out of retrieved field tendon samples.[52] Visual assessment and electrochemical measurements of OCP, LPR, and EIS were made in the

laboratory to investigate why severe corrosion occurred on some of the PT strands exposed to the deficient grout.

The measured OCPs for individual strands removed from failed tendon sections recovered from the Ringling Bridge were distributed between nearly -400 and +25 mV_{CSE}. Active corrosion was apparent in some specimens, evidenced by distinctively negative potentials. The researchers suggested that a wide range of potentials measured for strands exposed to segregated grout indicated locally varying corrosive environments. The potential difference was attributed to moisture, anion concentration (chloride and sulfate), oxygen concentration in the grout, and possibly macrocell corrosion.

Macrocell corrosion test specimens were also constructed. The top section contained normally hardened grout and corrosion-free strands taken away from the corroding tendon location. The bottom section contained segregated grout and corroded strands removed from the failed tendon location. The strand bundles in both sections were externally connected to measure macrocell current (I_{macro}) between them using a zero-resistance ammeter. The direction and magnitude of the macrocell current determined the corrosion tendency of the strands exposed to segregated grout and normally hardened grout. Figure 82 shows macrocell current data collected from three specimens (A, B, and C).

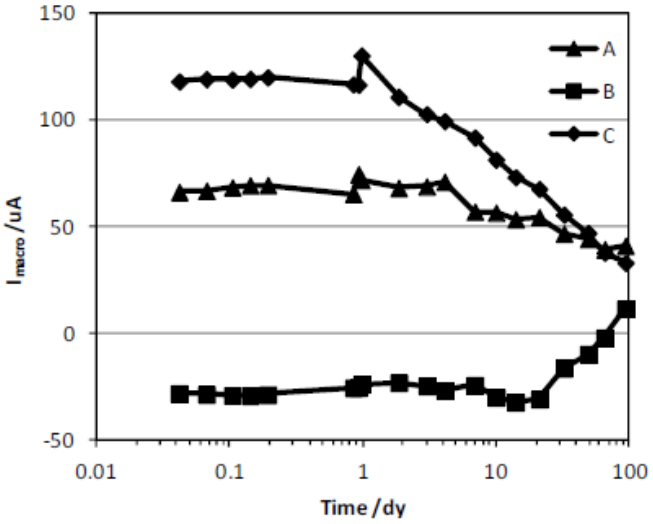

I_{macro} (uA [µm]) = macrocell current (microampere). dy = day.

Figure 82. Graph. Macrocell corrosion current data.[51]

Specimens A and B exhibited positive macrocell currents flowing from the bottom section to the top section, but their magnitudes decreased with time. The direction of the current flow indicated that the strands in the segregated grout were the macro-anode and those in the normally hardened grout the macro-cathode. The segregated grout provided a more corrosive environment than the normally hardened grout. In an earlier experiment, the segregated grout exhibited a much lower electrical resistivity than the normally hardened grout because of the high moisture content and high porosity in the former. The remaining specimen C started with negative current flow and then behaved like the other specimens near the end of the experiment.

The researchers thought the macrocell current decreased with time partly due to continuous hydration of the cement paste used to provide ionic coupling between two sections during specimen fabrication. It was noted that the surface of the cement paste was not sealed, and thus oxygen might be readily available. Differential oxygen availability at the macro-anode and macro-cathode might provide larger macrocell polarization and possibly higher corrosion activities, which might have been present in the field. The apparent CRs expressed in terms of corrosion current (I_{corr}) determined by LPR and EIS increased after the top and bottom sections were electrically coupled. This behavior is shown in figure 83.

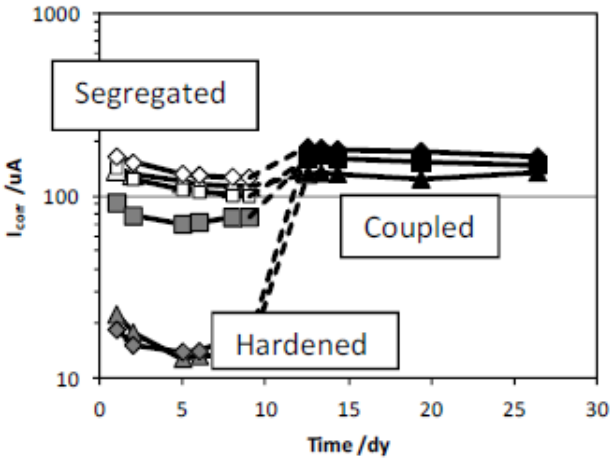

I_{corr} (uA [µA]) = corrosion current (microampere); dy = day.

A. Corrosion rate by LPR.

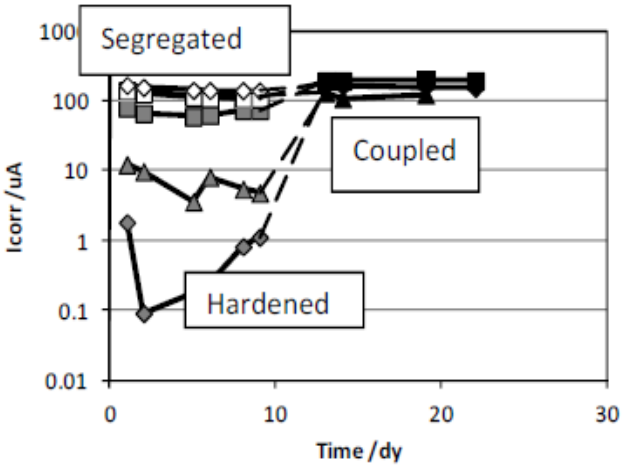

I_{corr} (uA [µA]) = corrosion current (microampere); dy = day.

B. Corrosion rate by EIS.

Figure 83. Graphs. Corrosion rate data from macrocell specimens.[51]

The researchers analyzed ionic concentrations, moisture content, pH of grout pore water, and chemical composition to characterize variations in the grout samples as part of grout analysis. Figure 81 shows distributions of moisture content, pH, chloride, and sulfate ions resided in five different grout conditions observed on a low anchor plate initially filled with segregated grout. Schematic grout conditions and a photograph are also provided to compare grout conditions and spatial distributions of pH, moisture content, and anion concentration data. Figure 85 shows actual concentration profiles of ionic species in different grout conditions using the data presented in figure 84 and other ions such as K^+, Na^+, Ca^{2+}, and nitrate (NO_3^{2-}).

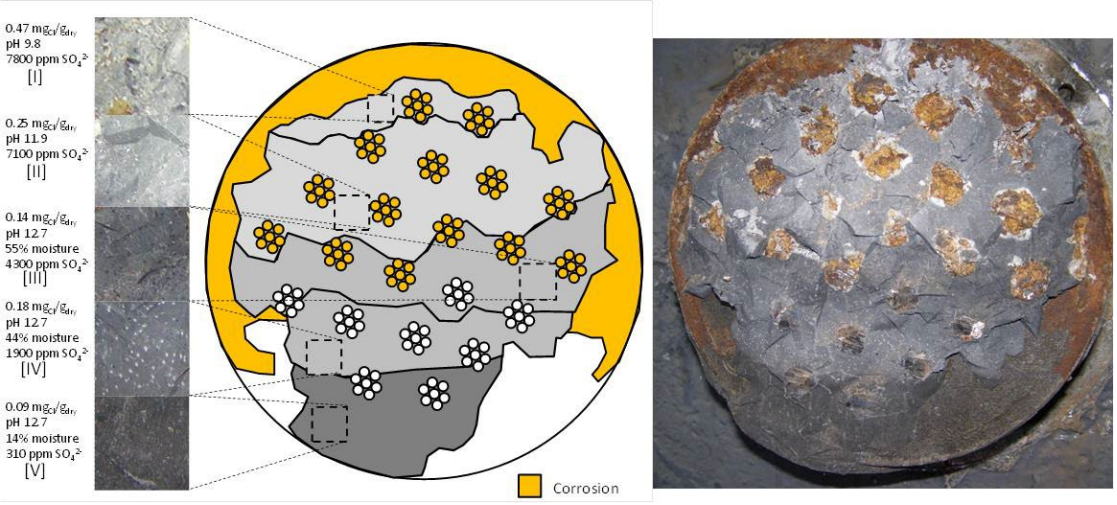

© 2014 FDOT.
mg_{Cl}/g_{dry} = chloride content in milligram per dry sample weight.

Figure 84. Photos. Distribution of moisture, pH, and anions in grout samples: Actual grout photos, schematic grout condition, actual anchor plate.[50]

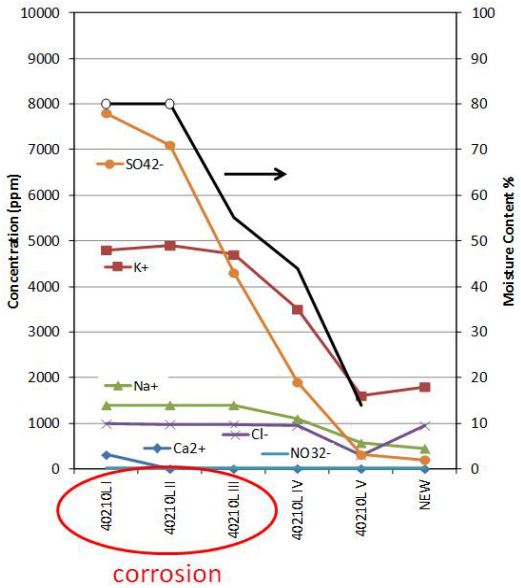

© 2014 FDOT.

A. Concentration profiles.

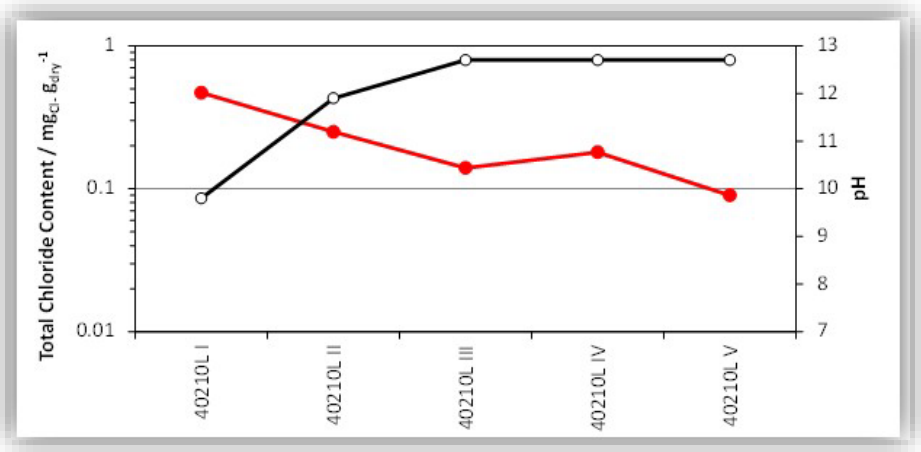

B. Chloride concentration (black line with open circles) and pH (red line with shaded circles).

Figure 85. Graphs. Ionic concentration profiles and pH shown in figure 84.[50]

Sulfate concentration and moisture content varied significantly, and segregated grout had much higher concentrations of sulfate, potassium, and sodium ions and lower concentrations of calcium ions than nonsegregated grout. The pH values of the segregated grout, determined by the ex-situ leaching method, were lower than those of the hardened grout.

As the degree of segregation got worse, sulfate concentration and moisture content increased, and pH decreased accordingly. The sulfate profile shown in figure 85-A, in conjunction with the appearance of corrosion, may suggest a sulfate threshold for corrosion. Based on this assumption, the researchers constructed a cumulative plot of the experimentally determined Ringling Bridge's sulfate to hydroxyl ratios ($[SO_4^{2-}]/[OH^-]$). This plot is shown in figure 86.

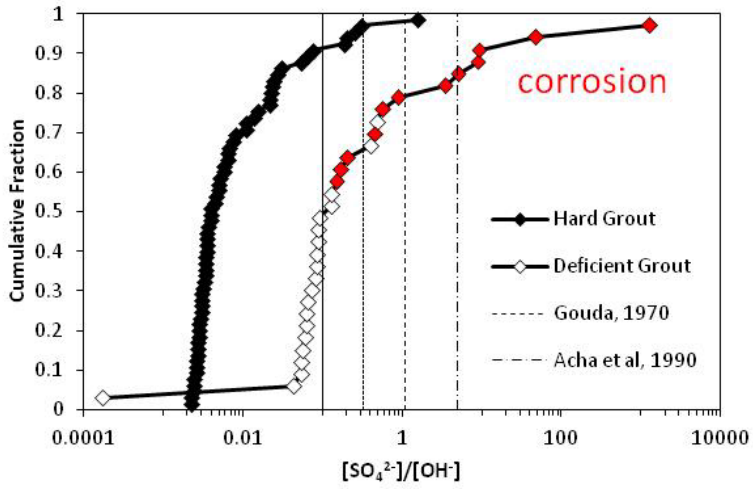

Figure 86. Graph. Cumulative plot showing $[SO_4^{2-}]/[OH^-]$ versus corrosion initiation.[50]

In the laboratory analysis, active corrosion conditions developed when sulfate weight with respect to the weight of grout powder exceeded a ratio of ~0.0007. This value corresponding to the sample conditions suggested that 0.15 was the threshold for typical grout pH environments. The researchers reported two sulfate thresholds suggested in the literature for corrosion in aqueous environments. When these sulfate thresholds were overlapped onto the experimental data shown in figure 86, the sulfate threshold determined for the Ringling Bridge was nearly one order of magnitude lower. It was learned that high sulfate concentration could be accumulated in deficient grouts without external sulfate sources. Even low concentrations of sulfate in well-hydrated grout might locally aggregate due to segregation. Significant early sulfate accumulation and the availability of sufficient levels were necessary to hinder a formation of stable passive film on the steel surface, but depassivation of steel by sulfate was otherwise difficult. As an initial assessment, it was hypothesized that sulfate ions played a role in corrosion initiation by generating sulfuric acid (H_2SO_4) and were thus related to the localized corrosion process.

The researchers also stated that moisture played an important role: High water content promoted grout deficiency. The effect of excess mixing water (15–20 percent above the manufacturer's recommended limit) was more significant than the prehydration of raw material prior to grout mixing.

13. VIRGINIA TRANSPORTATION RESEARCH COUNCIL [36,37,41]

Before 2001, PT tendon grouts used by VDOT were a mixture of water and cement (water-cement ratio <0.42), and sometimes an expansive admixture was added. Since then, prepackaged grout products for zero segregation, zero-bleed, zero shrinkage, low permeability, and adequate strength have been used after passing VDOT and independent laboratory tests. Still, segregated grout issues, including soft grout and voids, have been identified in the tendons filled with some prepackaged grout products. Possible reasons for the problems included incorrect batching and mixing, unreasonable tendon geometry and length, and high pump pressure.

A series of laboratory tests, including sieve analysis, were conducted for three prepackaged grout products at VTRC in 2012 to determine the effect of mixing water content on the segregation, length change, and compressive strength. Even though all the grout products passed the laboratory tests, they began to segregate when the mixing water above the manufacturer's recommended amount was added. All of them were badly segregated at a water-cement ratio of 0.65. Figure 87 shows a group photograph of three grout products at different water-grout powder ratios, and table 4 summarizes the sieve analysis results of grout products 2 and 3.

W/B = water-grout powder ratio.

Figure 87. Photo. Grout conditions at different water-to-grout powder ratios.[36]

Table 4. Results from sieve analysis of two grout products.

Sieve Number	Grout 2 Retained (percent)	Grout 3 Retained (percent)
16	0.1	0.2
30	0.5	0.1
40	0.0	0.0
50	51.1	0.3
100	38.0	3.0
200	8.0	11.2
Pan	1.7	85.2

The investigators also reported a mockup test result for the U.S. Route 460 segmental bridge project using two full-scale mockup tendons filled with grout 2 and grout 3. Each mockup had a 35-ft-long sloped section. With this arrangement, they were able to compare the performance of two grout products side by side. It was determined that grout 2 performed poorly compared to grout 3 because the former formed a bleed channel at 12 o'clock and developed soft/wet grout. These grouts also exhibited different retain percentages, as presented in table 4. The well performing grout 3 had much finer particles than the poorly performing grout 2. This finding may suggest how to predict grouts' relative performances using sieve analysis.

As an important verification step, the investigators recommended a full mockup experiment to prescreen potential grout-related problems in advance of any major PT projects involving grout. The mockup should include the most critical tendon situation (i.e., the greatest height change and length) using the same grout proposed for the project. During batching and grouting, the amount of mixing water in each batch must be carefully measured, and the grout bags should be weighed to provide the required water-grout powder ratio.

14. UNIVERSITY OF FLORIDA

University of Florida researchers carried out two research projects related to soft grout and alternative fillers to cementitious grout. The following sections summarize their key findings.

14.1 Soft Grout Study[110]

This research project was conducted in three phases to reproduce the soft grout encountered in several Florida PT bridges and determine its causes.

For the first phase of the study, a modified inclined tube test (MITT) was adopted to test prepackaged grout products and custom-formulated grout mixtures for bleeding tendencies and irregular grout formations, such as soft grout under simulated field conditions. The MITT used a bundle containing strands that were shorter in length than those used in the original inclined tube test. This modification facilitated easy duct cutting and sampling and the inspection of soft grout at the top, middle, and bottom of the specimen. It also helped with the subsequent moisture content measurement of the grout samples.

The study employed four commercially available, prepackaged grout products and plain portland cement grout with a superplasticizer with and without 35 and 45 percent pulverized limestone filler. Several variations were introduced in the MITT to simulate realistic soft grout conditions experienced in the field. Test variables included grout pumping pressure, a constricted duct, the volume of the mixing water (including 15 percent water added to the maximum recommended water dosage and residual water in the tube), the volume of a filler, the volume of a superplasticizer, shelf life, storage condition, and temperature. Apparent viscosity testing was conducted using a dynamic shear rheometer to determine if a correlation could be established between the rheology of the grout and the production of soft grout. Other common grout fresh property tests, including flow cone, wet density, unit weight, and pressure bleed, were also routinely conducted.

It was noted that none of the prepackaged grout tested with MITT produced bleed water or soft grout when the grout was mixed and installed by the manufacturer’s recommendations well before the expiration date printed on the bags. A prepackaged grout product (PT4) was prone to soft grout when the volume of mixing water was 15 percent higher than specified or when 256 oz. of water remained in the hose. The same product also produced soft grout when a constricted duct was used on one occasion. Further tests were conducted with PT4 in the tubes packed full of strands, high-temperature injection, pressurized conditions, strand placed in the top of the tube, etc. None of these conditions produced soft grout consistently. Therefore, it was concluded that excess water was the only factor to produce soft grout. Three other commercial products did not produce soft grout, regardless of test conditions.

Although plain cement grout with no fillers also produced soft grout, the probability of producing soft grout increased with filler and superplasticizer. All plain cement-based grouts showed visible bleed water after 1 h. After 24 h, plain cement grout without fillers reabsorbed bleed water, whereas those containing fillers produced bleed water.

Other supplementary tests for evaluating fresh grout properties, such as flow cone, unit weight, wet density, pressure bleed, sedimentation, and bleed readings on inclined tubes, did not indicate

that soft grout would be formed during the MITT. The soft grout produced in the laboratory contained excessive moisture content, between 60 and 80 percent, compared to less than 26 percent when the recommended maximum amount of water was used. This finding was consistent with the soft/wet grout samples obtained from the Ringling Bridge.

The second phase of the study investigated the effect of inert fillers on the production of soft grout and on bleeding in plain grout mixes formulated with three variables: percentages of ground calcium carbonate, dosages of high-range water reducer (HRWR) admixture, and water-cement ratios. The levels of HRWR varied so that each grout mixture achieved a dynamic viscosity below 3.6E-5 psi·s. The following conclusions were drawn from this study:

- For all tests conducted with grouts containing 0, 35, and 45 percent additional filler material, no bleed water was seen when the water-cement ratio was below 0.45.
- When the percentage of filler material increased, the amount of bleed water in the inclined tube for a given water-solid ratio increased.
- HRWR decreased the mixture's viscosity, increased the volume of bleed and segregation, and increased the moisture content near the exit region of the inclined tube.
- Inert filler material increased the tendency to produce soft grout in plain cement grout formulations in the presence of HRWR, requiring careful consideration for PT grout.
- Moisture content along the tubes filled with plain cement grouts and prepackaged grouts had very similar distributions whether the tubes contained soft grout or not.
- Tests resulting in soft grout consistently showed an excessively high moisture content level near the exit region for both the plain cement and prepackaged grout types. The moisture content ranged from 35 to over 50 percent.

The third phase of the study focused on prepackaged grouts' shelf life because long storage time appeared to make prepackaged grout more susceptible to the formation of soft grout under MITT, likely due to prehydration of the portland cement and degradation of the admixtures over time. Three exposure conditions, laboratory, field, and extreme, were adopted to expose the grout products, and then MITTs were conducted. Particle size analyses were conducted to determine if there was a correlation between soft grout and particle size due to prehydration. The following conclusions were drawn from the study:

- Prolonged storage time increased the likelihood prepackaged grouts would produce soft grout, even with favorable storage environments.
- All grouts with expired shelf lives produced soft grout.
- High temperature and high RH environments (95 ^{o}F and 95 percent RH) during storage of dry prepackaged grout material increased the probability of forming soft grout with significantly increased mean particle size.

- Standard methods for determining the shelf life of grout should be developed to ensure that PT grout will perform adequately after storage.

- Specific requirements for temperature and RH limits in storage environments are needed.

14.2 Flexible Filler Study[111]

The second research project was performed on flexible fillers to investigate the constructability of unbonded, multistrand tendons injected with flexible fillers. This project was divided into three areas.

The first research area involved the design, construction, and heating and injection procedures of full-scale PT tendon mockups. Four commercially available microcrystalline wax filler materials were chosen to evaluate their heating and injection procedures into five 200-ft-long mockups with profiles simulating internal and external tendons. Each tendon contained 19 0.6-inch prestressing strands in a four-inch-diameter HDPE duct. The strands were lightly stressed to distribute them in the duct, similar to the fully stressed tendons in the field.

Injection rates and venting procedures were varied among the five mockups, primarily in an effort to determine the most suitable approach. The wax barrels were heated to about 220 °F.

Temperature and pressure were measured during and after injection to track the behavior of the materials. The target injection rate ranged between 50 and 80 ft/min. It was observed that two tendons contained a void at the top of the duct's cross-section in the parabolic portion. In one case, venting was intentionally omitted. In the other case, the void was thought to be caused by inadequate venting procedures. Overall, all the strands in each mockup were well coated with filler material, despite the variation in the installation procedures.

In addition, a closed-form heat transfer model was developed and compared to the actual data gathered during the mockup injections. The model was to better understand the heat transfer process and estimate heat loss at the filler's front. The experimental data supported the applicability of the thermal model to a wide range of tendon lengths and material and injection parameters. After the model was validated with experiments, it was used to determine the sensitivity of filler temperatures to various field parameters (e.g., tendon length, ambient temperature, injection rate) that could provide critical guidance on the constructability of unbonded tendons with flexible fillers.

Pressure losses for different flow velocities and tendon lengths were also estimated to help decide injection pressure. Knowing the tendon geometry, hydraulic injection conditions, and filler material properties, this model could be used to compute the rate of cooling of a filler's front during injection. These data could then be used to determine a maximum length of continuous injection. A method for determining effective strand surface area was also developed for use in the thermal model.

The second research area was on the structural implications of the change from cementitious grout to flexible fillers. It focused on the flexural strength behavior of specimens with internal and external tendons. It was determined that the use of flexible fillers in internal and external tendons would result in a change in the contribution to the flexural strength of the specimens.

The third research area focused on developing a robust and cost-effective monitoring system for unbonded PT tendons. The change from bonded to unbonded tendons could lead to the development of an efficient tendon damage detection system as soon as a single wire break. For this purpose, analytical and experimental investigations were performed to develop an algorithm that can detect, locate, and quantify tendon damage by monitoring the strain distribution in the wedge plates of the anchors.

15. FLORIDA DEPARTMENT OF TRANSPORTATION[112]

FDOT carried out an in-house study to evaluate the effectiveness of an injectable corrosion inhibitor method, known as the impregnation method, to reduce or stop corrosion in grouted PT tendons. For this study, six control (untreated) specimens with no inhibitor and six specimens injected with a commercially available, silicon-based polymer corrosion inhibitor were prepared. Each specimen group was divided into two exposure conditions: The first six specimens were placed in a salt fog chamber utilizing a 5 percent NaCl solution, and the remaining six specimens were exposed to a 3 percent NaCl ponding solution. Figure 88 shows some of the specimens after exposure to the two different conditions.

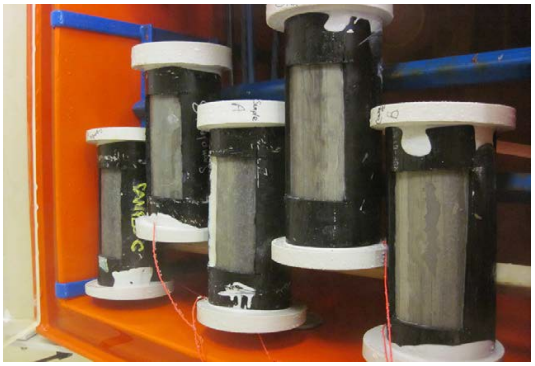

A. Specimens in a salt fog chamber.

B. Saltwater ponding specimens.

Figure 88. Photos. Impregnation test specimens.[112]

Corrosion potential data of the specimens in the salt fog chamber were collected using a copper-copper sulfate reference electrode to monitor changes in their corrosion tendencies twice a week. As shown in figure 89, the measured corrosion potential of the corrosion inhibitor-treated samples (samples A, B, and C) clearly showed more positive potentials—indicative of a passive state—with time than the control samples (controls A, B, and C).

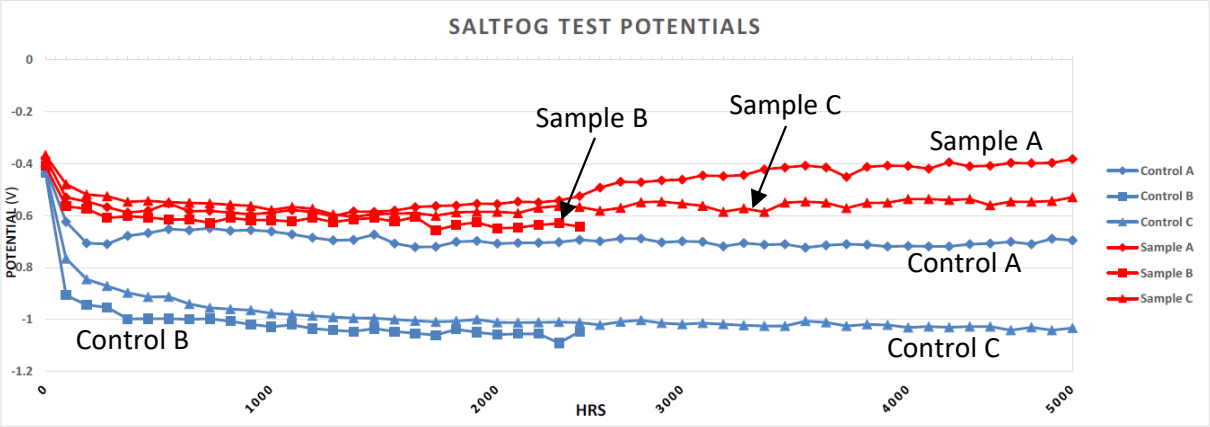

Figure 89. Graph. Corrosion potential data from salt fog chamber specimens.[112]

The LPR data of the ponding specimens were also collected to monitor their corrosion intensity because LPR is inversely proportional to CR. LPR measurements were made initially every week and then changed to bi-weekly at 1,008 h. The LPR data indicated that two of three corrosion inhibitor-treated specimens were not corroding. The third treated specimen exhibited polarization resistance values similar to the control specimens.

One salt fog chamber specimen and 2 saltwater ponding specimens per both the control and treated groups (a total of 6 specimens) were autopsied after 2,520 h of exposure testing. The remaining 6 specimens were autopsied after 5,208 h of exposure testing. Figure 90 and figure 91 show representative conditions of the control specimens after 5,208 testing h. Similarly, figure 92 and figure 93 show representative conditions of treated specimens after 5,208 testing h.

A. Exterior condition.

B. Interior condition.

Figure 90. Photos. Control specimen exposed to salt fog chamber.[112]

A. Exterior condition.

B. Interior condition.

Figure 91. Photos. Control specimen exposed to saltwater ponding.[112]

A. Exterior condition.

B. Interior condition.

Figure 92. Photos. Treated specimen exposed to salt fog chamber.[112]

A. Exterior condition.

B. Interior condition.

Figure 93. Photos. Treated specimen exposed to saltwater ponding.[112]

The accelerated corrosion testing in the salt fog chamber and saltwater ponding induced severe corrosion to the control specimens such that corrosion products were observed on all of their exterior surfaces even before the autopsy. On the other hand, the inhibitor-treated specimens exhibited virtually corrosion-free exterior surfaces.

When each specimen was split open to observe the condition of the embedded strands inside, all the control specimens had significant corrosion, but the treated specimens did not. One exception was observed at one end of treated specimen 3, which exhibited minor corrosion on about five percent of the strands near the exposed end, as shown in figure 93-B. The actual conditions of the specimens observed during the autopsy reflected the electrochemical data.

16. FLORIDA ATLANTIC UNIVERSITY[113]

This study aimed to characterize the corrosion protection properties of five microcrystalline wax products as flexible fillers. Some of the tests involved exposing coated strands/wires to high RH or outdoor environments. For another set of tests, three different fungi species (Fusarium oxysporum, Penicillium chrysogenum, and Aspergillus flavus) were introduced purposely by spraying to contaminate the five fillers mentioned above. Two types of steel specimens were prepared: 7-wire strand specimens and single-wire specimens. These specimens were first coated with flexible fillers and then exposed to fungi species.

This study confirmed that corrosion for the strands and single wires could start in areas where the flexible filler was removed, or a thin layer of the flexible filler remained. Airborne chloride and particulates in the exposure environment penetrated through the flexible filler and started corrosion in the presence of electrolyte film upon exposure to high RH. Flexible fillers contaminated with fungi also experienced more corrosion than those exposed to plain water due to microbiologically influenced corrosion (MIC). The investigated fungi species could utilize the waxes as a carbon source to cause different levels of MIC.

17. FEDERAL HIGHWAY ADMINISTRATION

FHWA studies have commenced since the discovery of chloride contamination in a prepackaged grout product in 2010 and the advent of the segregated grout problems, often with elevated levels of sulfate ions, encountered in the Ringling Bridge in 2011. Specifically, a series of four laboratory studies have been conducted at the FHWA Coatings and Corrosion Laboratory on the following topics:

- Chloride threshold.
- Sulfate-induced corrosion in segregated grout.
- Water-soluble sulfate concentrations in different grout conditions.
- Water-soluble sulfate ions' corrosivity.

The results of the research studies have been published in four FHWA reports so far. The major findings of these reports are summarized in the following sections.

17.1 Chloride Threshold Study[38,72]

In response to a nationwide problem caused by a chloride-contaminated prepackaged grout product, an accelerated corrosion testing program was carried out to determine chloride threshold value(s) for grouted PT tendons. No such information was available before that time. Domestic codes like the American Association of State Highway and Transportation Officials (AASHTO) and PTI allow either 0.08 percent acid-soluble (total) or 0.06 percent water-soluble chloride concentration by the weight of cement. In the foreign codes, the allowable total chloride concentration limit varies between 0.023 percent (Japanese code) and 0.2 percent (EN) by weight of cement. Although it was known that corrosion risk generally increased as chloride concentration increased, lower total chloride thresholds than the specified limits might be more appropriate depending on exposure conditions in the field. Thus, this laboratory study was launched to investigate this possibility.

The accelerated corrosion testing program consisted of three experimental tasks using three types of laboratory specimens. The prestressing steel of 0.6-in 7-wire strands was employed, and most of the specimens were stressed to 60 percent of GUTS. Single-wire specimens—made with center wires extracted from 7-wire strands—were tested for corrosion potential and CR by LPR after 24-h immersion in two different aqueous test solutions with pH values of 9 and 13.6 and 10 different chloride concentrations. Half of the specimens were stressed at 60 percent of GUTS, and the others were unstressed. Figure 94 presents their corrosion potential data (see figure 94-A) and CR data (see figure 94-B).

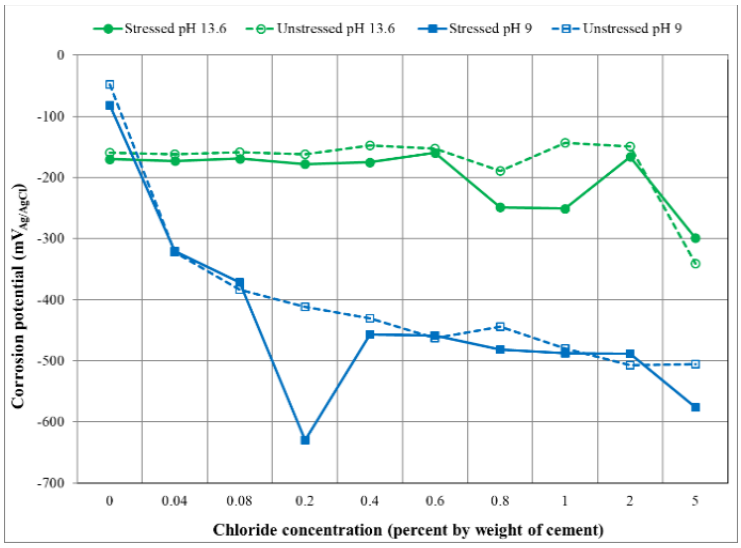

Source: FHWA.

A. Corrosion potential data.

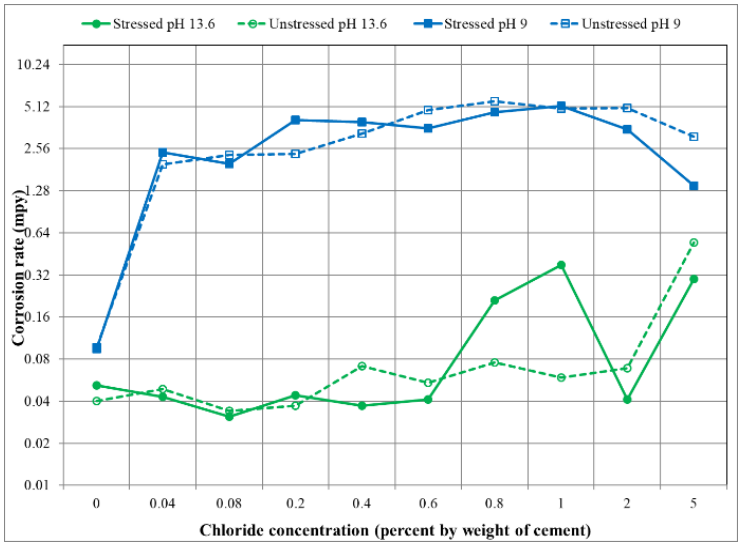

Source: FHWA.

B. Corrosion rate data.

Figure 94. Graphs. Corrosion data from center wires in different aqueous solutions.[72]

The passive film protected the wires immersed in the pH 13.6 solutions, as evidenced by more positive corrosion potentials than -200 mV versus silver-silver chloride reference electrode ($mV_{Ag/AgCl}$) and a very low CR (less than 0.05 mpy) up to 0.6 percent chloride concentration. Beyond the concentration, CR increased except for the 2 percent chloride data. The effect of stress on CR did not show a consistent trend, regardless of chloride concentration.

For the wires tested in the pH 9 solutions containing 0.04 percent and higher chloride concentrations, corrosion potentials became progressively more negative as chloride concentrations increased. Conversely, the matching CRs went up sharply compared to the CRs of

the chloride-free pH 9 and the CRs of all the pH 13.6 solutions. The observed reduction of CR at 5 percent chloride concentration was thought to be caused by limited dissolved oxygen in the presence of excessive chloride ions. Again, there was no consistency observed regarding the effect of stress on the CR.

The electrochemical testing data for aqueous solutions suggested that the PT strand could tolerate up to 0.6 percent chloride contamination without significant corrosion in carbonation-free, high-pH grout. However, in carbonated grout, active corrosion could be initiated by as little as 0.04 percent chloride concentration—below the AASHTO-specified chloride limit of 0.08 percent by weight of cement. Once corrosion started in the low-pH environment, the level of CR depended on chloride concentration.

To make the grouted single-strand and multistrand specimens stressed at 60 percent of GUTS, the same prepackaged grout product known to contain elevated levels of chloride ions was employed. After a chloride-free grout batch was acquired to avoid unintended chloride contamination, appropriate amounts of NaCl were admixed to produce eight levels of chloride-contaminated grout mixes containing 0, 0.08, 0.20, 0.40, 0.60, 0.80, 1, and 2 percent chloride by weight of cement. The fabricated specimens went through an accelerated corrosion testing scheme: successive two-week subcycles of ambient (77 °F and 60 percent RH), hot and humid (104 °F and 90 percent RH), ambient, and freezing and drying (14 °F and 40 percent RH).

During the six-mo testing period, three full cycles were completed. A group of control specimens was also kept in an ambient laboratory environment. For grouted specimens with a void, small amounts of water and fresh air were periodically introduced into the void to simulate water-recharging events. The collected electrochemical data were corrosion potential, CR (single-strand specimens only), macrocell corrosion current density (multistrand specimens only), and apparent grout resistance and resistivity.

For the single-strand grouted specimens, 0.4 percent was the lowest chloride concentration to make mean corrosion potential become gradually negative in ambient and hot and humid conditions, and mean CR became progressively higher. In the freezing and drying cycles, the corrosion of all specimens decreased to a negligible state, regardless of chloride concentration.

A general trend observed from the multistrand specimens was that more pits associated with intensive macrocell corrosion were found on the segments closer to the grout/void interface when chloride concentrations were 0.8 and 1 percent. When chloride concentration was between 0.08 and 0.6 percent, no measurable pits were found at all.

Based on these test results, two chloride thresholds were established for the strands encased in the normally hardened grout. The first chloride threshold was 0.4 percent by weight of cement. This value was the lowest concentration to initiate the corrosion of strands by forming a small number of pits on the strand surface. The second chloride threshold was 0.8 percent by weight of cement. At this critical concentration, corrosion started intensifying in terms of the number of pits and the pit depth associated with the corrosion propagation process.

17.2 Sulfate-Induced Corrosion in Segregated Grout[72,114]

During the autopsy of the multistrand specimens employed for the chloride threshold study, severe corrosion was observed at the grout/void interface of three specimens containing 0, 0.4, and 2 percent chloride concentrations. Figure 95 shows the grout/void interface of a chloride-free multistrand specimen after the duct was removed.

Source: FHWA.

A. Strands at grout/void interface.

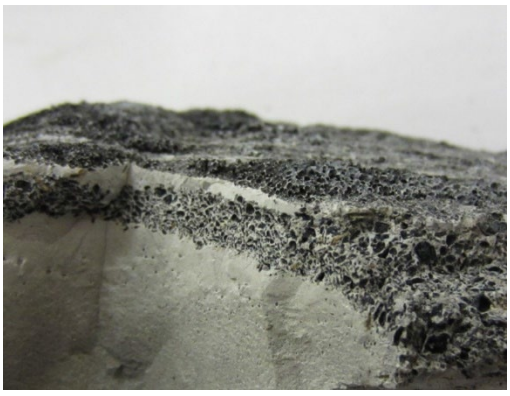

Source: FHWA.

B. Cross-section of the interface.

Figure 95. Photos. Chloride-free multistrand specimen.[72]

The interface was covered with a thick black deposit (see figure 95-A), which penetrated the top layer of the interface (see figure 95-B). The black deposit layer was porous and contained numerous small black particles. They appeared to be remnants of grout segregation. Figure 96 shows a closeup of corroded wires after a strand segment in contact with the porous grout layer shown in figure 95-A was removed and dismantled.

Source: FHWA.

Figure 96. Photo. Close-up of corroded wires from a strand segment that came into contact with the porous grout layer.[72]

Severe corrosion damage can be seen in the area near the grout/void interface despite a chloride-free condition. Figure 97 shows another severely corroded strand in the 0.4 percent chloride multistrand specimen. Its deterioration was revealed only after the bottom section of the void/grout interface was broken off during the de-tensioning process.

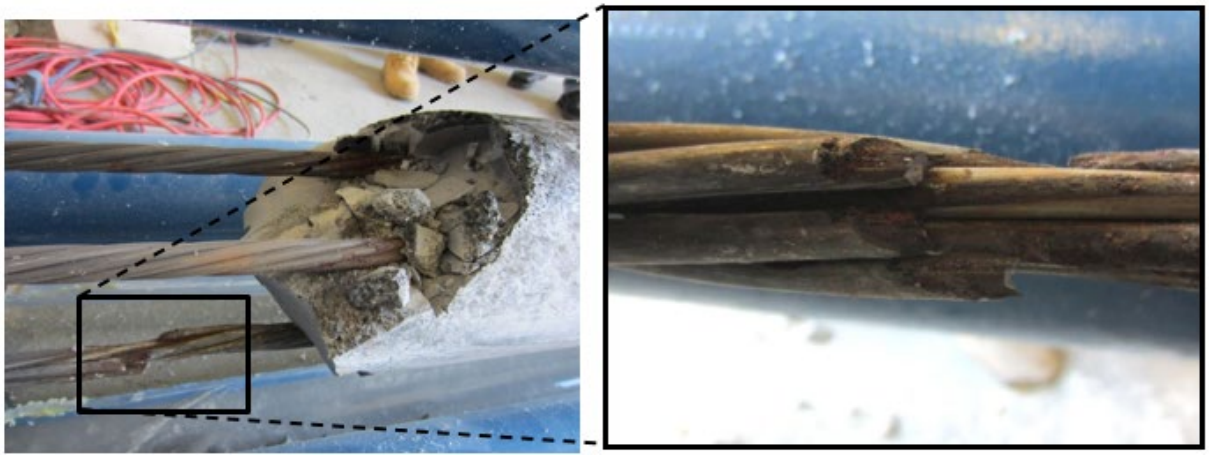

Source: FHWA.

Figure 97. Photos. Severely corroded strand in a 0.4 percent chloride multistrand specimen: Opening the interface and three broken wires.[72]

Three wires of one stressed strand were fractured by excessive stress concentrated in the corroded areas with significant section loss (see figure 97-B). The interfacial grout looked identical to the grout fragment of the chloride-free multistrand specimen shown in figure 95.

The discovery of severe corrosion, even in the absence of chloride ions, triggered a small laboratory investigation using an IC instrument. The investigation analyzed water-soluble sulfate ions in black deposits removed from interface fragments of the 0, 0.2, and 0.4 percent chloride multistrand specimens. For reference purposes, a raw grout powder sample and three normally hardened bulk grout samples collected from 0, 0.08, and 0.4 percent chloride multistrand specimens were also analyzed.

The raw grout powder contained 0.9 percent of water-soluble sulfate ions by weight of cement, whereas the black particles and the black deposit layer collected from the chloride-free multistrand specimen contained three times higher water-soluble sulfate ions. The elevated level of water-soluble sulfate ions in these samples was thought to be responsible for the unexpected corrosion damage observed in the chloride-free grout.

The grout fragments of the 0.4 percent chloride multistrand specimen did not contain sufficient black deposit material to perform ion chromatography analysis, so it could not be determined whether excessive water-soluble sulfate ions on its interface were also responsible for the fracture of the three wires shown in figure 97. The other grout samples taken from the areas free of the black deposit layer contained negligible water-soluble sulfate ions. The remaining sulfate analysis data indicated that the sulfate ions resided in the normally hardened grout samples were chemically bound evenly in the cement paste, and little could be leached out.

After corrosion damage was observed in the segregated grout layer and the water soluble sulfate ions were found there, the second accelerated corrosion testing study was conducted as part of the development of a model to forecast the failure of deficient grout in PT tendons. This spin-off study was performed to investigate the propensity of strand corrosion in the presence of water-soluble sulfate ions under several conditions, including grout segregation and carbonation. Three prepackaged grout products were employed.

The stressed and unstressed center wires were embedded in the voided grout specimens, made either with normally hardened grout or segregated grout. The segregated grout mixes were intentionally produced with 35 percent more water than the grout manufacturers' recommendations. The wires were exposed to 0, 0.4, 0.8, and 1.5 percent sulfate concentrations by weight of cement, which were admixed into 48 fresh grout mixes or introduced by injecting the pH 8 and 13.6 water containing specific sulfate concentrations into the artificial voids.

A total of 63 stressed wire specimens per grout product were tested at 104 °F and 80–95 percent RH. To simulate recharging water events, 0.34-oz solutions were injected several times. Ambient exposure testing at 77 °F was also performed with 12 specimens (four stressed and eight unstressed) per grout product. The corrosion of the wire specimens was nondestructively monitored by measuring macrocell corrosion current, LPR, and grout electrical resistance. At the end of the testing, the wires were extracted and cleaned, and then the pit depth was measured with a digital pit gauge.

All visible corrosion damages were concentrated at or near the grout/void interface. In figure 98, for example, figure 98-A shows a severely corroded wire near a segregated grout/void interface within a two-inch-diameter, 12-inch-long grouted specimen that was longitudinally cut in half along its length. Figure 98-B shows a closeup of the corroded wire after it was cleaned. This particular wire specimen (diameter = 0.205 inches) had been stressed at 60 percent GUTS and periodically exposed to a 0.8 percent sulfate concentration dissolved in recharging water with a pH of 8 for 200 d at 104 ºF.

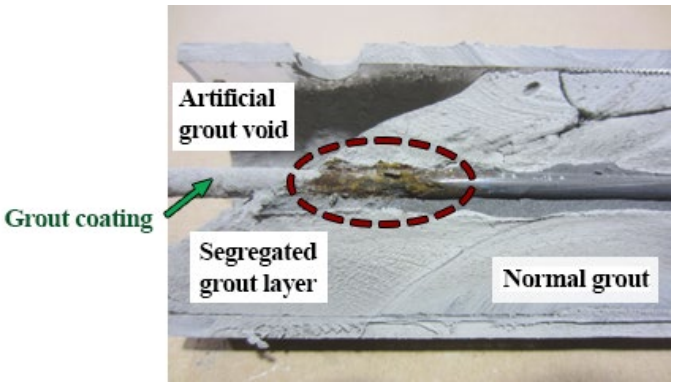

Source: FHWA.

A. Corroded wire at the interface.

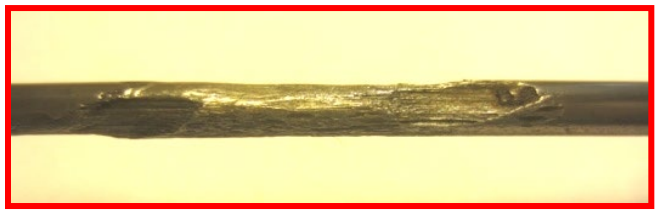

Source: FHWA.

B. Closeup of the cleaned wire.

Figure 98. Photos. Corroded wire in segregated grout/void interface.[114]

Accelerated corrosion testing was able to produce significant corrosion damage in the segregated grout layer in the presence of sulfate ions. The maximum pit depth was 48.5 mils, which was equivalent to 88.5 mpy. This example, although it involves a stressed single-wire and not a 7-wire strand, still illustrates the severity of macrocell corrosion in undesirable exposure conditions. These conditions may include segregated grout contaminated with elevated levels of water-soluble sulfate ions. In contrast, wire specimens exposed to normally hardened grout were hardly influenced by pH changes from 13.6 to 8.0 and changes in sulfate concentration.

It was concluded that when grout segregation occurred during the grout injection process, water-soluble sulfate ions and black particles—presumably, black carbon from silica fume—were released from the fresh grout mixture into the bleed water and floated to the high point. As the bleed water that had collected at the top was reabsorbed into the grout during the curing stage, a segregated grout layer could be formed at the grout/void interface. This defective grout resulted in a porous layer due to abnormally high water-cement ratios, entrapped air bubbles, and silica fume particles that could be dispersed within the segregated grout layer or settled on top of the interfacial layer. Since the porous layer could hold water like a sponge for a longer period than the nonporous layer, it could provide a corrosive condition for the strands in contact with the segregated grout. When an excessive amount of sulfate ions was liberated from the segregated grout and accumulated in the porous layer, a more serious corrosive condition was formed at the grout/void interface. Consequently, grout segregation created a more corrosive condition than the normally hardened grout in the low pH environment.

17.3. Sulfate Concentrations in Different Grout Conditions[115]

A third laboratory study was performed to investigate how water-soluble sulfate ions could be present in various types of grout samples made of three prepackaged grout products. These commercially available grout products were designated as products 1, 2, and 3. Products 1 and 2 were acquired just before starting this study, but product 3 consisted of leftovers from previous FHWA laboratory studies to see how the expired grout behaved. They were labeled #1 old product 3 and #2 old product 3. For each product, three four-by-eight-inch cylindrical specimens were fabricated in three batches (one more batch was made with an opened bag of #2 old product 3). The fourth cylindrical specimen of each product was made by adding 0.5 lb of water to the remaining mix after the third cylindrical specimen was cast. These four specimens were made to investigate each product's grout segregation tendency in the presence of a modest amount of extra water.

The product 1 and product 2 specimens containing the recommended water dosages showed a light or dark gray color. Their extra-water specimens appeared porous with many air bubbles in different sizes due to grout segregation. The product 3 specimens showed the worst appearance, and their color variation was the largest. The product 3 specimens made with extra water exhibited the most porous top surfaces, with thick, black deposit layers due to excessive grout segregation. These specimens mimicked the black top layer shown in figure 95 and used the same grout (#2 old product 3).

The water-soluble sulfate contents in the laboratory grout samples were analyzed. Figure 99 summarizes their mean water-soluble sulfate concentration data.

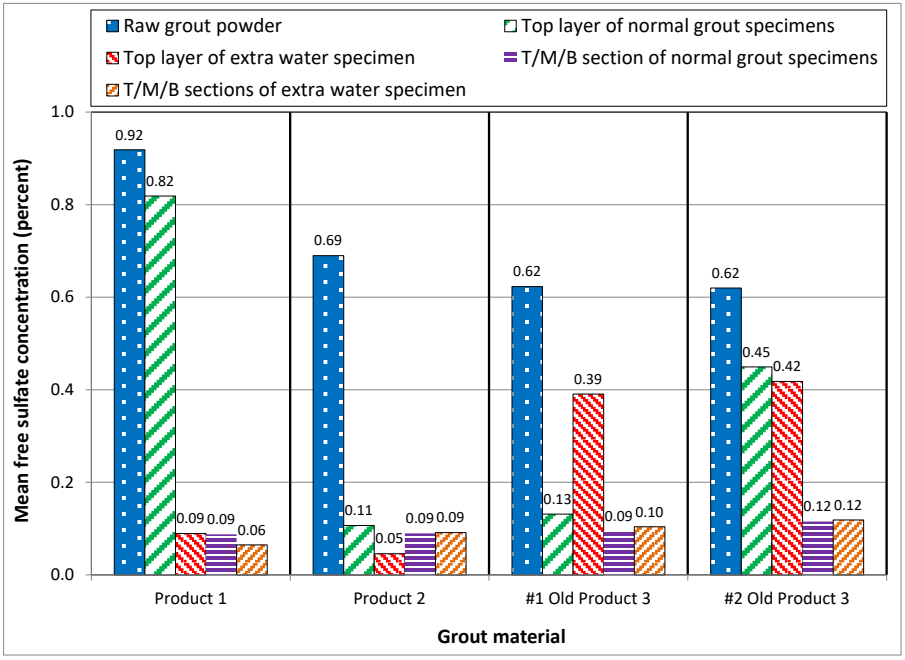

Source: FHWA.
T = top; M = middle; B = bottom.

Figure 99. Graph. Mean water-soluble sulfate concentration data in various types of grout samples.[115]

Individual water-soluble sulfate concentrations in the raw grout powders ranged from 0.35 to 1.01 percent by weight of sample, and their mean water-soluble sulfate concentrations were between 0.62 to 0.92 percent. When the grout powders were mixed with water and cured, most of the water-soluble sulfate ions became bound to the hardened cement paste through the hydration process. As such, water-soluble sulfate concentrations were drastically reduced to around 0.1 percent in all the grout specimens, including the extra water specimens. However, a higher level of water-soluble sulfate ions was consistently found in the segregated top grout layer than in the normally hardened bulk grout. Moreover, products 1 and 3 released more water-soluble sulfate ions in the top surface layer, irrespective of water volume, than product 2, suggesting that the liberation of water-soluble sulfate ions depended on the segregation characteristics of individual grout products.

The petrographic examination and chemical analyses of two field grout samples retrieved from the Ringling Bridge grout sample determined that 100 times higher water-soluble sulfate concentrations were more frequently found in pore water and soft/wet grout samples than in dried and hardened normal grout samples. The total sulfur content of the soft grout sample was also 3.5 to 5 times that of the hardened grout sample. It was likely that the water-soluble sulfate ions migrated through water movement as part of the grout segregation process. Consequently, the water-soluble sulfate ions were concentrated in the soft (segregated) grout. It was also revealed that the sulfate ions were contained in fine particles of the raw grout powder (smaller than 0.2 mils).

It was concluded that prepackaged, premixed grout products did not guarantee the uniform and consistent quality of raw ingredients packaged in individual bags. Also, unpredictable segregation behaviors could be encountered, even for laboratory specimens prepared in a reasonably controlled environment. These conditions could lead to highly variable water-soluble sulfate concentrations in the cement paste, especially in the top surface layer of the segregated grout. One particular grout product was more prone to inducing segregation and releasing water-soluble sulfate ions into the segregated grout than the other grout products, especially when it passed the recommended shelf life.

17.4 Corrosivity of Sulfate Ions[115]

The fourth and last laboratory study was conducted through two rounds of accelerated corrosion testing in aqueous test solutions that simulated grout pore water (and bleed water). A total of 784 center wires extracted from the 7-wire strand segments were prepared for this study. Different experimental conditions were introduced in terms of pH, stress level, strand supplier, surface condition, anion concentration, and temperature. Four target pH solutions were prepared to simulate different degrees of carbonation, which were considered the most critical factor for sulfate-induced corrosion. The target pH values (actual pH in the first and second rounds of testing) were 8 (7.8, 8); 10 (10, 9.8); 12.5 (12.4, 11.9); and 13.6 (13.4, 13).

The first round of testing was to determine the corrosivity of water-soluble sulfate ions in the simulated grout pore water. Each of four pH solutions was divided into nine anion-containing test solutions: five sulfate concentrations (0.2, 0.4, 0.8, 1.5, and 3 percent by weight of cement) and four chloride concentrations (0.08, 0.4, 0.8, and 2 percent by weight of cement). Anion-free solutions were prepared as controls, and the historically much-studied chloride was included as a

baseline for judging the corrosivity of sulfate ions. In addition, two equal concentrations of chloride and sulfate ions (0.4 and 0.8 percent by weight of cement) were intermixed to investigate the corrosion behavior of two competing anions in the same solution. Some specimens were tested at 60 percent of GUTS to investigate the effect of stress on corrosion activities, and the others were unstressed. The majority of the tests were performed at 77 ºF and 104 ºF, and a limited number of tests were performed at 40 ºF.

The second round of testing was to determine whether the surface condition of the wires could influence sulfate-induced corrosion behavior under different pH environments. Therefore, each of the four pH solutions was divided into eight sulfate-containing test solutions, including three lower sulfate concentrations (0.05, 0.10, and 0.15 percent by weight cement) to supplement the first round of testing. No more tests were conducted in chloride solutions, and all tests were performed without stress at 77 ºF and 104 ºF only. For as-received wire condition, the wires were gently wiped with a paper towel so that the factory-applied lubricant remained as undisturbed as as possible. For the cleaned wire condition, the lubricant was removed by wiping the wires several times with a rag soaked with denatured alcohol, and then a final cleaning was done with a paper towel.

Figure 100 shows mean corrosion potential data (see figure 100-A) and mean CR data (see figure 100-B) from the first and second round of testing conducted in the one sulfate-free and eight sulfate concentrations dissolved in various pH solutions at 77 °F. The legend includes the target pH values and the actual pH values for the first and second test rounds.

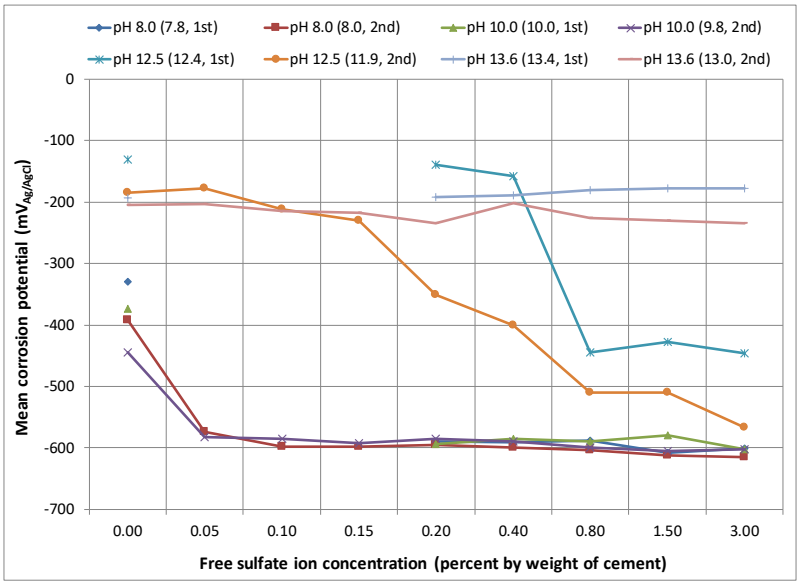

Source: FHWA.

A. Mean corrosion potential data.

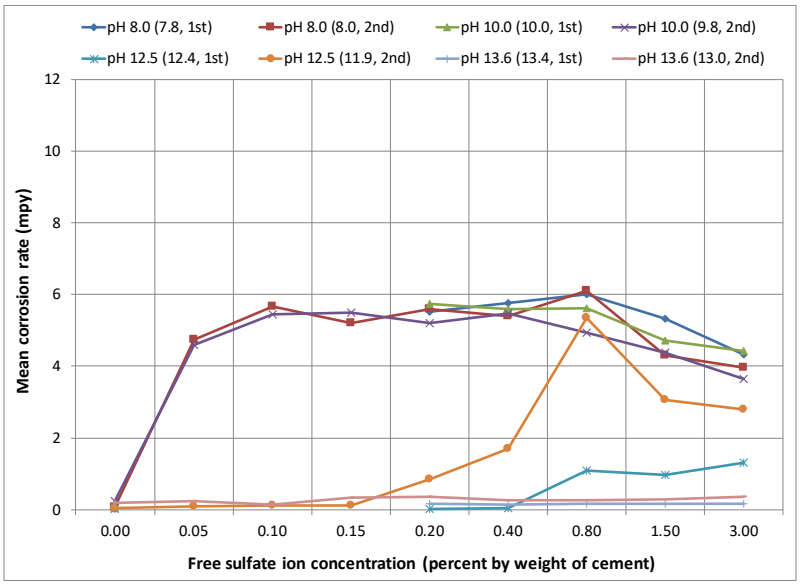

Source: FHWA.

B. Mean corrosion rate data.

Figure 100. Graphs. Corrosion data in sulfate solutions at 77 °F.[(115)]

Overall, the electrochemical data can be summarized as follows:

- Sulfate-influenced corrosion behaviors of the wires, such as reactions to chloride, depended on ionic concentration, pH, and temperature. Sulfate-free conditions yielded virtually zero CRs, regardless of pH and temperature.
- The key factor that determined the corrosivity of both anions was pH, as follows:
    - The sulfate and chloride ions exhibited similarly high corrosion tendencies in terms of corrosion potential and CR in the neutral and weak alkaline solutions.
    - The chloride ions acted more aggressively than the sulfate ions at a nominal pH of 12.5.
    - Both anions showed equally negligible corrosion at a nominal pH of 13.6.
- Equal concentrations of sulfate and chloride ions behaved similarly in the neutral and weak alkaline solutions, but chloride ions became more aggressive than sulfate ions in the high pH solutions, irrespective of temperature.
- Both anions exhibited temperature-dependent behavior:
    - Corrosion was more severe at 104 °F than at 77 °F under identical testing conditions.
    - Mean CRs measured at 40 °F were less than 10 percent of those measured at 77 °F, independent of anion concentration.

It was concluded that sulfate ions should be as detrimental as chloride ions to PT strands if the strands were exposed to carbonated grout or moist air in the grout voids, but negligible sulfate-induced corrosion damage would be expected in high-pH environments.

18. EUROPEAN RESEARCH WORK

The grout tests were performed at the Center for Experimental Research and Studies of Building and Construction (CEBTP).[116,117] The researchers used translucent ducts that contained 7-wire strands, were 15 ft long, and inclined approximately 30 degrees from the horizontal. The realistic tendon setup made it possible to observe the bleed-water phenomenon.

Maximum grout segregation was produced when the degree of inclination was between 30 and 60 degrees. The researchers noticed that separation occurred by gravity between the heavier cement suspension and the lighter mineral species (particularly ettringite and portlandite) formed during the hydration process. If certain conditions were met with a superplasticizer, the mineral species moved upward with air bubbles along the tube. At the end of the test, a layer of whitish paste surrounded by yellowish bleed water was formed at the highest point of the tube. The bleed water was surrounded by a space filled with air. It was determined that the degree of bleeding depended on the duct's geometry, and the presence of the strands could amplify the volume of air and water with a filtering effect. The whitish paste hardened quickly when in contact with air.

Mineralogical analyses showed that the material was primarily made up of ettringite (40 percent), portlandite (20 percent), and calcite (20 percent). The calcite was thought to be formed by the carbonation of the portlandite. The remainder of the paste contained a high concentration of admixtures and sulfates. The yellowish bleed water had a composition close to the interstitial solution of a cement paste with very strong alkalinity (pH 13.8). Certain discharged ingredients were combined with a settlement of the grout. This phenomenon was amplified by the presence of a superplasticizer, which could cause incompatibility with the cement in some cases. In turn, the incompatibility resulted in the grout's instability during the dormant phase of the grout set.

Nurnberger reported the risk of strand fracture due to hydrogen-induced SCC that resulted from the joint action of prestressing steel properties and hydrogen.[118] Hydrogen can be produced through cathodic reaction under certain neutral and acid conditions. The bleed water created severe pits as deep as 39 mils within a few weeks. The chemical analysis of the bleed water is seen in table 5.

Table 5. Results of chemical analysis of bleed water (pH = 10 ~ 13).

Ionic Species	Concentration (ppm)
Sulfate	1,900–5,200
Chloride	130–180
Potassium	3,600–7,300
Sodium	180–370
Calcium	60–90

It was believed that large amounts of sulfate and potassium ions leached out of the raw ingredients in the grout, such as the gypsum in the cement, aggregates, and water.

Blactot et al. conducted a series of laboratory tests with unstressed steel cables in two de-aerated aqueous solutions and simulated segregated grouts to investigate the effects of the deficient grouts and exposure conditions on SCC.[119] Two assumptions were made, as follows:

- The steel cables were exposed to mechanical stress.
- The steel cables were exposed to a dual-grout condition in the ducts: normal cement grout and segregated grout that possessed a high pH (close to 14) and sulfate ions but no oxygen.

The researchers theorized that, under these assumptions, some sections of the cables were favorable to generating hydrogen atoms or molecules via cathodic reaction, which could diffuse into the steel structure. Following this generation, SCC assisted by HE could occur and lead to the wire fracture. It was speculated that a specific layer present on cold-drawn prestressing steel strands broke up and thus generated a high susceptibility to corrosion. In the end, the researchers concluded, based on their key findings, that sulfate ions had little influence on active/passive transition and SCC in de-aerated, high-pH environments, regardless of sulfate concentration. It was also reported that corrosion potential did not depend on the concentration of sulfate ions, either.

As mentioned briefly in chapter 3, one of the external tendons in an unidentified bridge in Italy failed less than two yr after construction. The bridge was a segmental, PT box girder-type with external tendons consisting of 27 7-wire, high-strength steel strands located inside grouted HDPE ducts.[79,80,120] Laboratory investigations were carried out using two segments of the failed tendon. Approximately 24 percent of the original wires were missing, including two complete strands and several center wires. Each of the remaining wires was visually examined to identify the type of fracture, the fracture's location from the anchor head, and the extent and depth of the corrosion damage. Failed wires by corrosion-induced section loss and ductile necking accounted for 15.3 and 29.1 percent of the failed wires, respectively. The remaining 55.6 percent had failed due to a mixture of corrosion and necking. Many localized corrosion morphologies exhibited shallow damage, but deep corrosion attacks similar to chloride-induced pitting corrosion were also observed on the wires. Corrosion attacks were randomly distributed along the length of the inspected steel samples. Residues of whitish, unhardened paste were also found on recovered steel surface.

Although normally hardened grout filled the tendon samples in most cases, deficient grout with consistency and color similar to that found in the failed tendon could be observed. The grout extracted from the second tendon segment was nonhomogeneous, and three different areas were identified: First, the bottom part had a gray, hardened cement paste. Second, an intermediate part consisted of a whitish, friable material. Third, an upper part had a whitish, damp paste with a plastic consistency. When the damp grout from the upper part was dried out for about 24 h, it became friable like the grout in the intermediate part. The moisture content of the grout at the time of sampling approached the absorption of the sample, and the grout along the duct was still

saturated with water. Shallow corrosion damage was observed on 12 of the 27 strands, particularly those in contact with the whitish substance.

A detailed examination was carried out with more than 60 grout samples collected in different parts of the failed tendon and others removed afterward. The segregated and nonsegregated samples were used to investigate their compositions and microstructures and corrosive parameters. The grout samples were classified into four types by their consistency and color, as follows:

- Type G—Hardened grout with typical features, including gray color.
- Type B—Hardened grout with a dark gray (almost black) color.
- Type W—Segregated, unhardened whitish grout containing a plastic paste (wet) or a weak and friable material (dry).
- Type P—Hardened light gray grout containing black spots between type W and G grouts.

Type G grout found along the duct exhibited typical composition, microstructure, and properties of the normally hardened grout. This grout allowed full passivation of the steel. Type B grout was occasionally found at the bottom of the duct. It was a denser, hydrated cement paste with a lower water-cement ratio but still allowed passivation of the steel. Thus, no corrosion attacks were found in the areas where the strands were embedded in G and B grouts.

Type W grout and voids and—to a lesser extent, type P grout and voids—were found in the inclined part of the tendons near the anchorages, only on the opposite side of the grout injection. Grout voids were also found in some cases in the upper part of the duct. It was speculated that grout segregation occurred on the opposite side of the grout pumping port during the injection or early hydration stage. In most cases, only traces of this grout were observed, usually in the form of a thin stripe on the top of the duct. However, a large quantity of W grout was found in few cases. Type P grout could rarely be detected from the surface.

Localized pitting corrosion was observed only in the areas in contact with type W grout. CRs of the order of several millimeters per yr could be estimated. In some cases, the entire cross-section of the wire was depleted. Shallow corrosion attacks were occasionally observed on steel embedded in type P grout. No broken wires were found at the injection side, and the number of strands with corrosion damage deeper than 39 mils was minimal.

The segregated W grout contained much higher and more variable amounts of alkalis (mean composition of sodium oxide [Na_2O] and potassium oxide [K_2O] were 1.1 and 1.6 percent by dry mass, respectively) and sulfate ions (6.3 percent) than the nonsegregated grout. Particularly, sulfate concentration in the segregated grout was nearly twice that of the nonsegregated grout. Thermal analyses showed a lower calcium hydroxide ($Ca[OH]_2$) in the segregated grout than in the nonsegregated grout. This finding can be explained by the fact that, as the concentration of alkalis increases, the solubility of $Ca(OH)_2$ decreases, and it precipitates as portlandite. Type G grout had values of alkalis and sulfate ions in the expected range for normally hydrated cement paste and much lower than those found in W and P grouts. Type B grout contained the lowest

contents of alkalis and sulfate ions. The acid-soluble chloride concentrations were negligible to initiate corrosion in all grout types.

The grout pH values were in the upper range (≥ 13), regardless of the grout's color and consistency. Assuming that the alkali present in the W grout was completely dissolved in water to form potassium hydroxide (KOH) and sodium hydroxide (NaOH), the investigators calculated that the theoretical pH of the solution was around 14.3. Despite such a high pH, corrosion products were detected on the strand surface that emerged from type W grout. XRD analyses identified the presence of ettringite ($Ca_6Al_2[SO_4]_3[OH]_{12}\cdot 26H_2O$), calcite ($CaCO_3$), FeOOH, and magnetite (Fe_3O_4) in brownish corrosion products. The formation of goethite and magnetite suggested a lack of oxygen.

The researchers thought that, due to the high pH of the segregated grout and the negligible chloride concentration, the usual causes of steel corrosion in concrete—carbonation and chloride—could not be responsible for the rapid corrosion failure of the tendon. The SCC by HE was also excluded. After several laboratory experiments, the researchers presented a macrocell corrosion theory to explain why the corrosion attacks were so severe and fast. According to their theory, once corrosion initiated at localized spots in the interstices in the 7-wire strands, two different corrosion cells were established: an anode inside the interstices and a cathode on the rest of the passive steel surface.

The small anodic area was coupled with a much larger cathodic area where the passive wires could cover at least one or two orders of larger surface area than the anode. The segregated, wet grout also exhibited very low electrical resistivity (an order of 50 ohm-cm) due to its high ionic concentrations, high porosity, and high moisture content. These factors augmented already significant macrocell corrosion by an unfavorable surface area ratio. Researchers believed that such a condition resulted in high penetration rates of localized anodic areas on strands exposed to segregated grout.

19. ADDITIONAL INTERNATIONAL STUDIES

A research study carried out by the Indian Institute of Technology provided a unique insight into grout-related issues by focusing on the fresh grout properties of commonly used PT grouts in India.[121] A two-stage test program was carried out to evaluate seven types of grouts available in India: One plain cement grout with a water-cement ratio of 0.4; three plasticized expansive admixture grouts used in major infrastructure projects in India; and three prepackaged grouts, including high-performance grouts used in developed countries and other grouts that were manufactured in India.

It was observed that the most common cementitious grout materials used in India and some of the prepackaged grout products failed to meet the requirements of the existing standards and even the specifications given by the manufacturers. Every grout material had a set of mixing variables for its optimal performance, but site-dependent parameters like ambient temperature and speed of grout mixing could affect these properties and influence their performance. Many of the techniques developed in the laboratories under ideal situations produced different results in the field. For example, efflux time could be adopted as a quality control parameter to assess pumpability and fluidity, but not as a screening factor in selecting grout materials. The

researchers concluded that actual site practice was a critical factor for determining actual grout quality.

Additionally, Harder and Webster discussed the durability of more than 300 facilities in Canada containing unbonded mono-strand PT systems in their report "Durability of Post-Tensioning Tendons: Canadian Experience," which was published in *fib Bulletin No. 15: Durability of Post-Tensioned Tendons.*[122] Even though their report focused on unbonded PT tendons, an important finding in it was that the ambient temperature of a structure and the amount and extent of moisture were two major factors related to the failure of PT strands.

Also of interest, al-Amoudi carried out a comprehensive investigation to evaluate the corrosion performance of reinforced concrete constructed with plain cement (types I and V) and blended cement (made with fly ash, silica fume, and blast furnace slag) exposed to unique environments where sulfate ions existed concomitant with chloride ions, as in eastern Saudi Sabkha soil.[123] His work aimed to understand the influence of sulfate ions on the chloride-induced corrosion of reinforcing steel in concrete. Even though his findings were not directly related to the corrosion of prestressed steel strands, his work addressed the role of sulfate ions in the corrosion of steel in high-pH conditions, such as in cases where cementitious grout materials were used.

According al-Amoudi's data, both low sulfate (0.55 percent) and high sulfate (2.1 percent) concentrations yielded no clear trend as to the effect of sulfate concentrations on the time to initiate steel corrosion when the identical chloride concentration (15.7 percent) was maintained in the study. The time to corrosion initiation was not dominantly controlled by the conjoint presence of sulfate and chloride ions. Instead, in the mixed chloride-sulfate environments, the corrosion mechanism for corrosion initiation was governed by chloride ions because they diffused much faster than sulfate ions.

However, an increase in the corrosion current density—another indication of how fast corrosion reaction occurs—was observed consistently when sulfate concentration increased. For example, the corrosion current density of steel exposed to the low sulfate-chloride condition was higher than that of steel in the pure chloride solution. Moreover, corrosion current density values were even higher in the high sulfate-chloride environment than in the low sulfate-chloride environment. This trend was observed irrespective of cement type.

CHAPTER 5. CORROSION MECHANISMS RELATED TO PT TENDONS

This chapter discusses, based on what has been presented in chapters 3 and 4, corrosion mechanisms responsible for PT tendon corrosion in various exposure conditions. Exposure conditions to be examined include strands fully embedded in normally hardened grout and segregated grout, partially exposed strands in different grout conditions, and fully exposed bare strands in grout voids. Corrosion morphologies observed in the field will also be presented. Lastly, sulfate-induced corrosion, a recently discovered problem, will be examined in association with grout segregation.

1. THE LOCALIZED CORROSION OF 7-WIRE STRANDS

This section briefly discusses the basic electrochemistry of localized corrosion caused by the breakdown of the passive film—a kind of oxide film—formed on reinforcing bars and prestressed steel strands exposed to a highly alkaline environment (typically pH 12.5 or higher) provided by cementitious materials such as concrete, mortar, and grout. This invisible and protective passive film prevents the steel from corroding until harmful anions, like chloride and sulfate ions, or carbonation of the cementitious paste compromise the film's integrity. As discussed in chapter 4, a common surface coating on prestressed strands is $ZnPO_4$, and imperfections in the coating can also allow corrosion to initiate.[104]

Figure 101 schematically shows a representative polarization behavior of steel and alloys that are called active-passive metals. This schematic potential-log current density *(E*-log *i)* illustration exaggerates the important anodic behavior of drastically reduced corrosion current density in the passive zone.

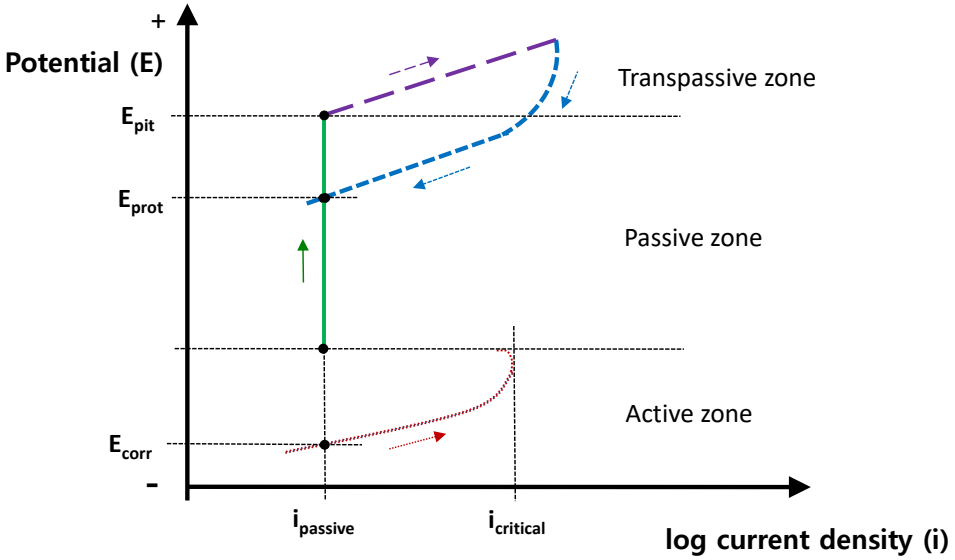

Source: FHWA.

Figure 101. Illustration. Major characteristics of active-passive metals presented in a *E*-log *i* diagram.

One way to make the S-shaped anodic polarization curve for metal is the CPP technique, which uses a potentiostat and a computer that can control the applied potential and measure the responding current (or current density) during polarization experiments. The initial upward anodic polarization from its corrosion potential (E_{corr}), indicated by the red dotted curve, gradually increases current density (i). This region is called the active zone, where the CR of the metal progressively increases with an increasingly upward potential and increasing i.

After anodic polarization progresses and i exceeds a critical value ($i_{critical}$), current density decreases substantially to a passive state level ($i_{passive}$). At $i_{passive}$, a passive film starts building up on the metal surface in the presence of oxygen, and the metal corrodes at a much lower rate. With further anodic polarization in the positive direction, indicated by the solid green line, the CR remains very low. This region is called the passive zone.

When the polarized potential reaches a sufficiently positive potential, the pitting potential (E_{pit}), and beyond, pits can nucleate and grow on the metal surface. This region is indicated by the slanted long dashed purple line and is called the transpassive zone. Oxygen also starts evolving in this zone because of water dissociation. After reaching a preset peak potential, the potentiostat reverses the polarization in the negative direction. This step is shown by the downward curve marked with square blue dots. The potential where the reversed and the forward anodic polarization curves intersect is called the protection potential (E_{prot}), or repassivation potential. No pitting corrosion occurs below E_{prot}. At any potential between E_{prot} and E_{pit}, no pits can form but existing pits can grow. E_{pit} is the primary potential related to corrosion of the reinforcing rebars and strands.

Active-passive metals are most susceptible to localized corrosion in three forms: pitting corrosion, crevice corrosion, and intergranular corrosion. But only the first two forms are relevant to the 7-wire steel strand embedded in cementitious grout. Localized corrosion usually proceeds in two stages: corrosion initiation and corrosion propagation. Corrosion initiates at local spots and crevices in the presence of chloride or sulfate ions. Once corrosion initiates locally, it propagates. An unfavorable ratio between the small surface area of the macro-anode and the large surface area of the macro-cathode can aggravate the rate of localized corrosion.

Pitting corrosion initiates when a corrosion cell is established between a small active area (anode) containing a damaged passive film (or $ZnPO_4$ coating) and a large passive area (cathode) covered with an intact passive film (or $ZnPO_4$ coating). Figure 102 shows a schematic illustration of a pitting corrosion cell with the following notations:

- OH^-: Hydroxyl ion.
- H^+: Hydrogen ion.
- O_2: Oxygen molecule.
- $2e^-$: Two electrons.
- Fe^{2+}: Ferrous ion.
- Cl^-: Chloride ion.

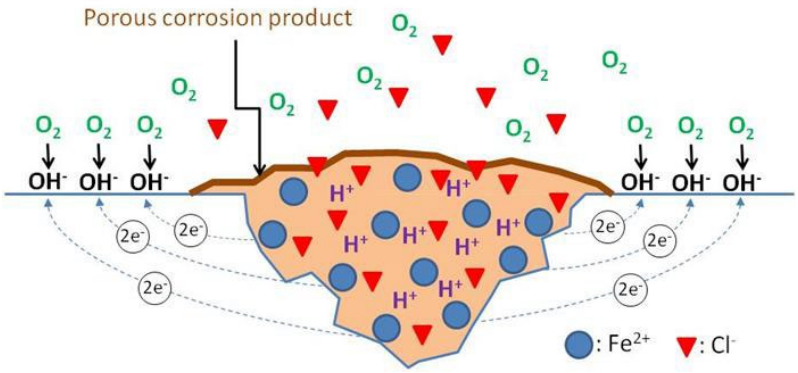

Source: FHWA.

Figure 102. Illustration. Pitting corrosion mechanism.(72)

Two electrochemical reactions occur simultaneously at the anode and the cathode in neutral and alkaline environments, according to the equations in figure 103 and figure 104, respectively.

$$Fe \rightarrow Fe^{2+} + 2e^-$$

Figure 103. Equation. Oxidation reaction at the anode.

$$O_2 + 2H_2O + 4e^- \rightarrow 4OH^-$$

Figure 104. Equation. Reduction reaction at the cathode (in neutral/alkaline environment).

The above electrochemical reactions indicate that the corrosion process produces positively charged Fe^{2+} in what becomes a pit and negatively charged hydroxyl ions (OH^-) on the protective steel surface. The OH^- increase the pH on the steel surface.

In acidic, oxygen-starved environments, even though the anodic reaction is identical, different reduction reactions consume electrons coming from the anode through a metallic path, according to the equations shown in figure 105 and figure 106, respectively.

$$O_2 + 4H^+ + 4e^- \rightarrow 2H_2O$$

Figure 105. Equation. Reduction reaction at the cathode (in acidic environment).

$$2H^+ + 2e^- \rightarrow H_2$$

Figure 106. Equation. Reduction reaction at the cathode (in de-aerated environment).

Crevice corrosion, another form of localized corrosion, initiates at geometrically confined spaces where the electrolyte becomes stagnant. In PT strands, crevices are naturally formed between two adjacent outer wires and between the outer wires and the center wire. Figure 107 illustrates a case of two outer wires separated by a small gap.

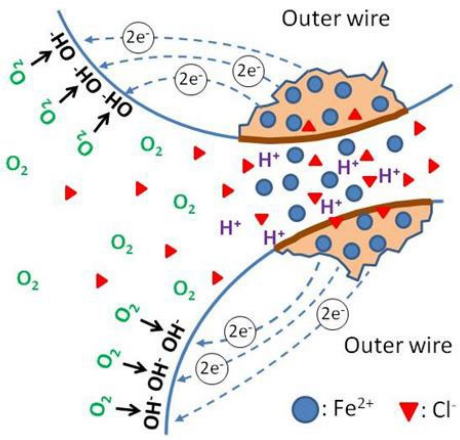

Source: FHWA.

Figure 107. Illustration. Crevice corrosion mechanism in 7-wire strand.[72]

Inside the crevice, the oxygen reduction reaction shown in figure 104 continues to consume dissolved oxygen. Eventually, the oxygen is unable to be replenished in the confined space and is depleted. However, the oxygen reduction reaction can be sustained outside the crevice because enough dissolved oxygen is present in the bulk electrolyte. This condition can establish a differential aeration cell, where the crevice becomes the macro-anode (from a lack of oxygen) and the rest the macro-cathode (from abundant oxygen).

The anodic reaction inside the crevice produces ferrous ions and supplies electrons to the cathodic area outside the crevice, according to figure 103 and figure 104. A Georgia Institute of Technology study noted that strand geometry could negatively impact corrosion resistance due to the interstitial crevices created by the six outer wires wrapped around the center wire.[104] The 7-wire strand specimens needed 67 percent less chloride ions to initiate corrosion than the single-wire specimens, as per figure 78. The 7-wire strand also facilitates water transport along its length through the interstitial crevices.

Once pitting corrosion or crevice corrosion initiates—albeit, by different mechanisms—corrosion propagates through the same mechanism of self-propagation and the autocatalytic process. To maintain charge neutrality in a charge gradient, negatively charged chloride and sulfate ions in the bulk electrolyte electro-migrate into the pit or crevice. The anions entering the pit or crevice react with the ferrous ions to form corrosion products by the equations shown in figure 108.

$$Fe^{2+} + 2Cl^- \rightarrow FeCl_2$$

A. For chloride.

$$Fe^{2+} + SO_4^{2-} \rightarrow FeSO_4$$

B. For sulfate.

Figure 108. Equations. Chemical reactions inside the pit and the crevice.

The accumulated anions further compromise the passive film and lead to active localized corrosion. The reaction products, $FeCl_2$ and $FeSO_4$, can be further hydrolyzed to ferrous hydroxide ($Fe(OH)_2$) and hydrochloric acid (HCl) or H_2SO_4 by the reactions shown in figure 109.

$$FeCl_2 + 2H_2O \rightarrow Fe(OH)_2 + 2HCl$$

A. Formation of hydrochloric acid.

$$FeSO_4 + 2H_2O \rightarrow Fe(OH)_2 + H_2SO_4$$

B. Formation of sulfuric acid.

Figure 109. Equations. Formation of ferrous hydroxide and acidification.

The acidification inside the pit and crevice creates an increasingly aggressive environment via an autocatalytic process. Severe acidification can drop the pH to less than 3. The outer corrosion product, ferrous hydroxide, can be converted to ferric hydroxide ($Fe[OH]_3$), commonly known as red rust, when in contact with more oxygen, according to the equation shown in figure 110.

$$Fe(OH)_2 + 1/4O_2 + 1/2H_2O \rightarrow 2Fe(OH)_3$$

Figure 110. Equation. Formation of ferric hydroxide.

In an oxygen-starved environment, the $Fe(OH_2)$ can be transformed into a final corrosion product, magnetite (Fe_3O_4), according to the equation shown in figure 111.

$$3Fe(OH)_2 \rightarrow Fe_3O_4 + H_2 + 2H_2O$$

Figure 111. Equation. Formation of magnetite.

Magnetite is more thermodynamically stable than $Fe(OH)_2$ and exhibits a blackish color.

2. ESTABLISHMENT OF MACROCELL CORROSION

Macrocell corrosion can occur between two physically separated anodic and cathodic areas. Severe macrocell corrosion can be established for the steel strands between an actively corroding small area at the segregated grout/void interface (or carbonated bleed water/air interface) and a passive large surface area in sound grout (or a high pH solution). A thin layer of hydrated grout on the steel surface will not be protective if it becomes carbonated upon exposure to external air or water. A high RH (higher than the critical value of 60 percent) would accelerate the subsequent corrosion in the void space. Corrosion at the grout/void interface may be sustained for months after a water-recharging event or a temperature drop condensates previously absorbed bleed water in segregated grout.[29,96]

Figure 112 illustrates a severe case of macro-cell corrosion for a 7-wire strand passing through three environments: normally hardened grout with a high pH; a carbonated thin layer of segregated grout; and a grout void filled with humid air (high RH), O_2, and CO_2. Th illustration also includes a thin layer of bleed water, which is susceptible to carbonation.

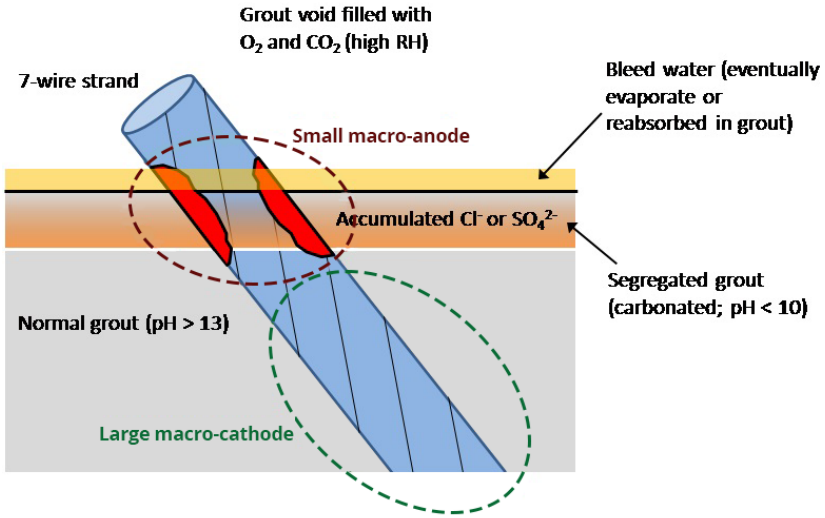

Source: FHWA.

Figure 112. Illustration. Schematic of macrocell corrosion in segregated grout.

Four components required for the macrocell corrosion mechanism are identified as follows:

1. Macro-anode: A 7-wire strand section exposed to the segregated grout layer/bleed water that is carbonated and contains elevated levels of anions and alkaline ions. The initially formed bleed water can be evaporated or reabsorbed into the segregated grout, which leads to a high amount of moisture and low grout electrical resistivity. Moist air containing O_2 and CO_2 may fill the grout void. As seen in the equation in figure 103, strand corrosion liberates ferrous ions and electrons.

2. Macro-cathode: A 7-wire strand section embedded in protective, normally hardened grout possessing high pH. As seen in the equation in figure 104, it consumes electrons traveling from the macro-anode and produces OH^-.

3. Electrolyte: Grout material (both hardened and segregated) in contact with the 7-wire strand. It carries the ions between the macro-anode and macro-cathode. Since segregated grout has a low electrical resistivity, the macrocell current can travel a significant distance through the defective grout. Also, negatively charged sulfate or chloride ions (or both) increase electrical conductivity.

4. Metallic path: The entire 7-wire strand serving as a metallic path for transporting electrons from the macro-anode to the macro-cathode.

Microcell (or local action cell) corrosion is not discussed here because it is a dominant form of uniform corrosion involved with numerous tiny anodes and cathodes in a finite metal surface area. Even though the electrochemical reactions for micro- and macro-corrosion cells are the same, the macro-anode and macro-cathode are physically separated, and the affected anodic and cathodic surface areas are much larger than those related to the microcell corrosion.

Figure 113 schematically shows an *E*-log *i* diagram for steel strands as soon as macrocell corrosion starts. Another *E*-log *i* diagram describing polarization behavior after the macrocell corrosion reaches a steady state is omitted here.

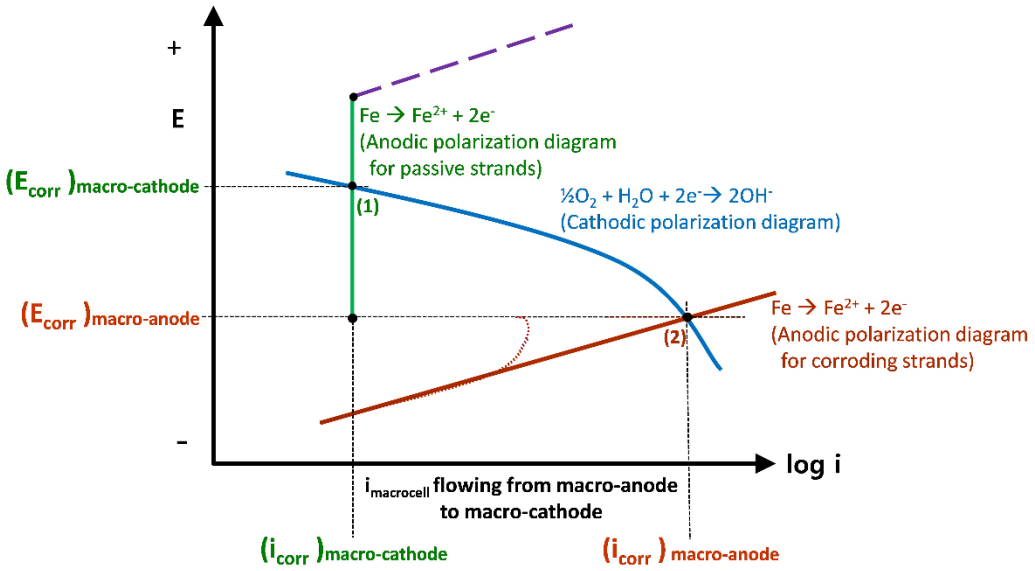

Source: FHWA.

Figure 113. Diagram. Potential-log current density diagrams of different anodic and cathodic behaviors.[72]

Two situations, termed cases 1 and 2, can occur for macrocell corrosion of grouted PT tendons. Case 1 is related to a passive anodic polarization diagram (the upward solid green line), for a noncorroding strand exposed to normally hardened grout without harmful elements. It intersects with a cathodic polarization diagram (the curved blue line). In this case, a relatively positive corrosion potential and low corrosion current density result. They are indicated by $(E_{corr})_{\text{macro-cathode}}$ and $(i_{corr})_{\text{macro-cathode}}$, respectively, in figure 113. This case represents a typical grouted PT tendon exhibiting a very low or negligible CR because of high-quality grout.

Case 2 involves an active anodic polarization diagram (the diagonal red line) of an actively corroding strand in the segregated grout or other undesirable conditions that cannot protect the strand. It intersects with the same cathodic polarization diagram as for Case 1. In this situation, a relatively negative corrosion potential and high corrosion current density result. They are indicated by $(E_{corr})_{\text{macro-anode}}$ and $(i_{corr})_{\text{macro-anode}}$, respectively, in figure 113. This case describes the active corrosion state experienced by the corroding strand due to deficient grout. When the strand itself electrically connects the strand sections in Cases 1 and 2 and establishes the macrocell corrosion, a strand section in case 1 acts as the macro-cathode and another section in case 2 as the macro-anode. The potential difference between cases 1 and 2 ($[(E_{corr})_{\text{macro-cathode}} - (E_{corr})_{\text{macro-anode}}]$) determines the magnitude of the driving force for the macrocell corrosion.

Macrocell corrosion damage takes place only at the macro-anode and is proportional to the net macrocell corrosion current density ($[(i_{corr})_{\text{macro-anode}} - (i_{corr})_{/\text{macro-cathode}}]$). Because the CR is proportional to the corrosion current density, it is inversely proportional to the surface area. In

other words, the rate of macrocell corrosion is largely determined by the surface area ratio between the macro-anode and the macro-cathode. Severe corrosion damage can occur at the macro-anode if the surface area ratio of the macro-anode to the macro-cathode becomes small, a so-called “small anode-large cathode” situation. A good example of severe macrocell corrosion damage is shown in figure 98.

3. CORROSION MORPHOLOGIES

Grouted PT strands can suffer from uniform corrosion and localized corrosion, depending on exposure conditions, which can vary locally. This section presents representative corrosion morphologies observed on corroded wires that are products of uniform corrosion, pitting corrosion, and crevice corrosion. The examined wires were extracted from actual corroded 7-wire strands in the field and then acid-cleaned to remove adhered corrosion products.

Uniform corrosion typically causes negligible to minor section loss and is not usually critical to load-carrying capacity. If measurable corrosion damage is observed, a digital micrometer may be used to quantify section loss. Figure 114 shows an example of uniform corrosion damage.

Figure 114. Photo. Uniform corrosion damage on an outer wire.[84]

On the other hand, a localized attack by pitting corrosion or crevice corrosion can be critical because of the significantly reduced cross-sectional area. Pitting corrosion initiates at discrete spots where the protective passive film is compromised, or other imperfect surface conditions exist. Figure 115 shows autopsy photographs of a single strand specimen that was buried in a 0.4 percent chloride-contaminated grout for six months.[72] Figure 115-A shows the as-opened condition. A small rust spot matching the pit development indicated by a red arrow can be seen. Figure 115-B shows a magnified small pit formed on the circled strand surface after it was cleaned.

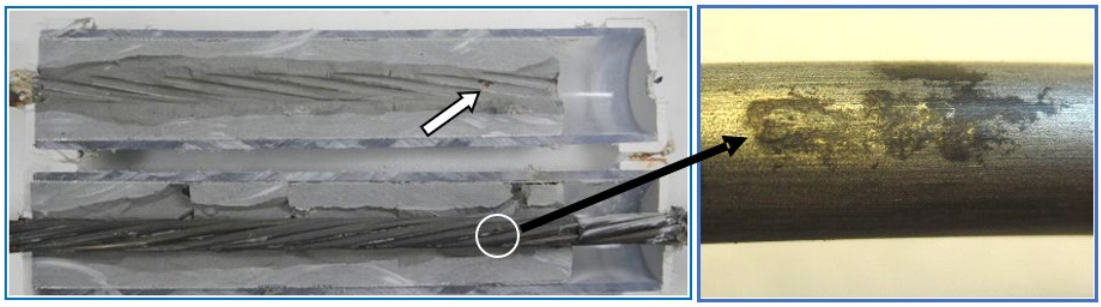

Source: FHWA.

Figure 115. Photos. Pitting corrosion on a single strand specimen: Opened single strand specimen and closeup of a pit.[72]

Figure 116 shows two small pits (see figure 116-A) and several shallow pits (see figure 116-B) formed on two outer wires exposed to a 0.8 percent chloride grout. These photographs show discrete and shallow pits associated with the initial stage of pitting corrosion damage.

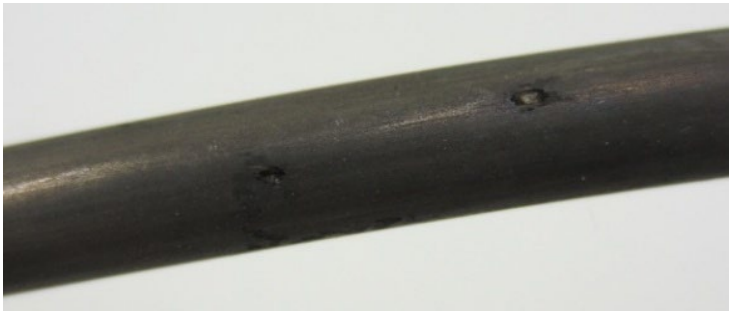

Source: FHWA.

A. Two small pits.

Source: FHWA.

B. Several shallow pits.

Figure 116. Photos. Pitting corrosion on two outer wires.[72]

Pitting corrosion damage can grow by merging multiple small pits laterally and also penetrating deeper. Figure 117 features five photographs showing progressive pitting corrosion damage observed on five outer wires extracted from randomly selected field strand samples.

A. Growing pitting damage.

© 2017 Seoul City Facility Management.

B. Elongated pitting damage.

© 2017 Seoul City Facility Management.

C. Severe pitting damage.

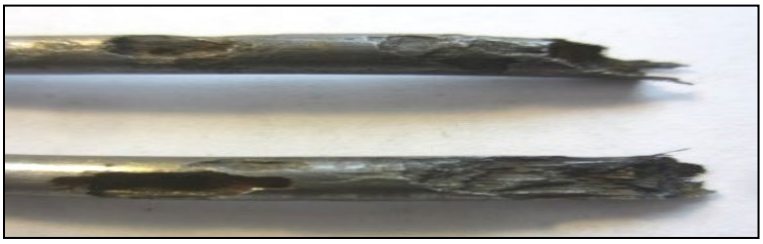

© 2017 Seoul City Facility Management.

D. Fractured wires—Plan view.

© 2017 Seoul City Facility Management.

E. Fractured wires—Front view.

Figure 117. Photos. Examples of progressive pitting corrosion damage.(84)

Figure 117-A shows pitting corrosion damage from the merging of multiple small pits, similar to those in figure 116-B. Figure 117-B shows more advanced damage from figure 117-A. Figure

117-A and figure 117-B also show the fibrous texture of corrosion damage due to preferential mass consumption along the wire drawing direction. Figure 117-C shows a nearly fractured wire due to an intensive pitting attack. Figure 117-D and figure 117-E show different views of two wires that were finally fractured by pitting corrosion, which is the ultimate form of corrosion damage and developed from the intensive pitting attack shown in figure 117-C.

Crevice corrosion can occur at the interstitial site inside the 7-wire strand. Figure 79 shows the imperfect $ZnPO_4$ line (type 2 defect) along the spiral line formed by rubbing the wires with each other. Those interstitial sites can be filled with bleed water and a very lean grout mix in severely segregated grout and become a potential site for crevice corrosion. For example, figure 118 shows the origin of crevice corrosion in a corroding 7-wire strand.

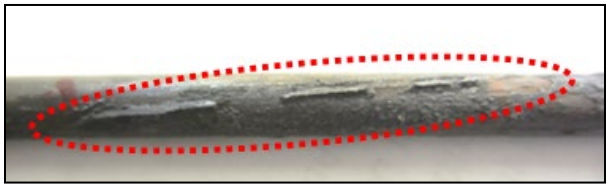

A. Before removing grout residues.

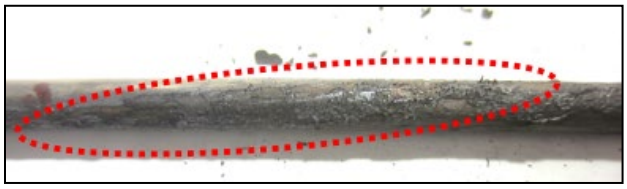

B. After removing grout residues.

Figure 118. Photos. Corrosion damage at the interstitial site.[84]

Figure 118-A shows dried grout residues adhered to a center wire along a spiral interstitial site. Figure 118-B shows crevice corrosion damage beneath the grout residues after they were removed. Figure 119 shows close-up photographs of five wires exhibiting different stages of crevice corrosion damage after cleaning. The wires were from randomly selected 7-wire strands.

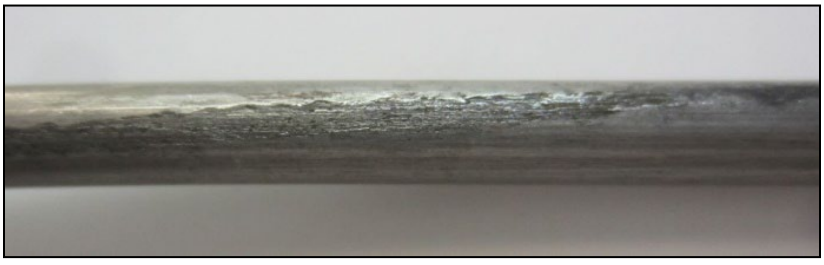

A. Minor damage.

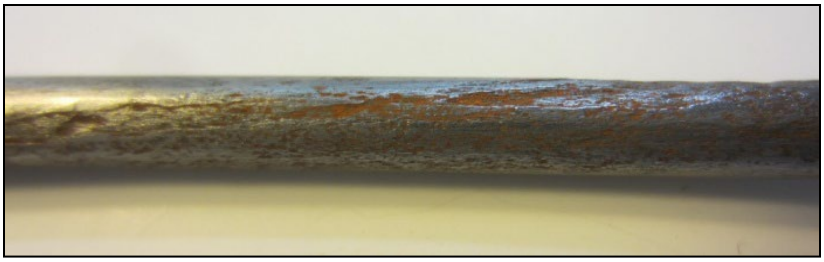

B. Moderate damage.

C. Deeper damage.

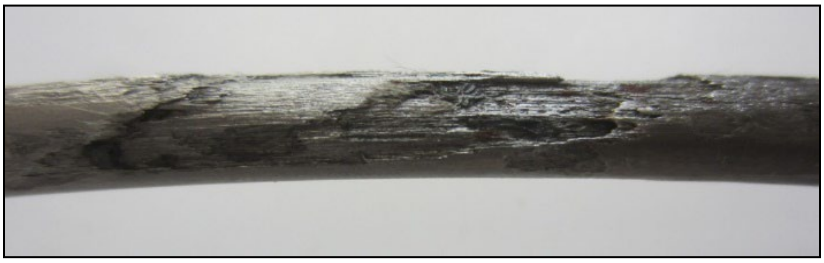

D. More advanced damage.

E. Severely damaged wire.

Figure 119. Photos. Examples of progressive crevice corrosion damage.[84]

Figure 119-A shows slightly indented, shallow corrosion damage along a spiral interstitial site. Figure 119-B through figure 119-E show progressively advancing corrosion damage from the condition shown in figure 119-A. These examples illustrate how crevice corrosion progresses on individual wires and eventually results in wire fractures.

When corrosion of the wires and ultimately the strands cause a tendon to fail, some wires corrode in two, and the remaining wires rupture by necking. This type of ductile fracture is caused by overstressing and shows cup-and-cone-shaped fracture ends. Two examples of the cup-side fracture are shown in figure 120.

A. Fractured wire example 1.

B. Fractured wire example 2.

Figure 120. Photos. Wire ends showing ductile fracture.[84]

In some cases, the fractured wires show a zig-zag-shaped texture without recognizable reduction of the cross-sectional area. Two representative examples are shown in figure 121.

A. Fractured wire example 3.

B. Fractured wire example 4.

Figure 121. Photos. Fractured wire ends showing little area reduction.[84]

Although these examples were not scientifically determined to be caused by brittle fracture, they resembled brittle fracture. It is important to recognize the possibility that the brittle fracture can occur by EIC, i.e., SCC, corrosion fatigue, and by HE. Some instances of EIC in PT tendons have been reported.[74,118]

4. CORROSION CHARACTERISTICS OF DIFFERENT GROUT CONDITIONS

Generally, the corrosion process of the grouted PT tendons should be the same as that of reinforcing steel in concrete, thanks to passivity offered by a high-pH, cementitious grout. The cementitious grout also serves as a physical barrier to water, O_2, and CO_2. In addition, it provides a structural contribution to grouted internal tendons. However, grout's physical condition can vary locally, and strand corrosion can be influenced by, at a minimum, the following factors:

- Condition of $ZnPO_4$ coating.
- Size and frequency of grout voids.
- Exposure of steel surface area.
- Concentration of O_2 and CO_2 inside the tendon, especially within grout voids.
- RH in grout voids.
- Ambience of temperature.
- Degree of grout hydration.
- Degree of grout segregation.
- Corrosivity of bleed water in terms of pH and concentration of chloride and sulfate ions.
- Characteristics of the strand/segregated grout interface, in terms of the following:
  - The pH.
  - The porosity.
  - The moisture content (and amount of absorbed bleed water).
  - The concentration of chloride and sulfate ions.
  - The electrical resistivity.

- Condition of bulk grout, in terms of the following:
  - The extent of carbonation.
  - The concentration of chloride and sulfate ions.
  - The cracks.
  - The moisture content.
  - The electrical resistivity.

As a minimum, water, O_2, grout voids, and a low pH environment are needed to initiate corrosion. Once water exists in the tendon, it can remain for an extended time because of the relatively well-sealed PT tendon hardware. If grout voids are present, water (or moisture) alone with no or a negligible concentration of chloride and sulfate ions can initiate localized corrosion after pH drops to a neutral level. A low pH environment can be introduced by atmospheric CO_2 in the grout voids, carbonated bleed water, leaking water from the deck and anchorage zone, acidification, or a combination of these factors. The following section discusses the corrosion characteristics of PT strands exposed to normally hardened grout and segregated grout.

4.1 Normally Hardened Grout

In an ordinary situation, carbonation-induced corrosion is unlikely because strands are isolated within a high-pH, protective, normally hardened (i.e., nonsegregated) grout. Even though there are circumferential cracks along the tendon length, there has been no evidence that such grout cracks can initiate corrosion as long as the encasing ducts are crack-free.

However, chloride-induced corrosion can occur when a sufficient amount of chloride ions exists in the presence of moisture and O_2. Typical sources of chloride ions include marine environment and deicing salts carried in the leaking water from the deck surface. (Please see references 14, 16, 17, 64, and 85.) The FHWA's chloride threshold study determined that chloride threshold values for corrosion initiation and corrosion propagation in normally hardened grout were 0.4 and 0.8 percent by the weight of the cement, respectively.[72]

4.2 Segregated Grout

4.2.1 Characteristics of Segregated Grout

The discovery of moist, claylike grout was noted as early as the 1970s. Observations of soft/wet and chalky grout began to appear in international and domestic literature in the 1980s. These conditions are typical signs of segregated grout, which occurs inconsistently and is likely to occur in isolated sections of a bridge. As a result, the segregated grout issue remained mostly unnoticed by most PT bridge owners, maintenance engineers, and contractors in the United States until the two tendons on the Ringling Bridge in Sarasota, Florida failed in 2011 due to rapid corrosion in the presence of segregated grout.[27,35,50]

The deficient grout is classified into two categories: physically deficient grout and chemically deficient grout.[124] Neither type of grout can provide good protection to strands, and their durability should be questioned. Segregation of grout is a root cause of grout deficiency. It has been recognized that the segregation phenomenon can occur in neat portland cement grout, with or without admixtures, and with prepackaged grout products.

No matter what grout material is used, excessive mixing water appears to be a common denominator for producing segregated grout.[41,110] Suppose excessive water exists in the fresh grout mix. In that case, solid particles, such as hydrated or unhydrated cement particles, settle by gravity (sedimentation) during grout pumping and the initial set of fresh grout. Simultaneously, the lighter grout ingredients, such as silica fume and admixtures, air bubbles, and bleed water, move upward along the bleed channel at the 12 o'clock position in a tendon. Consequently, bleed water, silica fume/admixtures (if present), and most air bubbles are collected at the high point of the tendon. Other contributing factors that aggravate the segregation phenomenon include vibration, grout fillers, incompatible admixtures, expired grout, the filtering action of the 7-wire strand, and unfavorable field conditions. These unfavorable conditions may include prolonged storage, elevated temperature, high RH, prolonged downtime before the initial set, pump cavitation, excessive pumping height, and poor workmanship.

Typically, segregated grout possesses many features, as follows:

- Physically different texture, including some or all of the following:
    - Soft/wet, claylike paste, which becomes friable upon drying in air.
    - Whitish, chalky paste.
    - A sedimented layer containing silica fume particles.
    - White, powdery grout.
- Weak cement paste (low compressive strength) produced by high water-cement ratio.
- Various grout voids of different sizes and densities, especially large voids formed after bleed water evaporation or reabsorption.
- Bleed water (eventually evaporated or reabsorbed into segregated grout).
- High moisture content.
- High grout porosity.
- Unhydrated or incompletely hydrated cement paste.
- Varying water-cement ratios and colors within the deficient grout.
- Uncertain corrosivity (many PT tendons containing soft/wet grout have not experienced corrosion, even after an extended period).
- Elevated levels of water-soluble sulfate, potassium, and sodium ions.
- Low level of calcium hydroxide.

Any grout deficiencies, singly or collectively, can compromise protective properties and lead to strand corrosion. Grout voids, the most common form of physically deficient grout, are formed by reducing grout volume during the sedimentation process. They are also created by entrapped air and evaporation or reabsorption of bleed water into the grout. In some cases, extended grout

voids are formed inside horizontal tendon sections due to entrapped air in the duct or blockage by lumps of stiff/solidifying grout. The strands exposed in the isolated voids are not at risk if the duct is sealed and the voided areas are dry or if the strands are covered with a sound grout coating. What is not known is how long these conditions can continue to protect the strands.[7,75,84]

On the other hand, when voids are present and water is available, there is a risk of corrosion. In the presence of CO_2 in the voids, carbonation-induced corrosion can begin once grout pH drops below 10. When the temperature drops below the dew point, occasional condensation by residual moisture trapped inside the duct and air voids can be another source of water in the tendons.[29,85]

While the concentration of chloride ions is very low in bleed water samples, the level of sulfate ions can be substantially high. The initial pH of the bleed water can be higher than 12.2. However, when pH is reduced due to carbonation, the strands are susceptible to corrosion from the bleed water alone. Consequently, the passivity of the steel is lost, and extensive pitting corrosion damage can be observed within a few weeks near the bleed water/air interface and on the exposed and submerged portions of the strands. Some studies reported that carbonated bleed water was corrosive, particularly if it contained expansive admixture. (See references 33, 88, 98, and 119.) According to a field investigation, the measured pH of the undisturbed white powdery layer formed by grout segregation was 8 ± 1.[29]

4.2.2 Role of Water-Soluble Sulfate Ions

Segregated grout may contain much higher and more variable soluble ions (alkalis and sulfate ions) and lower calcium content than nonsegregated grout. Large amounts of sulfate and potassium ions can leach out of construction materials such as gypsum in cement and aggregates, leading to their accumulations in the segregated grouts without external sulfate sources. As the concentration of alkalis increases, the solubility of $Ca(OH)_2$ decreases and precipitates as portlandite. Therefore, a lower concentration of $Ca(OH)_2$ is found in the segregated grout than in the nonsegregated grout. Like in the bleed water samples, a low concentration of chloride ions is typically found in the segregated grout. (See references 39, 52, 85, and 109.)

Most of the sulfate ions initially available in raw grout powder become bound in the hardened grout. However, variable amounts of water-soluble sulfate ions can be released into the segregated grout under certain conditions. The sulfate liberation mechanism is still largely unknown. Still, a petrographic analysis determined that the segregated grout retained significantly higher (100 times) sulfate ions in pore water and moist soft/segregated grout than the dried and normally hardened grout. This finding suggested that water-soluble sulfate ions migrate toward the areas with a higher amount of moisture.[115]

Like in ordinary concrete and normally hardened grout, chloride-induced corrosion and carbonation-induced corrosion can take place in segregated grout. However, PT strands exposed to segregated grout can also suffer from sulfate-induced corrosion under certain conditions. The last corrosion mechanism is unique to the grouted PT tendons. As discussed in chapter 4, localized corrosion damage was observed on the strands exposed to the segregated grout containing no chloride. A high concentration of water-soluble sulfate ions (2.7 percent by weight

of cement) and silica fume particles were contained in the porous top layer of the segregated grout. The observed corrosion damage was concentrated around the segregated grout layer.[72]

If segregated grout becomes carbonated, the water-soluble sulfate ions are as aggressive as chloride ions. Concentrated ionic species in the segregated grout also help lower the electrical resistivity of the grout, which can facilitate macrocell corrosion. On the other hand, if the grout is not carbonated, the strands embedded in the segregated grout do not initiate corrosion, irrespective of sulfate concentration.[84,114,115]

5. AN INFERRED CORROSION MECHANISM IN SEGREGATED GROUT

Based on the findings from the literature review, field investigations, and laboratory studies, a sequence of hypothetical events is presented here to understand how PT strand corrosion initiates and progresses in segregated grout. Since it is known that a significant amount of chloride ions is unlikely to be released into the segregated grout, the effect of the chloride ions is not considered here. Two prerequisite conditions are involved in this hypothetical case, as discussed below.

The first condition is that the use of excess mixing water produces segregated grout. Additionally, the quality of the mixed grout can be worse if grout bags pass the manufacturer's expiration date and are stored improperly.[110,115,125]

The second condition is related to steel passivity. For example, suppose water-soluble sulfate ions are present in carbonated bleed water and grout. In that case, the strands become vulnerable to both carbonation-induced and sulfate-induced corrosion due to the compromised passive film.

First, a grout mix containing excessive water is pumped into a tendon through a grout injection port, and grout segregation can occur along the duct, especially in the inclined sections. The worst grout condition may exist at the farthest distance (the opposite end) from the grout injection point because the segregation process continues as the already-segregated grout is forced to move through the space between the duct wall and the strands under pumping pressure. Several unexpected events, such as pump cavitation, idling, prolonged pumping, and entrapped air can also promote grout segregation or clogging during the grouting operation.

In addition, the filtering effect of the 7-wire strand may augment the segregation process. If residual water remains in the duct after duct cleaning and hydrostatic testing, the segregation problem can be further aggravated. After grout injection is completed and all the valves are closed, grout segregation may continue, and bleed water builds up. Figure 122 and figure 123 illustrate the occurrence of the segregated grout followed by the formation of bleed water, respectively.

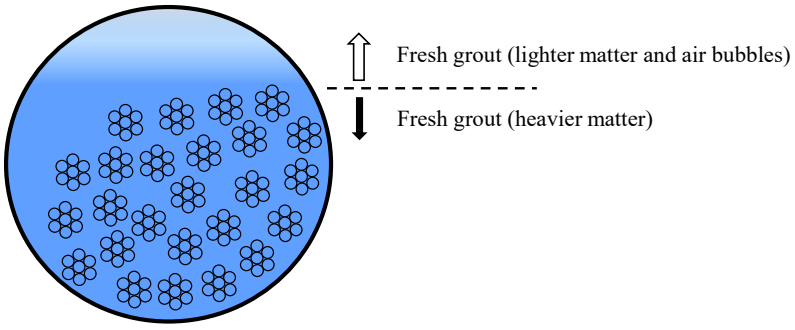

Source: FHWA.

Figure 122. Illustration. Commencement of grout segregation.

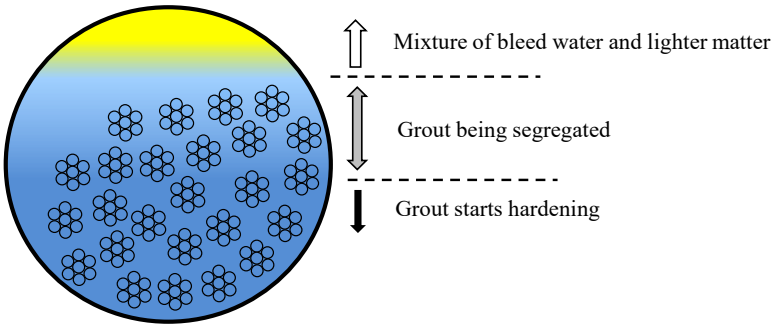

Source: FHWA.

Figure 123. Illustration. Formation of bleed water.

Typically, segregated grout has a weak, porous, or soft/wet texture (sometimes powdery or chalky) due to a high water-cement ratio and tiny air bubbles. It exhibits a white or light gray color containing elevated levels of sodium and potassium ions. If water-soluble sulfate ions are released during the segregation process, most of them are accumulated in the bleed water and segregated grout, especially in the top layer. A sedimented silica fume layer may also be situated on the segregated grout's top surface after bleed water disappears. At the end of the segregation process, the duct is filled with grout in various conditions, including nonsegregated, mildly segregated, heavily segregated, and a mixture of bleed water and little solid grout material. This condition is illustrated in figure 124.

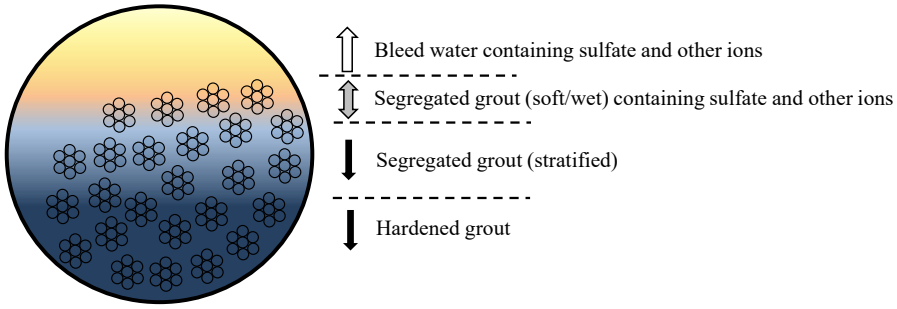

Source: FHWA.

Figure 124. Illustration. Continued grout segregation and bleeding process.

Some portion of the bleed water and the watery grout mixture can flow back toward a low point due to gravity upon the absence of pumping pressure. As a result, some strands can be exposed without grout protection or covered with a thin grout coating. Evidence of such a possibility is shown in figure 28. The top surface of the dried grout exhibited a wrinkled texture, which consisted of a collection of small downward ridges (indicated by three arrows in figure 28). It can be speculated that these ridges might have been carved by residual bleed water flowing back down along the inclined tendon while the segregated grout layer was still wet and soft. Eventually, grout voids may form at high points and along inclined sections.

The bleed water evaporates or is reabsorbed into the segregated grout, and additional grout voids may form. If the tendon is not perfectly sealed, newly created voids can gradually fill over time with moist air containing O_2 and CO_2. This condition is illustrated in figure 125.

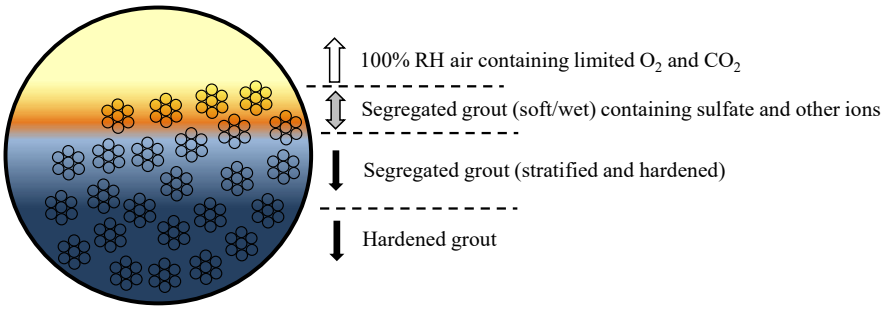

Source: FHWA.

Figure 125. Illustration. Formation of a void after the disappearance of bleed water.

Subsequently, carbonation-induced corrosion can initiate on bare strands and those covered with a thin grout coating. However, the depth of grout carbonation may not be significant to initiate corrosion as long as the carbonated grout layer is in direct contact with the exposed strand surface. Figure 126 depicts carbonation-induced corrosion in segregated grout containing sulfate ions and other ion species.

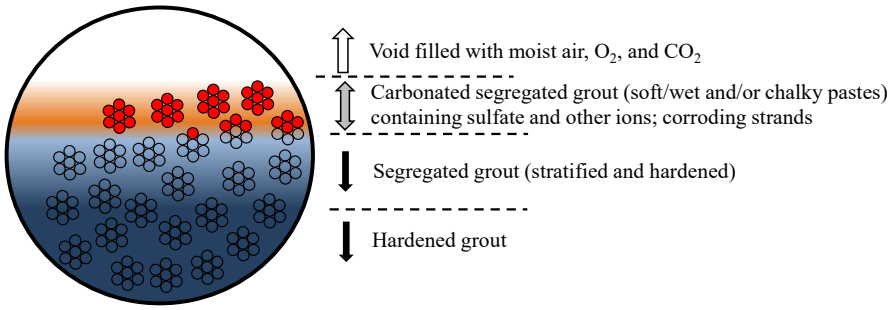

Source: FHWA.

Figure 126. Illustration. Carbonation-induced corrosion.

Since the CR increases to unacceptable levels at RH above the critical value of 60 percent, any excess moisture remaining in the voids and the segregated grout may become significant. When the ambient temperature rises, the rate of corrosion increases as well. Thus, the total amount of corrosion damage is influenced by the duration of high RH and the elevated temperature.

Water-soluble sulfate ions facilitate a much more aggressive corrosion attack when the segregated grout is carbonated.

Field investigations of the Ringling Bridge tendon failures indicated that significant corrosion damage—including strand fractures—was frequently observed on strands exposed to large grout voids and those beneath thin, segregated grout coating. In addition, an elevated level of sulfate ions was also found in the segregated grout. One example is schematically shown in figure 127, based on a photograph of the actual case shown in figure 27.

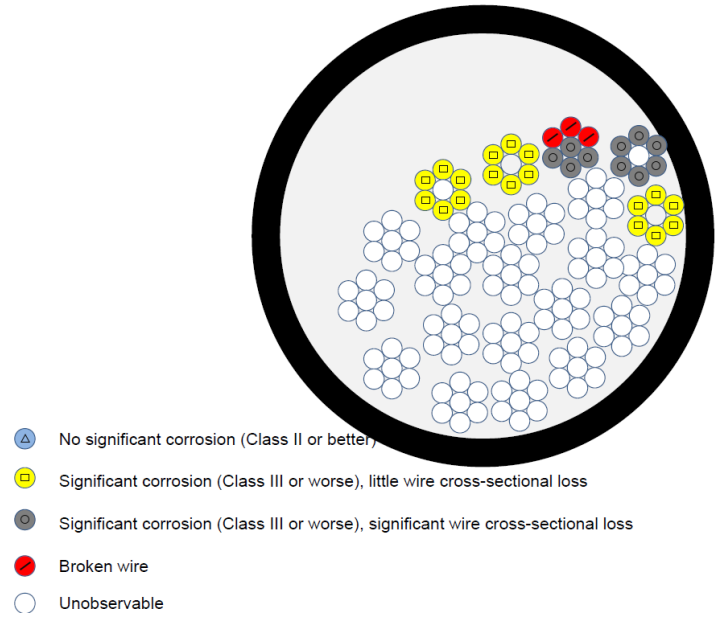

Figure 127. Illustration. Schematic representation of various corrosion conditions in a corroded external tendon.[49]

The strands exposed to the void or covered with very thin grout coatings suffered from intensive corrosion. In contrast, those buried in grout did not show corrosion damage, regardless of grout condition. Moreover, carbonation-induced corrosion can be worsened if macrocell corrosion is established between corroding—while exposed to grout voids—strands serving as a macro-anode and those embedded in the grout, irrespective of whether the grout is normally hardened or segregated. The residual bleed water, a thin segregated grout coating, and/or a good-quality grout coating can act as an electrolyte if they are in contact with the macro-anode.

CHAPTER 6. CORROSION CONTROL METHODS

Remediation options for grouted PT tendons depend on many factors, including cause of corrosion, structure type, type and extent of damage, level of confidence required, and cost. This chapter discusses currently available corrosion control methods that include the following:

- The EIT system.
- Temporary corrosion protection.
- Cathodic protection.
- Repair and regrouting of tendons containing deficient grout.
- The impregnation method.
- Flexible fillers.
- Corrosion-resistant strands.
- Drying air.
- Injecting inert gas.

Due to the extensive technical breadth of each method, only basic information is presented in this chapter.

1. THE ELECTRICALLY ISOLATED TENDON SYSTEM[1,2,90,94,126-130]

The EIT system was developed to provide better protection and condition monitoring of grouted internal PT tendons. Electrically isolated anchor heads, corrugated plastic ducts, and special care at grout vent tubes are employed to achieve electrical isolation from the surrounding reinforcing steel network. A plastic trumpet is also tightly connected to the duct inside the anchorage to isolate the strand from the cast iron bearing anchorage. The EIT and the reinforcing steel network need separate electrical cables to be brought together in the monitoring boxes.

During construction, pressure testing is performed immediately before grouting, with all air vents closed and end caps sealed. The duct is pressurized with air, and the leakage rate is monitored using a flow meter. Upon grout injection, the grout inlets and air vents are filled with grout, which can create an electrolytic path to the surrounding concrete and act as a defect in the duct. Therefore, it is essential to seal all the grout inlets and air vents with a leak-tight plastic cap. Electrical impedance data can also be used for quality control during the tendon installation.

Once the construction is completed, the EIT system monitors the impedance between the prestressing steel inside the tendon and the reinforcing steel network. The impedance measurement method uses a portable impedance meter to measure each of the impedance components, i.e., resistance (R), capacitance (C), and inductance (L). A measured value is a total impedance from the grout in the duct, the plastic duct itself, and the concrete surrounding the duct to the reinforcing steel. In an equivalent circuit modeling, the grout and concrete are (at least in the range of measuring frequencies between 100 and 1000 Hz) treated as pure resistances and the plastic duct as a parallel capacitance. Any system-related imperfections (e.g., not fully closed grout vents) and defects in the duct are represented as an ohmic resistance in a parallel circuit. Both R and C values depend on the tendon length: R decreases with the length, and C is proportional to the length.

The specific resistance ρ (= R x length) in ohm-m and specific capacitance Cs (= C/length) in farad/m are used for quality control. The loss factor D is the ratio of R and C, which is independent of the tendon length. The requirement for comprehensive corrosion protection—electrical isolation of the prestressing steel from the reinforcement and water tightness of the protective envelope—is satisfied if the grouted tendon complies with the specified limit of ρ. If a short circuit (R <10 ohms) between prestressing steel and the reinforcement exists through a damaged duct or defective electrical isolation, the measured values of C and D are meaningless. If ρ is greater than 1,000 kohm-m, the EIT is thought to maintain perfect electrical isolation with no defects present.

For long-term monitoring, the impedance values can be analyzed over time to provide information about the condition of the corrosion protection system. It is important to monitor the temperature as well at the time of measurement because temperature variations can influence impedance readings. A continuous increase of impedance with time is expected thanks to the hydration of the grout and concrete surrounding the tendon. If impedance data deviate from a steadily increasing trend line, the deviations can be early warning signs that the corrosion protection system is breached. In other words, the EIT system can detect the existence and/or development of hidden defects in the corrosion protection system throughout the structure's service life when water (with or without chloride ions) penetrates the grouted duct through the defects.

However, the EIT system cannot accurately identify the location of a defect along the length of the monitored tendon. Moreover, as discussed in chapter 4, a laboratory study at the University of Texas at Austin reported that their EIT system was barely monitorable. More hands-on experience and a longer monitoring period may be needed to determine the long-term effectiveness of the EIT system.

2. TEMPORARY CORROSION PROTECTION[1,2,20,131]

Prestressing steel should be stored in a dry and clean location at the job site, off the ground, and with sufficient ventilation to protect from moisture. In exceptional cases, it may be stored in an air-conditioned area. For extended periods of storage, applying oils to the prestressing steel can be a good temporary protection solution. Preferably, the manufacturer should apply the oils at the shop. The protective oils should not contain substances potentially harmful to the steel and do not need to be removed before applying permanent protection because they are effective for a limited duration, on the order of a few months. Also, these oils should not have a negative effect on the bond strength between the steel and grout.

A laboratory study testing 19 water-soluble oils used in PT applications and other potential candidates from the metalworking industry was conducted.[132] The study confirmed the good performance of one commercial product and multiple oils produced in the United States under six-month saltwater exposure testing. Their bond reduction was between 31 and 65 percent, whereas bond reduction from emulsifiable oils varied from 30 to 97 percent. As a result, four oil products were recommended for large-scale testing.

The most common temporary protection method is to coat the prestressing steel with water-soluble oils or vapor phase inhibitors (VPIs). VPIs may pose health risks and are only effective if

the tendon is completely sealed. Other materials, including sodium silicate and biodegradable soap, usually used as a coolant for cutting metal, have also been used. Except for VPIs, these materials can have the added benefit of reducing friction losses during post-tensioning if they are applied to the strands before stressing. Tendons should not be flushed even when oils are used. Water retained in the ducts can have adverse effects on grout's bleed resistance. Other options for temporary corrosion protection include sealing the ducts to prevent moisture entry, continuous pumping of dry air through the ducts, and purging with compressed air or dry gas.

Another study done in Switzerland evaluated different temporary protection systems.[(2)] After tendons were protected with a commercially available emulsified inhibitor oil, stressed, and left for six months in ducts without grouting during winter, some tendons exhibited only insignificant traces of rust near the tendon ends. It was apparent that this product had provided very effective protection. Two other temporary corrosion protection methods were also investigated. The first method tested, filling tendons with nitrogen gas, did not provide the expected level of protection. The tendons still showed a significant amount of corrosion comparable to that of reference tendons without any temporary protection. The effectiveness of nitrogen gas for temporary protection was inconclusive, and the method was difficult to implement in practice. The second method tested, continuous dry air blowing, provided some protection. However, signs of corrosion were more common than with the inhibitor product and extended over a larger portion of the tendon length. This method may be considered when temporary protection is not applied to the prestressing steel before installation. Overall, the inhibitor oil provided the best and most fully satisfactory protection of prestressing steel for the investigated duration of six months.

The most effective, proven method for temporary corrosion protection is to seal the tendons as quickly as is practicable during the duration between the completion of stressing and the initiation of grouting. Once the tendon is stressed, all tendon ends and vents should be sealed to avoid the ingress of water into the duct system before cementitious grout quickly fills the tendons. Leaving prestressing steel inside the duct without temporary or permanent corrosion protection for an extended time can create durability problems, including tendon failures. Figure 128 shows pitting corrosion observed during construction on stressed strands that were exposed to moist air in an empty duct for an extended period before grouting.

Source: FHWA.

A. An excavated tendon.

Source: FHWA.

B. Closeup of pitting corrosion.

Figure 128. Photos. Pitting corrosion damage on stressed strands in an empty duct.

Many specifications limit the length of time between stressing and grouting. For example, the PTI *Guide Specification for Grouting* gives maximum time limits for grouting depending on the ambient humidity: 7 d in a very damp atmosphere (RH >70 percent) or over or near saltwater, 20 d in a moderate atmosphere (RH = 40–70 percent), and 40 d in a very dry atmosphere (RH <40 percent).[21] If these limits are exceeded, temporary corrosion protection is required.

3. THE IMPREGNATION METHOD [41,44,132-135]

The impregnation method was recently developed as a corrosion mitigation solution for new and existing grouted PT tendons subjected to high RH, moisture, grout voids, chloride ions, and sulfate ions. An injected substance is advertised to displace moisture, form a protective barrier on exposed steel surfaces, and impregnate surrounding grout to form a barrier against moisture and oxygen. Since moisture or a high RH also lowers grout's electrical resistance and may increase the CR of steel, moisture removal should be its essential function. This corrosion mitigation method utilizes a formulated low-viscosity, dual-acting, hydrocarbon-silicon-polymer resin.

Before the impregnation process begins, the tendon is tested with air for leaking, and all leaking spots are repaired. The tendon's moisture content is also tested to ensure the strands, voids, and grout are not saturated with water. Next, the resin is pumped through interstitial spaces in the grouted 7-wire strands without releasing the tension on the prestressing strands. Injection into the tendon's interior is made from the grout caps at the anchorage or by installing a port at an intermediate tendon section. Figure 129 illustrates how the impregnation method is executed from an exposed tendon end.

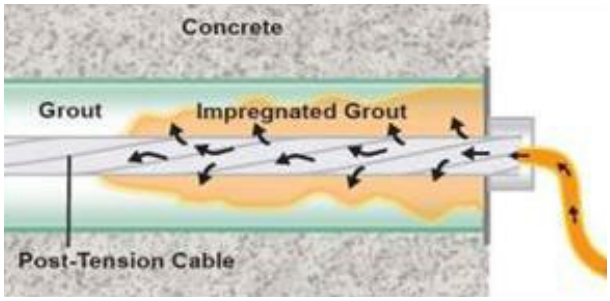

Figure 129. Illustration. Schematic of impregnation from the end of an exposed tendon.[134]

The corrosion protection properties of the impregnation material were evaluated in a laboratory experiment with the steel plates without any surface preparation.[134,135] Impregnation material was applied to one-half of each steel plate. The samples were then exposed to a periodic saltwater spray. The treated side of the steel surface was protected well compared to the untreated side. Similar results were obtained when this test was repeated with exposure to seawater spray and sulfate spray.

More laboratory tests were conducted using treated and untreated bare 7-wire strand samples and strands embedded in a prepackaged grout material. By applying a voltage from each strand sample to a counter-electrode, these samples were forced to corrode in anodic potentiostatic testing. Test results of impregnated and untreated samples indicated that impregnation effectively reduced the total current up to 95 percent under potentiostatic testing. The same testing on void-free grout samples with and without chlorides showed that the impregnation-treated samples exhibited an 81.4 percent reduction in corrosion current when compared to the untreated samples. As reported in chapter 4, an in-house study conducted at FDOT also observed good performance for impregnated specimens in corrosive exposure conditions.

Another research report pointed out the advantages of the impregnation method when it was applied to the high-capacity PT foundation anchors, as follows:[132]

- The process requires access only at the individual strand ends at the anchor head, which can stay in tension. Wicking action along the center wire carries the chemical down the strands.

- The chemical forms a flexible polymer coating when it sets after 24 h, preventing oxygenated water from reaching and corroding the strands.

- The chemical fills the pores in the existing grout with a wicking action, which is limited by the porosity and permeability of the grout and the chemical's viscosity.

- The process requires very little maintenance. When the components set, the moisture protection lasts a long time, unless harsh chemicals affect the polymer coating.

Three drawbacks were also mentioned in the report, as follows:

- Chemical impregnation covers existing corrosion and mixes with existing water. The strands should be cleaned and dried (and must remain dry) before and during the process. Water emulsifies the chemical polymer before it sets, reducing the effectiveness of the moisture seal function.

- In some areas, the tendon may not become completely covered due to grout voids where there is no wicking action. As such, impregnation may be unsuitable for ungrouted tendons because it would require an excess of chemicals.

- Environmental concerns exist.

Other concerns also exist. To avoid long-term issues for PT tendons that have been exposed to external water or bleed water, the strands must be dried first by a drying technique before injection. Otherwise, the chemical will combine with the water, causing it to emulsify. The strand-drying procedure may require installing pressurized gas input ports and does require a means to provide gaseous flow so that evaporation can occur. Confirming the tendon is dry to its bonded length is difficult to accomplish. The chemical takes 24 h to become impervious to water. If corrosion is already present before the chemical impregnation process begins, rust will be encapsulated under the impregnation chemical. In certain conditions, moisture may be trapped inside a pit formed by corrosion, which may continue the corrosion process unless the impregnated coating shuts down the ingress of oxygen.

Or suppose there is a void in the grout, and the chemical being injected through the tendon has no grout to push against and penetrate. Without grout surrounding the strands, the chemical may not completely coat that part of the exposed strands and may ooze from the strands without reaching the bottom of the tendon—or the chemical may only travel around the center strand of the tendon and protect the inside unless the entire duct is filled with the chemical.

The impregnation method was tried on selected PT bridges in Florida. Additionally, four external tendons in the Varina-Enon Bridge in Virginia were treated in July 2015 at the cost of $12,222 per tendon (mobilization for $3,947 and injection for $8,275). As the first step, air communication and tendon moisture testing was performed. The average RH in the four tendons was 90 percent (the highest RH was 94 percent) compared to an ambient RH of 63 percent. These RH readings were significantly higher than those measured in Florida PT bridges. Many leaks were found during air testing and injection testing, and thus injection was delayed until all the leaks were sealed using epoxy paste or fiber-reinforced polymer. Eventually, all the tendons were successfully impregnated. The volume of material required to impregnate the tendons was significantly more than expected and more than what was used to impregnate the Florida bridge tendons, possibly due to more voids and defects in the grout. Figure 130 shows the condition of two tendons after they were treated.

Source: FHWA.

A. One northbound tendon.

Source: FHWA.

B. One southbound tendon.

Figure 130. Photos. Two external tendons treated with the impregnation method.

According to field trials, the injected impregnation material traveled as far as 250 ft along a tendon's end.[134] It could impregnate up to 100 ft in each direction when injected from a mid-point location. Figure 131 shows an opened area exhibiting impregnated strands and the surrounding grout.

Figure 131. Photo. Impregnated strands and grout.[134]

The impregnation method left a corrosion-resistant film on the exposed steel surface and penetrated the grout for an additional layer of protection surrounding the strands. However, the aforementioned field trials did not report what kind of monitoring technique would be used to determine this method's effectiveness with time.

4. FLEXIBLE FILLERS[1,15,111,136,137,138]

Flexible filler materials have been used in Europe as an alternative to cementitious grout in unbonded tendons. The use of alternative fillers started when the Service d'Etudes Techniques des Routes et Autoroutes **(**SETRA), the Technical Department for Transport, Roads, and Bridges in France, issued new requirements to abandon the use of cementitious grout in external tendons in February 2001.[137] These new requirements were followed by the publishing of the European Technical Approval Guide 013 on post-tensioning systems by the European Organization for Technical Assessment in June 2002.[138]

Wax and grease are the primary flexible filler materials. The waxes used are homogeneous, hydrophobic, and have metal adhesion properties. They are made of saturated hydrocarbons with high percentages of ramified chains. In particular, microcrystalline wax, one type that is used, is obtained from heavy components of distillation. The microcrystallization enables its flexibility and its properties of adhesion to various supports and surfaces. It is preferable to grease for service at higher temperatures because of the stability in its crystalline structures. In contrast, the grease used is a mix of oil and soap with anti-corrosion additives. It is preferable for service at lower temperatures and where low friction is required because it is a more homogeneous mixture than wax. However, grease can bleed and separate over time.

For applications where there is no need for low friction (e.g., with injection after stressing and sheathed strand not embedded in grout or concrete), wax may be preferred by most suppliers over grease because its crystalline structure provides greater long-term stability.

France seems to be the largest microcrystalline wax user on unbonded external PT tendons but still continues to fill internal tendons with cementitious grout. Germany also uses wax for prefabricated tendons only. From 1970 to 2000, the United Kingdom built 10 bridges with either grease or wax-filled tendons, but flexible fillers are no longer specified there. South Carolina's Arthur Ravenel Jr. Bridge, also known as the Ravenel Bridge, used microcrystalline wax in its anchorages. Most other countries in Europe and Asia do not use flexible fillers systematically in PT construction. Instead, flexible fillers have been used on cable-stayed bridges in Japan, Europe, the United States, Mexico, and various other countries worldwide.

The injection of flexible filler materials needs special equipment (pumping equipment, heater, and mixer) and procedures. Handling the filler materials heated to over 200 °F can be a safety problem for installation crews and people staying near the operation. Therefore, care must be taken to ensure that pumps and hoses are intact and in good working order, connections are tight and secure, and all personnel wear the appropriate and mandatory protective gear. At pumping pressure ≤ 90 psi, potential leaks are minimized.

Heating the materials to a uniform temperature before the filling operation can be difficult in the field. The wax is typically heated to 230 ºF. The temperature of the heated filler needs to be maintained above its melting point during injection into the ducts. This requirement can be problematic on long tendons in colder climates. If the wax cools sufficiently in the duct during injection, the wax can thicken and cause the duct to leak or burst due to additional backpressure.

The pros and cons of flexible fillers, from the standpoint of construction and maintenance, are as follows.

Pros:

- Tendons are restressable or replaceable.
- Wax filling and injection in the duct are fast (only 2–3 min required to fill a long tendon).
- No wax testing is required on site.
- Improved personal safety is needed for exposure to excessive heat from the molten wax in case of duct rupture.
- Loss of prestressing force is incremental.

Cons:

- Special safety measures are required for personnel during hot wax filling.
- Special equipment is required for heating and pumping.
- A thicker HDPE duct is required.
- The wax is about seven times more expensive than cementitious grout.
- There is a potential for bursting and duct bulging and deforming.
- There is a potential for leaking and deforming at pumping pressures between 90 and 225 psi.
- There is a potential for duct bursting at pumping pressures greater than 225 psi.

Furthermore, since all tendons filled with flexible fillers are fully unbonded, additional design implications should be considered for shear, ultimate strength, cracks, and deflection control. While there is no impact on use in external tendons, it is necessary to increase total strands 10 to 15 percent for use in internal tendons. The combined use of bonded and unbonded tendons can minimize the design impact.

Flexible fillers provide corrosion prevention in unbonded PT tendons, prohibit the circulation of gases or liquids within the strand duct and in the anchorage zone, reduce friction between metallic components, and avoid fretting corrosion**.** In particular, wax protects the prestressing steel by keeping water away from the steel thanks to its hydrophobic and metal-adhering properties. However, flexible fillers such as heated waxes flow like real liquid. If not properly installed, they may develop the same installation defects as grout, i.e., air pockets and voids. When they cool, these materials can shrink and cause cracks and voids. This behavior is a particular concern in colder climates, where the temperature difference between the coldest time of the yr and the injection time can be over 200 °F. As discussed in chapter 4, a laboratory study carried out by the University of Florida observed voids at high points and the cracking of filler materials in their laboratory specimens. The study revealed the difficulties of achieving void-free tendons and avoiding cracks in filler materials.

The impact of filler defects on corrosion protection and fillers' long-term stability under service conditions is unknown, especially in the event of frequent exposure to water if the duct system does not maintain water tightness. Based on what is known about other petroleum-based products, material degradation may be possible during a service life of 75 to 100 yr. Steel coated with flexible fillers has been observed to corrode due to the following reasons:

- Water ingress-related corrosion observed with early grease-type flexible fillers and sheathing. In some cases, chlorides also contributed.

- Poor quality of flexible fillers observed, along with poor workmanship.

- MIC caused by bacteria and fungi.

PTI issued a technical note in 2015 that discussed the merits and limitations of potential filler materials. It was intended to guide owners and designers in making the appropriate choice for a given structural application. FDOT specified the use of wax to fill all external tendons and selected internal tendons in 2016. VDOT also specified flexible fillers for unbonded external

tendons and grout for bonded internal tendons in the same yr. Filling tendons with flexible filler instead of cementitious grout may allow strand replacement if sufficient access is provided at the anchor ends. According to FDOT, the use of wax filler will increase 15 to 26 percent above similar grouted systems for pay item cost and 0.5 to 2.4 percent higher than a similar grouted system for superstructure cost but less than 1 percent for total project cost.[137]

Currently, there is limited experience with flexible fillers in PT applications in the United States High-quality workmanship is required for successful filling and appropriate handling of combustible materials at high temperatures. Therefore, extensive training is needed to develop a qualified workforce familiar with the injection of flexible fillers and capable of doing a consistent, high-quality job.

5. CORROSION RESISTANT STRANDS[2,10,88,90-94,104,139-146]

There are other types of 7-wire strands that possess higher corrosion resistance than conventional bare strands. They include epoxy-coated, hot-dip galvanized, and solid stainless steel. Figure 132 shows all four types of the 7-wire strand products currently available in the U.S. market. The solid stainless steel shown in the figure is the 2205 duplex stainless steel.

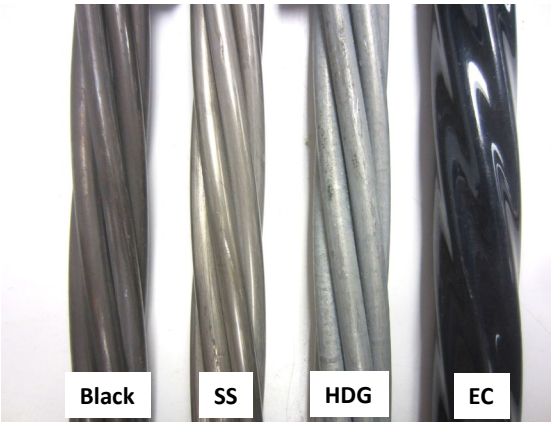

Source: FHWA.
Black = conventional; SS = solid stainless steel; HDG = hot-dip galvanized; EC = epoxy-coated.

Figure 132. Photo. Four types of 7-wire strand materials.

Protective coatings applied to prestressing steel started to appear in the literature as early as the mid-1960s. Various types of protective coatings were applied to 0.25-inch-diameter prestressing steel specimens, and numerous tests evaluated their performance in laboratory environments. It was determined that hot-dip galvanized, epoxy-coated strands performed well, but neither met all the requirements for an ideal coating.

Prestressing steel coatings should have specific properties, including no adverse effect on the strength or ductility of the steel, sufficient flexibility, ductility to withstand stranding during manufacturing, and elongation during stressing without cracking or peeling. Coatings should not have a detrimental effect on the bond between steel and concrete or grout and should be able to

withstand handling, placement, and stressing without damage. The following discusses three types of corrosion-resistant strands.

5.1 Epoxy-Coated Strand

Epoxy-coated strand was manufactured to meet the requirements of the following American Society for Testing and Materials International (ASTM) standards:

- *ASTM A882/A882M-04a: Standard Specification for Filled Epoxy-Coated Seven-Wire Prestressing Steel Strand.*(140)
- *ASTM A416/A416M-18: Standard Specification for Low-Relaxation, Seven-Wire Steel Strand for Prestressed Concrete.*(139)

The *ASTM A882/A882M-04a* was withdrawn in 2019. The specified physical properties of the epoxy coating used for prestressing strands were significantly different from those used for mild steel reinforcement. Epoxy coating is very tough but is ductile and good at bonding to the steel. It should also be durable and resistant to abrasion. According to the *ASTM A882/A882M-04a*, the finished coating thickness can range from 15 to 45 mils. A bare 7-wire strand meeting the *ASTM A416/A416M-18* requirements is mechanically cleaned and then preheated to 572 ºF before the coating is applied using the electrostatic spray method.

Epoxy-coated strand is available in two configurations: conventional and flow-filled coated strands. The conventional epoxy-coated strand is produced by spraying around its exterior circumference with a thick epoxy coating. The flow-filled coated strand is manufactured by spraying the coating after spreading the outer six wires from the center wire. In this way, interstices between the individual wires are filled with the plastic-state epoxy coating before the wires are restranded. Figure 133 shows two cross-sections of the flow-filled epoxy-coated strand (see figure 133-A) and the conventional bare strand (see figure 133-B).

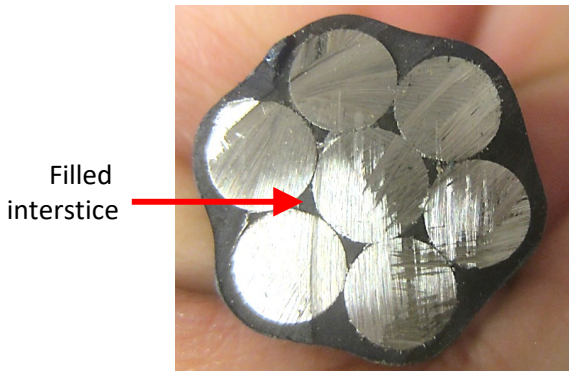

Source: FHWA.

A. Flow-filled epoxy-coated strand.

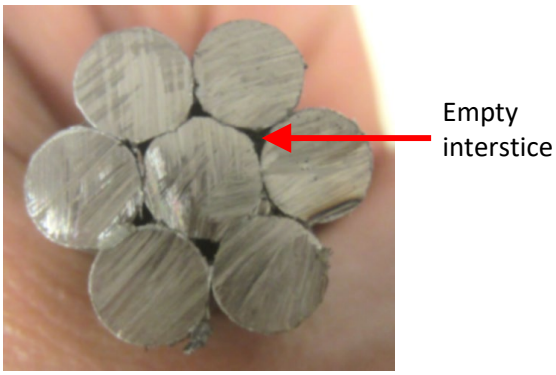

Source: FHWA.

B. Conventional bare strand.

Figure 133. Photos. Cross-sectional views of two types of 7-wire strand materials.

At present, only flow-filled coated strand is available, either with a smooth surface or with grit particles embedded on the coating surface. The epoxy-coated strand with a smooth surface is intended for use in applications where the bond is not critical, such as unbonded external PT tendons and stay cables. Smooth epoxy coating is not a replacement for the sheathing used in mono-strand PT systems. The epoxy-coated strand with a grit-impregnated coating is intended for use in bonded PT tendons and pretensioned applications.

Flow-filled epoxy coated strand is superior to bare and conventional epoxy-coated strands because flow-filled epoxy coating prevents water from traveling through the strand interstices. However, concerns have been raised because wedges at the anchor heads break the epoxy coating, and corrosion can develop under the damaged coating between the marks created by the wedge teeth. The significance of corrosion at the wedge locations may vary. In bonded PT tendons, corrosion at the wedge locations should not significantly affect the structure's integrity. However, in unbonded PT tendons or stay cables, anchorage failure due to corrosion at the wedges can lead to failure of the tendons or cables. In these situations, additional protection should be provided at the wedge locations. Currently, epoxy-coated strand in PT applications and stay cables requires special wedges that bite through the epoxy coating and into the underlying strands. Strand tails should also be coated with the manufacturer's recommended epoxy patch material.

5.2 Hot-Dip Galvanized Prestressing Strand

Hot-dip galvanized 7-wire strand suitable for prestressing applications is commercially available in standard sizes from 3/8 to 0.6 inches in diameter. Before galvanizing, the single wires need to meet the requirements of grade 270 strand per ASTM A416/A416M when fabricated to the corresponding finished strand size. During production, the wires are individually coated in zinc and then stranded. The minimum density of zinc coating for the strand ranges from 0.90 to 1 oz/ft^2.

As zinc is anodic to steel in the electromotive force series, the zinc’s sacrificial action protects the steel by suppressing corrosion of the underlying steel at the coating damages. However, the CR of zinc can also be high in a highly alkaline environment, such as grout, because it is an

amphoteric material (i.e., corrosion susceptible in acidic as well as alkaline conditions). While it is popular in Europe and Japan, the use of the galvanized strand is not common in North America. The possibility of HE for galvanized high-strength steel is still controversial as contradictory test results exist. The effects of zinc galvanizing on the bond of a prestressing strand are not fully known at this time.

Some laboratory studies reported that hot-dip galvanized strand could delay the onset of corrosion, but it performed worse than alternative strand materials. In many cases, the exterior wires exhibited corrosion on the zinc coating as well as the underlying steel, and heavy corrosion also occurred on the inner wires. Also, galvanizing cold drawn wire for a prestressing strand may reduce the tensile strength of the wire and degrade relaxation properties: the ultimate elongation of the wire may increase, and the elastic modulus of the 7-wire strand typically decreases. The FHWA TA 5140.25 Background section c(3) says the following:

> "The galvanizing process affects the mechanical properties of steel. It has been reported that ultimate tensile strength can be reduced by as much as 5 percent and fatigue strength by 20 percent. With some steel formulations there may also be changes in ductility. The possibility of hydrogen embrittlement due to the galvanizing process has been suspected. However, there is no hard evidence to support this suspicion. In the case of galvanized wire or strand encapsulated in grout, the zinc coating may react with some cements releasing hydrogen gas. This reaction is apparently dependent upon the cement alkalis, type of steel, and the composition of the zinc coating. When galvanized strand is embedded in cementitious grout, the corrosion rate of zinc itself is accelerated. As a result, zinc as an anode or sacrificial metal coating does not perform the same as in atmospheric conditions."

This TA was rescinded in January 2020.[142]

5.3 Stainless Steel Strands

High-strength stainless-steel strands made with different alloys have demonstrated excellent corrosion performance in laboratory studies.[104] Stainless steel alloys 2205 and 2304 showed the most promising results as corrosion-resistant prestressing strands. The highest corrosion resistance of the 2205 duplex alloy was thought to be from its 3.2 percent Mo content.

More studies are needed to quantify this type of strands' corrosion resistance in specific conditions, including exposure to carbonated bleed water and segregated grout contaminated with different concentrations of anions.

6. REGROUTING[99,132]

Regrouting procedures must be determined based on the geometric characteristics (length, cross-section, volume, and so on) of preexisting voids. According to a Texas A&M University study reviewed in chapter 4, the PG and PVG methods repaired voids more economically than the VG method did. Although the different grouting repair methods did not show significant differences in their filling capability at a 95 percent confidence level, the PG method seemed to exhibit a lower filling capability than the others. Thus, the PVG method was recommended for filling voids in the field.

A list of four requirements for suitable grouting material follows:

- A properly flowing grout mixture to fill the duct.
- A specific amount of time for the reabsorption of any bleed water inside the duct.
- Grout properties of adherence and strength.
- Resistance to freezing.

Quality control is an essential element in the grouting process, and care must be taken to follow the manufacturer's directions. The pumping pressure must be maintained at an adequate level, depending on the grout hose, a possible vertical rise of the duct, and the length to be regrouted. It was reported that unintended corrosion problems could be developed between the existing and repair grouts.

Whenever possible, regrouting should start at a low point. Comparing the void volume to the actual volume of grout injected will determine if further grouting will be necessary. In many cases, not all voids can be filled, and thus voids will still exist. Inspection holes may be drilled to see the duct interior using a borescope. This extra step can increase the likelihood of filling all voids in the duct but may be impractical for a large number of voids. The borescope inspection is recommended for situations where large, continuous duct regions were left ungrouted or partially filled.

7. THE DRYING AIR AND INERT GAS TECHNIQUE[2,146]

Lowering the RH below the critical value of 60 percent is one effective way of controlling corrosion. Inert gases can be used to remove moisture and suppress corrosion because the moisture evaporates in moving gases while oxygen is being removed.

For unbonded PT tendons experiencing corrosion, a gas-purging technique was developed and tested in Canada in the early 1990s. Dry gas was circulated in the duct until free water was removed and the internal RH was sufficiently lowered. The dry gas purging system can remove the water before repairs and then continuous operation with an automated control system.

The flow of nitrogen gas can dry out both the water and wet grout in the tendon. A drying system can maintain a positive pressure of nitrogen gas to a grouted tendon as long as it maintains airtightness. The gas can be dissipated in the grout through the porosity, cracks, and voids. If there are voids in the grouted tendon, pressure can be maintained in the voids by exceeding the gas escaping flow through the porous grout.

Pressurization with inert gas can reduce water intrusion into voided tendons when sufficient pressure is maintained. However, if the tendon leaks through the duct wall and gaps in the tendon system, the actual implementation of this method can be difficult. Also, the method requires the maintenance of special equipment throughout the entire operation. Additionally, the pressure required to move water from around the strands and reach the anchor zone can be large.

8. CATHODIC PROTECTION[2]

The application of cathodic protection to prestressing strands has been rare for two reasons. First, if the magnitude of a potential shift during the cathodic protection is excessive, the water

dissociates into hydrogen gas and oxygen in a neutral and alkaline environment. As a result, atomic hydrogen may penetrate the high-strength prestressing steel matrix and cause HE. The likelihood of experiencing HE would be greater under an impressed current cathodic protection system than under sacrificial anode cathodic protection systems due to the higher possibility of applying excessive protection current.

The second reason is the shielding effect of the internal ducts. The metal ducts should receive most of the protection current and shield the prestressing steel inside. Also, the plastic ducts block the protection current because it is an effective insulator. This shielding effect reduces the effectiveness of cathodic protection on PT strands. However, the cathodic protection technique can still be useful to protect reinforcing steel around the internal tendons and the exterior surfaces of the metal ducts from corrosion.

9. OTHER CONSIDERATIONS [36,37,88,90,91,107-110,121]

The primary source of chloride penetration into internal tendons is through the corroded galvanized metal ducts. Therefore, galvanized ducts should not be used in aggressive environments. Instead, the plastic duct should always be used. All anchorages should be fitted with permanent grout caps, as these can reduce the risk of water entering through the anchor heads. Also, similar metals should be used in anchorage components to prevent galvanic corrosion among dissimilar metals.

The performance of any grout material can be influenced by site-dependent parameters such as ambient temperatures and mixing operations. Many of the techniques developed in laboratories under ideal situations may differ from those encountered in the field. The on-site grouting practice and the use of suitable grout materials are critical for determining the quality of the actual grout to be used in a specific construction project. Therefore, a full-scale mockup test is recommended for every major construction project to identify problems before grout installation. The mockup should include the most complicated tendon profile, in terms of the largest height change and length, and use the same grout selected for the project. Also, during grout mixing work, the water in each batch must be carefully measured, and individual grout bags should be weighed to maintain the required water-grout powder ratio accurately.

REFERENCES

1. *Fib*. 2005. *Fib Bulletin No. 33: Durability of Post-Tensioning Tendons*. Lausanne, Switzerland: FIB International.

2. American Concrete Institute (ACI) Committee 222 (ACI 222.2R-14). 2014. *Report on Corrosion of Prestressing Steels*. Farmington Hills, MI: ACI.

3. Poston, R.W. and Wouters, J.P. 1998. *Durability of Precast Segmental Bridges, NCHRP [National Cooperative Highway Research Program] Web Document 15.* Project 20-7/Task 92. Washington, DC: NCHRP, Transportation Research Board (TRB).

4. Clark, G. 2011. "Durable Post-Tensioned Concrete Structures." *Technical Report No. 72*. Presented at the *Concrete Bridge Development Group*.

5. Trejo, D., Hueste, M., Gardoni, P., Pillai, R., Reinschmidt, K., Im, S., Kataria, S., Hurlebaus, S., Gamble, M., and Ngo, T. 2009. *Effect of Voids in Grouted Post-Tensioned Concrete Bridge Construction: Volume 1—Electrochemical Testing and Reliability Assessment*. Report No. FHWA/TX-09/0-4588-1. Austin, TX: TxDOT.

6. Woodward, R.J. 1989. "Collapse of a Segmental Post-Tensioned Concrete Bridge." *Transportation Research Board* 1211: 38–59. Washington, DC: TRB.

7. Woodward, R.J. 2001. "Durability of Post-Tensioned Tendons on Road Bridges in the UK." *Fib Bulletin No. 15: Durability of Post-Tensioned Tendons:* 1–10. Lausanne, Switzerland: FIB International.

8. Schutter, G.D. 2013. *Damage to Concrete Structures*: 31–33. CRC Press, Taylor and Francis Group: Boca Raton, FL.

9. Nasser, G.D. 2008. "The Legacy of the Walnut Lane Memorial Bridge." *Structure Magazine*: 27–31. Chicago, IL: The National Council of Structural Engineers Association (NCSEA), ASCE's [American Society of Civil Engineers'] Structural Engineering Institute (SEI), and the Council of American Structural Engineers (CASE).

10. Freyermuth, C.L. 1991. "Durability of Post-Tensioned Prestressed Concrete Structures." *Concrete International* 13, no. 10: 58-65. Farmington Hills, MI: ACI.

11. ASBI. 2007. *Durability Survey of Segmental Concrete Bridges, 3rd Edition*. Buda, TX: ASBI.

12. Freyermuth, C.L. 2001. "Status of the Durability of Post-Tensioning Tendons in the United States." *Fib Bulletin No. 15: Durability of Post-Tensioning Tendons*: 43-50. Lausanne, Switzerland: FIB International.

13. ASBI. 2012. *Durability Survey of Segmental Concrete Bridges, 4th Edition.* Buda, TX: ASBI.

14. Garcia, P., Theryo, T.S., and Womble, S. 2006. "Overview of PT Tendons Corrosion Investigation, Repairs and Mitigation." Presented at the *US Army Corrosion Summit.* Clearwater Beach, FL.

15. Vallier, R.W. 2014. "Flexible Filler Material for Post-Tensioned Systems." Presented at the *2014 FDOT Design Training Expo*. Daytona Beach, FL: FDOT.

16. Sagues, A. and Rowers, R.G. 2006. "Mechanism and Detection of Corrosion of Post-Tensioned Tendons in Florida Bridges." Presented at the *2006 PTI Technical Conference and Exhibition*. Reno, NV: PTI.

17. FDOT. 2002. *New Directions for Florida Post-Tensioned Bridges, Vol. 1: Post-Tensioning in Florida Bridges*. Tallahassee, FL: FDOT.

18. FDOT. 2010. "Segmental Bridges—It's a Construction Technique With Design Implications." Presented at the *2010 FDOT/FTBA [Florida Transportation Builders' Association] Construction Conference*. Orlando, FL: FDOT/FTBA.

19. Theryo, T.S. 2016. "Durability Issues and Improvement Strategy of Post-Tensioned Bridges in the United States." Presented at the *3rd International Conference on Sustainable Civil Engineering Structures and Construction Materials*. Bali, Indonesia.

20. PTI. 2019. *Specification for Grouting of Post-Tensioned Structures*. Farmington Hills, MI: PTI.

21. PTI and ASBI. 2019. *PTI/ASBI M50.3-19, Specification for Multistrand and Grouted Post-Tensioning.* Farmington Hills, MI and Buda, TX: PTI and ASBI.

22. *Fib*. 2002. *Fib Bulletin No. 20: Grouting of Tendons in Prestressed Concrete: Guide to Good Practice Prepared by Fib Task Group 9.8: Grouting.* Lausanne, Switzerland: FIB International.

23. ISO. 2012. *Grout for Prestressing Tendons—Part 1. Basic Requirements (14924-1); Part 2—Grouting Procedures (14824-2); Part 3—Test methods (14824-3)*. 14824. Geneva, Switzerland: ISO.

24. European Committee for Standardization (CEN). 2007. *EN 445: Grout for Prestressing Tendons—Test Methods, English Version.* Brussels, Belgium: CEN.

25. CEN. 2007. *EN 446: Grout for Prestressing Tendons—Grouting Procedures, English Version.* Brussels, Belgium: CEN.

26. CEN. 2007. *EN 447: Grout for Prestressing Tendons—Basic Requirements, English Version.* Brussels, Belgium: CEN.

27. Pouliotte, J. 2012. “PT Grouting and Corrosion Issues in Florida.” Presented at the *AASHTO T-9 (Bridge Preservation) Committee Meeting*. Austin, TX: AASHTO.

28. Schokker, A. 2012. *Development of Best Practices for Inspection of PT Bridges in Minnesota*. Report No. 2012-09. St. Paul, MN: Minnesota DOT.

29. Hartt, W.H. and Venugopalan, S. 2002. *Corrosion Evaluation of Post-Tensioned Tendons on the Mid-Bay Bridge in Destin, Florida*. Report No. not available. Gainesville, FL: FDOT.

30. Ghorbanpoor, A. 2000. *Condition Assessment of External PT Tendons in the Mid-Bay Bridge*. Report No. not available. Gainesville, FL: FDOT.

31. www.nwf.dailynews.com. 2022. “Mid-Bay Bridge Could Be Closed ‘A Couple of Weeks’” (web page). https://www.nwfdailynews.com/news/20190109/mid-bay-bridge-could-be-closed-a-couple-of-weeks, last accessed January 28, 2022.

32. Sinclair Broadcast Group, Inc. 2022. “Mid-Bay Bridge Closed, Emergency Repair Underway” (web page). https://weartv.com/news/local/mid-bay-bridge-closed-emergency-repairs-underway, last accessed January 28, 2022.

33. Powers, R.G., Sagues, A.A., and Virmani, Y.P. 2004. *Corrosion of Post-Tensioned Tendons in Florida Bridges*. Report No. FL/DOT/SMO/04-475. Gainesville, FL: FDOT.

34. Theryo, T. and Garcia, P. 2004. “Sunshine Skyway Bridge Post-Tensioned Vertical Tendon Corrosion Investigation: Summary of Findings.” *Segmental Bridges* 57, no. XIX: Number 1. Tampa, FL: Parson Brinckerhoff.

35. Theryo, T. 2014. “Selected Post-Tensioned Bridge Investigations in the Last 15 Years.” *Presented at the FHWA/FDOT Grout Meeting*. Gainesville, FL: FHWA/FDOT.

36. Sprinkel, M.M. 2015. “VDOT Experience With Grouts and Grouted Post-Tensioned Tendons.” *PTI Journal* August 2015: 51-61. Farmington Hills, MI: PTI.

37. Sprinkel, M.M. 2016. “Tendon Issues.” *Bridge Design & Engineering Journal*, 85: 94-95. London, UK: Hemming Group, Ltd.

38. FHWA. 2012. *Literature Review of Chloride Threshold Values for Grouted Post-Tensioned Tendons.* Report No. FHWA-HRT-12-067. Washington, DC: FHWA. https://www.fhwa.dot.gov/publications/research/infrastructure/structures/bridge/12067/12067.pdf, last accessed January 28, 2022.

39. Moore, M., Reed, M., and Pearson, J. 2008. “Appendix I.1: I-295 Varina-Enon Cable Stay Bridge Materials Testing of Samples From Tendon 10-E and 1302-W”; “Appendix B.4: Site Visit Report No. 1.” *Final Report (I-295 Varina-Enon Bridge Tendon Replacement for the VDOT)*. Exton, PA: Figg Bridge Engineers, Inc.

40. Parsons Brinckerhoff, Inc. and Siva Corrosion Services, Inc. 2013. *Evaluation of Grout and Strands at 13 Tendon Locations and Selected Vertical PT Bars at Fixed Piers*. Report No. 40111. Richmond, VA: VDOT Structure and Bridge Division.

41. Sprinkel, M.M. and Napier C. 2013. "Post-Tensioned Grout Update (Design, Specifications, Material & Construction." Presented at *Virginia Concrete Conference*. Richmond, VA: VDOT.

42. Sprinkel, M.M. 2017. "Performance of Post-Tensioned Bridges." Presented at *Virginia Concrete Conference*. Richmond, VA: VDOT.

43. Sprinkel, M.M. 2018. "Update on Post-Tensioned Structures in Virginia." Presented at VDOT Central Office." Richmond, VA: VDOT.

44. Sprinkel, M.M. 2016. "Preservation of Post-Tensioned Tendons in the Varina-Enon Bridge." Presented at the *2016 International Bridge Conference*. Pittsburg, PA: Engineers' Society of Western Pennsylvania (ESWP).

45. The Times. 2009. "INDOT [Indiana DOT] Takes Hard Look at Bridges Similar To Cline Ave" (web page). https://www.nwitimes.com/news/local/lake/article_b4cbb7ee-1621-50f1-ad3c-c27ea5711320.html, last accessed March 11, 2020.

46. The Times. 2009. "Firm Asked for Cline Ave. Limits Week Before Closure" (web page). https://www.nwitimes.com/news/local/lake/firm-asked-for-cline-ave-limits-a-week-before-closure/article_f804b508-123d-53cb-9198-d733cc908c24.html, last accessed March 11, 2020.

47. Frost, J., Madlem, T., Kline, D., and Crigler, J. 2006. "Unique and Effective Sampling Method Saves Money and Time." *Structure Magazine,* October 2006: 42-45. Chicago, IL: NCSEA, ASCE's SEI, and CASE.

48. Construction Headline. 2020. "Introduction to Box Girder Bridge" (web page). http://constructionheadline.com/box-girder-bridge/, last accessed March 11, 2020.

49. Paredes, M. 2013. "Update on Corrosion Failure of Post-Tensioned Tendons in Florida Due to Thixotropic Grout Segregation." Presented at *Corrosion/2013*. Orlando, FL: National Association of Corrosion Engineers (NACE) International.

50. Lau, K. 2014. "Corrosion Post-Tensioned Tendons in Presence of Deficient Grout." Presented at the *FHWA/FDOT Grout Meeting*. Gainesville, FL: FHWA/FDOT.

51. Lau, K. 2016. *Corrosion of Post-Tensioned Tendons With Deficient Grout*. Report No. BDV29-977-04. Gainesville, FL: FDOT.

52. Lau, K., Lasa, I., and Paredes, M. 2011. *Corrosion Development of PT Tendons With Deficient Grout: Corrosion Failure in Ringling Causeway Bridge, Draft Report.* Gainesville, FL: FDOT State Materials Office.

53. Lau, K., Lasa, I., and Paredes, M. 2013. *Corrosion Failure of Post-Tensioned Tendons in Presence of Deficient Grout, Paper No. 2600.* Presented at *Corrosion/2013*. Orlando, FL: NACE International.

54. Paredes, M. 2013. "PT Grout Segregation." Presented at the *AASHTO T-18 (Bridge Management, Evaluation, and Rehabilitation) Committee Meeting*. Portland, OR: AASHTO.

55. Kerr, R. 2014. "FDOT Post-Tensioning and Grout Field Investigation and Findings." Presented at the FHWA/FDOT Grout Meeting. Gainesville, FL: FHWA/FDOT.

56. Jacobsen, J.J. and Theryo, T.S. 2016. "Ringling Bridge External Tendons Investigation and Repair." Presented at a *FDOT District 7 Meeting*. Tampa, FL: FDOT.

57. Corven Engineering, Inc. 2010. *Evaluation of the Plymouth Avenue Bridge—Preliminary Investigations*. Report No. not available. Minneapolis, MN: City of Minneapolis Public Works Department.

58. Schokker, A. 2018. "Achieving Durability in Post-Tensioned Structures: A Look at Lessons We Have Learned (or Need to)." Presented at the *Structural Engineering Seminar Series*. Duluth, MN: University of Minnesota.

59. Star Tribute. 2010. "Corroded Cables To Keep Minneapolis Bridge Closed" (web page). StarTribute.com. Last visited December 28, 2010.

60. Structurae. 2018. "Repair of the Plymouth Avenue Bridge in Minneapolis, USA" (web page). https://structurae.net/en/products-services/repair-of-the-plymouth-avenue-bridge-in-minneapolis-usa, last accessed March 11, 2020.

61. Post and Courier. 2018. "Corrosion 'Exploded' Cable in Wando Bridge, Sending Grout Flying 100 Feet." https://www.postandcourier.com/politics/dot-corrosion-exploded-cable-in-wando-bridge-sending-grout-flying/article_bfff0fa0-7568-11e8-a1a7-0bfbef6a71fe.html, last accessed March 11, 2020.

62. Theryo, T. S. 2010. "*Walk-Through Inspection Brief Report*." Presented at an unnamed meeting. Place unknown: Parsons Brinckeroff.

63. Infrastructure Corporation of America, Parsons Brinkerhoff, Inc., and CONCORR Florida, Inc. 2011. *Wando River Bridge—Preliminary External Tendons Investigation Phase I*. Final Report No. not available. Columbia, SC: South Carolina Department of Transportation.

64. Siva Corrosion Services, Inc. 2017. *I-526 James B. Edwards Bridge Over the Wando River in Charleston, SC: Failed Tendon Investigation*. Draft Report No. 1001028-02. Charleston, SC: HDR/ICA.

65. HDR. 2018. “I-526 Wando River Bridges—Phase I: Status Issues Report and Meeting Minutes.” Notes from *Phase I Meeting*. Columbia, SC: South Carolina Department of Transportation.

66. Applied Technical Services, Inc. 2018. *Metallurgical Failure Analysis of a Bridge Post-Tensioning Tendon*. Report No. DC294717. West Chester, PA: Siva Corrosion Services, Inc.

67. CTL Group. 2018. *Strand Tensile Tests*. Report No. 251761. West Chester, PA: Siva Corrosion Services, Inc.

68. Collins Engineers, Inc. 2017. *I-526 Eastbound and Westbound Over the Wando River Pier Assessment*. Report No. not available. Charleston, SC: HDR/ICA.

69. Infrastructure Corporation of America, Parsons Brinkerhoff, Inc., and CONCORR Florida, Inc. 2011. *Wando River Bridge–Preliminary External Tendons Investigation Phase I*, Draft Report No. Not Available. South Carolina Department of Transportation, Columbia, SC.

70. Merrill, B.D. 2010. *Grout Testing and Analysis of Carbon Plant Road Over IH 37*. Memorandum CSJ: 0074-06-215. Austin, TX: TXDOT.

71. Shahawy, M. and Cox, W.R. 2005. “Critical Evaluation and Condition Assessment of Post-Tensioned Bridges in Texas.” *Journal of the Transportation Research Board* CD 11-S: 257–264. Washington, DC: TRB.

72. Lee, S.K. and Zielske, J. 2014. *An FHWA Special Study: Post-Tensioning Tendon Grout Chloride Thresholds*. Report No. FHWA-HRT-14-039. Washington, DC: FHWA. http://www.fhwa.dot.gov/publications/research/infrastructure/structures/bridge/14039/14039.pdf, last accessed March 11, 2020.

73. Chauvin, M.R. 2017. *Considerations for Development of Inspection and Remedial Grouting Contracts for Post-Tensioned Bridges*. Report No. 2017-04. St. Paul, MN: Minnesota Department of Transportation.

74. Godart, B., Lacombe, J., and Aubagnac, C. 2015. “Failures of External Tendons in Prestressed Concrete Bridges: Causes, Investigations, Remediation and Prevention.” Presented at the *2015 IABSE Conference—Structural Engineering: Providing Solutions to Global Challenges*. Geneva, Switzerland: IABSE.

75. Pearson-Kirk D., Collard-Jenkins, S., and Solan, B. 2004. “The Performance of Post-Tensioned Bridges.” Presented at the *2004 Concrete Bridge Conference*. Charlotte, NC: National Concrete Bridge Council.

76. Pearson-Kirk D., Collard-Jenkins, S., Theryo, T., and Chandra, V. 2004. “Improving the Durability of Segmental Bridges.” *Segmental Bridges* XIX, no. 57. Tampa, FL: Parsons Brinckeroff.

77. VSL International Ltd. 2002. *Grouting of Post-Tensioning Tendons: VSL Report Series 5*. VSL International Ltd.: Subingen, Switzerland. https://www.semanticscholar.org/paper/GROUTING-OF-POST-TENSIONING-TENDONS-5-VSL-Report-Tendons/1aaef440ad3d3d8ac58a34572534b3d0181c5f45, last accessed March 30, 2022.

78. Weiher, H. and Zilch, K. 2006. "Condition of Post-Tensioned Concrete Bridges—Assessment of the German Stock by a Spot Survey of Damages." Presented at the *First International Conference on Advances in Bridge Engineering*. Brunel University, UK: Brunel University.

79. Carsana, M. and Bertolini, L. 2016. "Characterization of Segregated Grout Promoting Corrosion of Posttensioning Tendons." *Journal of Materials in Civil Engineering* 28, no. 6. Reston, VA: American Society of Civil Engineers.

80. Carsana, M. and Bertolini, L. 2015. "Corrosion Failure of Post-Tensioning Tendons in Alkaline and Chloride-Free Segregated Grout: A Case Study." *Structure and Infrastructure Engineering* 11, no. 3: 402-411. London, UK: Publisher Taylor & Francis.

81. Bazzucchi, F., Restuccia, L., Ferro, G.A. 2018. "Considerations Over the Italian Road Bridge Infrastructure Safety the Polcevera Viaduct Collapse: Past Errors and Future Perspectives." *Frattura ed Integrità Strutturale (Fracture and Structural Integrity)* 46. Cassino, Italy: Frattura ed Integrità Strutturale. https://pdfs.semanticscholar.org/6ba7/5b9695bfc5cdd05c4504ae684c4bd5feb2b9.pdf?_ga=2.14264887.1467920448.1615753391-952880209.1615753391, last accessed March 14, 2021.

82. Gilles, I.P. "Internal Post-Tensioning Tendons: Many Problems and Sometimes Solutions." *Service Public de Wallonie*. Brussels, Belgium. http://www.mtq.gouv.qc.ca/portal/page/portal/Librairie/Publications/fr/ministere/recherche/17e_colloque/10_mai_13h30.pdf,%20last%20accessed%20March%2011,%202020, last accessed March 11, 2020.

83. Mutsuyoshi, H. 2001. "Present Situation of Durability of Post-Tensioned PC Bridges in Japan." *Fib Bulletin No. 15: Durability of Post-Tensioned Tendons: 75–88*. Lausanne, Switzerland: FIB International.

84. Korea Institute of Bridge and Structural Engineers and Korea Concrete Institute. 2017. *Tendon Failure Investigation and Follow-Up Research Studies, Final Report.* Seoul Metropolitan Facilities Management Corporation: Seoul, South Korea.

85. Ma, H.N. et al. 2019. *Investigation Report on Prestressing Tendon Failure Incident at Concrete Viaduct of Shenzhen Bay Bridge—Hong Kong Section*. Hong Kong Highways Department: Hong Kong. https://www.hyd.gov.hk/en/district_and_maintenance/structures/doc/SBB_HK_Investigation_2019.pdf, last accessed November 16, 2020.

86. Thompson, N.G., Lankard, D., and Sprinkel, M. 1991. *Improved Grouts for Bonded Tendons in Post-Tensioned Bridge Structures*. Report No. FHWA-RD-91-092. Washington, DC: FHWA.

87. Ghorbanpoor, A. and Madathanapalli, S.C. 1992. *Performance of Grouts for Post-Tensioned Bridge Structures*. Report No. FHWA-RD-92-095. Washington, DC: FHWA.

88. Salas, R.M., Schokker, A.J., West, J.S., Breen, J.E., and Kreger, M.E. 2004. *Conclusions, Recommendations and Design Guidelines for Corrosion Protection of Post-Tensioned Bridges*. Report No. FHWA/TX-04/0-1405-9. Austin, TX: TxDOT.

89. Shokker, A., Koester, B.D., Breen, J.E., and Kreger, M.E. 1999. *Development of High Performance Grouts for Bonded Post-Tensioned Structures*. Report No. 1405-2. Austin, TX: TxDOT.

90. Kilduff, A.L., Moyer, K.L., McCool, G.E., Ahern, M.E., and Breen, J.E. 2013. *Corrosion Resistance Recommendations From Long-Term Exposure Testing of Post-Tensioning Systems*. Report No. FHWA/TX-13/0-4562-5F. Austin, TX: TxDOT.

91. Kalina, R.D. 2009. *Comparative Study of the Corrosion Resistance of Different Prestressing Strand Types for Use in Post-Tensioning of Bridges*. Master's Thesis. The University of Texas.

92. MacLean, S. 2008. *Comparison of the Corrosion Resistance of New and Innovative Prestressing Strand Types Used in Post-Tensioning of Bridges.* Master's Thesis. The University of Texas.

93. McCool, G.E. 2010. *Evaluation of Corrosion Resistance of New and Upcoming Post-Tensioning Materials After Long-Term Exposure Testing.* Master's Thesis. The University of Texas.

94. Moyer, K.L. 2012. *Assessment of Long-Term Corrosion Resistance of Recently Developed Post-Tensioning Components.* Master's Thesis. The University of Texas.

95. Wang, H. and Sagues, A.A. 2005. *Corrosion of Post-Tensioning Strands: Final Report.* Report No. BC353 RPWO#33. Gainesville, FL: FDOT.

96. Wang, H., Sagues, A.A., and Powers, R. 2005. "Corrosion of the Strand-Anchorage System in Post-Tensioned Grouted Assemblies." Paper No. 05266. Presented at the *Corrosion 2005 Conference*. Houston, TX: NACE International.

97. Bricker, M.D. and Schokker, A. 2005. *Corrosion From Bleed Water in Grouted Post-Tensioned Tendons.* PCA R&D Serial No. 2547. Skokie, IL: PCA.

98. Shokker, A. and Musselman, E. 2008. *Varina-Enon Grout Evaluation Report, Appendix I.2, Final Report.* Figg Bridge Engineers, Inc.: Exton, PA.

99. Trejo, D., Hueste, M., Gardoni, P., Pillai, R., Reinschmidt, K., Im, S., Kataria, S., Hurlebaus, S., Gamble, M., and Ngo, T. 2009. *Effect of Voids in Grouted Post-Tensioned Concrete Bridge Construction: Volume 2—Inspection, Repair, Materials, and Risks*. Report No. FHWA/TX-09/0-4588-1. Austin, TX: TxDOT.

100. Trejo, D., Pillai, R.G., Hueste, M.D., Reinschmidt, K.F., and Gardoni, P. 2009. "Parameters Influencing Corrosion and Tendon Capacity of Post-Tensioning Strands." *ACI Materials Journal*, March–April: 144–153. Farmington Hills, MI: ACI.

101. Kataria, S. 2008. *Assessment of Grouts for Constructability and Durability of Post-Tensioned Bridges*. Master's Thesis. Texas A&M University.

102. Texas Departmental Material Specifications. 2004. "DMS-4670: Grouts for Post-Tensioning." TxDOT: Austin, TX. http://ftp.dot.state.tx.us/pub/txdot-info/cst/DMS/4000_series/pdfs/4670.pdf, last accessed March 11, 2020.

103. Merrill, B.D. 2012. "TxDOT PT/Grout Issues." Presented at a webinar. Austin, TX: TxDOT. http://ftp.dot.state.tx.us/pub/txdot-info/brg/0212_webinar/merrill.pdf, last accessed March 11, 2020.

104. Moser, R.D. 2011. *High-Strength Stainless Steels for Corrosion Mitigation in Prestressed Concrete: Development and Evaluation*. Ph.D. dissertation. Georgia Institute of Technology.

105. Osborn, A.E.N., Lawler, J.S., and Connelly, J.D. 2008. *Acceptance Tests for Surface Characteristics of Steel Strands in Prestressed Concrete*. NCHRP Report 621. Washington, DC: TRB.

106. O'Reilly, M., Darwin, D., and Browning, J. 2012. *Corrosion Performance of Prestressing Strands in Contact With Dissimilar Grouts*. Report No. SL Report 12-1. Topeka, KS: Kansas Department of Transportation.

107. Rafols, J.C. 2012. "Corrosion of Post-Tensioned Tendons Repaired With Dissimilar Grout." Master's thesis. University of North Florida.

108. Lau, K., Paredes, M., and Powers, R. 2013. "Corrosion Evaluation of Repair-Grouted Post-Tensioned Tendons in Presence of Bleed Water." Paper No. 2604. Presented at the *Corrosion 2013 Conference*. Orlando, FL: NACE International.

109. Lau, K., Powers, R., and Paredes, M. 2012. *Corrosion of Post-Tensioned Tendons Repaired with Dissimilar Grout Phase II—Corrosion Evaluation of Repair-Grouted Post-Tensioned Tendons in Presence of Bleed Water*. Report No. not available. Gainesville, FL: FDOT.

110. Hamilton, H.R. 2014. *Simulation of Prepackaged Grout Bleed Under Field Conditions*. Revised Draft Final Report No. BDK75 977-59. Gainesville, FL: FDOT.

111. Hamilton, H.R. and Rice, J.A. 2017. *Replaceable Unbonded Tendons for Post-Tensioned Bridges*. University of Florida. Report No. BDV31-977-15. Gainesville, FL: FDOT.

112. Bergum, K. and Risher, T. 2017. *Evaluation of a Silicon Based Polymer Corrosion Inhibitor for Post-Tensioned Tendons*. Interim report. Gainesville, FL: FDOT.

113. Castaneda, C.F. 2017. *Flexible Filler Corrosion Protection of Unbonded Post-Tension Tendons.* Master's thesis. Florida Atlantic University.

114. Hartt, W.H. and Lee, S.K. 2018. *Corrosion Forecasting and Failure Projection of Post-Tensioned Tendons in Deficient Cementitious Grout.* Report No. FHWA-HRT-17-074. Washington, DC: FHWA. https://www.fhwa.dot.gov/publications/research/infrastructure/bridge/17074/17074.pdf, last accessed March 11, 2020.

115. Lee, S.K. 2021. *Corrosivity of Water-Soluble Sulfate Ions in Simulated Grout Pore Water Solutions and Different Types of Grout Samples*. Report No. FHWA-HRT-21-052. Washington, DC: FHWA.

116. Godart, B. 2001. "Status of Durability of Post-Tensioned Tendons in France." *Fib Bulletin No. 15: Durability of Post-Tensioned Tendons:* 25–42. Lausanne, Switzerland: FIB International.

117. Chaussin, R. and Chabert, A. 2001. "Strategies for Improvement—Approach in France." *Fib Bulletin No. 15: Durability of Post-Tensioned Tendons:* 235–244. Lausanne, Switzerland: FIB International.

118. Nurnberger, U. 2001. "Corrosion Induced Failure Mechanisms." *Fib Bulletin No. 15: Durability of Post-Tensioned Tendons:* 89–101. Lausanne, Switzerland: FIB International.

119. Blactot, E., Brunet-Vogel, C., Farcas, F., Gaillet, L., Mabille, I., Chaussadent, T., and Sutter, E. 2007. "Electrochemical Behavior and Corrosion Sensitivity of Prestressed Steel in Cement Grout." *Simulation of Electrochemical Processes II*: 267–276. South Hampton, UK: WIT Press.

120. Bertolini, L. and Carsana, M. 2011. "High pH Corrosion of Prestressing Steel in Segregated Grout." *Modeling of Corroding Concrete Structures*: 147–158. Place of publication not available: RILEM [International Union of Laboratories and Experts in Construction Materials, Systems and Structures].

121. Kamalakkannan, S., Thirunavukkarasu, R., Pillai, R. and Santhanam, M. 2013. "Assessment of Grouts for Post-Tensioning Applications." Presented at the *Raikar 2013*. Mumbai, India. https://www.researchgate.net/publication/324562340_ASSESSMENT_OF_GROUTS_FOR_POST-TENSIONING_APPLICATIONS, last accessed March 12, 2020.

122. Harder, J. and Webster, N.R. 2001. “Durability of Post-Tensioning Tendons: Canadian Experience.” *Fib Bulletin No. 15: Durability of Post-Tensioned Tendons:* 51–71. Lausanne, Switzerland: FIB International.

123. Al-Amoudi, O.S.B. “Protection of Reinforced Concrete Structures in Chloride-Sulfate Exposure.” Paper No. 07279. Presented at the *Corrosion 2007 Conference*. Nashville, TN: NACE International.

124. Hartt, W.H. 2014. “Failure Forecasting for Corroding Bonded Post-Tensioning Tendons Containing Chemically Deficient Grout.” Presented at the *FHWA/FDOT Grout Meeting*. Gainesville, FL: FHWA/FDOT.

125. Hamilton, T.R. 2014. “Evaluating PT Grout Segregation with the Modified Inclined Tube Test.” Presented at the *FHWA/FDOT Grout Meeting*. Gainesville, FL: FHWA/FDOT.

126. Elsener, B. 2008. “Monitoring of Electrically Isolated Post-Tensioning Tendons.” *Tailer Made Concrete Structures*: 231–236. London, UK: Taylor & Francis Group.

127. Cercone, C., Naito, C., Corven, J., Pessiki, S., Keller, W., and Pakzad, S. 2015. *Designing and Detailing Post-Tensioned Bridges To Accommodate Non-Destructive Evaluation: Subtask 11.1 Literature Review*. Report No. 14-01. Bethlehem, PA: Advanced Technology for Large Structural System (ATLSS) Engineering Research Center, Lehigh University.

128. FHWA. 2018. *Designing and Detailing Post-Tensioned Bridges To Accommodate Nondestructive Evaluation*. Report No. FHWA-HIF-18-029. Washington, DC: FHWA.

129. FHWA. 2019. “Electrically Isolated Post-Tensioning Tendons for More Durable Bridges: Accelerated Market Readiness brochure.” Washington, DC: FHWA. https://www.fhwa.dot.gov/bridge/concrete/amr_eit.pdf, last assessed June 19, 2021.

130. Naito, C. and Cercone, C. 2019. “Implementation of an Electrically Isolated Tendon Post-Tensioning System in the United States.” *Aspire Magazine*, Spring Issue: 36–37. Chicago, IL: PCI.

131. Schokker, A., Rueda, E.S., Breen, J. and Kreger, M. 2004. “Testing of Oils as Temporary Corrosion Protection and Update on Progress With New Materials for PT.” Presented at the *2004 PTI Conference Technical Session 7 (Durability of Post-Tensioned Structures)*. Farmington Hills, MI: PTI.

132. Miller, E.L., White, B.C., Haskins, R.W., Ebeling, R.M., and Evans, J.A. 2017. *An Investigation of Corrosion Mitigation Strategies for Aging Post-Tensioned Cables*. Report No. ERDC/ITL TR-17-1. Vicksburg, MS: US Army Corps of Engineers.

133. Whitmore, D.W. and Beaudette, M.R. 2016. “Impregnation of Post-Tensioning Tendons.” *Aspire Magazine*, Winter 2016: 36-37. Chicago, IL: PCI.

134. Whitmore, D.W. and Lasa, I. 2014. “Cable Impregnation for Post-Tension Grouting Problems.” Presented at the *Transportation 2014: Past, Present, Future—2014 Conference and Exhibition of the Transportation Association of Canada*. Montreal, Canada: Transportation Association of Canada. http://conf.tac-atc.ca/english/annualconference/tac2014/s-33/whitmore.pdf, last accessed March 12, 2020.

135. Whitmore, D.W. 2015. “PT Impregnation for Post-Tension Corrosion Problems.” Presented at the *TRB Annual Meeting Corrosion Committee (AHD45)*. Washington, DC: TRB.

136. PTI. 2015. *Selection of Filler Material for Multistrand PT Tendons, Technical Note 19*. Farmington Hills, MI: PTI.

137. Theryo, T.S. 2014. “Flexible Post-Tensioned Duct Filler Materials as Alternative to Cement Grout.” Presented at the *2014 Virginia Concrete Conference*. Richmond, VA: VDOT.

138. European Organization of Technical Approvals (EOTA). 2002. *Guideline for European Technical Approval of Post-Tensioning Kits for Prestressing of Structures*. Brussels, Belgium: ETAG 013, EOTA. http://www.sgpstandard.cz/editor/files/stav_vyr/dok_es/eta/etag/013_en.pdf, last assessed June 19, 2021.

139. ASTM. 2018. ASTM A416/A416M-18: *Standard Specification for Low-Relaxation, Seven-Wire Steel Strand for Prestressed Concrete*. Volume 04.02. ASTM: West Conshohocken, PA.

140. ASTM. 2010. ASTM A882/A882M-04a: *Standard Specification for Filled Epoxy-Coated Seven-Wire Prestressing Steel Strand* [withdrawn in 2019]. ASTM: West Conshohocken, PA.

141. ASTM. 2014. ASTM A475-03: *Standard Specification for Zinc-Coated Steel Wire Strand*. Volume 01.06. ASTM: West Conshohocken, PA.

142. FHWA. 2020. *Technical Advisory: [Rescinded] Cable Stays of Cable-Stayed Bridges*. Washington, DC: FHWA. https://www.fhwa.dot.gov/bridge/t514025.cfm, last accessed March 21, 2020.

143. Moore, D.G., Klodt, D.T., and Hensen, R.J. 1970. *Protection of Steel in Prestressed Concrete Bridges*. NCHRP Report 90. Washington, DC: TRB.

144. Hamilton, H.R., Breen, J.E., and Frank, K.H. 1995. *Investigation of Corrosion Protection Systems for Bridge Stay Cables*. Report No. 1264-3F. Austin, TX: TxDOT.

145. PCI. 1993. “Guidelines for the Use of Epoxy-Coated Strand, Ad Hoc Committee on Epoxy-Coated Strand.” *Prestressed Concrete Institute (PCI) Journal*, July-August: 26-32. Chicago, IL: Precast/Prestressed Concrete Institute.

146. ASTM. 2020. *ASTM A1114/A1114M-20: Standard Specification for Low-Relaxation, Seven-Wire Steel, Grade 240 [1655], Stainless Steel Strand for Prestressed Concrete*. Volume 01.04. ASTM: West Conshohocken, PA.

147. Vector Corrosion Technologies. 2020. "Post-Tech PT Cable Drying: Unbonded Post-Tensioned Concrete Structures." Vector Corrosion Technologies: Winnipeg, Canada. https://www.vector corrosion.com/uploads/content/15002 2012Apr 30%20Post-Tech%20PT%20Cable%20Drying.pdf?force_download, last accessed March 12, 2020.

HRDI-30/09-22(WEB)E